Université Pierre et Marie Curie

Ecole doctorale Complexité du Vivant (ED515)

Centre Interdisciplinaire de Recherche en Biologie, Collège de France

Cortical stiffness : a gatekeeper for spindle positioning in mouse oocytes

Présentée par Agathe Chaigne

Thèse de doctorat de Biologie Moléculaire et Cellulaire du Développement

Dirigée par Marie-Emilie Terret

Présentée et soutenue publiquement le 4 Juillet 2014

Devant un jury composé de :

Mme Sophie Louvet	Présidente
Mr Guillaume Halet	Rapporteur
Mr Péter Lénárt	Rapporteur
Mr Laurent Blanchoin	Examinateur
Mr Matthieu Piel	Examinateur
Mme Marie-Emilie Terret	Examinateur
Mme Marie-Hélène Verlhac	Membre invité

Remerciements

Je voudrais d'abord remercier tous les gens de la Science (avec un S majuscule) :

Mon inestimable jury: Laurent Blanchoin, Guillaume Halet, Peter Lénart, Sophie Louvet et Matthieu Piel. Merci d'avoir accepté de juger mon travail.

Tous les gens qui m'ont aidé lors de cette thèse et en particulier mon comité de thèse, Arnaud Echard, Alexis Gautreau et Matthieu Piel, one more time, qui ont vraiment fait avancer mon travail d'une façon extrêmement productive.

Marie-Hélène alias The Big Boss pour m'avoir accueillie dans ton labo et donné les moyens de faire plein de trucs marrants, d'aller tirer sur des ovocytes à Curie. Tu donnes à tous les gens du labo la possibilité de faire, d'essayer, de se tromper ; ce n'est pas donné à tout le monde et je t'en remercie. Merci aussi de m'avoir appris à dire JE, parfois.

Marie-Emilie alias The Boss pour m'avoir proposé un sujet cool, pour m'avoir super encadrée, pour avoir discuté de Top Chef avec moi, pour m'avoir soutenue tout le temps et m'avoir remonté le moral quand j'ai fait la même manip pendant 6 mois en modifiant la concentration d'agarose 3 pM par 3 pM. J'ai vraiment passé une thèse formidable, à la fois passionnante et détendue et c'est en grande partie grâce à toi ! Ta façon d'encadrer tes étudiants, de leur manifester ton intérêt et ta patience comme tu le fais, tout en étant toujours disponible pour tout le monde te rend irremplaçable.

Isabelle à la fois pour ton aide précieuse, tes conseils et ta rigueur dans le travail, mais aussi et surtout parce que je suis très contente de te connaître. Discuter avec toi m'aura souvent permis de comprendre les autres.

Maria pour tes innombrables conseils et anecdotes, et parce qu'on s'est bien marrées (comme des vils petits scarabées). Ta confiance en toi m'a donné de la force pour défendre mes idées.

Agnieszka you gave me a great lesson of courage. You are a strong woman, the kind that holds the whole world (and sometimes the whole lab!) on her shoulders, and you are still very missed in the lab.

Gosia , for a few fun parties at « La plage de Jérémie » with way too much vine (and sometimes even vodka). Good luck for everything is the future !

Isma et **Joanne** on ne se connaît pas encore très bien mais je suis sûre que ça va très bien marcher pour vous.

Stéphane parce que la première fois qu'on s'est rencontré tu m'as comparée à Audrey

Hepburn dans « Vacances Romaines », et pour toutes tes idées en labmeeting.

Pascale on ne s'est pas beaucoup connu mais tu m'as accueillie très gentiment alors que j'étais un peu stressée.

Jessica je te remercie surtout pour avoir démarré ce projet que j'ai adoré suivre, et parce que tu t'es donné la peine de venir me voir juste pour m'expliquer comment analyser de la photoactivation.

Toute l'équipe de **Cécile Sykes**, en particulier **Pierre Nassoy** pour ses idées, **Kévin** et **Joël** pour le crawfish etouffé de New Orleans, et surtout mon inestimable collègue et ami **Clément** avec qui j'ai passé de longues heures enfermée dans une cave à critiquer ses goûts musicaux (pourris, il faut bien le reconnaître) en regardant mes ovocytes se déformer (ou pas). On se sera quand même bien marré dans cette cave.

Nir Gov and **Raphaël Voituriez** for thinking that modeling spindle migration in a mouse oocyte is a good idea and for being able to say « is it quadratic? » in front of a biologist audience without blinking.

Tous les gens de l'étage: la Fekrije team et la Alexander team (en particulier **Marion** pour les descentes de pression).

Tous les gens qui m'ont aidée: **Jean-Pierre**, **Frédéric**, tous les animaliers (big up à **Seb** (malgré sa passion du PSG) pour m'avoir appris à buter les souris mos sans me faire mordre), **Claudette**, **Nicole**, **Sophie**, **Sidonie** pour toutes les commandes, conventions, machins à signer, **Jérémie** pour les appels et textos de type « y a un machin qui s'allume pas et le microscope fait un bruit chelou, je cours ? ».

Tous les gens qui m'ont donné des plasmides, inhibiteurs, machins, en particulier **Sophie Louvet**, **Franck Perez**, **Alexis Gautreau** (one more time), **Katja Wassmann**.

Je dois maintenant remercier tous mes amis (de la Science et d'ailleurs)

Claire, Hector, Florent, Imen, Filipe, Henri, Charlotte, Lauriane, Ludo, Rémy, Rémi, Morgan, Isabelle, Anne-So, Chou, Marianne, François, Claire B, Manu, Audrey, Lara, **Alexis**, **Edouard** (special thanks pour avoir répondu un long mail à mes questions pendant tes vacances en t'excusant de ne pas pouvoir faire mieux !) **Clémence, Alice, Benjamin** et tous les autres. Je ne vais pas vous dire à tous pourquoi je suis contente de vous avoir parce que franchement, ça serait trop long, et puis vous le savez déjà, bande de moules.

Je remercie aussi tous les gens qui ont été à un moment ou un autre mentor ou moteur

dans mon embryon de carrière scientifique (ne nous emballons pas) :

Mr Le Nechet qui m'a donné envie de faire de la bio, tous mes profs de prépa de Nantes et de Paris, en particulier mes profs de bio Mr Auger et Périlleux (alias PP) et Mme Bonhoure, et aussi Toby sans qui je n'aurais JAMAIS eu 14 en maths à l'ENS et Dejan pour ses commentaires dithyrambiques sur mes copies de chimie orga, les gens que j'ai côtoyé à l'ENS, les profs de la prépa Agreg d'Orsay en particulier Patrick Pla, Hélène Vincent-Schneider et Samuel Rébulard.

Je remercie mes sponsors (non officiels)

Mariage Frères, La compagnie anglaise des thés, Kenzo, Labeyrie, Beillevaire, La Belle-iloise, Le Foie de Morue, Top Chef, HBO (Winter is coming), Mark Knopfler, Renaud, Puccini, Eminem, Scotland, l'Angélique Confite.

Enfin je dois remercier ma famille en général et la Famille en particulier (en mode mafia)

Tous **les Lahouze** pour la contrebande de confit et foie gras pour les soirs de manips ratées.

Tous les Chaigne : **Pierre**, **Brigitte**, **Caroline**, **Olivier**, **Antoine** et **Charlotte** et en particulier **Benjamin** qui trouve que la Science c'est marrant mais un peu bizarre et quand même galère.

Tous les Baron en particulier **George, Eric, Nana, Julien** (que j'ai copieusement bassiné avec mes histoires de graphiques), **Olivier, Nadine, Max, Théo et Estelle** qui doivent trouver ce que je fais très étrange aussi.

Une pensée pour tous ceux qui ne sont plus là.

Et surtout, merci à la **Chaigne** team : **Daniel** l'autre docteur es science qui sera toujours mon héros, **Pascale** la théoricienne de la lèvre supérieure rigide qui sera toujours mon pilier. Vous avez toujours été exigeants avec nous, ce n'est pas toujours facile (it is the less that we can say), mais je n'en serai pas ici sans vous et ne nous voilons pas la face, faire et défaire c'est toujours travailler. Merci aussi surtout à ma grande sœur **Marion** (ça n'a pas raté, patron !) et ma petite sœur **Héloïse** (spéciale dédicace pour les tutoriaux Adobe Illustrator personnalisés) pour avoir fait semblant de lire mon papier et commenté sur le joli machin qui s'épaissit, et m'avoir écouté râler. Et aussi **Gibbon**.

Ce travail est dédié à **Benoît**, pour tout et le reste. Here's looking at you, kid.

Table of content

Abbreviations list

Prologue

Introduction

A) Actin and cell division

1) Actin and its partners

a) G-actin and F-actin

α. G-actin monomers

β. F-actin filaments

Figure 1: Polarity of actin filaments

χ. Actin polymerization mechanisms

b) Actin nucleators

α. Arp2/3, a branched actin filaments nucleator

Role

Structure and activity

Figure 2: Arp2/3 and branched actin nucleation

Activation

Figure 3: NPF type I structure

β. Formins, nucleator and/or elongator?

Role

Structure

Figure 4: The Formin family

Activity

χ. Other types of nucleators

Figure 5: Structure of WH2-mediated actin nucleators

Spire

JMY

Cordon-Bleu

Leiomodin

c) Modulation of actin nucleation

α. Actin associated proteins

F-actin organizing proteins

Figure 6: Actin interacting proteins

F-actin Motors

Figure 7: Myosin-II and F-actin

β. Transduction pathways associated with actin polymerization

Rho GTPases

Figure 8: Actin and Rho-GTPases

MAPK pathway

Figure 9: The MAPK pathway

Figure 10: Transduction pathways associated with actin dynamics

2) The roles of actin in mitotic cell division

a) Overview of mitotic cell division

α. The basic steps of mitotic cell division

Figure 11: The steps of mitosis

Figure 12: Spindle organization during mitosis

β. Asymmetric divisions

Figure 13: Simplified scheme of asymmetric divisions

b) The roles of actin in mitotic cell division

α. Cortical actin filaments

β. Cytoplasmic actin filaments

χ. Actin flows

B) Meiotic maturation in mouse oocyte

1) Meiosis and the female gamete formation

a) Overview on meiosis

Figure 14: Overview on Meiosis

b) A series of cellular arrests

Figure 15: Mouse meiotic maturation

2) Meiotic maturation in the mouse

a) Cellular particularities of oocytes

b) Progression of mouse meiotic maturation

α. Prophase I and recombination

β. Meiosis resumption

χ. Spindle formation

Figure 16: Spindle formation in mouse oocyte

δ. Spindle migration

ε. Homologous chromosome segregation and polar body extrusion

ϕ. Spindle reformation and anchoring

Figure 17: Actin flow and Metaphase II spindle

γ. Later events

3) Breaking the symmetry in the oocyte

a) Absence of polarity factors in Prophase I

α. None of the usual suspects

β. A slightly off-centered nucleus

b) Spindle migration

α. Visualization of actin in cells

UtrCH

Lifeact

Controversies

β. Role of F-actin

Figure 18: F-actin meshwork during Meiosis I in the mouse oocyte

χ. Force generation

Figure 19: Force generator in mouse Meiosis I spindle migration

c) The role of Mos

Figure 20: Mos/MAPK during mouse meiotic maturation

d) Formation of the actin cap and polarization of the oocyte

Figure 21: Actin cap formation in Meiosis I

C) The physics of cell division

1) The physical parameters describing cell mechanics

a) Tension

α. Micropipette aspiration

Figure 22: Micropipette aspiration and determination of cortical tension

β. AFM

χ. Optical trap

b) Cytoplasmic viscosity

Figure 23: Micropipette aspiration and measure of the cell viscosity

c) Elasticity/Plasticity

d) Models and scales

2) Physical constraints on a dividing cell

a) From outside the cell

Figure 24: Mechanical constraints and spindle positioning in non-polarized cells

b) From inside the cell

α. Cortical tension, spindle formation and robustness

Figure 25: Increased cortical tension allows proper spindle formation in mitosis

β. Cortical tension and spindle motion in mouse oocyte

Figure 26: F-actin network and cortical tension in mouse oocytes, a contradiction?

χ. Cell mechanics and cytokinesis

Figure 27: Shape instabilities, blebbing and pressure release during cytokinesis

D) Situation of the problem

Results

A soft cortex is essential for asymmetric spindle positioning in mouse oocytes

Cortical stiffness: a Gatekeeper for spindle positioning in mouse oocyte (in preparation)

Discussion and perspectives

A) Cooperation of two actin networks in positioning the Meiosis I spindle

1) Relationships between the two actin networks

2) Cortical tension: a catalyst for forces unbalance

B) Actin network architecture influences Myosin-II activity

C) Multiple roles for cortical tension?

1) A role for cortical tension in spindle formation?

Figure 28: Spindle defects in Meiosis I oocytes harboring a low cortical tension

2) A role for cortical tension in the switch between symmetric and asymmetric acentriolar division?

Figure 29: A role for cortical tension in mediating the switch between symmetric and asymmetric divisions in acentriolar cells?

References

Annexes

Abbreviations list

-/-: homozygous mutant allele

ABP: Actin Binding Protein

ADF/Cofilin: Actin Depolimerization Factor/Cofilin

ADP: Adenosine di Phosphate

AFM: Atomic Force Microscope

AI: AutoInhibitory domain

APC-C: Adenomatous Polyposis Coli C terminal fragment

APC/C: Anaphase Promoting Complex/Cyclosome

aPKC: atypical Protein Kinase C

Arp2/3: Actin related protein 2/3

ARPC1-5: actin-related protein complex-1-5

ATP: Adenosine tri Phosphate

B: Basic binding domain

cAMP: Cyclic Adenosine 3',5'-MonoPhosphate

CapZ: Capping Protein Z

CC: Coil-Coiled

CDK1: Cyclin Dependent Kinase 1

COBL: Cordon-Bleu

CP: Capping Protein

CRIB: Cdc42-Rac Interactive Binding domain

CSF: CytoStatic Factor

DAD: Diaphanous Autoinhibitory Domain

DD: Dimerization Domain

Diaph1/2: Diaphanous 1 and 2

DID: Diaphanous Inhibitory Domain

DOC1R: Deleted in Oral Cancer 1 Related

DRF: Diaphanous Related Formin

E3KARP: NHE3 kinase A regulatory protein

EBP50/NHE-RF: ERM Binding Protein 50 or Na+/H+ Exchanger Regulatory Factor

Ect2: Epithelial Cell Transforming 2

ENA/VASP: Enabled/Vasodilator-Stimulated Phosphoprotein

ERK: Extracellular signal-regulated kinases

ERK1/2: Extracellular signal-Regulated Kinase 1 and 2

ERM: Ezrin, Radixin, Moesin

F-actin: Filamentous actin

FAK: Focal Adhesion Kinase

FERM domain: Four-point one, Ezrin, Radixin, Moesin domain

FH1-FH2: Formin Homology domain 1 and 2

FMN1/2: Founding Mammalian Formin 1 or Formin-1 and Formin-2

FSI: Formin-Spire Interaction domain

G-actin: Globular actin

GAP: GTPase Activating Proteins

GBD: GTPase Binding domain

GDP: Guanosine Di Phosphate

GEF: Guanine nucleotide Exchange Factor

GFP: Green Fluorescent Protein

GTP: Guanosine Tri Phosphate

HURP: Hepatoma Up-Regulated Protein

JMY: Junction-Mediating regulatory protein

kDa: kiloDalton

L: Linker

LH: Luteinizing Hormone

LMOD1-3: Leiomodin 1 , 2 and 3

MAP: Microtubule Associated Protein

MAPK: Mitogen Activated Protein Kinase

MAPKAPK2: MAPK-Activated Protein Kinase 2

mDia: mammalian Diphanous

MEK: MAPK/ERK kinase Kinase

MISS: MAPK Interacting and Spindle Stabilizing

MLCK: Myosin Light-Chain Kinase

Mos: Moloney murine Sarcoma virus

MPF: M-phase Promoting Factor

MTOC: MicroTubule Organizing Center

N-WASP: Neural Wiskott-Aldrich Syndrome Protein

Non-DRF: Non Diaphanous Related Formin

NPF: Nucleation Promoting Factor

NuMA: Nuclear Mitotic Apparatus

P: polyProline domain

PAK1-3: P21-Activated protein Kinase 1, 2 and 3

Par-3/6: Partitioning defective 3 and 6

PB1/2: Polar Body 1 and 2

PDZ domains: Postsynaptic-density protein of 95 kDa, Discs large and Zona occludens-1 domain

Pi: inorganic Phosphate

PICK1: Protein Interacting with C Kinase 1

PCM: PeriCentriolar Material

PKA: Protein Kinase A

PRD: Prolin-Rich Domain

PtdIns(4,5)P_2: PhosphatidylInositol 4,5-bisphosphate

Ran: Ras-related Nuclear protein

RBD: Rho-Binding Domain

RCC1: Regulator of Chromosome Condensation 1

SAC: Spindle Assembly Checkpoint

SAF: Spindle Assembly Factor

SCAR: Suppressor of Cyclic AMP Repressor

SHD: SCAR Homology Domain

SOP: Sensory Organ Precursors

Spir: Spire

Spire1/2: Spire 1 and Spire 2

TBR: Tubulin-Binding Region

TIRF: Total Internal Reflection Fluorescence

Tmod: Tropomoduline

TPX2: Targeting Protein for the Xenopus kinesin xklp2

WAHD1: WASH Homology Domain 1

WASH: WASP and Scar Homologue

WASP: Wiskott-Aldrich Syndrome Protein

WAVE: WASP-family Verprolin-homologous protein

WCA domain: WASP-homology-2 (WH2 or W; also called verprolin-homology) domain; Central (also called cofilin-homology or connector) domain; Acidic domain

WHAMM: WASP Homologue associated with Actin, Membranes and Microtubules

WMD: WHAMM Membrane-interaction Domain

Prologue

Asymmetric divisions are very important because they allow the formation of two different daughter cells thus generating cell diversity. Meiotic divisions during the formation of the female gamete, the oocyte, are examples of asymmetric divisions: in that case, the purpose of the divisions is to remove half of the DNA content to form an haploid cell, so that when it fuses with an haploid sperm it forms a diploid zygote. But, especially in species where eggs are laid such as Xenopus, asymmetric divisions are also very important to retain most of the cell cytoplasm in the oocyte, which contains maternal stores indispensable for further embryonic development. Hence, these divisions are highly asymmetric in size ensuring the segregation of chromosomes with minimum cytoplasmic loss.

The first female meiotic division (Meiosis I) in the mouse is peculiar because the asymmetry of the division depends on an off-center spindle positioning that is not microtubule dependent as in most mitotic cells but only actin dependent (Longo and Chen, 1985). Furthermore, it was shown recently that cortical tension, a parameter that accounts for cortex stiffness, decreases during Meiosis I (Larson et al., 2010), which is a very puzzling observation for two reasons. First, a very dense F-actin meshwork is formed during Meiosis I (Azoury et al., 2008; Schuh and Ellenberg, 2008) which we would expect to stiffen the cortex. Second, oocytes are round cells stable in shape, similar to mitotic cells that round up at the onset of mitosis because of an increase in cortical tension absolutely required for proper spindle function (Kunda et al., 2008; Lancaster et al., 2013).

During my PhD, I was interested in this drop in cortical tension and its role in spindle positioning. The goal of my PhD was first to understand where this drop was coming from and how it was related to F-actin present in the mouse oocyte, and second what was its role during Meiosis I. To this end, I also developed new physical approaches to study mechanical properties of the cytoskeleton in the oocytes that did not exist previously in the lab.

In the first part of the introduction, I will present F-actin and its partners playing a role in cell division in general and mouse meiotic divisions in particular. I will then present mouse meiotic divisions with a focus on spindle migration mechanisms during Meiosis I. Finally, I will discuss the mechanical properties of cells with an emphasis on cortical tension and their known roles in cell division.

INTRODUCTION

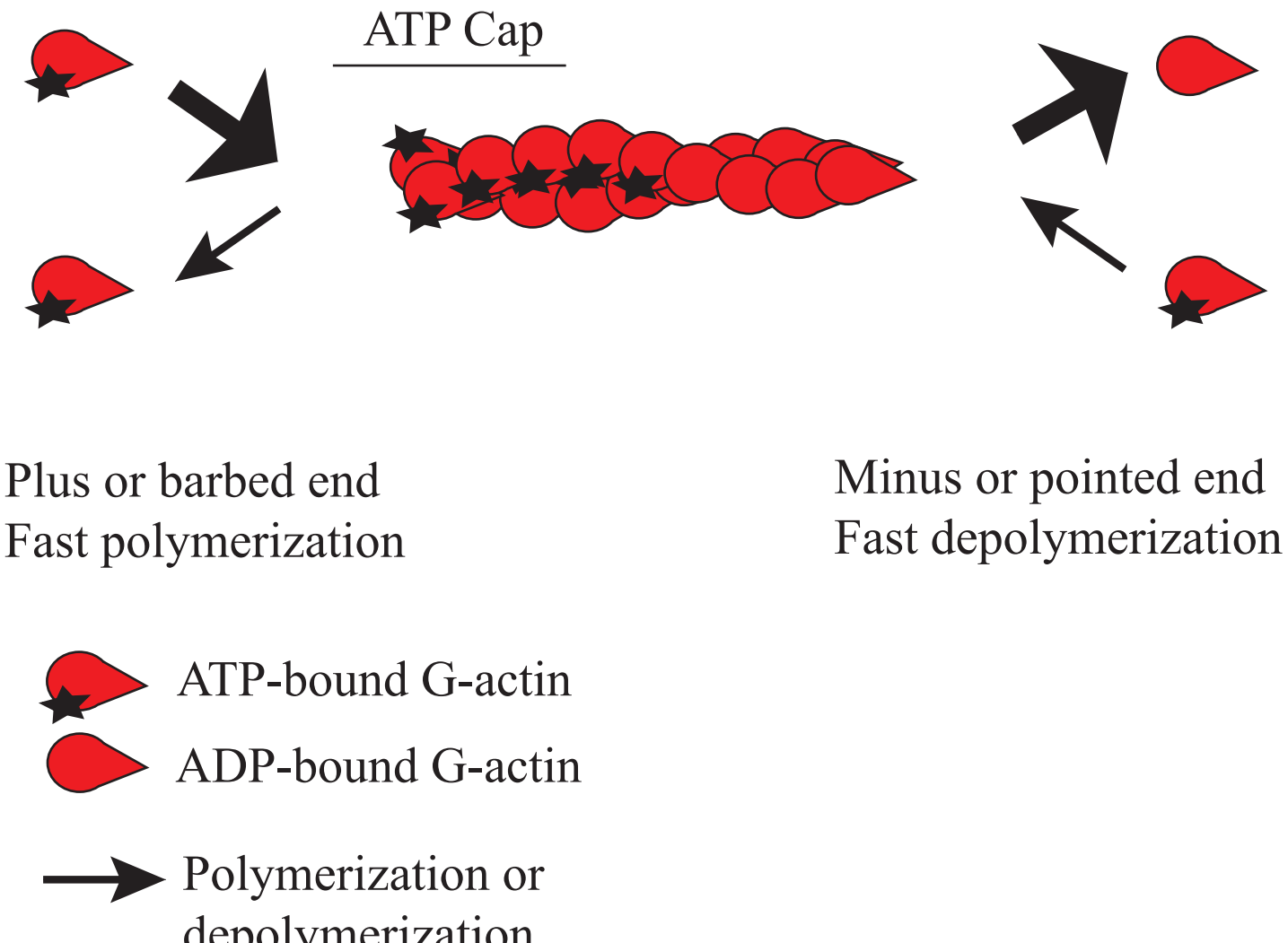


Figure 1: F-actin polarity and polymerization

A) Actin and cell division

1) Actin and its partners

Actin is one of the most abundant proteins in cells; it has a major role in building the cytoskeleton, which confers to the cell its specific architecture. It is a very highly conserved protein among species and is involved in many cellular processes such as cell motility, cell division and intracellular trafficking.

a) G-actin and F-actin

Actin is present in almost all eukaryotic cell types. It is found in cells as monomers (globular actin or G-actin) or polymers (fibrillar actin, F-actin or microfilaments).

α. G-actin monomers

Actin monomers are 42 kDa proteins. In Vertebrates, three different isoforms have been identified: α-actin, β-actin and γ-actin. These isoforms are thought to sustain different functions in cells probably due to differences in their localization or their ability to bind proteins (for review see (Perrin and Ervasti, 2010)). Each monomer has a globular conformation and possesses a cleft that can bind Mg^{2+} and ATP (Adenosine Tri Phosphate), and hydrolyze ATP in ADP (Adenosine Di Phosphate) +Pi (inorganic Phosphate). In cells, G-actin is often associated with Profilin, a protein that has been shown to inhibit F-actin polymerization (Schutt et al., 1993; Perelroizen et al., 1994).

β. F-actin filaments

F-actin filaments consist of multiple actin monomers polymerized in an oriented fashion and forming an helix. The ATP-bound cleft in each monomer is oriented towards a particular end of the proto-filament. This extremity is able to polymerize faster than the other: it is called “plus-end” or “barbed-end” as opposed to “minus-end” or “pointed-end” (Figure 1).

When the actin monomer is added on a growing filament, it has a bound ATP molecule, which can then undergo hydrolysis. Therefore, because of the difference in polymerization rates between the two extremities, the plus-end of the actin filament is richer in ATP-bound monomers than the minus-end, thus forming an ATP-cap that might play a role in stabilizing the filament (Figure 1) (Blanchoin et al., 2000a).

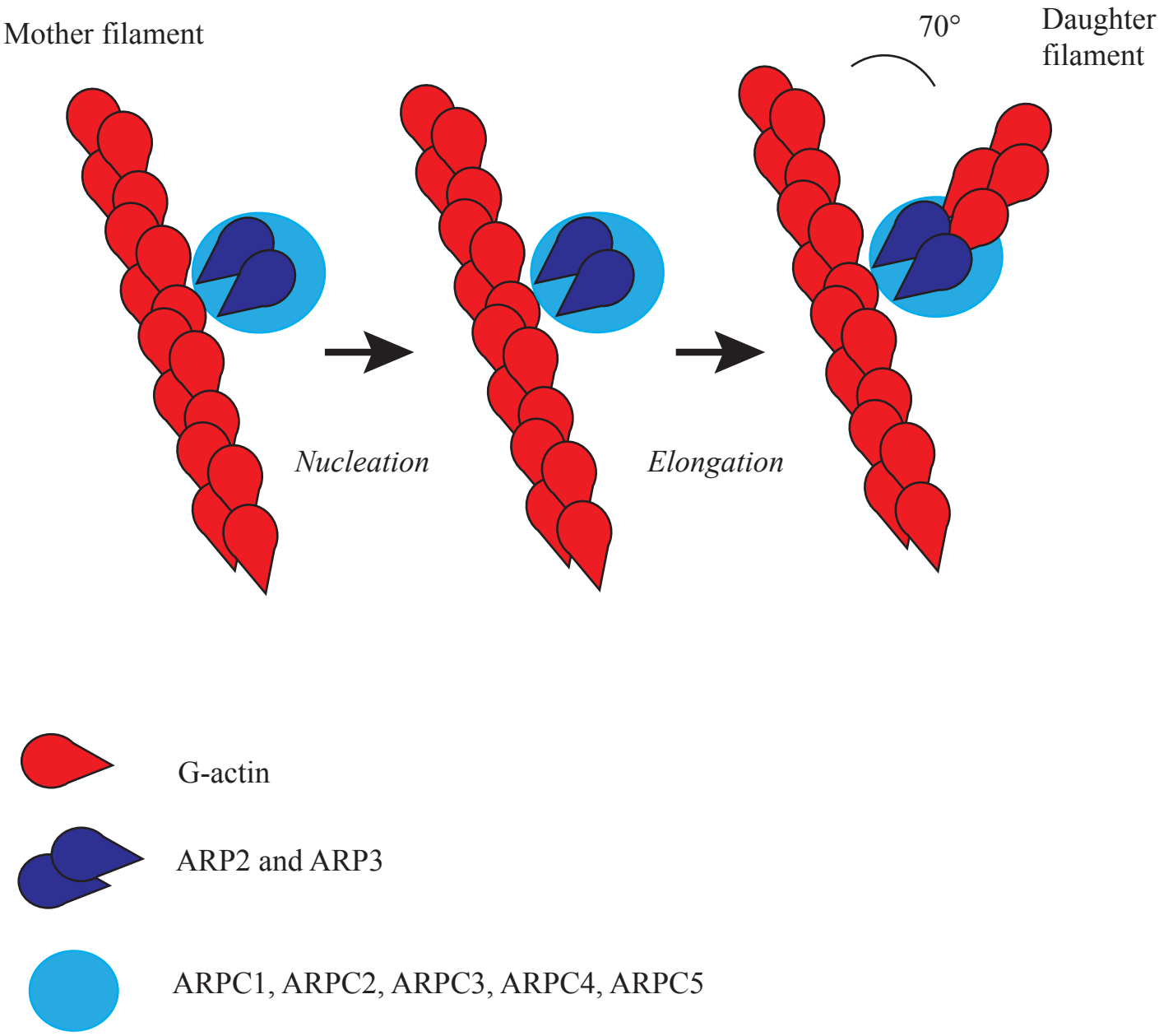


Figure 2: Arp2/3 and branched actin nucleation

χ. Actin polymerization mechanisms

F-actin filaments start to polymerize when G-actin reaches a threshold concentration called the critical concentration. De novo filament polymerization is achieved in two steps: the nucleation and the elongation. As mentioned before, the critical concentration is different at each end of the filament. In living cells, the critical concentration is reached and F-actin is at steady state.

The nucleation step, which is the formation of a seed of three monomers, is a slow process because the formation of an actin dimer is not thermodynamically favorable. However, the addition of the third monomer stabilizes the trimer and provides a starting point for elongation of the filament. The elongation step is a very favourable and quick reaction.

Actin filaments can undergo polymerization and depolymerization at both ends. But their rate is different leading to a process called treadmilling: even when there is actin assembly on the barbed end and disassembly on the pointed end the filament can harbor a constant length.

b) Actin nucleators

As mentioned before, the crucial event for filament polymerization is nucleation. Actin nucleators are a group of proteins that promote actin nucleation in cells (for review, see (Campellone and Welch, 2010)).

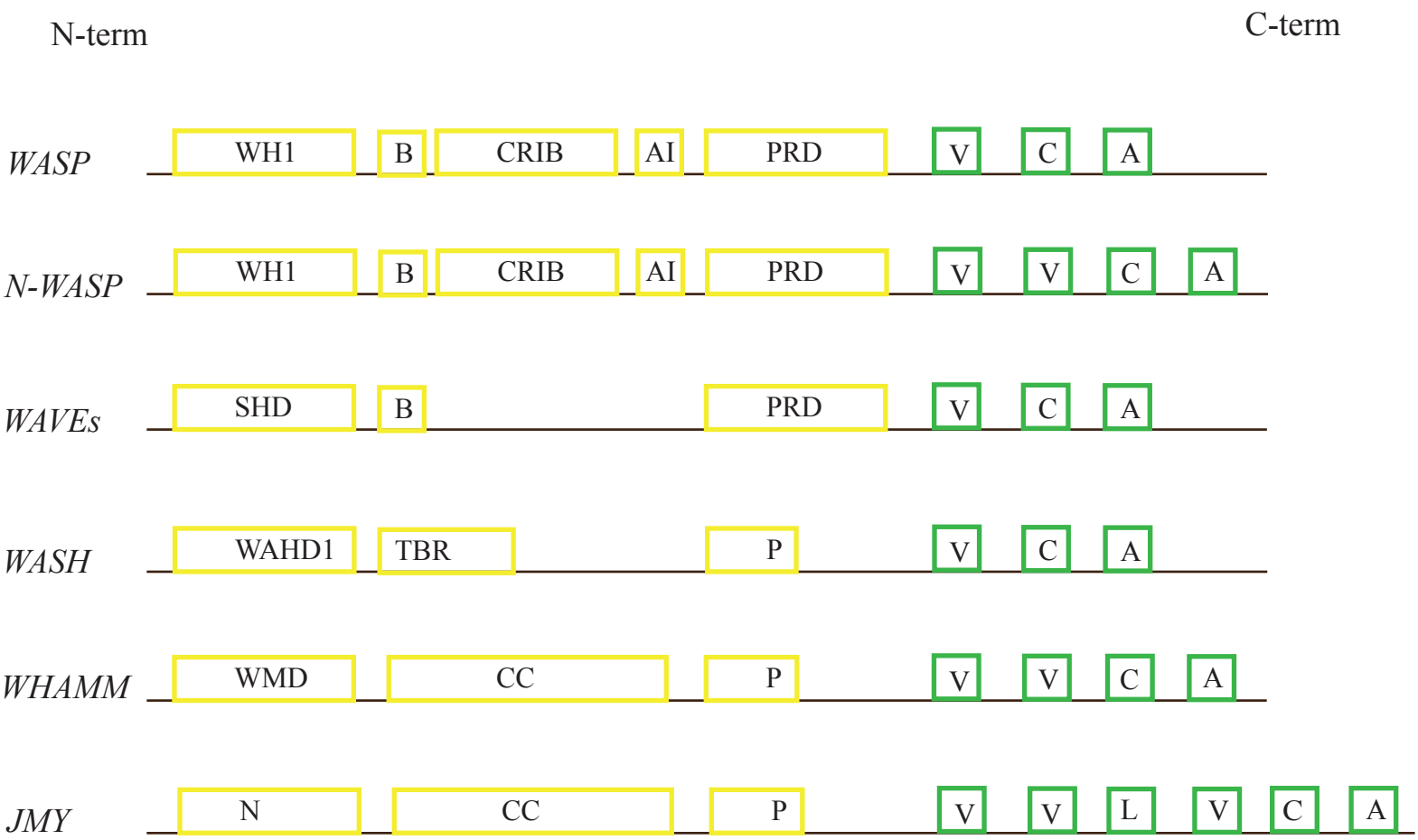
α. Arp2/3, a branched actin filaments nucleator

Role

The Arp2/3 complex is involved in many cellular processes, involving in particular a change in the architecture of the cell at its periphery. Indeed, Arp2/3 is localized and activated at the cortex of many cell types (see below). It has been involved for example in lamellipodia formation of migrating cells (Blanchoin et al., 2000b), during vesicular trafficking (Campellone et al., 2008), endocytosis (Kaksonen et al., 2006) and phagocytosis (May et al., 2000). It also plays a key role during mouse meiotic divisions that I will detail later on, promoting their asymmetry in size (Sun et al., 2011a; Chaigne et al., 2013).

Structure and activity

Arp2/3 is composed of seven subunits (ARP2, ARP3, ARPC1, ARPC2, ARPC3, ARPC4, ARPC5) forming a 220 kDa complex (for review, see (Goley and Welch, 2006; Rotty et al., 2013)), which is able to nucleate branches on a pre-existing actin filaments at a



Regulatory motifs

WH1: WASP Homology 1 domain
B: Basic binding
CRIB: Cdc42–Rac Interactive Binding
AI: AutoInhibitory domain
PRD: Prolin-Rich Domain
SHD: SCAR Homology Domain
WAHD1: WASH Homology Domain 1
TBR: Tubulin-Binding Region
P: Polyproline
WMD: WHAMM Membrane interaction Domain
CC: Coil-Coiled
N: N-term

Nucleation motifs

V: WASP Homology domain 2
C: Connector
A: Acidic region
L: Linker

Figure 3: Type I NPF Structure

70° angle (Figure 2). The ability of this complex to nucleate actin filaments comes from the structural similarities between the ARP2 and ARP3 subunits and G-actin (Machesky et al., 1994; Kelleher et al., 1995). ARP2 and ARP3 bind to the pointed end of daughter filaments, thus probably providing a stable actin dimer-like structure allowing further elongation whereas ARPC2 and ARPC4 bind to the mother filament. The Arp2/3 complex seems to exist in two conformational states: opened and closed, the latter being the active conformation leading to creation of new branches (Smith et al., 2013).

Activation

For its nucleating activity, the Arp2/3 complex needs to be activated through a family of proteins called the NPF (Nucleation Promoting Factor) family (for review see (Campellone and Welch, 2010)).

Class I NPFs possess a characteristic VCA (or WCA) domain which is composed of a WH2 domain (also known as VH2 for Verprolin Homology domain 2), a connector domain (C), and an acidic domain (A). The VCA domain promotes the Arp2/3 complex-mediated nucleation by allowing the binding of G-actin (through the V motif) and Arp2/3 (through the CA motif) (Marchand et al., 2001) (Figure 3). Type I NPFs include WASP (Wiskott-Aldrich Syndrome Protein) which has also been shown recently to nucleate unbranched filaments in the absence of Arp2/3 (Urbanek et al., 2013), N-WASP (Neural WASP), three isoforms of SCAR/WAVE (Suppressor of Cyclic AMP Repressor/WASP-family Verprolin-homologous Protein) (Machesky et al., 1999), WASH (WASP and Scar Homologue) (Linardopoulou et al., 2007), WHAMM (WASP Homologue associated with Actin, Membranes and Microtubules) (Campellone et al., 2008) and JMY (Junction-Mediating regulatory protein) which can also nucleate unbranched actin filaments in the absence of Arp2/3 (Zuchero et al., 2009). Although the precise mechanism of Arp2/3 activation by the VCA is not completely elucidated, recent single molecule fluorescence colocalization techniques have further demonstrated that it stimulates both Arp2/3 binding to the mother filaments and Arp2/3 branching activity (Smith et al., 2013). Biochemical studies on WASP have shown that Arp2/3 is able to bind two VCA-containing molecules at once (Padrick et al., 2011), which could explain this dual function. Several type I NPFs have been shown to play a role during mouse meiotic divisions (Sun et al., 2011b, 2011a; Huang et al., 2012; Chaigne et al., 2013; Liu et al., 2012), that I will discuss later.

NPF can in turn be activated, for example Wave2 is phosphorylated in culture cells by ERK/MAPK (Extracellular signal-Regulated Kinases/Mitogen Activated Protein Kinase)

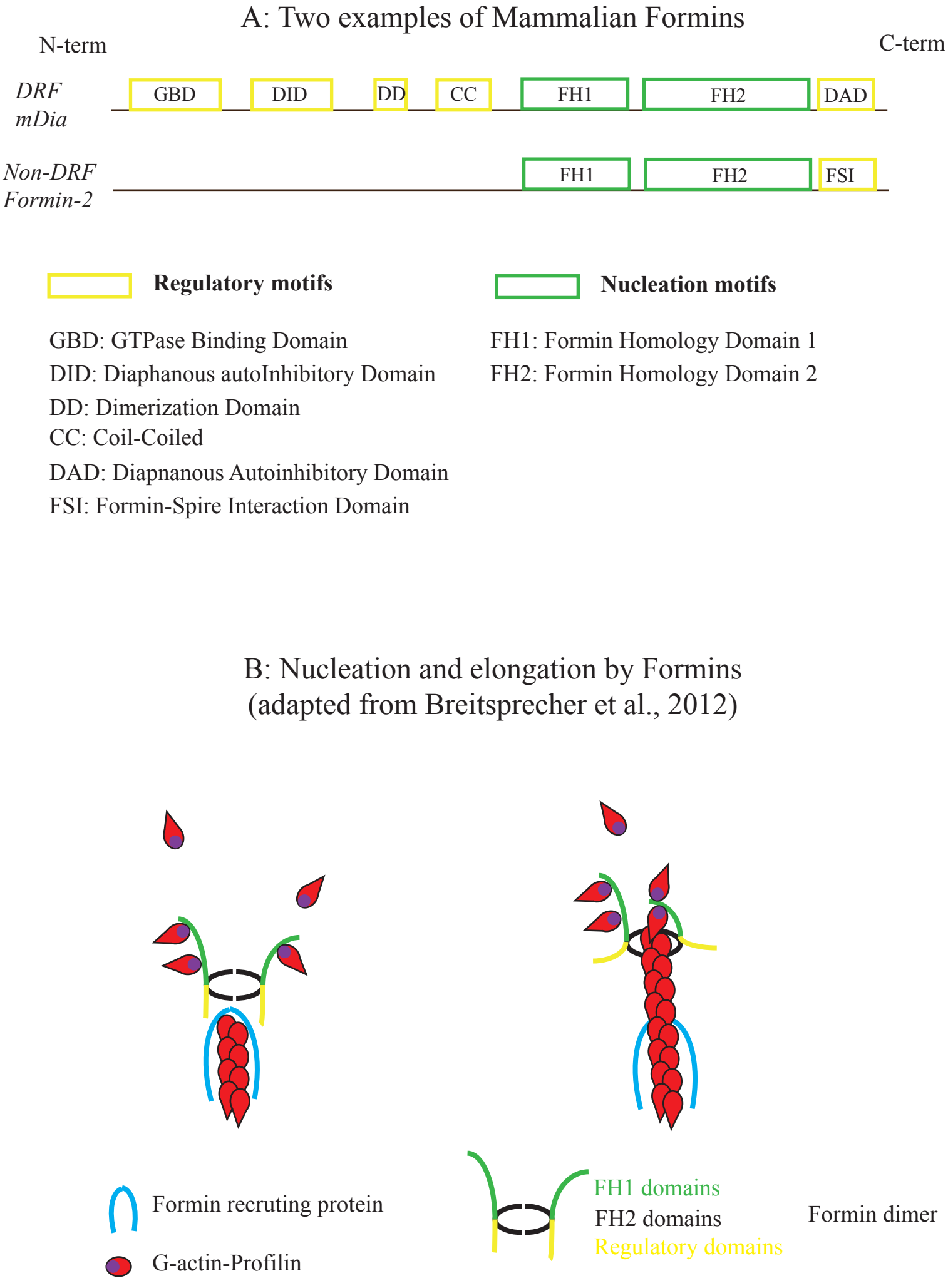


Figure 4: Formin structure and function

(Nakanishi et al., 2006; Mendoza et al., 2011) adding another level of complexity (for review see (Mendoza, 2013)). Furthermore, they possess in their N-terminal parts motifs important for their regulation, for example some of them can be targeted to the membrane and activated via interaction between the Basic (B) domain (Figure 3) and membrane phospholipids such as PtdIns(4,5)P_2 (PhosphatidylInositol 4,5-bisphosphate), explaining the many roles for Arp2/3 at the cell membrane.

Class II NPF such as Cortactin lack complete VCA domains, but they have acidic domains at their amino terminus that bind the Arp2/3 complex and tandem repeat domains that bind F-actin. They also activate Arp2/3 but in a less potent manner (Uruno et al., 2001; Weaver et al., 2001).

Arp2/3 activity is also dependent on ATP which binds to the subunits ARP2 and ARP3 in the same way that it binds to G-actin (Dayel et al., 2001). Its role is still controversial today, but it seems to promote a change in the conformation of the complex (Goley et al., 2004), a change in its affinity for the NPFs (Dayel et al., 2001), and its hydrolysis may also play a part in remodeling the F-actin network by promoting debranching (Martin et al., 2006).

Finally, several classes of negative regulators of the Arp2/3 complex have been identified in the past few years, including PICK1 (Protein Interacting with C Kinase 1) (Rocca et al., 2008) and Arpin (Dang et al., 2013). Very preliminary experiments conducted in the lab showed that overexpressing these proteins has no effect on mouse meiotic divisions (unpublished data).

β. Formins, nucleator and/or elongator?

Role

Like the Arp2/3 complex, Formins are also involved in cell migration, but also in cell polarity and cytokinesis. Furthermore, they seem to be able to stabilize microtubules and as such have recently been shown to play a role in cell division (for review see (Chesarone et al., 2010)).

Structure

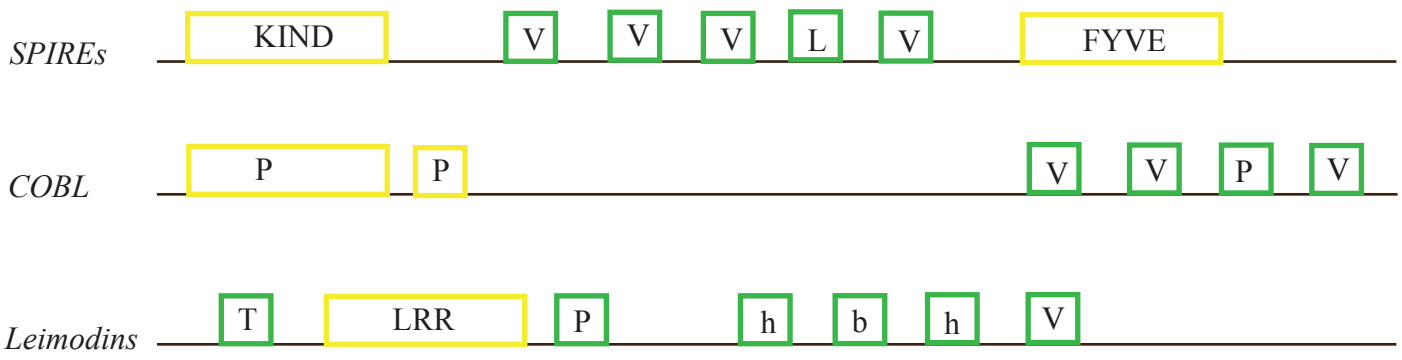
Contrary to Arp2/3, the Formins are very potent nucleators of unbranched F-actin filaments (Figure 4). In all Formins, the C-terminal domain possesses the nucleating activity; it comprises the FH1 (Formin Homology 1) and FH2 (Formin Homology 2) domains (Figure

4A). The FH1 domain binds to G-actin-Profilin whereas the FH2 domain forms a donut-shaped dimer with an adjacent Formin around the barbed end of the growing F-actin filament (Figure 4B). The N-terminal part is variable according to the subfamilies and contains domains important for the control of the protein activity. The exact sequence of these domains can vary considerably from a subfamily to another and among species. There are two classes of Formins in Mammals (Figure 4A): the Diaphanous-Related Formins (DRFs), subdivided in three families, and the Non-Diaphanous-Related Formins (Non-DRFs), subdivided in four families. Among the Non-DRF class, the FMN family comprises two members, FMN1 (Founding Mammalian Formin 1 or Formin-1) and FMN2 (Founding Mammalian Formin 2 or Formin-2). Formin-2 in particular is expressed in mouse oocytes (Evsikov et al., 2006) and brain and plays a key role during mouse meiotic divisions, promoting their asymmetry in size (Leader et al., 2002; Dumont et al., 2007a; Azoury et al., 2008; Li et al., 2008; Schuh and Ellenberg, 2008). FMN1 and 2 both possess a Formin-Spire interaction domain (FSI) (see below).

Activity

The precise mechanism of actin nucleation by Formins is not yet understood. It seems that many Formins need another protein to start nucleating F-actin. For example, a recent study *in vitro* has shown by TIRF (Total Internal Reflection fluorescence) microscopy that the protein APC-C (Adenomatous Polyposis Coli C terminal fragment) would be one of these proteins: it recruits actin monomers which serve as a nucleation seed and mDia1-C (a DRF Formin), which is then propelled and acts as a processive elongator (Breitsprecher et al., 2012) (Figure 4B). It seems that similarly, other Formins would need the binding of another molecule to nucleate actin; for example, the C-terminal part of Formin-2 is able to bind via its FSI motif to Spire-1 (Figure 4A), an actin binding protein which can nucleate F-actin *in vitro* (Pechlivanis et al., 2009). In addition, the fly Formin Cappuccino, a non-DRF Formin, also interacts *in vitro* and *in vivo* in the oocyte with Spire (Rosales-Nieves et al., 2006; Quinlan et al., 2007). Thus, Formins should not be considered only as nucleators but also as elongators, as shown also in mouse oocytes (see part **B)***3)b)*β) (Pfender et al., 2011; Montaville et al., 2014).

In contrast to the Arp2/3 complex, Formins are processive proteins that cap the barbed-end of the growing filaments (Pruyne et al., 2002; Sagot et al., 2002) (Figure 4B). The 2 FH2-domains bind transiently to the barbed end, somehow promoting a very potent filament elongation whereas the FH1 domains bind to G-actin-Profilin, probably then acting by



Regulatory motifs

KIND: Kinase non-catalytic domain
FYVE: Fab1, YoTB, Vac1 and eeA1 domain
LRR: Leucin-rich repeats

Nucleation motifs

V: WASP Homology domain 2
h-b-h: helix-basic-helix
P: Polyproline
T: Tropomyosin- and actin-binding helices
L: Linker

Figure 5: Structure of WH2-mediated actin nucleators

increasing the local concentration in G-actin (Vavylonis et al., 2006).

χ. Other types of nucleators

Spire

Spire contains four WH2 domains required for actin nucleation that bind actin and in addition possesses a G-actin binding linker between the third and fourth WH2 domains (Quinlan et al., 2005) (Figure 5). The precise mechanism for F-actin polymerization is not yet completely understood, but evidence suggests that G-actin binds to the tandem WH2 domains and the actin-binding linker thus forming a linear core of three monomers (Quinlan et al., 2005). Spire can work on its own or cooperate with Formins. Mammalian Spire1/2 (Spire 1 and Spire 2) bind to FMN1 and FMN2 (Pechlivanis et al., 2009) and allow the polymerization of F-actin in the cytoplasm of mouse oocytes (Pfender et al., 2011; Montaville et al., 2014), a process that I will detail later.

JMY

As mentioned before, in addition to its role as a NPF for the branched actin nucleator Arp2/3, JMY is able to nucleate actin filaments by itself (Zuchero et al., 2009). It is composed of three WH2 domains, a C domain and an A domain like for all class I NPFs (see Figure 3). Similarly to Spire, JMY possesses an actin-binding linker between the second and third WH2 domains that are involved in the formation of a new actin seed (Zuchero et al., 2009).

Cordon-Bleu

COBL (Cordon-Bleu) has three WH2 domains that bind G-actin *in vitro* (Ahuja et al., 2007), but contrary to JMY and Spire no predicted actin-binding linker (Zuchero et al., 2009) (Figure 5). Although the precise mechanism has not been demonstrated, it is assumed that these domains provide a trimeric seed for further unbranched filament elongation (Ahuja et al., 2007).

Leiomodin

The Leimodin family comprises three members, LMOD1, LMOD2 and LMOD3 that are muscle proteins. They possess two actin-binding domains and a WH2 domain (Figure 5). These three actin-binding domains are predicted to allow further polymerization from this nucleated seed (Chereau et al., 2008).

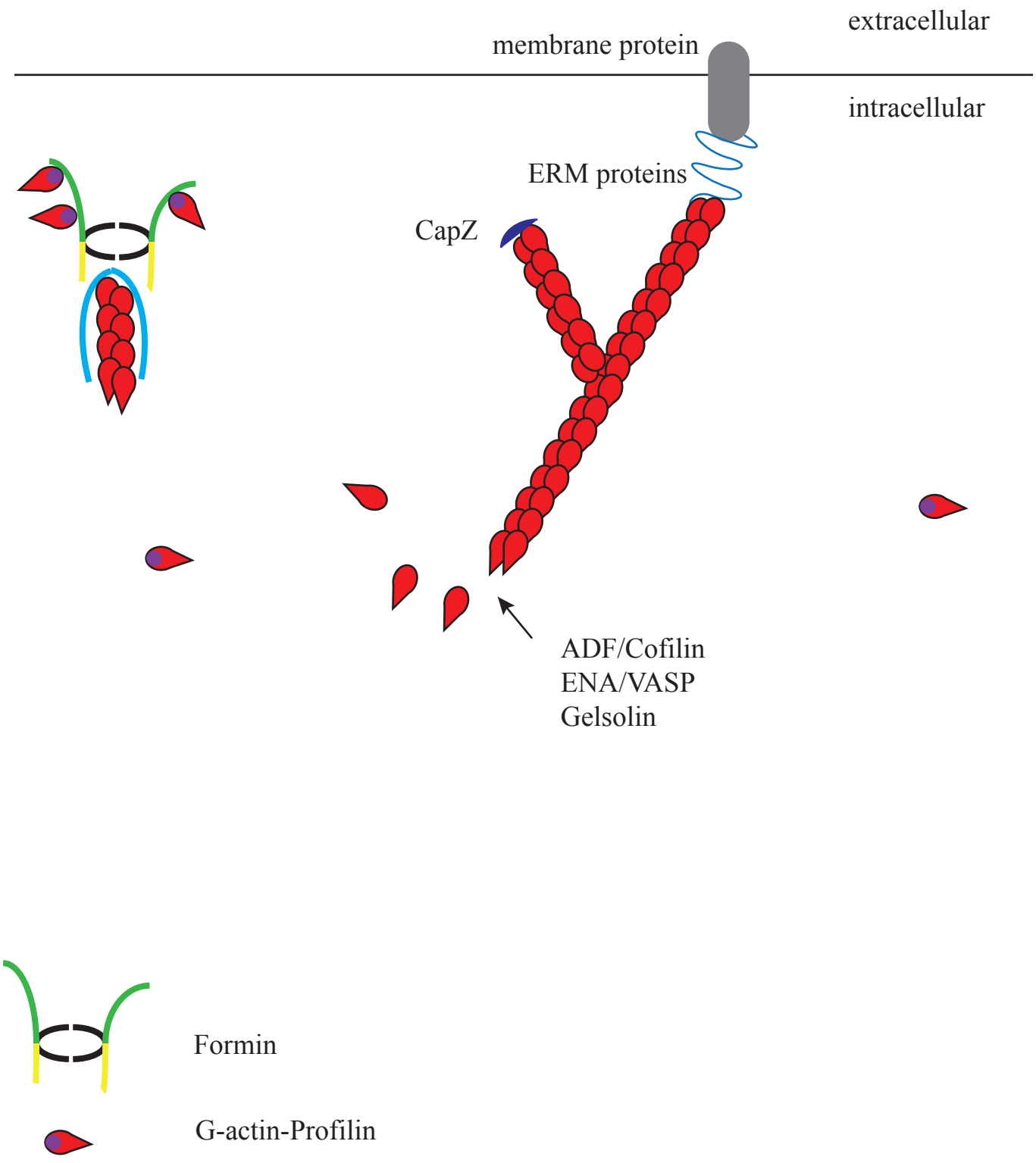


Figure 6: Actin-interacting proteins

c) Modulation of actin nucleation

Actin is a central protein in cells and as such interacts with many other proteins in order to regulate its function in time and space. We will discuss some proteins that have direct interactions with F-actin filaments, and some of the many transduction pathways that lead to modifications of the actin cytoskeleton.

α. Actin associated proteins

There are many actin-associated proteins, such as G-actin sequestering proteins, F-actin stabilizing or destabilizing proteins, F-actin organizing proteins and F-actin motors (Figure 6).

G-actin sequestering proteins

As mentioned before, G-actin in cells is often bound to Profilin (Schutt et al., 1993; Perelroizen et al., 1994). This binding promotes addition of actin monomers at barbed ends of filaments (Vavylonis et al., 2006).

Thymosine β4 is a small protein of the WH2 motif-containing protein family known for sequestering actin monomers (dos Remedios et al., 2003). It caps the actin monomers at both ends and competes with Profilin (Irobi et al., 2004), but can also bind to F-actin with a low affinity and destabilize the filaments (Carlier et al., 1996).

F-actin destabilizing proteins

ADF/Cofilin (Actin Depolimerization Factor/Cofilin) is a family of F-actin depolymerizing proteins (Bamburg et al., 1980), that comprises ADF and Cofilin in Vertebrates. These proteins possess binding sites for G-actin and F-actin and are responsible for the destabilization of F-actin in various ways, for example severing, increasing the off-rate at the pointed-end or direct depolymerization (dos Remedios et al., 2003).

Gelsolin is a superfamily comprising among others Gelsolin, Villin, and Severin (also called Fragmin); they all contain at least one gelsolin repeat (Kwiatkowski et al., 1986). Gelsolin binds to F-actin and upon Ca^{2+} fixation induces a change in conformation thats leads to the severing of the filament from their barbed ends (Robinson et al., 1999).

A less understood family is the ENA/VASP (Enabled/Vasodilator-Stimulated Phosphoprotein) family. ENA/VASP binds to G-actin, F-actin and Profilin and could act by preventing the capping of the filaments, inhibit Arp2/3 dependent nucleation or promote unbranching (for review see (Krause et al., 2003)).

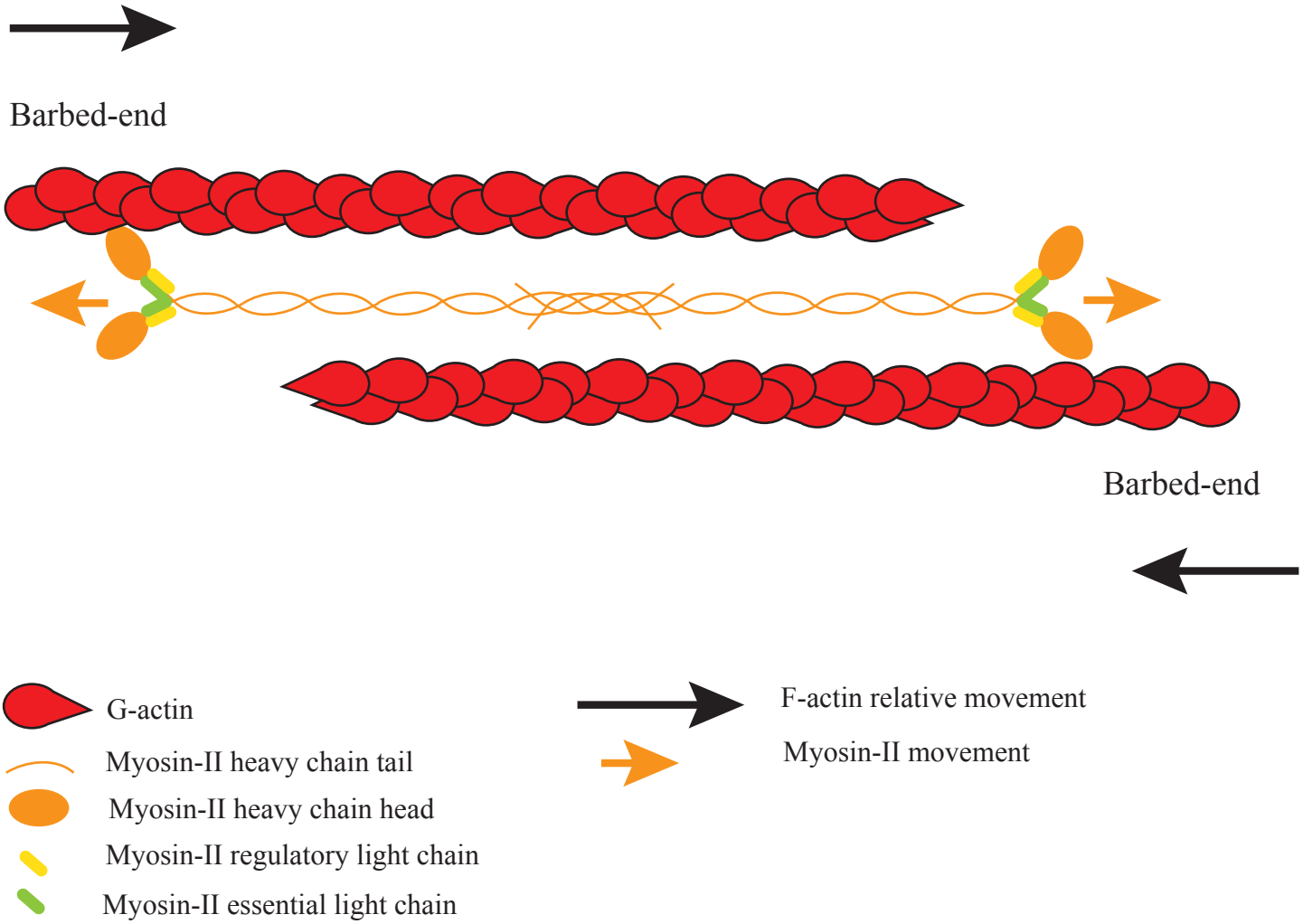


Figure 7: Myosin-II and F-actin

F-actin stabilizing proteins

The barbed-end of microfilaments can depolymerize very fast. However, in cells, they are stabilized by actin capping proteins proteins (for review see (dos Remedios et al., 2003) such as CapZ (Capping protein Z, also called CP for capping protein) (Casella et al., 1987). There are also proteins that stabilize the minus ends of the filaments, for example Tropomodulin (Tmod) that binds to pointed ends in presence of Tropomyosin.

F-actin organizing proteins

Many proteins such as Fimbrin, Actinin α, Villin, Spectrin organize actin filaments in higher order actin structure. Here, we will focus on another class of actin-organizing proteins, the ERM (Ezrin, Radixin, Moesin) proteins.

Ezrin, Radixin and Moesin are closely related proteins (Sato et al., 1992), they all possess a FERM (Four-point one, Ezrin, Radixin, Moesin) domain at their N-terminal parts. This domain is thought to have a clover leaf configuration such as it needs to bind to a ligand to unfold and thus allow the binding of F-actin to the C-terminal part of the protein (Bretscher et al., 2002). These proteins associate with the cytoplasmic tail of membrane protein such as the cell surface glycoprotein CD44 (Tsukita et al., 1994), but also with two scaffolding proteins EBP50/NHE-RF (ERM Binding Protein 50 or Na+/H+ Exchanger Regulatory Factor) and E3KARP (NHE3 kinase A regulatory protein) that themselves bind to a variety of membrane protein (Yun et al., 1998). Thus, ERM proteins are an interface between the plasma membrane and the actin cortex underneath (Charras et al., 2006) (Figure 6). Due to their close relation with the cell periphery, ERM proteins have been proposed to play various roles in cell cortex mechanics (for review see (Neisch and Fehon, 2011)) for example during blebbing (Charras et al., 2006) or during cell rounding at the onset of mitosis (Carreno et al., 2008; Kunda et al., 2008). In particular, it seems that upon activation, ERM proteins acting as crosslinkers between the actin cytoskeleton and the membrane force the F-actin filaments to become parallel to the cortex thus increasing the cortical tension of the cell and promoting cell rounding (Kunda et al., 2008). In mouse oocytes, cortical tension has also been shown to depend on ERM proteins (Larson et al., 2010), I will detail this process below (part **C**)*2)b)*β).

F-actin Motors

Myosins are motor proteins that can bind to actin; as such they form together a functional unit. Myosins possess a conserved motor domain on their "head" part, or N-terminal part and a variable "tail" at their C-terminal extremities. There are many different

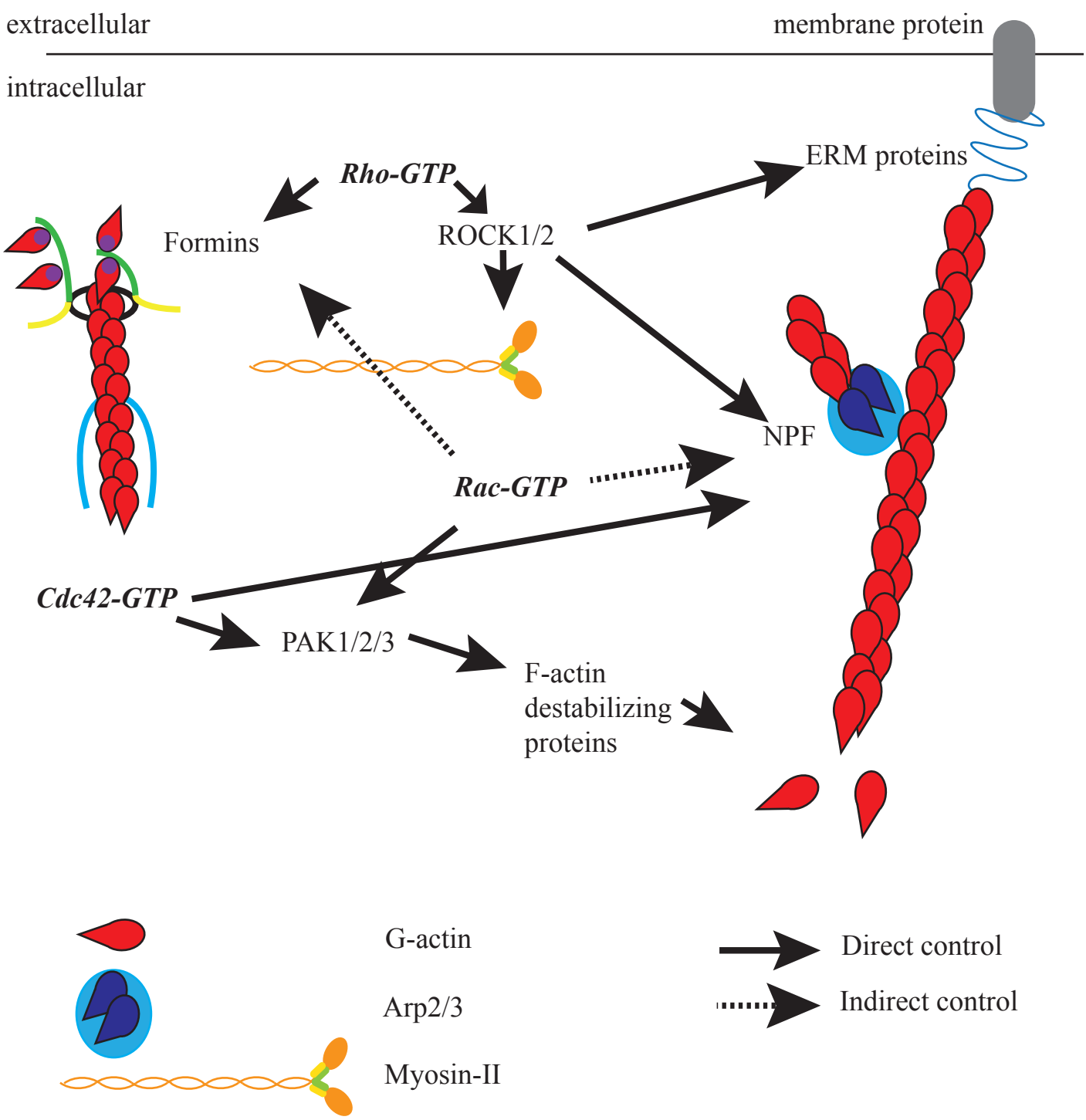


Figure 8: Actin and Rho GTPases

Myosins that are divided in thirty five families (Bloemink and Geeves, 2011). All but Myosin-VI are able to walk along the actin filaments towards the plus-end through ATP hydrolysis-mediated changes in Myosins' "head" conformation. The tail domain contains motifs that can be important for the specific function of a specific Myosin, for example cargo transport or dimerization. Two Myosins play an important role during mouse meiotic divisions, Myosin-II and V; I will discuss it later. Myosin-X is also peculiar because it binds both to F-actin and microtubules in vitro and in Xenopus oocytes (Weber et al., 2004) and embryos (Woolner et al., 2008; Woolner and Papalopulu, 2012).

Myosin-II is one of the most studied Myosins. It is present in particular in the muscle and is named so because it has two "heads", the very long tail of the two heavy chains supercoilling, thus forming a head-to-tail dimer (Figure 7). They also possess four light chains associated with each "head". Myosin-II has a small processivity, which means that it can walk only on a short distance on the actin filament, but at a high speed. Myosin-II can be phosphorylated at several sites. Phosphorylation of the light chain by MLCK (Myosin Light-Chain Kinase) is of crucial importance because it unfolds the protein and allows F-actin-Myosin interactions (for review see (Hong et al., 2011)).

Myosin-Va and Myosin-Vb have also been shown to walk along actin filaments but moreover they can transport cargos (for review see (Hammer and Sellers, 2012)). This process seems to be used either for short distance transport or in cells lacking centrosomes for long distance transport for example in the mouse oocyte (Schuh, 2011), suggesting that this is an alternate pathway for the canonical microtubule/Dynein/Kinesin track (Hammer and Sellers, 2012).

Interestingly, Myosin activity depends on the architecture of the F-actin network. For example *in vitro*, Myosin-VI and Myosin-II induce a contraction followed by a disassembly of a branched actin network of antiparallel filaments, whereas parallel filaments with their barbed-end oriented towards the same direction would not contract or disassemble (Reymann et al., 2012). Moreover, it has also been shown in the amoeba Dictyostelium discoideum that Myosin-II binds preferentially to stretched F-actin filaments (Uyeda et al., 2011). Thus, the orientation, the architecture and tension of the F-actin filaments play a part in the activity of Myosins.

β. Transduction pathways associated with actin polymerization

There are many transduction pathways that control the actin cytoskeleton. We will

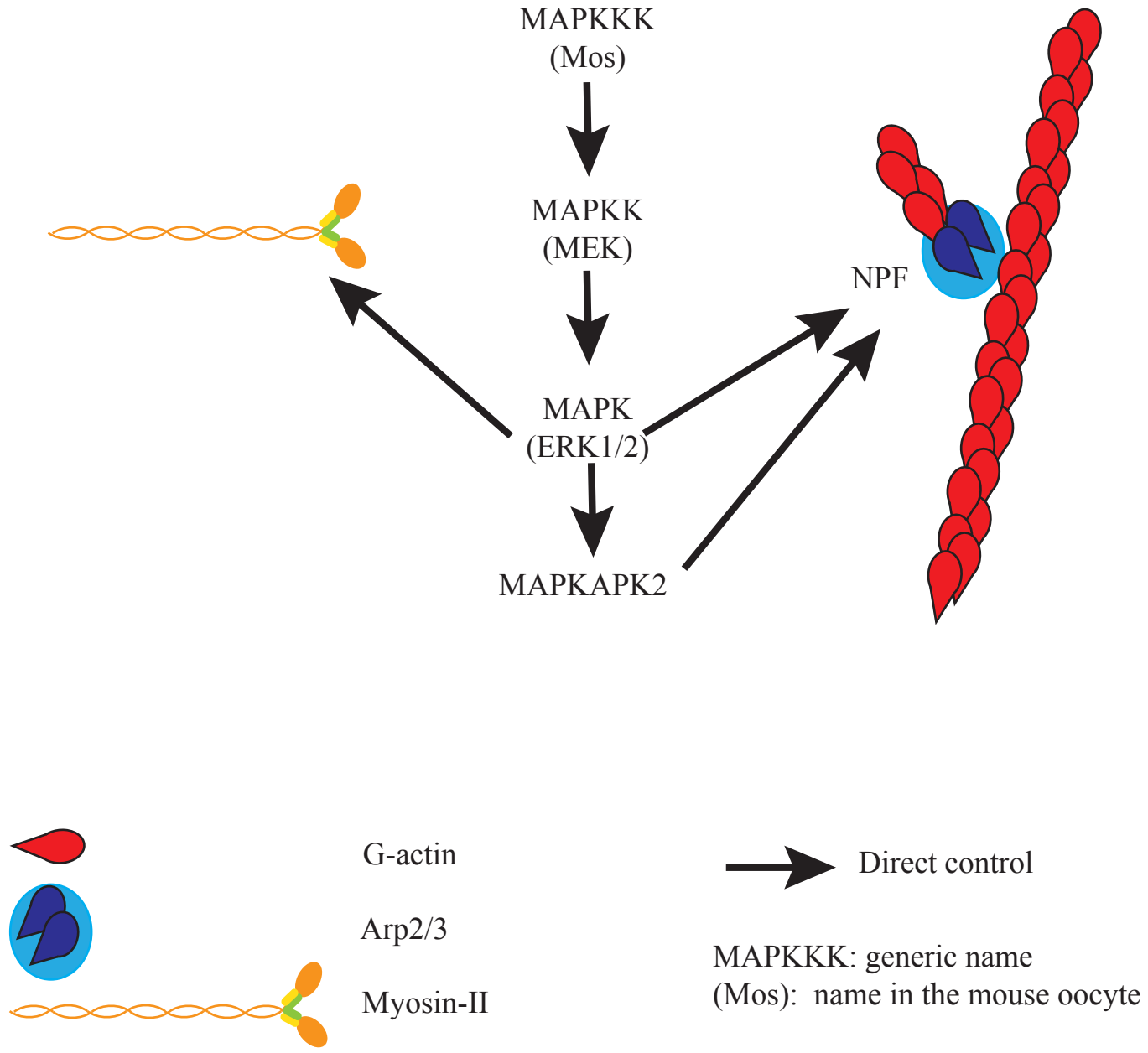


Figure 9: Actin and the MAPK pathway

only present here the pathways that are relevant in mouse oocytes.

Rho GTPases

The Rho family of small GTPases includes Rho, Rac and Cdc42. These small molecules act as molecular switches; they exist bound to GTP (Guanosine Tri Phosphate), which is their active state, and GDP (Guanosine Di Phosphate). The switch between these states is mediated by GAPs (GTPase Activating Proteins) and GEFs (Guanine nucleotide Exchange Factor) (Jaffe and Hall, 2005). Rho has been shown very early on to have a major role in the control of the actin cytoskeleton and especially on stress fibers and focal adhesion (Paterson et al., 1990). Then Rac and Cdc42 were shown to control respectively the formation of lamellipodia, which are the leading edge of migrating cells, and filopodia, the cytoplasmic projections of migrating cells (for review see (Pullikuth and Catling, 2007)); these two structures rely on actin cytoskeleton.

The Rho GTPases have many downstream effectors (Figure 8) (for review see (Jaffe and Hall, 2005)). For example, Rho controls the Formins Diaph1 (Diaphanous 1) and Diaph2 (Diaphanous 2), Rock1 (Rho-associated, Coiled-coil-containing protein Kinase 1 or Rho Kinase 1) and Rock2 (Rho-associated, Coiled-coil-containing protein Kinase 2 or Rho Kinase 2) which in turn activate the phosphorylation and thus activation of Myosin-II light chain, activates WASH in Drosophila oocytes (Liu et al., 2009) and ERM proteins (Bretscher et al., 2002). Rac controls PAK1, PAK2 and PAK3 (P21-Activated protein Kinase 1, 2 and 3) which regulate Cofilin, an F-actin destabilizing protein, thus controlling actin depolymerization; it also interacts indirectly with a DRF Formin, mDia (mammalian Diaphanous) and Wave2 (Goh et al., 2012). Cdc42 controls WASP and N-WASP, which activates Arp2/3-dependent F-actin assembly, and the PAK family.

MAPK pathway

The MAPK (Mitogen-activated protein kinase) pathway is composed of a cascade of proteins phosphorylating each other, namely upstream a MAPKKK (MAP Kinase Kinase Kinase), then a MAPKK (MAP Kinase Kinase) and downstream a MAPK (MAP Kinase), which is a Serine/Threonine Kinase (Figure 9). In Mammalian oocytes, the ones expressed are respectively Mos (Moloney murine Sarcoma virus), MEK (MAPK/ERK Kinase) and ERK1/2 (Extracellular signal-Regulated Kinase 1 and 2). The MAPKs ERK1/2 have many substrates and are known for controlling the actin cytoskeleton in several ways. In cells, it has been shown to mediate Arp2/3 dependent nucleation via phosphorylation of the NPF Wave2

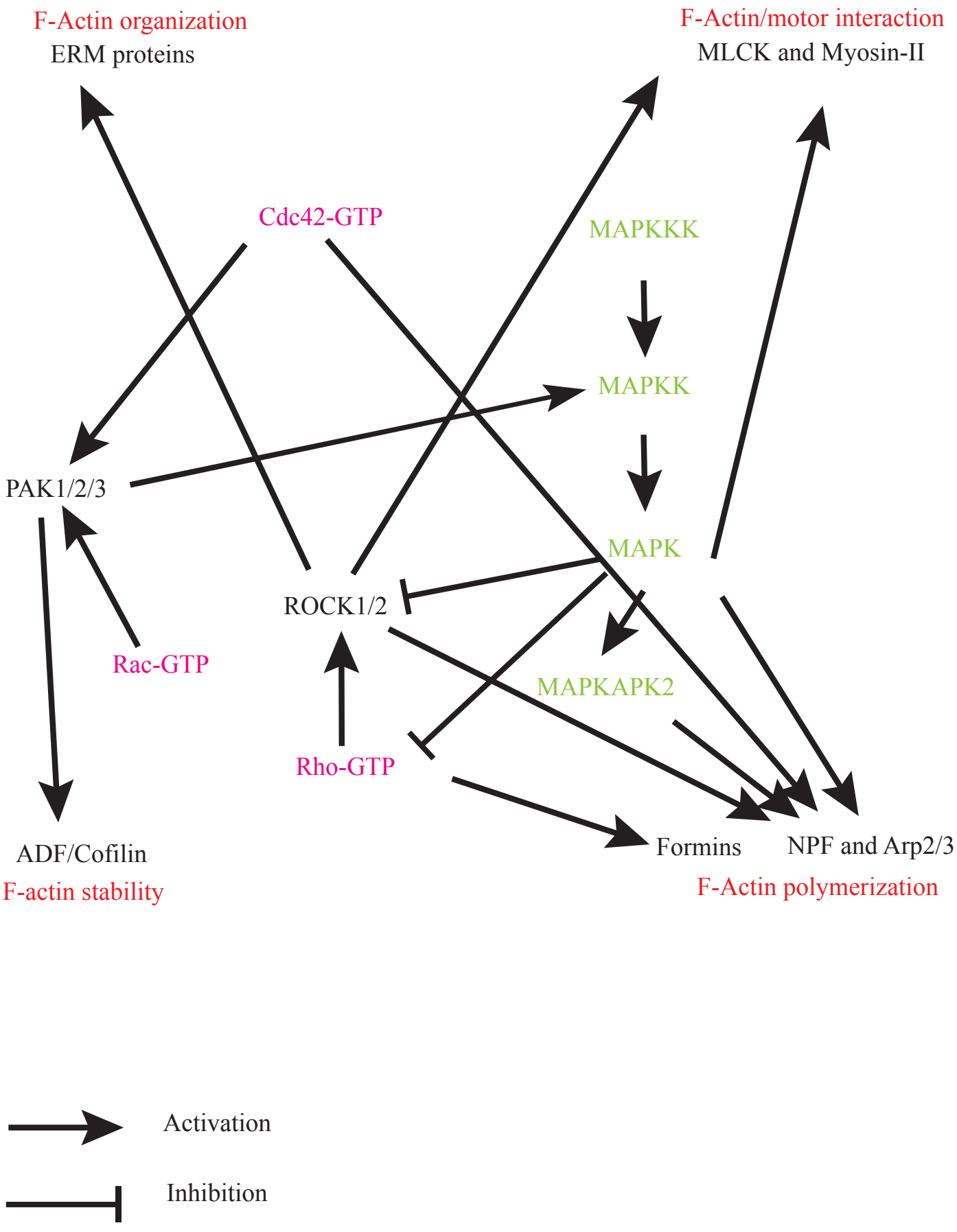


Figure 10: Transduction pathways associated with actin dynamics

(Nakanishi et al., 2006; Mendoza et al., 2011). In neutrophils, the MAPKAPK2 (MAPK-Activated Protein Kinase 2), a downstream effector of the MAPKKK has been shown to directly mediate Arp2/3 phosphorylation (Millard et al., 2003). Furthermore, ERK1/2 can phosphorylate MLCK and thus activate Myosin-II *in vitro* (Suizu et al., 2000).

In addition, the MAPK pathway and the Rho pathway are interconnected, bringing another level of complexity (Figure 10); it has been shown in various contexts that MEK can be activated by PAK (Pullikuth and Catling, 2007). Furthermore, MAPK can also modulate Rho signaling, for example focal adhesion remodeling during cell migration requires ERK activation of FAK (Focal Adhesion Kinase), which itself has been shown to inhibit Rho and ROCK (Pullikuth and Catling, 2007).

2) The roles of actin in mitotic cell division

a) Overview of mitotic cell division

α. The basic steps of mitotic cell division

Cell division produces two daughter cells from a mother cell. During S phase, the DNA is replicated. Then for somatic cells mitosis follows, producing two daughter cells with the same amount of DNA as the mother cell. The challenge of cell division is to separate correctly the chromosomes and the cytoplasm between the two daughter cells, errors during cell division leading to aneuploidy and potential tumorigenic processes.

Mitosis is divided into four steps: prophase, metaphase, anaphase, telophase (Figure 11). During prophase, the replicated DNA is condensed into chromosomes composed of two sister chromatids, which progressively align on the metaphase plate during prometaphase. When the chromosomes are fully aligned and under equal tension on the microtubule spindle at metaphase, anaphase is triggered. The spindle is essential to align the chromosomes. It is composed of microtubules, very labile Tubulin α and Tubulin β polymers that can quickly polymerize and depolymerize. Microtubules are nucleated from MTOCs (MicroTubule Organizing Centers), which are usually centrosomes composed of two centrioles and pericentriolar material (PCM) comprising proteins such as γ-Tubulin and pericentrin. At mitosis onset, centrosomes duplicated during S phase separate and rapidly promote spindle bipolarization as they constitute the spindle poles. From these nucleating structures, microtubules organize as astral microtubules connecting the spindle to the cell cortex,

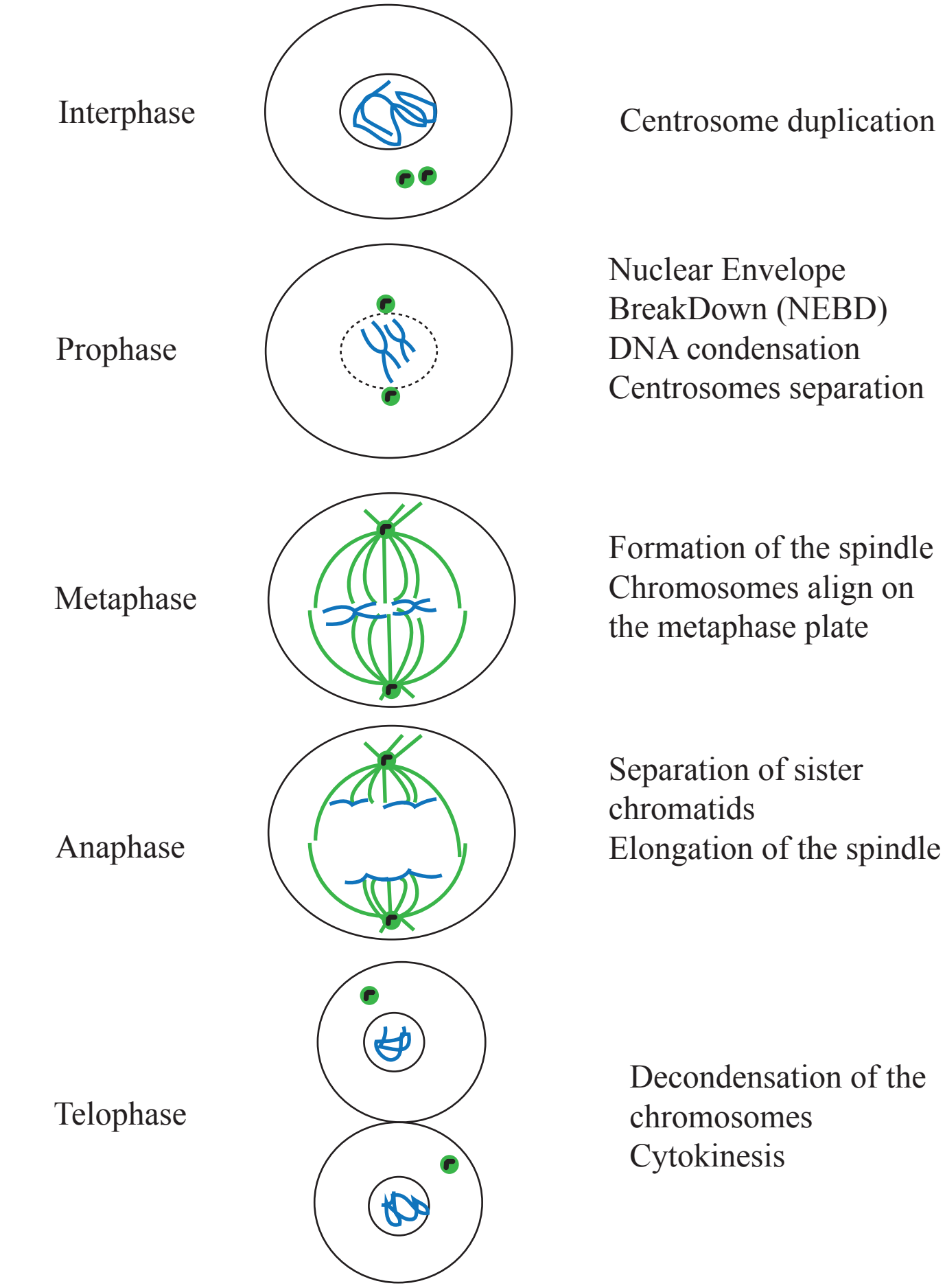


Figure 11: The steps of mitosis

kinetochore microtubules connecting the kinetochores of the chromosomes to the spindle poles (referred also as K-fibers when stabilized), and polar microtubules that can slide with respect to each other via microtubule specialized motors and mediate spindle elongation at anaphase (Figure 12). Finally, cytokinesis is the separation of the two daughter cytoplasms after telophase. Cytokinesis always occurs in the middle of the microtubule spindle. Thus the division plane is specified by the position of the metaphase plate of the spindle.

β. Asymmetric divisions

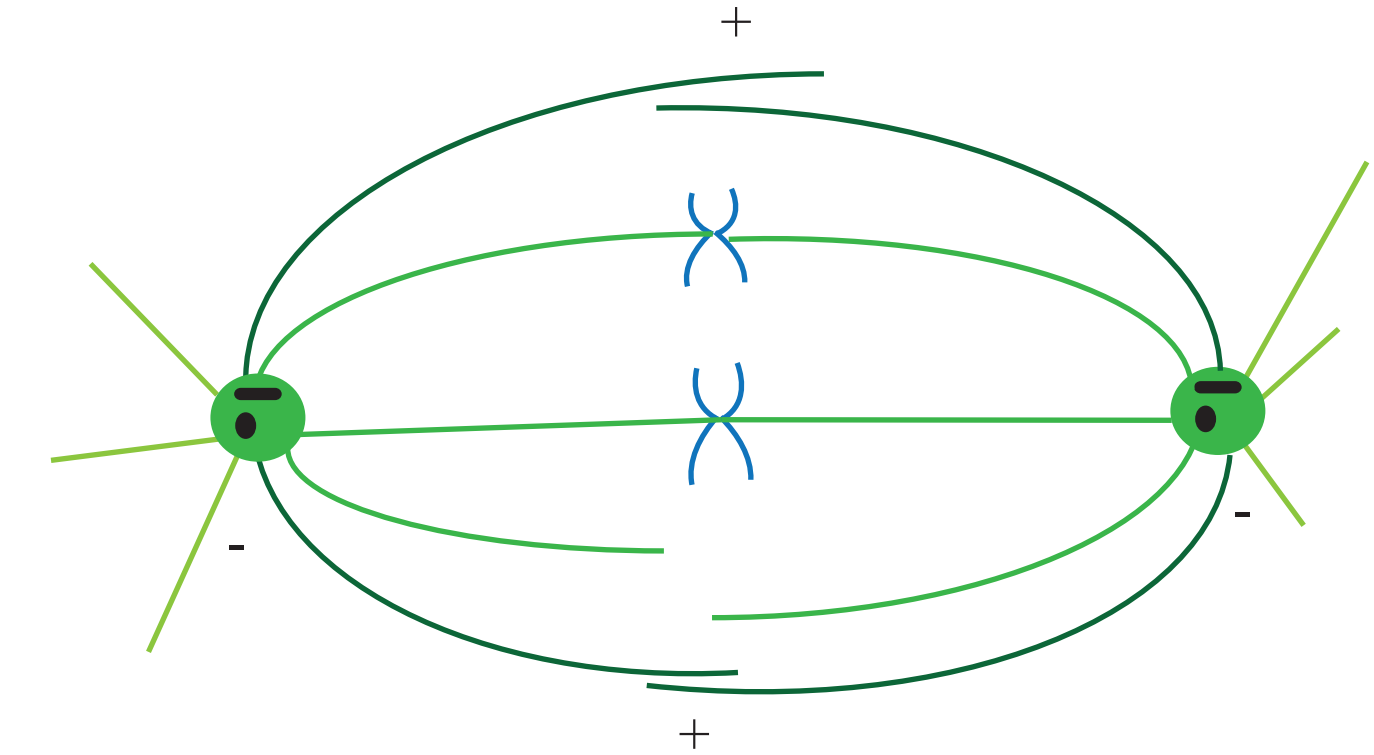
Asymmetric divisions produce two different daughter cells, allowing these two cells to have different fates. This is very important for example during development to promote cell diversity as stem cells self-renew and at the same time produce differentiated cells. It can also allow the partitioning of the genome with minimum cytoplasm loss, for example in female meiosis where half of the DNA needs to be extruded from the future oocyte but most of the cytoplasm containing maternal stores has to be retained. In addition to their role in development and adult life, defects in asymmetric cell divisions are associated with a variety of pathologies (for reviews see (Powell et al., 2010; Lu and Johnston, 2013; Terret et al., 2013)). The asymmetry of the division can be in composition, in size or both (Figure 13). We will focus here only on the asymmetry in size of the division, which occurs during female meiosis.

The asymmetry in size of the division is a consequence of the off-center positioning of the spindle in the cell, since the division plane is specified by the position of the metaphase plate of the spindle. In mitosis, the spindle is positioned through interaction between astral microtubules emanating from spindle poles and the cell cortex. The microtubule minus-end directed motor Dynein located at the cell cortex produces a pulling force on the spindle (Colombo et al., 2003) via astral microtubules (for review see (McNally, 2013; Moore and Cooper, 2010)). Although microtubules play a major part in cell division because they organize and position the spindle, growing evidence shows that actin is actively involved in cell division as well. We will focus here on the role of actin in mitosis and will discuss meiosis later.

b) The roles of actin in mitotic cell division

α. Cortical actin filaments

In mammalian cells, cortical actin is involved in spindle orientation. Indeed, stereotypical divisions become random when cells are treated with F-actin depolymerization



DNA

Astral microtubules

Polar microtubules

Kinetochore microtubules forming K-fibers

Centrosome with two centrioles and Pericentriolar Material

Figure 12: Spindle organization during mitosis

drugs (Théry et al., 2005; Toyoshima and Nishida, 2007). This is also the case in Xenopus embryos where disruption of F-actin leads to spindle mispositioning in the outer epithelial cells (Woolner et al., 2008). Cortical F-actin probably mediates spindle positioning through interactions between the actin cortex and astral microtubules (Toyoshima and Nishida, 2007). Indeed Myosin-X, a Myosin able to interact with microtubules and actin (Weber et al., 2004), is also required for spindle orientation (Toyoshima and Nishida, 2007; Woolner et al., 2008). In addition, it was recently shown that in mammalian cells a subcortical pool of actin is rotating around the cell and helps the cell to read external constraints coming from its environment in order to position its spindle accordingly (Fink et al., 2011). Thus, it is very possible that cortical F-actin, whose localization at the cortex could follow the external constraints coming from cell adhesions for example, mediates spindle positioning through interactions between Myosin-X and astral microtubules (for review see (Almonacid et al., 2014)).

In addition to its role on spindle orientation, cortical actin is essential for spindle morphogenesis by increasing cortical rigidity and thus contributing to cell rounding at mitosis onset in Drosophila cells (Carreno et al., 2008; Kunda et al., 2008). The increase of cortical rigidity is mediated by ERM-dependent actin localization in these cells (Carreno et al., 2008; Kunda et al., 2008). Cell rounding is crucial for proper spindle morphology since cells impaired of Moesin habor spindle defects (Kunda et al., 2008; Lancaster et al., 2013). Indeed, the spindle cannot form in a too confined environment: when the cell is flat, the microtubules are too small to reach and capture the chromosomes (Lancaster et al., 2013). In addition, without cell rounding, the spindle cannot position accurately. This could be because the cortex needs to be stiff in order for the microtubules to be properly anchored and thus properly pull on the spindle (Kunda et al., 2008). Thus, by mediating the cortex mechanical properties, cortical F-actin plays a crucial part in spindle morphogenesis and positioning (for review see (Kunda and Baum, 2009)).

β. Cytoplasmic actin filaments

Whereas the role of cortical F-actin has been investigated for a while, the role of cytoplasmic actin is still unclear, especially since it is hard to visualize cytoplasmic pools of actin (see part **B)***3)b*)α). In yeast, actin cables have been shown to control spindle morphogenesis and function (for review see (Sandquist et al., 2011)). Although their precise role is not yet known, actin cables have also been detected during mitosis, for example in Xenopus embryos (Woolner et al., 2008). In plants where there are no centrioles, F-actin

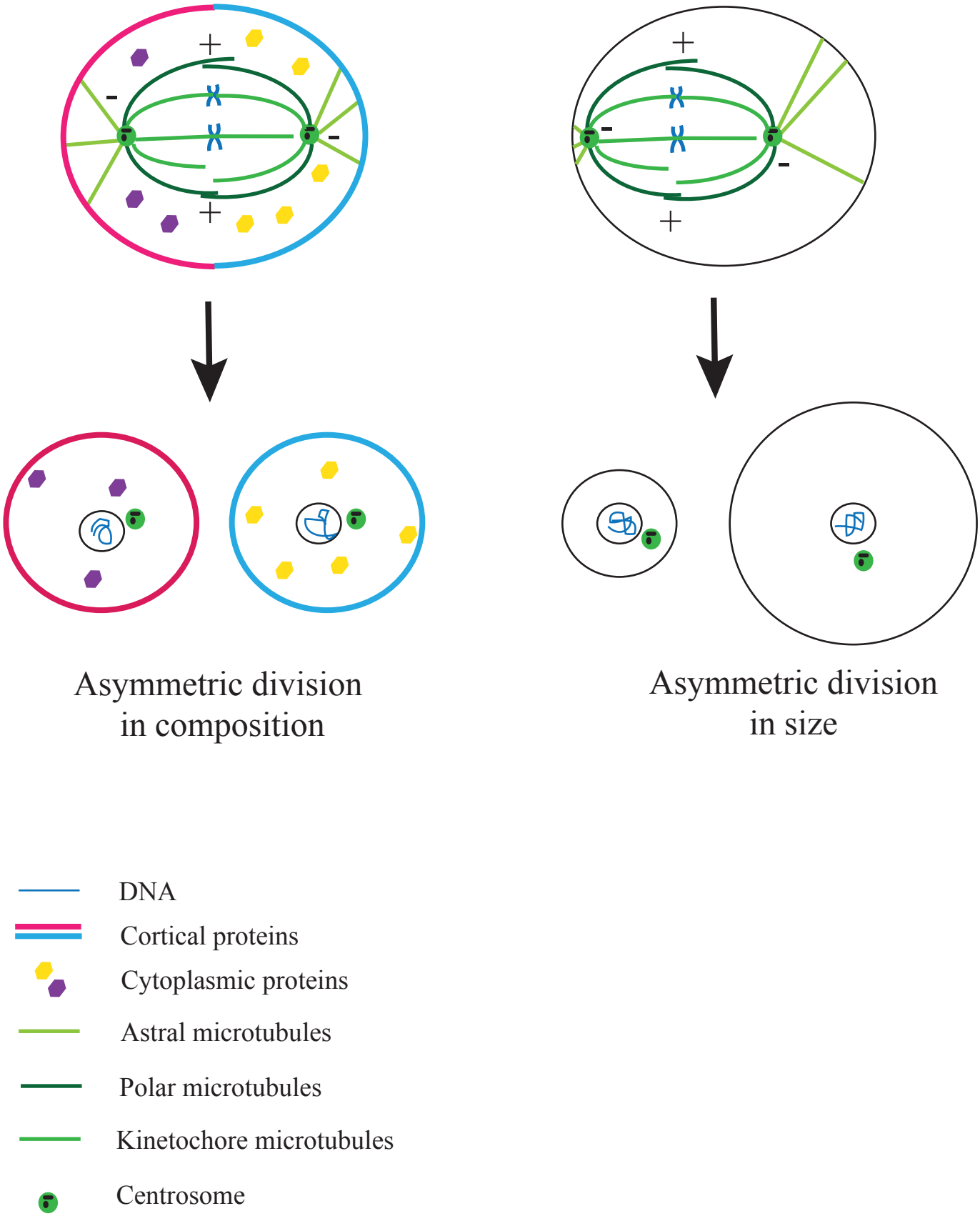


Figure 13: Simplified scheme of asymmetric divisions

cables running along the mitotic spindle have been reported (for review see (Sandquist et al., 2011)). Whether it is also the case in animal cells remains elusive, but it is possible since in many vertebrate embryos cytoplasmic actin seems to be up-regulated during M-phase (Field et al., 2011).

In Drosophila syncitial embryos, cytoplasmic actin seems to play a role in preventing the movement of the nuclei at the onset of mitosis, whereas nuclei are free to move in interphase (von Dassow and Schubiger, 1994). Similarly, in Drosophila oocytes, a F-actin meshwork is delaying a cytoplasmic streaming because when the F-actin meshwork is dismantled, the cytoplasmic streaming starts earlier (Dahlgaard et al., 2007). Thus, in that case, the F-actin acts as a "brake" to prevent cytoplasmic motion (Field and Lénárt, 2011).

χ. Actin flows

Actin flows correspond to streaming movements of the actin cytoskeleton. They have first been described in lamellipodia of migrating cells. It has been shown in mitotic cells by monitoring the motion of beads in the cytoplasm that a cortical streaming due to contractions mediated by Myosin-II is responsible for spindle formation and in particular centrosome separation (Rosenblatt et al., 2004). Actin flows have also been implicated in the maintenance of the Metaphase II spindle at the cortex in mouse oocytes, that I will discuss later (Yi et al., 2011). A recent report also shows that in Xenopus oocyte extracts, actin flows develop spontaneously, under the dependence of F-actin nucleators (Pinot et al., 2012).

B) Meiotic maturation in mouse oocyte

Meiosis is the cell division leading to the formation of gametes, oocytes and spermatozoids. Generally speaking, it consists of two successive divisions without an intermediate DNA replication phase: the daughter cells thus contain half of the mother cell DNA such as upon fertilization the two haploid gametes form a diploid zygote. We will focus here on female meiosis only and on the formation of the female gamete, the oocyte.

1) Meiosis and the female gamete formation

a) Overview on meiosis

Meiosis is a series of two divisions (Figure 14). The first division is called Meiosis I and the second Meiosis II. Every step of the division is referred to as I or II, depending on

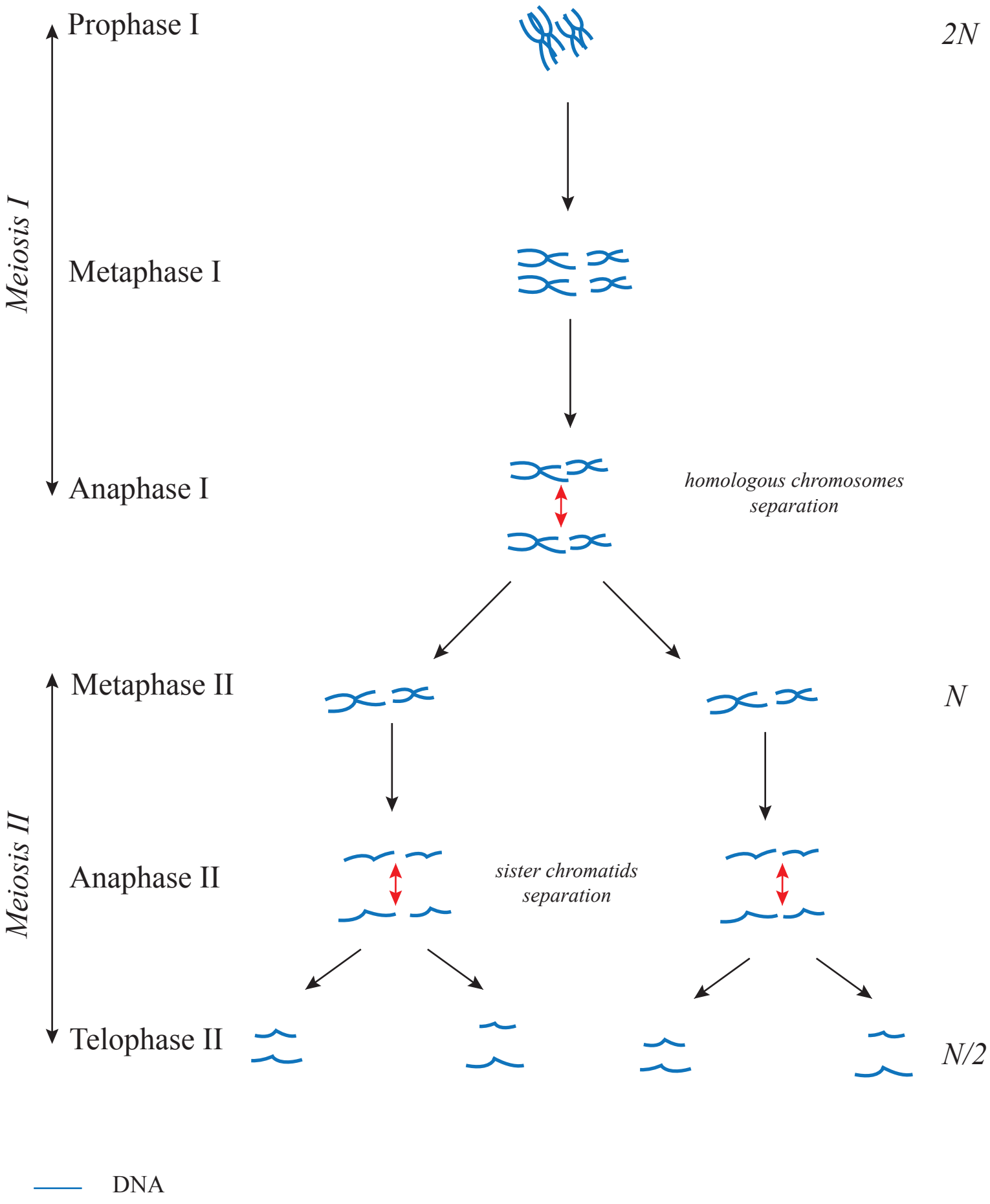


Figure 14: Overview on Meiosis

whether it belongs to the first or second meiotic division. Meiosis I is a very atypical division, first because the homologous chromosomes are able to exchange parts of their DNA during Prophase I via the crossing overs, bringing genetic diversity, and second because at anaphase I homologous chromosomes segregate instead of sister chromatids. Meiosis II however resembles mitosis with separation of sister chromatids.

b) A series of cellular arrests

In the female vertebrate, the stock of incompetent oocytes is present at birth since oocytes enter meiosis during embryonic development and stay quiescent, arrested in Prophase I (Prophase of first meiotic division) until puberty. Then, upon periodic hormonal stimulation, a few oocytes depending on the species will enter a differentiation phase called growth phase. A peak of the sexual hormone LH (Luteinizing Hormone) will trigger meiosis resumption and the entry into the divisions per se, a phase known as meiotic maturation (Figure 15). The divisions will however stay incomplete because the oocyte experiences a second block in Metaphase II (Figure 15). This block will be overcome by fertilization that will trigger Meiosis II exit. If the block in Prophase I is universal, the second block depends on the species: in Metaphase II for vertebrates, in Metaphase I for most other species for example.

Meiosis is temporally regulated by the MPF (M-phase Promoting Factor) which is a complex promoting the entry to M phase of all Eukaryotic cells. It is composed of two subunits, CyclinB and CDK1 (Cyclin Dependent Kinase 1). CyclinB is the regulatory subunit; its synthesis and degradation are tightly controlled in all dividing cells. In oocytes arrested in Prophase I, MPF activity, sustained by the catalytic unit CDK1, is maintained low because cAMP (Cyclic Adenosine 3',5'-MonoPhosphate) level is high. Indeed, cAMP indirectly regulates CDK1 activity by promoting its inhibitory phosphorylation (for review see (Holt et al., 2013)). cAMP is produced by the oocyte and surrounding follicular cells. Furthermore, CyclinB level is also maintained at a low level (Ledan et al., 2001) in Prophase I. When oocytes are removed from the ovaries, the level of cAMP drops allowing spontaneous exit from Prophase I and the initiation of meiotic maturation (Conti et al., 1998). This allows to artificially synchronize a pool of oocytes and have them complete Meiosis I at the same time. Alternatively, the addition of nucleotide derivatives in culture medium can mimic cAMP endogenous role and allow the maintenance of oocytes in Prophase I for several hours.

MPF activity increases slowly during Meiosis I (Verlhac et al., 1994) and diminishes abruptly when chromosomes are fully aligned on the metaphase plate, following CyclinB degradation and thus triggering Meiosis I exit (for review see (Holt et al., 2013)). Eventually,

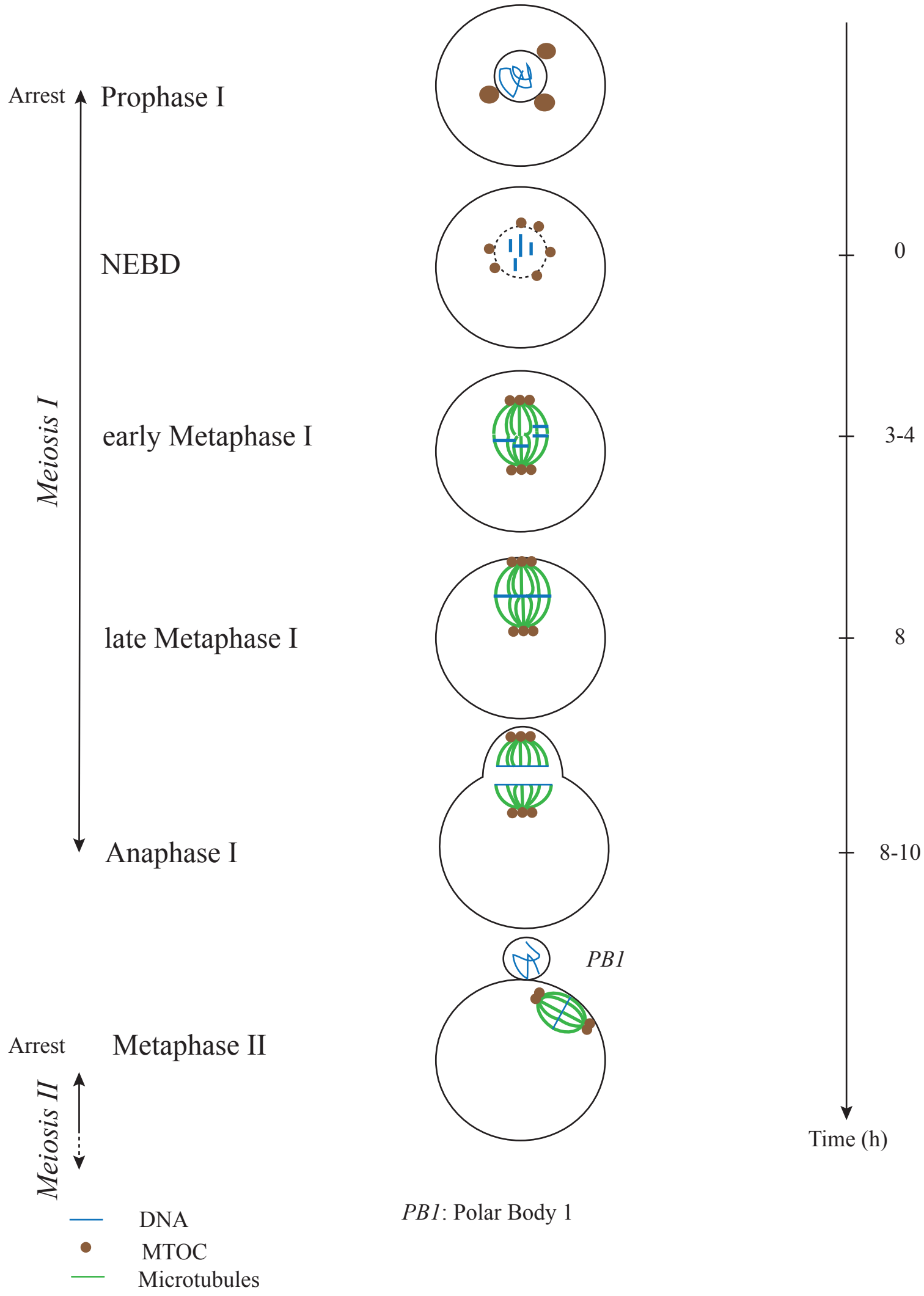


Figure 15: Mouse meiotic maturation

MPF activity is rapidly restored by CyclinB resynthesis, allowing entry into Meiosis II and Metaphase II arrest. Fertilization will trigger CyclinB degradation, the drop in MPF activity and Meiosis II exit.

2) Meiotic maturation in the mouse

a) Cellular particularities of oocytes

Oocytes are very peculiar cells. A first particularity of oocytes in general is that they are very big cells; for example, a fully-grown mouse oocyte has a diameter of 80 μm. A second particularity of most oocytes is that, as plant cells, they lack true centrosomes, centrioles being lost during the growth phase (Szollosi et al., 1972). Instead, their microtubules are nucleated by multiple MTOCs (MicroTubule Organizing Centers) devoid of centrioles. These MTOCs, that are cortical in small oocytes, become efficient microtubule nucleators and relocate to the nuclear envelope at the end of the growth phase (Luksza et al., 2013). The lack of true centrosomes in oocytes imposes alternative modes of spindle assembly and positioning that I will discuss in detail below.

b) Progression of mouse meiosis

In this part, the general progression of meiotic maturation in the mouse oocyte will be described (Figure 15). We will explain the symmetry breaking event and its consequences in more details in the last part.

α. Prophase I and recombination

Prophase I is divided into subphases called Leptotene, Zygotene, Pachytene and Diplotene. These stages correspond to the steps in DNA recombination (chromosome condensation, pairing, crossing-over, resolution). DNA recombination allows the exchange of DNA portions between homologous chromosomes, hence allowing the formation of new gene combinations that increase genetic diversity among the species. In mammals, Prophase I is a very long process that lasts for years because it starts in the embryo and finishes during adulthood where the oocytes stay blocked in Diplotene of Prophase I until meiosis resumes. Then, oocytes, surrounded by follicular cells, undergo a growth phase where they acquire the capacity to resume meiosis; it is notably characterized by an enormous volume increase. At that stage, the oocyte does not harbor any sign of polarization except a slightly off-centered nucleus that was actively centralized at the end the growth phase (Brunet and Maro, 2007;

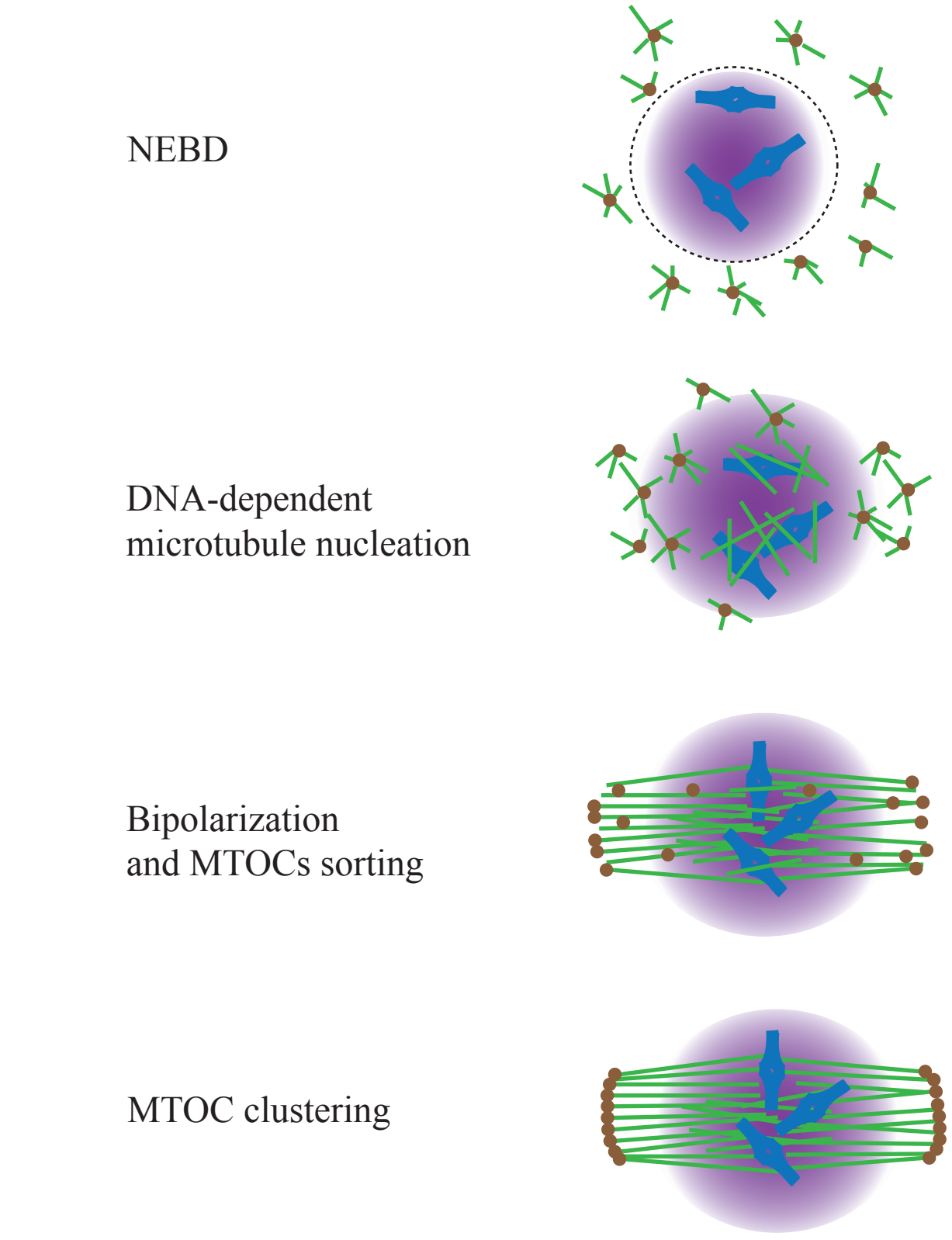


Figure 16: Spindle formation in mouse oocyte

Luksza et al., 2013) (see part **B)***3)a)*α).

β. Meiosis resumption

Meiosis resumption depends on a peak of the hormone LH that triggers a decrease in cAMP, which in turn increases the activity of CyclinB/CDK1 (see above) (for review see (Holt et al., 2013)). MPF activation then triggers chromatin condensation, Nuclear Envelope BreakDown (NEBD) and the formation of the first meiotic spindle.

χ. Spindle formation

In the mouse oocyte, the spindle forms where the nucleus was, which is close to the exact oocyte center but a little off-centered (see part **B)***3)a)*β). Contrary to mitosis, which is a short process (about 1h), meiosis is a long process (9h for mouse Meiosis I). In mitosis, centrosomes govern spindle formation and organization. Indeed, the spindle is formed by nucleation of microtubule from the two centrosomes that are separated in Prophase to form the spindles poles, hence it is immediately a bipolar structure; microtubules then elongate and make contacts with the chromosomes. The contacts are stabilized, forming K-fibers when microtubules reach the kinetochore. This dominant way of spindle formation in mitosis is known as the "search and capture" model (Mitchison et al., 1986). In addition to centrosomes acting as major microtubule nucleating centers, microtubules can also be nucleated specifically around the chromosomes in mitotic cells by the Ran-GTP (Ras-related Nuclear protein) pathway, also called the "local assembly" model (Kalab et al., 1999; Carazo-Salas and Karsenti, 2003). In oocytes, cells lacking true centrosomes, the Ran-GTP pathway is important and the spindle is built inside-out since microtubules are first nucleated around the chromosomes, the poles being formed in a second step (see below). Ran is a small GTPase that is active when bound to GTP and inactive when bound to GDP. Its guanine exchange factor RCC1 (Regulator of Chromosome Condensation 1) is localized on the chromosomes, thus Ran-GTP accumulates around the chromosomes, creating a gradient of Ran-GTP only around the chromosomes (Deng et al., 2007; Dumont et al., 2007b). Ran-GTP is able to locally activate SAFs (Spindle Assembly Factors) through their release from the inhibition of importins. These active SAFs, such as NuMA (Nuclear Mitotic Apparatus), TPX2 (Targeting Protein for the Xenopus kinesin xklp2) and HURP (Hepatoma Up-Regulated Protein) are then able to nucleate and organize microtubules around the chromosomes (Deng et al., 2007; Dumont et al., 2007b; Brunet et al., 2008; Breuer et al., 2010; Kolano et al., 2012) (Figure 16). Thus, microtubules are first nucleated only in the vicinity of the chromosomes, forming a

"microtubule ball" (Schuh and Ellenberg, 2007). Then, HURP allows the formation of a stable central array required for the proper sorting of MTOCs (Breuer et al., 2010) that were dispersed around the chromosomes at NEBD (Luksza et al., 2013; Schuh and Ellenberg, 2007); this is essential for spindle bipolarization, which takes two to three hours in the mouse (Figure 16). Spindle poles are formed later following the clustering of the MTOCs, under the control of NuMA (Kolano et al., 2012). Finally, K-fibers are formed late, detectable only around 5 hours after NEBD (Brunet et al., 1999; Kitajima et al., 2011; Lane et al., 2012). Accordingly, microtubules mainly form lateral attachment with chromosome arms until K-fiber formation (Brunet et al., 1999; Kitajima et al., 2011).

δ. Spindle migration

In most oocytes, meiotic divisions are very asymmetric in size, producing a very big cell, the oocyte, and two very small cells, the polar bodies (Figure 15). In the mouse, the asymmetry in size of the first meiotic division is due to the migration of the spindle from an almost central position to the cortex (Longo and Chen, 1985). This is again a long process that takes about 4 hours. Since oocytes are not polarized, there is no predetermined site of spindle migration, the spindle axis forming randomly (Verlhac et al., 2000). The only constraint is that the spindle always migrates along its long axis towards the closest cortex (Verlhac et al., 2000). In mitosis, the positioning of the spindle depends on interactions between astral microtubules and the cortex. In oocytes, there are no astral microtubules since they lack true centrosomes (Szollosi et al., 1972). Accordingly, it has been known for a long time that the migration of the spindle depends only on actin but not on microtubules (Longo and Chen, 1985) . We will describe the mechanism of actin-based spindle migration below in details (see part **B)***3)b)*β).

As the spindle moves closer to the cortex, a differentiated area, known as "actin cap" is formed under the control of the Ran-GTP gradient (Deng et al., 2007), polarizing the oocyte; we will come back to its formation below (see part **B)***3)d)*) .

ε. Homologous chromosome segregation and polar body extrusion

Toward the end of spindle migration, the spindle is perpendicular with respect to the cortex, with the chromosomes aligned on the metaphase plate (Figure 15). Anaphase occurs, separating the two sets of homologous chromosomes. Concomitantly, cytokinesis takes place allowing the extrusion the first polar body (PB1) that will eventually degenerate. PB1 extrusion depends on Cdc42 and the actin cap (Wang et al., 2013).

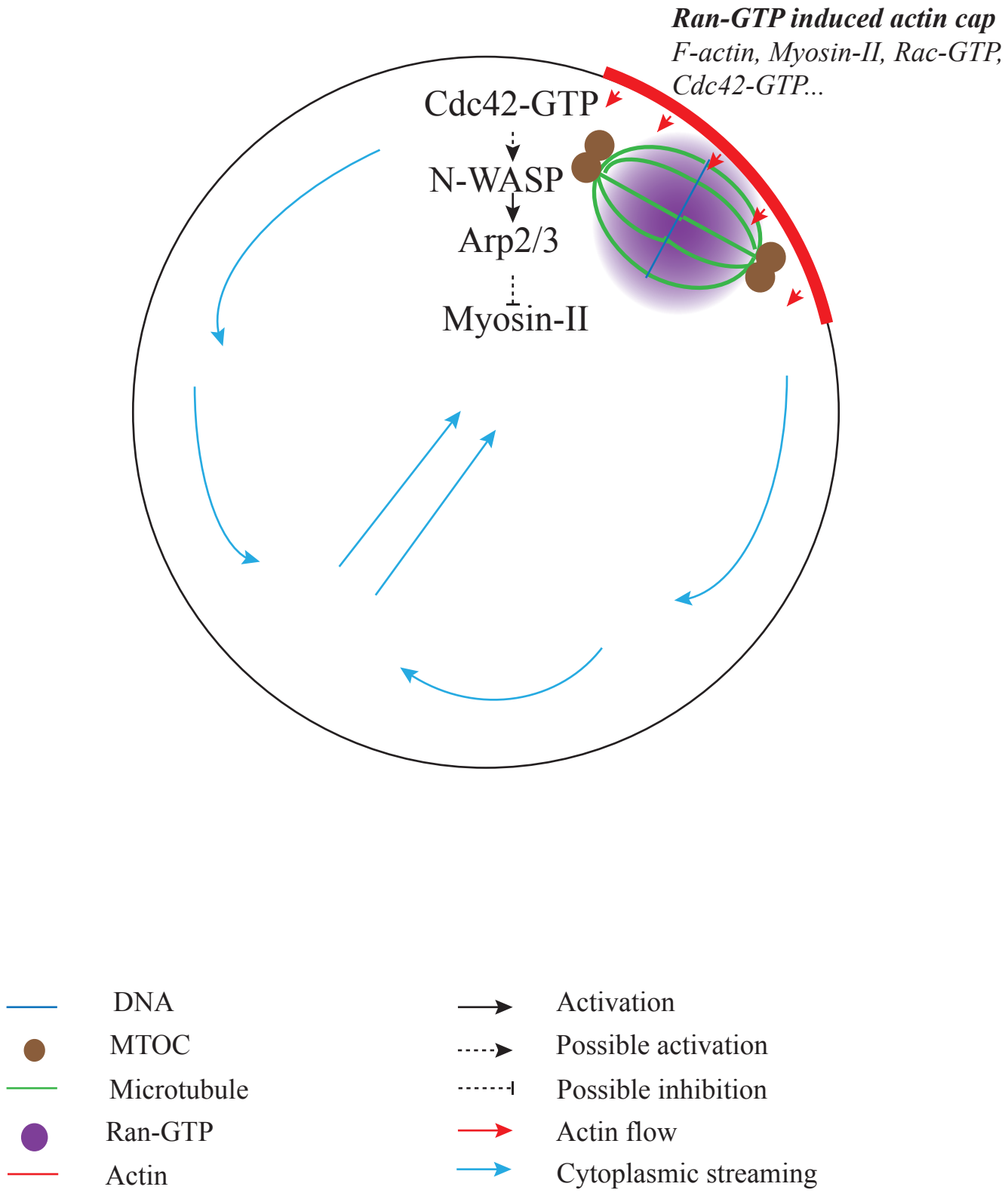


Figure 17: Actin flow and Metaphase II spindle

In mitotic cells, the Spindle Assembly Checkpoint (SAC) monitors chromosome attachment and blocks the cell in metaphase until all the chromosomes are properly aligned and under tension in the metaphase plate. The SAC inhibits the anaphase-promoting complex/cyclosome (APC/C), a multi-subunit E3 ubiquitin ligase that adds ubiquitin residues on a target protein triggering it to degradation by the 26S proteasome. Targets proteins for APC/C are CyclinB and Securin, a bound inhibitor to Separase. When chromosomes are not properly aligned on the metaphase plate, the SAC is active and inhibits APC/C. Securin and CyclinB are not degraded, inhibiting anaphase by sequestering Separase and thus leaving the cohesins maintaining sister chromatids together on the chromosomes, and inhibiting mitosis exit by keeping MPF activity high. Once all chromosomes are aligned and under tension on the metaphase plate, the SAC is turned off, APC/C is active and sends Securin and CyclinB for degradation. As a result, Separase is active and cleaves the cohesins leading to anaphase and CyclinB is degraded inducing to a drop in MPF activity and mitosis exit. The kinetochores are fundamental for SAC activity because they act as platforms to recruit the SAC signaling proteins (for review see (Musacchio and Salmon, 2007)). In meiosis, the SAC exists (Terret et al., 2003a; Wassmann et al., 2003; Homer et al., 2005; Niault et al., 2007; McGuinness et al., 2009) but is not very robust which probably explains why meiosis is highly error-prone (for review see (Jones and Lane, 2012)). For example, the SAC in meiosis does not always detect defects in chromosomes alignment on the metaphase plate, nor tension defects between the kinetochores (Gui and Homer, 2012; Kolano et al., 2012; Lane et al., 2012; Sebestova et al., 2012)

ϕ. Spindle reformation and anchoring

After the first polar body extrusion, the Meiosis II spindle reforms directly parallel and under the cortex and the oocyte arrests in Metaphase II until fertilization. The mechanism of spindle anchoring has been shown to depend on an F-actin flow reminiscent of the retrograde flow present at the leading edge of migrating cells (Figure 17) (Yi et al., 2011). This F-actin flow is required for spindle anchorage and depends on Arp2/3 since chemical inhibition of Arp2/3 arrests the flow and impairs spindle subcortical localization (Yi et al., 2011). Myosin-II acts in opposition to this cortical flow by contracting the cortex (Yi et al., 2011). It is possible that the actin cortical flow induces a cytoplasmic streaming responsible for pushing the spindle against the cortex (Yi et al., 2011). The Ran-GTP gradient is responsible for the Arp2/3 dependent streaming probably by local activation of the NPF N-WASP (Yi et al., 2011). Interestingly, Rac-GTP and Cdc42-GTP which colocalize with the actin cap in Meiosis

I (see part **B)***3)d)*) are also responsible for Meiosis II spindle anchoring (Dehapiot et al., 2013; Halet and Carroll, 2007). Furthermore, since WASP is also controlled by Cdc42-GTP respectively in some cells (see part **A)***1)c)*β) it is tempting to assume that in the oocyte Cdc42-GTP is acting upstream of N-WASP to promote this F-actin flow (Figure 17).

Vertebrate oocytes arrest in Metaphase II until fertilization, a process known as the CSF (CytoStatic Factor) arrest. During the CSF arrest, oocytes are blocked in metaphase because MPF activity is maintained high following APC/C inhibition by Emi2, inhibiting CyclinB degradation (Shoji et al., 2006). In vertebrate eggs (Sagata et al., 1989) and mouse oocytes, the Mos/MAPK pathway is required for the CSF arrest since *mos-/-* oocytes do not arrest in Metaphase II but instead activate parthenogenetically leading to teratomas and female sterility (Colledge et al., 1994; Hashimoto et al., 1994; Verlhac et al., 1996). In Xenopus egg extracts, the Mos/MAPK pathway directly controls Emi2 activity (Wu and Kornbluth, 2008) but this has not been addressed in mouse oocytes. Another difference is that P90Rsk (Ribosomal S6 kinase), a substrate of the Mos/MAPK pathway, does not control the CSF arrest in mouse as it is the case in Xenopus egg extracts (Dumont et al., 2005). The Mos/MAPK pathway also controls proper spindle morphology during the CSF arrest notably via MAPK substrates MISS (MAPK Interacting and Spindle Stabilizing) (Lefebvre et al., 2002) and DOC1R (Deleted in Oral Cancer 1 Related) (Terret et al., 2003b).

γ. Later events

After fertilization, the spindle will rotate and become perpendicular to the cortex, allowing the extrusion of the second polar body (PB2). The rotation process depends on F-actin (Zhu, 2002) and the GTPase RhoA (Zhong et al., 2005). The extrusion of the second polar body depends on Cdc42, RhoA and its upstream activator Ect2 (Epithelial Cell Transforming 2) and F-actin (Halet and Carroll, 2007; Elbaz et al., 2009; Dehapiot et al., 2013). Cytokinesis is also dependent on ROCK and Cofilin (Duan et al., 2014). The two pronuclei will then immediately form thus coupling the end of Meiosis II with the first mitotic division. After fertilization, CSF and MPF activity are immediatly lost (for review see (Kubiak et al., 2008)) whereas MAPK activity remains high until the pronucleus stage (Kalab et al., 1996; Verlhac et al., 1996) (Figure 20A).

3) Breaking the symmetry in the oocyte

In this part, I will focus on the breaking of symmetry, which leads to spindle

migration. I will show that the oocyte does not present obvious signs of polarity prior to spindle migration and how spindle migration itself polarizes the oocyte cortex, by inducing the formation of an actin cap.

a) Absence of polarity factors in Prophase I

α. None of the usual suspects

Mouse Meiosis I is a very asymmetric division in size, which produces two cells of very different sizes following spindle migration to the cortex. As mentioned before, asymmetric divisions in size are often mediated by an off-center positioning of the spindle induced by cortical cues, such as the polarity proteins Par-3, Par-6 (Partitioning defective 3 and 6) or aPKC (atypical Protein Kinase C) (for review see (Nance and Zallen, 2011)). However, in mouse oocytes, these proteins become asymmetrically located only after spindle migration (Vinot et al., 2004). As far as other organites or cytoskeleton determinants go, the oocyte does not seem to be polarized either before spindle migration: cortical granules (vesicles underneath the plasma membrane that will be exocytosed after fertilization) are evenly distributed, endoplasmic reticulum is homogeneous around the nucleus (FitzHarris et al., 2007), Rac-GTP is homogeneous at the plasma membrane (Halet and Carroll, 2007) and mitochondria are spread throughout the whole cytoplasm (Dalton and Carroll, 2013).

β. A slightly off-centered nucleus

In Prophase I, the nucleus is not at the perfect cell center but always slightly off-centered (Brunet and Maro, 2007). So far, this is the only sign of asymmetry before spindle migration that has been described. The initial position of the nucleus seems to be essential for efficient meiotic maturation because incompetent oocytes or oocytes from aged mice which harbor a decrease in meiosis efficiency have eccentric nuclei (Brunet and Maro, 2007).

b) Spindle migration

The symmetry-breaking event initiates spindle migration. As the cell is completely isolated after NEBD, it has to come from within the cell. As mentioned before, it does not depend on microtubules but on microfilaments (Longo and Chen, 1985). Indeed, when microtubules are chemically depolymerized, chromosomes are still able to migrate to the cortex (Verlhac et al., 2000).

α. Visualization of actin in cells

A very challenging point for studying the role of F-actin in cell division is first to be

able to visualize it and second not to modify its dynamics. In mouse oocyte, injecting directly G-actin tagged with fluorescent markers is not a potent tool because it leads to a very high background with no visible filaments (Azoury et al., 2008). In fixed cells, fluorescent derivatives of Phalloidin, a protein extracted from the toxic mushroom *Amanita phalloides* which binds tightly to F-actin and prevents depolymerization, thus often leading to cell death, is widely used, in particular in mouse oocytes (Pfender et al., 2011; Schuh, 2011; Holubcová et al., 2013). In live cells however the tools that are used to visualize F-actin rely on already studied protein-protein interaction, meaning that they were developed from protein domains interacting with F-actin. The main restriction with these probes is that they can compete with the endogenous proteins that they are derived from. In mouse oocytes, two probes have been extensively used.

UtrCH

This probe relies on the Calponin Homology (CH) domain of Utrophin, which is a non-muscle homolog of Dystrophin, a protein that binds F-actin to a protein of the plasma membrane in muscular cells. In Xenopus oocytes and echinoderm embryos, it binds to F-actin yet does not stabilize it (Burkel et al., 2007) and it has been widely used in mouse oocytes (Azoury et al., 2008; Schuh and Ellenberg, 2008; Azoury et al., 2011; Pfender et al., 2011; Schuh, 2011; Holubcová et al., 2013) and in Starfish oocytes (Mori et al., 2011).

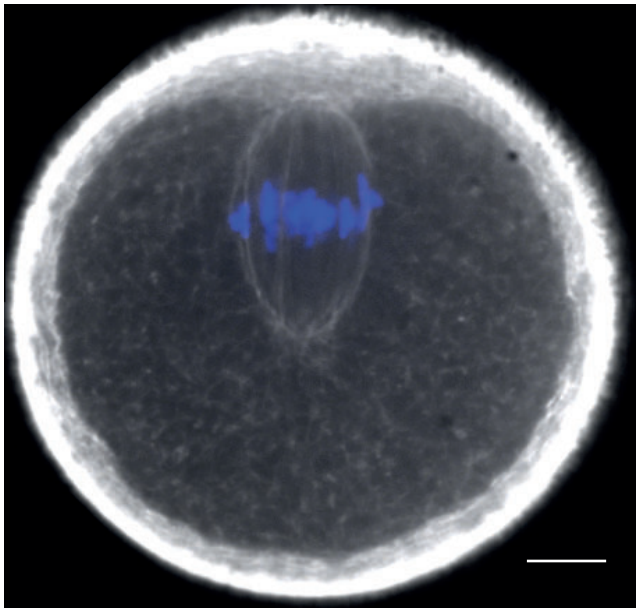
Lifeact

This probe (Riedl et al., 2008) has been derived from the ABP-140-GFP (Actin Binding Protein 140 described in yeast (Yang and Pon, 2002). ABP-140-GFP was described as having no striking effect on actin cable dynamics, but harboring a faint and easily photobleached fluorescence. Lifeact contains only a small part of ABP-140 amino acid sequence. It binds to G-actin preferentially compared to F-actin, thus it does not impair F-actin dynamics because of its overall low affinity (Riedl et al., 2008).

Controversies

Many controversies have arisen from the use of these different tools. The main issue is that not all of these probes can be used in every cellular context (for review, see (Field and Lénárt, 2011)). For example, Lifeact cannot detect some stress-induced actin structures (Munsie et al., 2009). In mouse oocyte there have been a lot of controversies because UtrCH was detecting a very dense F-actin network consisting of an actin cage surrounding the microtubule cage and a dynamic meshwork (Azoury et al., 2008; Schuh and Ellenberg, 2008),

A: Confocal spinning-disk image of F-actin organization in late Meiosis I (Chaigne et al., 2014, cover picture)



White: Gfp-UtrCH
Blue: DNA
Scale bar: 10 μm

B: Schematic of F-actin organization in mouse oocyte in late Metaphase I



Figure 18: F-actin meshwork in late Metaphase I in the mouse oocyte

whereas Lifeact was only detecting an actin cloud around the spindle (Li et al., 2008). However, UtrCH showed the same labeling as Phalloidin (Schuh, 2011) which might indicate that Lifeact does not recognize cytoplasmic filaments as well as UtrCH in this model system, although it recognizes very well cortical actin at the end of Meiosis I (Yi et al., 2011). This is probably due to the fact that it binds preferentially to G-actin, possibly very abundant around the spindle during Meiosis I. In addition, in this system, UtrCH has also been described as stabilizing F-actin when highly overexpressed (Holubcová et al., 2013). Thus, it remains very important to use these probes with caution.

β. Role of F-actin

The first indication of the potential nucleator involved in the architecture of actin filaments in mouse oocytes came from the study of the *fmn2-/-* (Formin-2 knock-out) mice. These mice are sterile and present defects in spindle positioning (Leader et al., 2002; Dumont et al., 2007a). The development of new techniques of F-actin visualization, namely the UtrCH probe, allowed the observation of a very dense F-actin meshwork nucleated progressively throughout Meiosis I (Azoury et al., 2008; Schuh and Ellenberg, 2008). This network consists of a very dynamic F-actin meshwork and an actin cage surrounding the microtubule spindle (Figure 18). As mentioned before, another team observed only a cloud around the microtubule spindle using Lifeact (Li et al., 2008) but concluded in a later study that this was probably due to an imaging artifact (Yi et al., 2011). This F-actin network, nucleated by Formin-2 since it is absent from *fmn2-/-* oocytes, is required for spindle migration (Leader et al., 2002; Dumont et al., 2007b; Azoury et al., 2008; Schuh and Ellenberg, 2008). Recently, it was further demonstrated that this network is actually nucleated by cooperation between Formin-2 and Spire1/2 (Pfender et al., 2011). As discussed before, Formin-2 can interact with Spire1/2 through its C-terminal FSI domain. Formin-2 and Spire1/2 are present at the surface of Rab11 positive vesicles (Schuh, 2011). Rab11 is a member of the Rab GTPases that are molecules involved in intracellular transport. These vesicles organize the cytoplasmic F-actin meshwork and seem to move in an outward fashion via the action of Myosin-V also present at their surface (Holubcová et al., 2013; Schuh, 2011); freezing of this meshwork by overexpression of UtrCH or vesicles depletion leads to impaired spindle motion therefore it was proposed that the vesicular system organizes the actin based long-range transport of the spindle (Holubcová et al., 2013).

Interestingly, an F-actin meshwork very similar to the one present throughout Meiosis I is already present in Prophase I but needs to be dismantled concomitantly to Formin-2

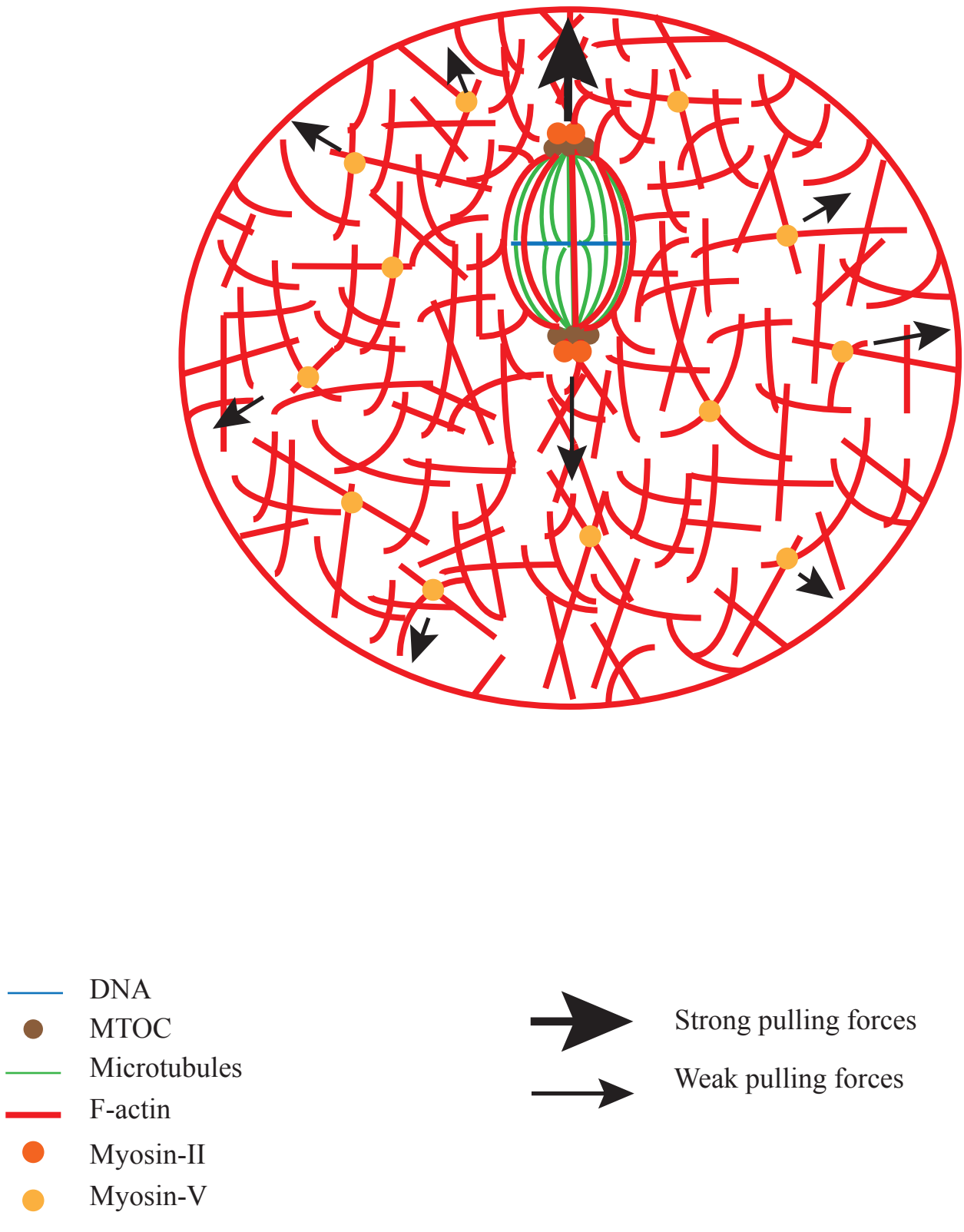


Figure 19: Force generator in mouse Meiosis I spindle migration

degradation before NEBD for proper spindle migration (Azoury et al., 2011). This is probably to allow the formation of a spindle in a constraint-free environment.

In addition to Formin-2 and Spire1/2, Arp2/3 (Sun et al., 2011a) and many of its NPFs such as Wave2 (Liu et al., 2012; Sun et al., 2011c), WHAMM (Huang et al., 2013) and JMY (Sun et al., 2011b; Liu et al., 2012) have been implicated in spindle migration, although the F-actin structure involved and its role in spindle migration had not been elucidated. The Rho-GTPase Cdc42 has also been shown to somehow control spindle migration (Na and Zernicka-Goetz, 2006) but this is probably an artifact of dominant negative mutant injection since the conditional knock-out of Cdc42 in oocytes does not impair spindle migration at all (Wang et al., 2013).

It is interesting to notice that F-actin driven chromosome movement is not restricted to mouse oocytes. In many oocytes, such as rat oocyte (Ai et al., 2008) or horse oocyte (Tremoleda et al., 2001), F-actin is present during Meiosis I spindle motion to the cortex. In starfish oocyte, the chromosomes also move to the cortex in an actin dependent fashion. In that case, the chromosomes are scattered in the nucleus in Prophase I, and they are translocated to the closest cortex (Lénárt et al., 2005). Even if starfish oocytes possess centrosomes and astral microtubules, chromosomes are out of reach for them, thus their translocation is actin dependent. However, contrary to mouse oocyte, in that case the network is contracting and pulling the chromosomes that are big compared to the size of the mesh like a “fishnet” (Lénárt et al., 2005; Mori et al., 2011). As discussed before, most oocytes lack true centrosomes. Thus, F-actin mediated transport is probably a conserved alternate pathway for chromosome positioning in cells lacking true centrosomes or with chromosomes out of reach of microtubules as in starfish.

χ. Force generation

There has been some debate over the force initiating spindle movement. It probably involves Myosin-II (Figure 19) since it is present at spindle poles and its inhibition impairs spindle migration (Simerly et al., 1998; Schuh and Ellenberg, 2008). Spindle migration is on average very slow (0,15 μm/min) (Schuh and Ellenberg, 2008) but it might consist of two phases, a first slow phase probably Myosin-II dependent and a second faster phase involving actin streaming mediated by Arp2/3 (Yi et al., 2013). This second phase would start when the chromosomes and their Ran-GTP associated gradient reach and differentiate the cortex, accumulating Rac-GTP (see below) (Figure 17).

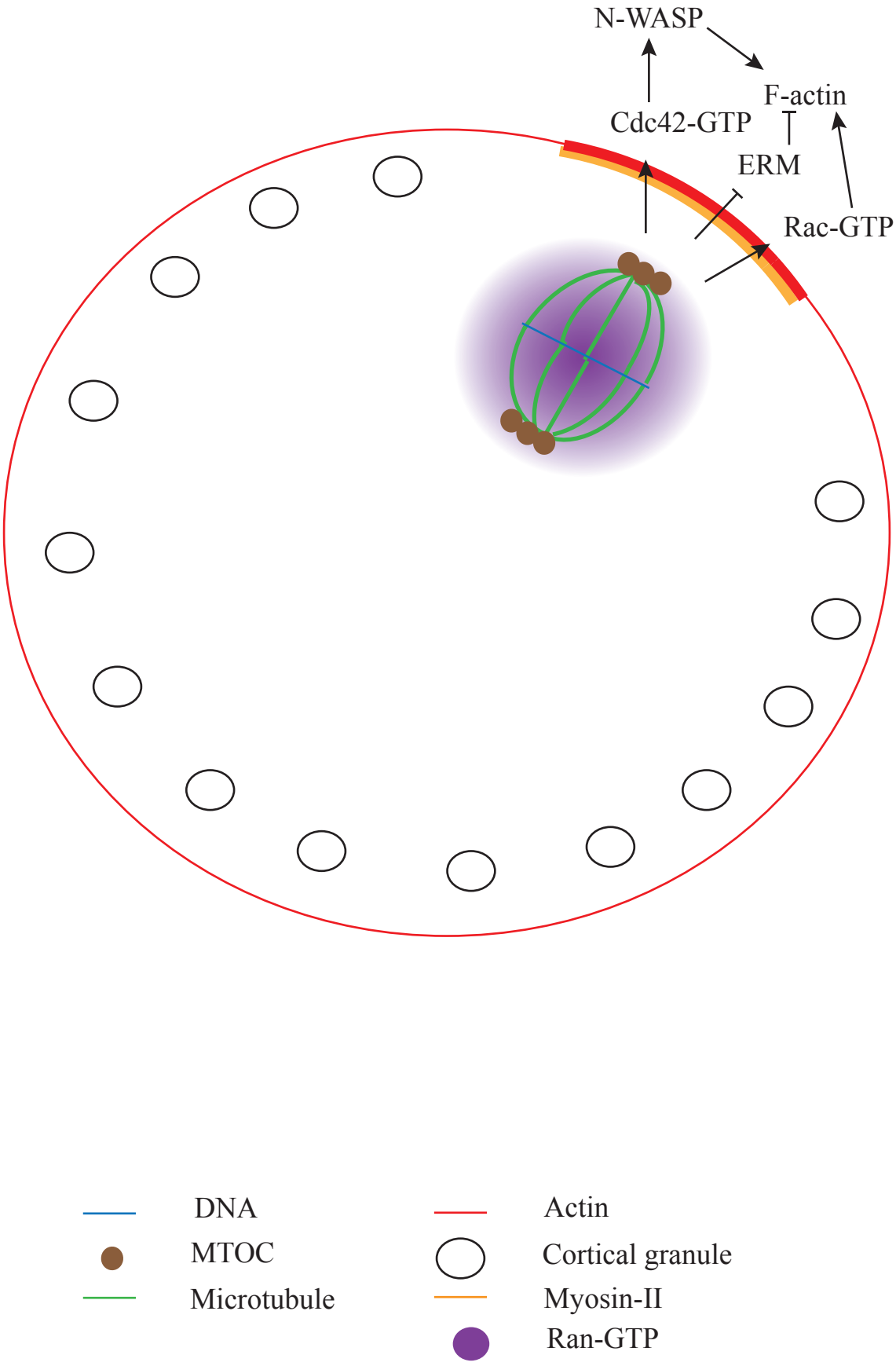


Figure 21: Actin cap formation in Meiosis I

Furthermore as discussed before, it was described recently that Spire1/2, Formin-2 and Myosin-V are colocalized at the surface of vesicles that are moving toward the cortex (Schuh, 2011). *In vitro*, Spire1/2 and Formin-2 cooperate to nucleate F-actin filaments by both sitting alternatively on the barbed end of filaments and mediating each other binding (Montaville et al., 2014). Similarly to the cooperation between APC-C and mDia1, it seems that Spire1/2 recruit Formin-2 at the Rab11 and Myosin-V positive vesicles (Montaville et al., 2014). When the movement of the vesicles is abolished, the spindle does not migrate; it was thus proposed that the outward movement of the vesicles could play a part in spindle migration by providing an additional driving force and a refined way of modulating actin meshwork architecture (Holubcová et al., 2013).

c) The role of Mos

Mos, the MAPKKK specifically expressed in the oocyte (Propst et al., 1987), in addition to its role on meiosis exit during the CSF arrest, has been involved in spindle migration.

Mos is synthesized progressively after NEBD and induces ERK1/2 activation around NEBD+3h (Verlhac et al., 1993, 1996) (Figure 20A). Mos artificial precocious expression can trigger meiotic resumption even in a non-permissive medium, which is a medium containing a high concentration of cAMP analogs (Verlhac, 2000). In *mos-/-* oocytes, polar bodies are abnormally big (Choi et al., 1996). This is because when Mos is absent, the spindle does not migrate, instead, one of the poles elongates at anaphase (Figure 20B) (Verlhac et al., 2000). Since the Mos/MAPK pathway controls F-actin polymerization and dynamics (see Part **A**.*1) c)* β), it is very possible that it plays a part in microfilament dynamics implicated in spindle migration. Furthermore, a study in the Cnidarian oocyte has shown that the role of Mos in spindle migration is conserved (Amiel et al., 2009). However, its precise role was not known.

d) Formation of the actin cap and polarization of the oocyte

After spindle migration, once the chromosomes are close to the cortex, a cortical differentiated area called “actin cap” is formed. This zone is devoid of microvilli compared to the rest of the oocyte cortex (Longo and Chen, 1985) and devoid of cortical granules (Ducibella, 1988). On the contrary, it is enriched in F-actin and Myosin-II (Simerly et al., 1998) and enriched in the polarity proteins Par6 and Par3 (Vinot et al., 2004; Duncan et al., 2005) (Figure 21). Actin cap formation depends on the Ran-GTP gradient surrounding the chromosomes (Deng et al., 2007; Dumont et al., 2007b). The Ran-GTP gradient in turn

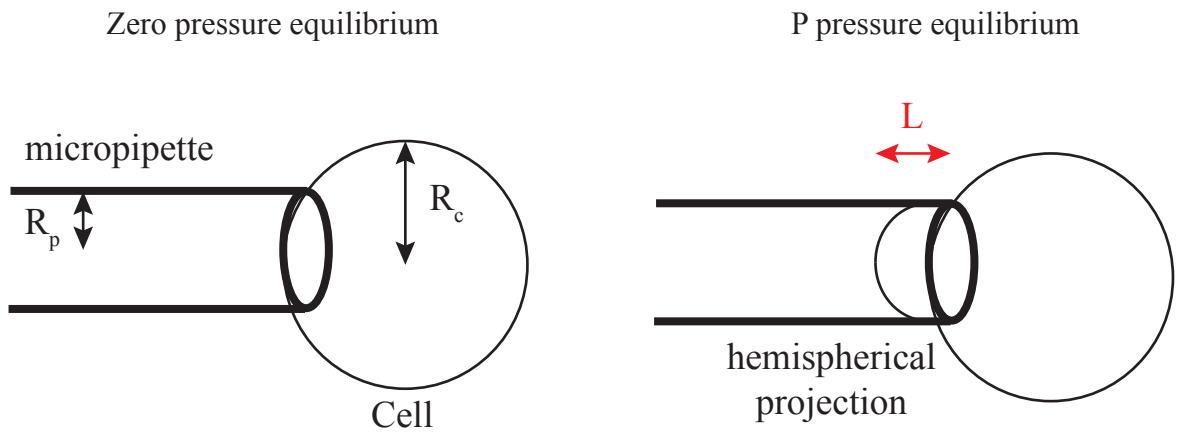
activates many downstream effectors leading to the formation of the actin cap. Ran-GTP induces F-actin accumulation by inducing a decrease in active ERM proteins above the chromosomes (Dehapiot and Halet, 2013). Ran-GTP is also responsible for the localization of Cdc42 which in turn controls the localization of the NPF N-WASP (Dehapiot et al., 2013). Rac-GTP also colocalizes with the actin cap thus probably promoting F-actin accumulation independently of ERM proteins (Halet and Carroll, 2007; Dehapiot and Halet, 2013) (Figure 21).

What could be the role of the actin cap? Since microvilli are required for sperm fusion, one possible role for this cap is preventing the fusion of the sperm too close to the Metaphase II spindle, thus preventing the mixing of the two sets of DNA before extrusion of the remaining half of the sister chromatids (Brunet and Verlhac, 2010). Activated oocytes with an impaired Ran-GTP gradient that do not harbor an actin cap cleave instead of extruding PB2, therefore the actin cap could also play a part in restricting the progression of the cleavage furrow and allowing the extrusion of a very small polar body.

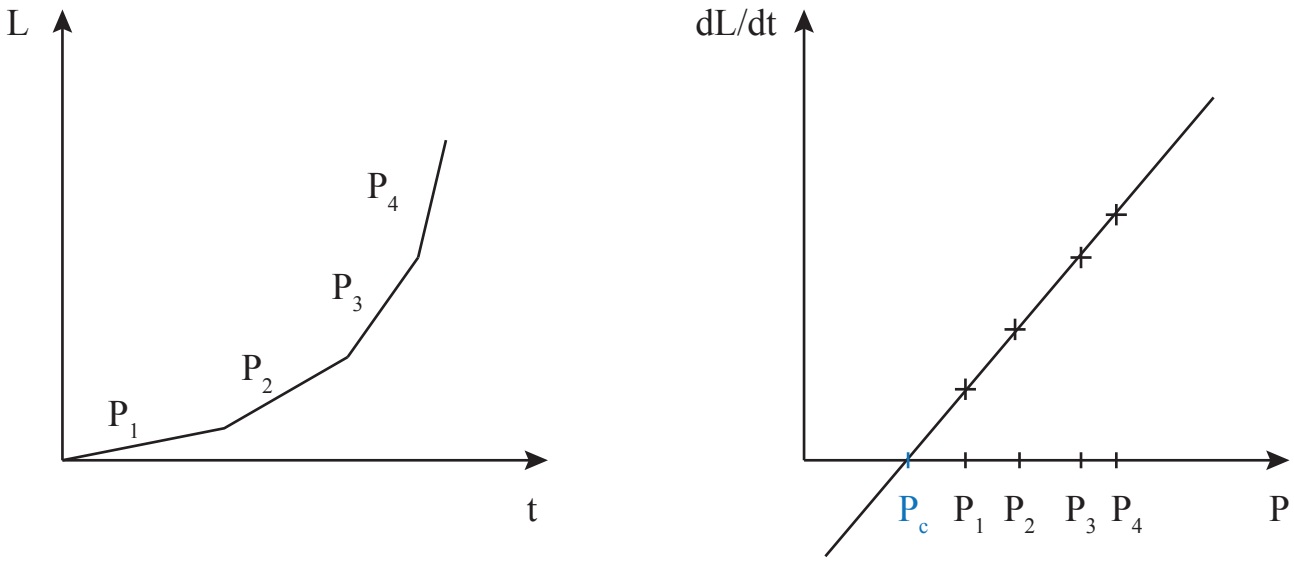
C) The physics of cell division

Mammalian cells are usually non-isolated mechanical systems as they often belong to a tissue and are therefore surrounded by other cells. This implies that cells entering mitosis have to integrate the physical constraints exerted by the surrounding cells to achieve proper division. However, mouse oocytes undergoing meiotic maturation can be considered as isolated cells. Throughout oogenesis in mammals, oocytes maintain physical contact with the surrounding follicular somatic cells via granulosa cell extensions known as transzonal projections and via gap junctions. Upon the LH stimuli, gap junctions between cumulus cells and mural granulosa are closed (Sela-Abramovich et al., 2006; Norris et al., 2008) and transzonal projections are retracted (Gilula et al., 1978). As a result the oocyte has no more connections with the surrounding follicular cells during meiotic divisions. Hence, the mechanical constraints on these cells are very different than the ones experienced by adherent cells. In this part, we will discuss cell mechanics during cell division, either when it is induced by the external environment or by the cell itself, and some of the techniques to access the mechanical properties of the cells. The techniques presented here are not exhaustive but are widely used to study cell division and mouse meiotic divisions in particular.

A: Experimental set-up for determination of the cortical tension by micropipette aspiration



B: Determination of the cortical tension by micropipette aspiration



$$\Delta P_c = 2T_c\left(\frac{1}{R_p} - \frac{1}{R_c}\right)$$

R_p: pipette radius
R_c: cell radius
L: length of the hemispherical projection inside the pipette
P: pressure
t: time

Figure 22: Micropipette aspiration and determination of cortical tension

1) The physical parameters describing cell mechanics

a) Tension

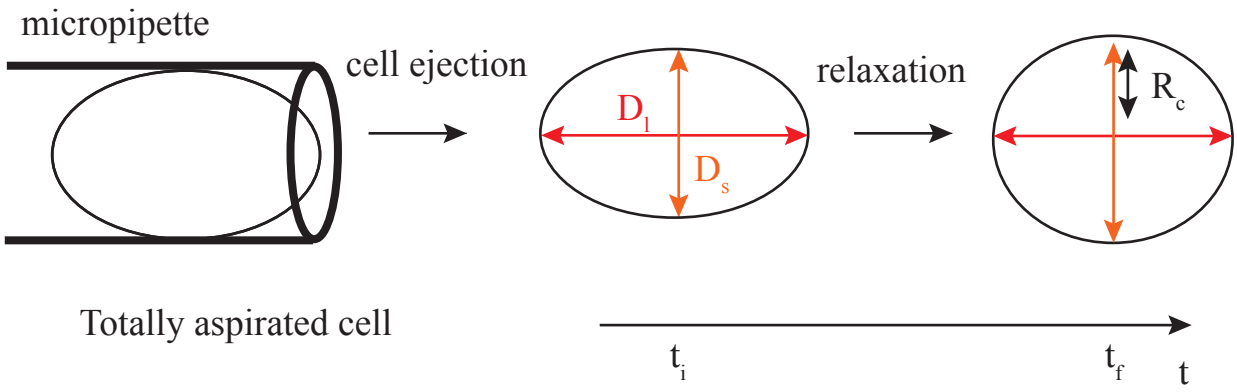
The surface tension governs cell mechanics at the interface between the cell and its environment. Let us consider a liquid drop. That drop will tend to minimize its contact surface with the environment. Surface tension actually corresponds to the energy that it would cost to expand the drop surface. It thus represents the equilibrium between the pressure exerted by the cell on its environment and the constraints exerted by the environment on the cell surface at any given time. In isolated cells, surface tension corresponds to the tension of the cell cortex, which is the sum of the tension exerted by the acto-myosin cortical cytoskeleton, the interaction between this cell cortex and the plasma membrane, and the plasma membrane tension itself (for review see (Lecuit and Lenne, 2007)). It is usually believed that the plasma membrane tension plays a minimal part in the total surface tension and that most of the cortical tension is due to the contractility of F-actin and Myosin-II. Indeed when the cortex is completely depolymerized, the residual tension is very small (Tinevez et al., 2009; Lieber et al., 2013).

There are several ways used today to measure surface tension. Most techniques are based on the fact that a cell will react to a small perturbation according to its tension. To produce such a perturbation, it is possible to aspirate the cell with a micropipette, deform it with an Atomic Force Microscope (AFM) or an optical trap.

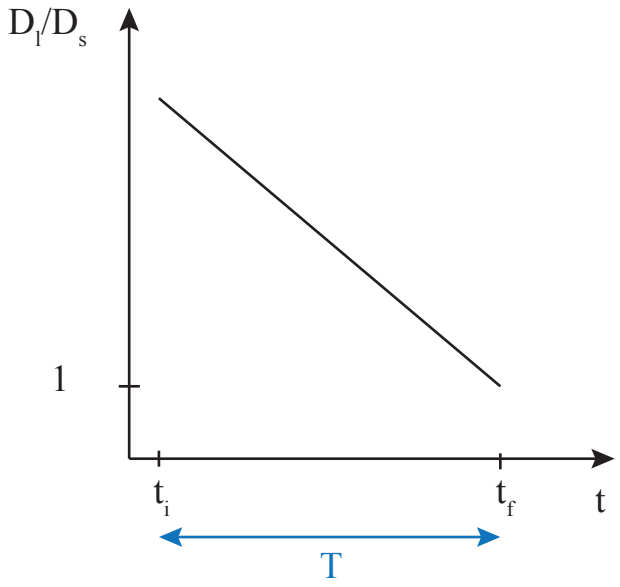
α. Micropipette aspiration

Micropipette can be used to aspirate cells and assess their tension (reviewed in (Hochmuth, 2000)). In this case, the cell surface is aspirated inside a glass pipette of known radius, and will form a hemispherical projection until it reaches a critical pressure (P_c) where it starts flowing into the pipette (Figure 22) (Evans and Yeung, 1989). Assuming that the cell behaves as a liquid drop, the cortical tension is bound by the Laplace law as $\Delta P_c = 2T_c(\frac{1}{R_p} - \frac{1}{R_c})$, where T_c is the cortical tension, R_p is the pipette radius, R_c is the cell radius and ΔP_c is the critical pressure. Hence, by monitoring the variation of length as a function of time $\frac{dL}{dt}$ of the hemispherical projection for different pressures P, it is possible to access the critical pressure P_c, which is the pressure where this variation would be null (Figure 22B). This technique has been notably used on mouse oocytes (Larson et al., 2010).

A: Experimental set-up for determination of the cell viscosity by micropipette aspiration and release



B: Determination of the cell viscosity by micropipette aspiration and release



$$T = \eta \frac{R_c}{T_c}$$

R_c: cell radius at steady state
D_l/D_s: larger diameter/smaller diameter
t: time
t_i/t_f: initial time/final time
T: total time
η: cell viscosity
Tc: cortical tension

Figure 23: Micropipette aspiration and measure of the cell viscosity

β. AFM

Atomic Force Microscopy relies on the attraction and repulsion between the sample and a small tip. Simply speaking, the small tip is moving at the surface of the sample and linked to a lever which movements are recorded. To assess cortical tension, the tip is pressed against the cell and its backward motion is assessed via measure of the lever motion (for an example of cell tension measurement by AFM, see (Stewart et al., 2011)).

χ. Optical trap

The optical trap consists of a very focused laser able to trap a bead. The bead can be coated so that it will stick to the membrane of interest. The resistance of the bead to the motion induced by the laser is proportional to the surface tension of the object of interest (for an example in cells see (Rai et al., 2013)).

b) Cytoplasmic viscosity

Generally speaking, the viscosity of a cell represents how hard it is to move an object inside the cytoplasm. Indeed, the viscosity of a fluid measures the resistance to its deformation by a known stress. The more viscous the fluid, the harder it would be to deform it or to put it in motion. Thus, the cytoplasmic viscosity will describe the global viscosity in the cytoplasm, and in a simple case the force applied on a spherical particle moving inside the cytoplasm will be proportional to that value of viscosity as given by Stokes law $\vec{F} = -6\pi\eta r\vec{v}$ where $\vec{F}$ is the force, η is the viscosity, r is the radius of the particle and $\vec{v}$ is the speed of the particle.

Measuring a cell internal viscosity is not an easy task. The simplest way to measure the viscosity of a system (macroscopic viscosity) is to use a rheometer (Valentine et al., 2005). Another way to measure viscosity is to induce small perturbations and record how the cell reacts to it, for example, by sticking two needles inside a mitotic spindle, one applying forces, and the other one responding to these forces while its position is monitored (Shimamoto et al., 2011). Another method is again to use micropipette aspiration. In this system, cells are completely aspirated inside a pipette of radius slightly smaller that the cell radius (Figure 23). The cells are then released and the time of recovery is recorded by simple measurement of the variation of the ratio between the bigger and the smaller diameter. This time is proportional to the ratio tension/viscosity (Lam et al., 2009). It is important to notice here however that this is a global viscosity that does not take into account possible differences

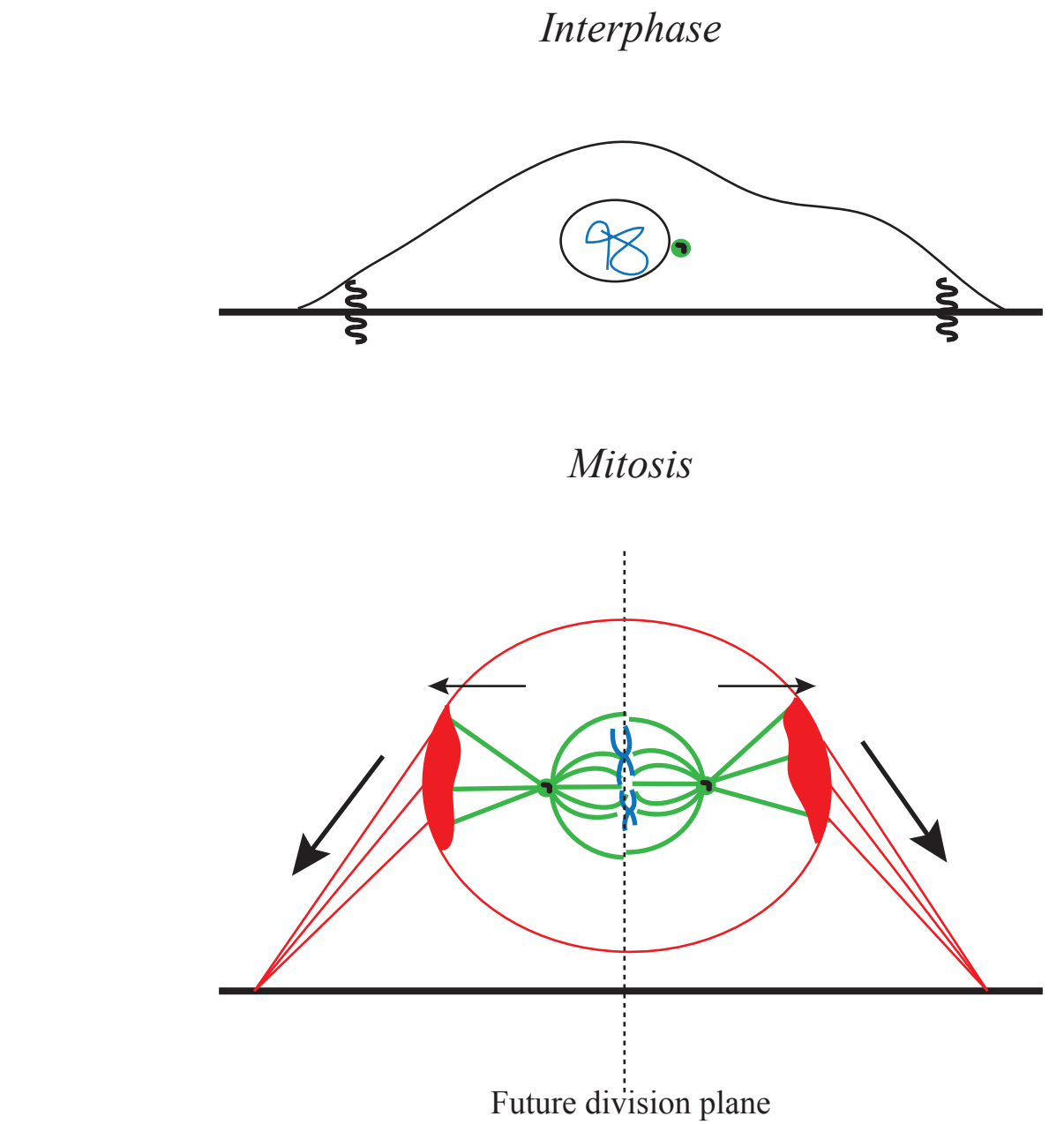


Figure 24: Mechanical constraints and spindle positioning in non-polarized cells

between the cytoplasm and the cell cortex or between different regions in the cytoplasm. To measure microscopic viscosity, optical tweezers can again be a useful tool to follow single particles.

c) Elasticity/Plasticity

Elasticity and plasticity are two opposite concepts that express the response of an object to a deformation. If the object is deformable and is able to maintain the induced deformation, it is a plastic object. However, an object that will be hard to deform and will go back to its original shape will be an elastic object. Cytoskeleton proteins and especially F-actin and Myosin-II are essential in organizing the shape of the membrane and cortex and their elastic or plastic response (Lecuit and Lenne, 2007).

d) Models and scales

The physical equations that are used to calculate various parameters such as cell tension from measures are based on models. For example, measurement of cortical tension by micropipette aspiration is based on the cell behaving like a liquid drop (Evans and Yeung, 1989). Thus, it is very important to check whether the model acutely describes the cell behavior. Furthermore, the question of time-scale is crucial when it comes to measuring forces. For example, as mentioned before, it is possible to measure the viscosity inside the mitotic spindle, but the response of the spindle to forces exerted on its small axis is elastic at short and long time-scale but viscous at intermediate time-scale (10-100s) (Shimamoto et al., 2011). In particular, processes that implicate cytoskeleton rearrangement can typically be relatively long. Thus, it is important to consider the time-scale of the biological event before choosing the measurement technique. Furthermore, as mentioned before, the question of scale is crucial. For example, monitoring the motion of 1 nm or 1 μm beads to measure viscosity would get access respectively to the cytoplasmic viscosity or to the cytoskeleton viscosity.

2) Physical constraints on a dividing cell

a) From outside the cell

In vitro, most cells grow on a substratum that can be constituted of either other cells and/or extracellular matrix. Generally speaking, the shape of the cell prior to cell division in non-polarized cells is thought to provide mechanical constraints that force spindle orientation (for review see (Théry and Bornens, 2006)). At the onset of mitosis, cells round up but

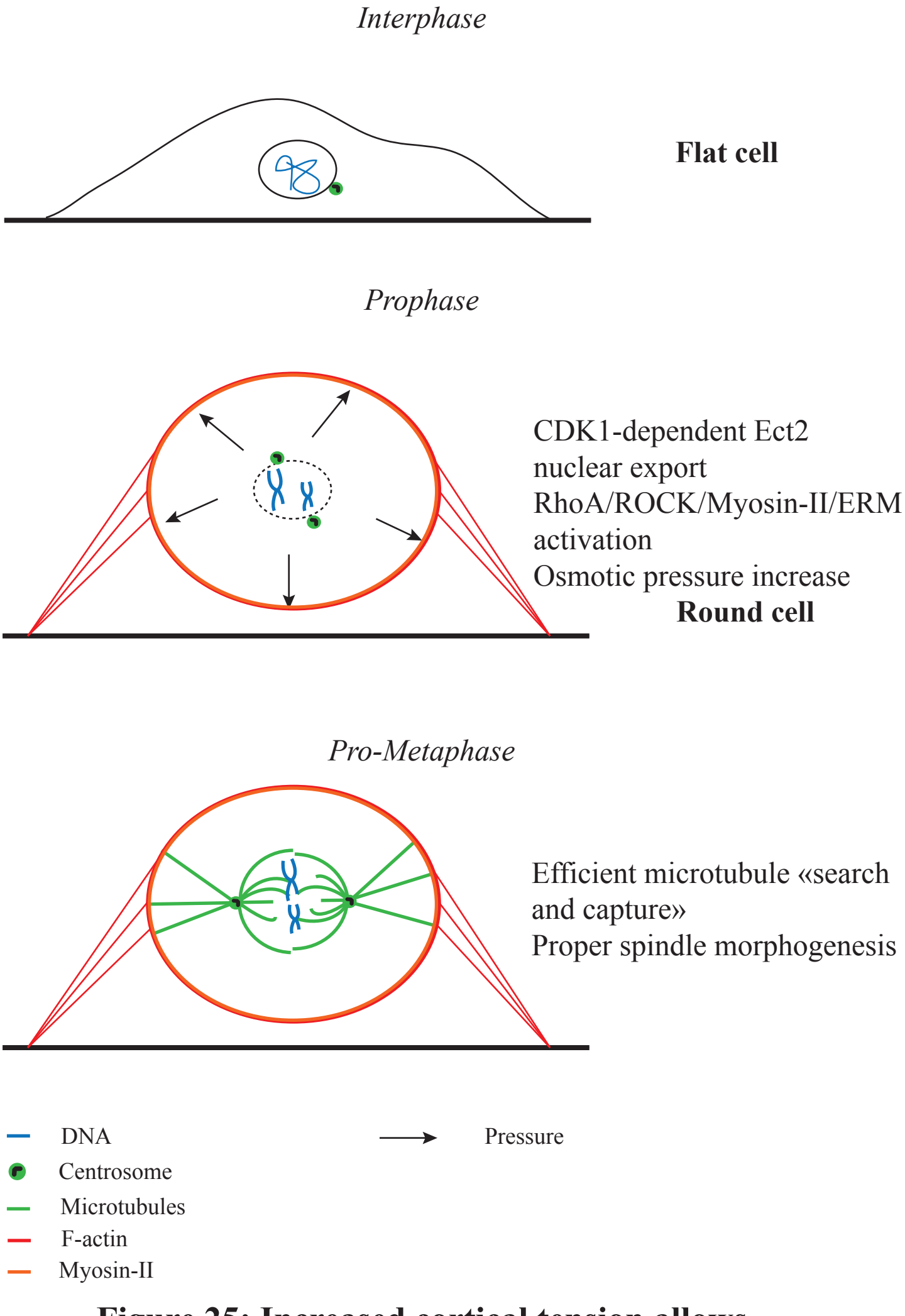


Figure 25: Increased cortical tension allows proper spindle formation in mitosis

maintain retraction fibers, which are cytoplasmic projections very rich in F-actin. By growing cells on stereotypical micropatterns, it was shown that the initial cell shape influences the position of the division axis through actin cortex heterogeneity at the cortex that are mediated by the position of the retraction fibers (Théry et al., 2005; Fink et al., 2011). These retraction fibers exert strong forces on the cell body (Fink et al., 2011). Furthermore, the force-field localizing actin at these precise spots is probably due to the presence of cell-matrix interaction proteins such as Integrins that can signal to the actin cytoskeleton (Toyoshima and Nishida, 2007). How F-actin structures then influence spindle positioning is still debated; the current hypothesis is that astral microtubules are in contact with these actin structures (Kunda and Baum, 2009) (Figure 24).

In vivo, cells usually have to divide in a tissue, surrounded by other cells. Thus, their external environment is another constraint that they have to overcome, adding more complexity compared to the case studied above. For example, during Zebrafish development, cells in the Enveloping Cell Layer divide in a stereotypical fashion because of an anisotropy in the tissue global tension; the cells preferentially divide along the main axis of tension (Campinho et al., 2013). By doing that, cells probably reduce the anisotropy of the tissue (Campinho et al., 2013).

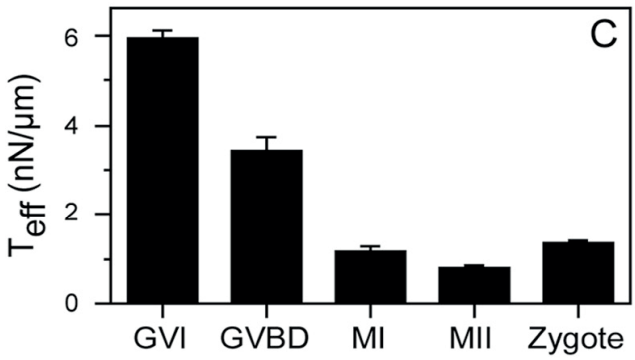
b) From inside the cell

α. Cortical tension, spindle formation and robustness

As discussed before, mitotic cells round up at the onset of mitosis. This could be a passive mechanism due to the loss of adhesion with the substratum. However, evidence shows that the rounding is actively driven by an increase in cortical tension (Kunda et al., 2008; Stewart et al., 2011). Furthermore, this increase is not due to the loss of adhesion since interphasic cells detached from their substratum experience only a slight increase in their cortical tension (Stewart et al., 2011). It was demonstrated that the increase in cortical tension is due to the actin cytoskeleton and ERM proteins (Carreno et al., 2008; Kunda et al., 2008) but also to an increase in osmotic pressure (Stewart et al., 2011). It was thus proposed that the role of the acto-myosin cortex is to ensure a uniform rounding throughout the whole cell (Lancaster et al., 2013).

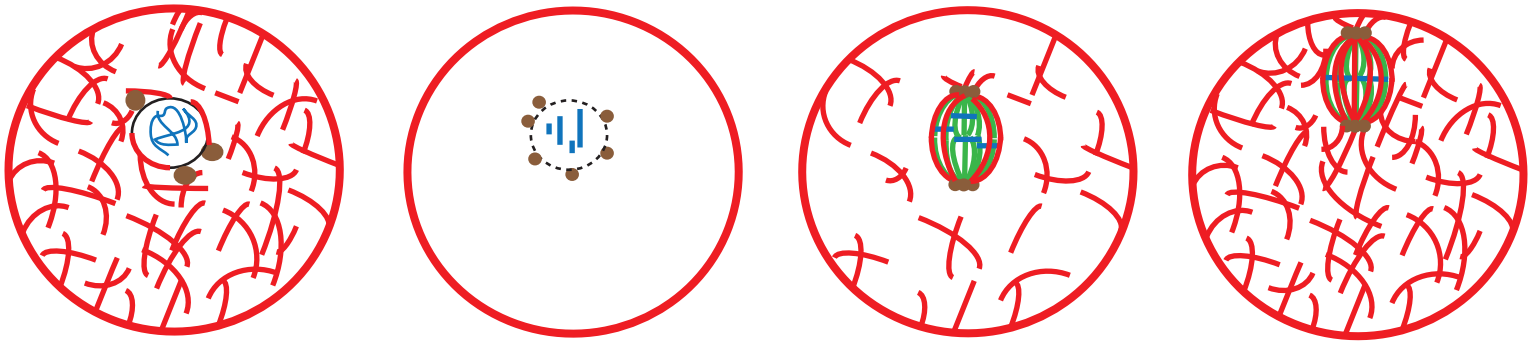
What could be the role of this increase in cell stiffness at mitosis onset? Cells knocked-down for the ERM protein Moesin show defects in spindle morphogenesis, thus showing that a stiff cortex is important for spindle formation and function (Carreno et al.,

A: Cortical tension in mouse oocytes (Larson et al., 2010)



GVI: Prophase I
GVBD: NEBD
MI/II: Metaphase I/II

B: F-actin organization during meiotic maturation



Prophase I *NEBD* *Early Metaphase I* *Late Metaphase I*

DNA
MTOC
Microtubules
F-actin

Figure 26: cortical tension and F-actin network in mouse oocytes, a contradiction?

2008; Kunda et al., 2008). It was further demonstrated that indeed the cell needs to undergo rounding because the spindle requires room to properly form (Lancaster et al., 2013), as flattened cells cannot properly capture chromosomes because they are out of reach for the microtubules; flattened cells also show defects in the maintenance of spindle poles (Lancaster et al., 2013).

It is also interesting to notice that rounding is coupled to mitosis entry because it is controlled by the MPF. Indeed, MPF phosphorylates a protein called Ect2, promoting its nuclear export (Matthews et al., 2012). Ect2 then acts upstream of RhoA, ROCK and Myosin-II, thus ensuring coordination between proper cell rounding and the progression of mitosis (Figure 25).

Since dividing cells are subject to both external and cell-driven forces, it is clear that the spindle has to be robust to get properly positioned without getting dismantled. The mechanical properties of mitotic spindles were assessed in Xenopus extracts and it was found that indeed, forces applied on the spindle long axis did not change the spindle architecture (Shimamoto et al., 2011). This is important because the forces that position the spindle in cells are precisely forces applied parallel to the spindle long axis (Figure 24) (Théry and Bornens, 2006). However along its short axis, the spindle behaves as a stiff solid on short time-scales, which probably prevents the spindle from being deformed by brutal and fast knocks and as a viscous liquid for intermediate time-scales which still allows chromosomes alignment on the metaphase plate (Shimamoto et al., 2011; Dumont, 2011).

β. Cortical tension and spindle motion in mouse oocyte

In mouse oocyte, the Meiosis I spindle is positioned by pulling forces exerted via a cytoplasmic F-actin meshwork and Myosin-II (Azoury et al., 2008; Schuh and Ellenberg, 2008). Recently, the mechanical properties of the oocytes were explored by micropipette aspiration (Figure 22): the cortical tension of the oocytes is high in Prophase I and drops during meiotic divisions (Larson et al., 2010) (Figure 26A). This is a very puzzling observation since oocytes are big round cells stable in shape throughout meiotic divisions and because concomitantly with spindle migration the F-actin meshwork is progressively nucleated, thus one would expect a build up in cortical tension rather than a drop, especially since the cortical tension actually decreases at NEBD at the same time that the cytoplasmic meshwork is dismantled (Figure 26B).

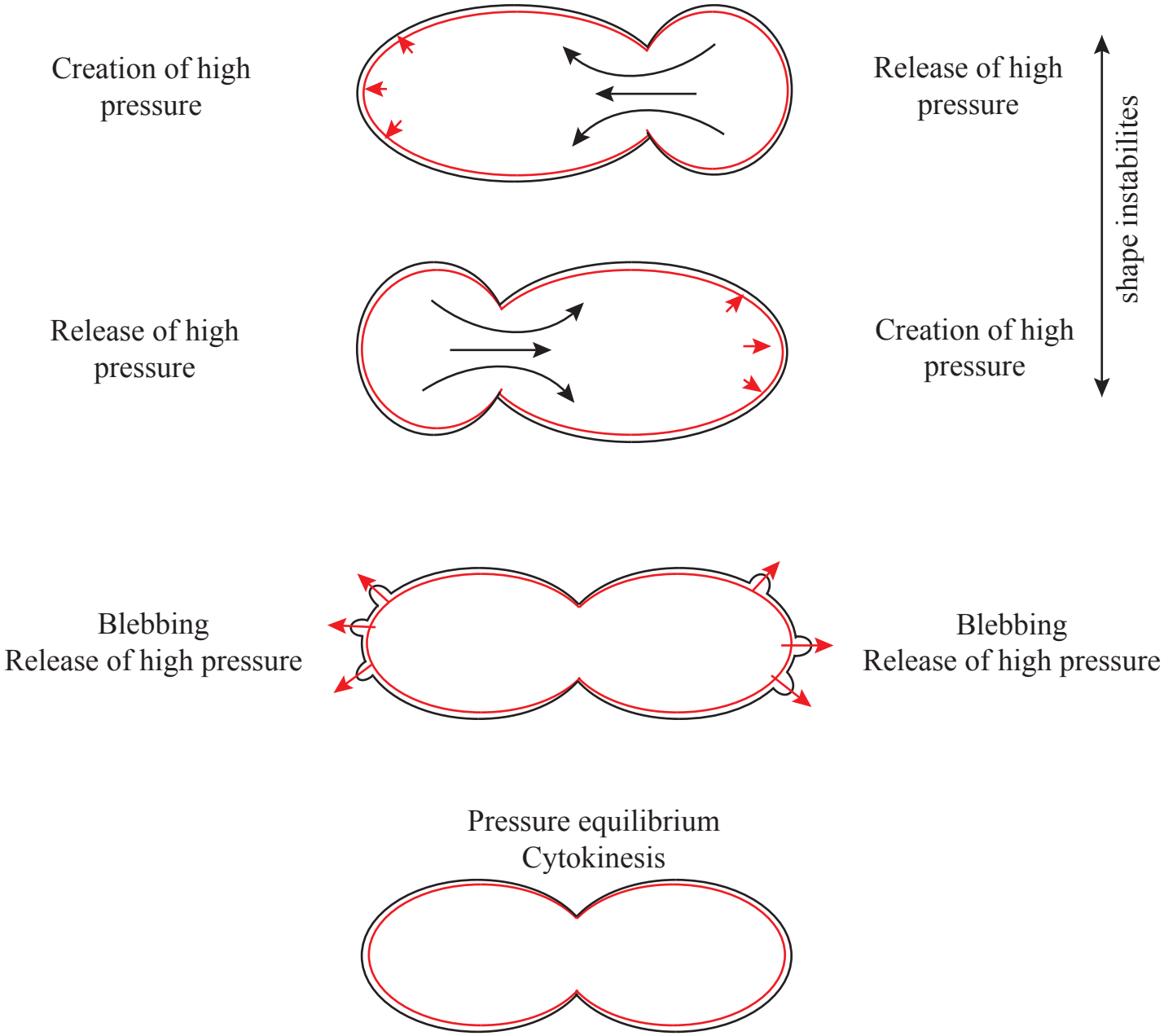


Figure 27: Shape instabilities, blebbing and pressure release during cytokinesis

χ. Cell mechanics and cytokinesis

Finally, cell mechanics is crucial for cytokinesis. Cytokinesis is due to an acto-Myosin-II dependent constriction at the cell equator, which is the position of the metaphase plate; hence it is easy to understand that it is very dependent on the mechanical properties of the cortex, since a very high cortical tension would probably be an obstacle to furrow ingression. It was indeed shown in fission yeast that turgor pressure prevents the contractile ring to close faster (Proctor et al., 2012). In Drosophila, some cells are even able to decrease their cortical tension by delocalization of Moesin at anaphase prior to cytokinesis (Kunda et al., 2012). In addition, the progression of the constriction furrow can be responsible for shape instabilities because the very high cortical tension due to F-actin and Myosin-II contraction will amplify a small asymmetry in the size of the daughter cells (Figure 27) (Sedzinski et al., 2011). A way to decrease the cortical tension could be to release pressure via blebs, which are little spheres containing only membrane but no cortex (Figure 27) (Sedzinski et al., 2011; Kunda et al., 2012).

Abscission (e.g. cutting of the cytoplasmic bridge between the two daughter cells), which is the last step of cytokinesis, has also been shown to depend on cortical tension. Indeed, abscission takes place only when the tension drops in the bridge, allowing the recruitment of the abscission machinery (Lafaurie-Janvore et al., 2013). The authors propose that when cells flatten after mitosis, they exert strong pulling forces on their substrate, and these forces are transmitted to the bridges; thus, when the cells are not fully spread, the forces that they have to develop are strong and abscission is delayed, allowing the cells to stay connected until they have reached a proper organization (Lafaurie-Janvore et al., 2013).

D) Situation of the problem

We have seen in this introduction that spindle migration to the cortex during mouse Meiosis I is a fundamental event promoting oocyte first asymmetric division. It has been known for a long time that this process is actin-dependent, but only recently the F-actin structures involved have been accurately visualized, thanks to the development of new F-actin probes.

During Meiosis I, a very dense and dynamic F-actin meshwork Formin-2 and Spire1/2 dependent is responsible for spindle migration. However, this meshwork is not contractile as it is the case in Starfish oocyte. Instead, Myosin-II located at both poles of the actin cage

surrounding the microtubule spindle seems to be the motor for spindle migration. Thus, it is not entirely clear how the F-actin meshwork promotes spindle migration.

Furthermore, the branched actin nucleator Arp2/3 and many of its NPF have been involved in spindle migration, but so far no study has identified the F-actin structure involved in spindle migration requiring Arp2/3-dependent nucleation.

Finally, a recent study has described a drop in cortical tension concomitant to spindle migration (Larson et al., 2010), a puzzling observation since oocytes are round cells that need to actively position their spindle; in mitotic cells, this is usually possible because of an increase in cortical tension. Moreover, the formation of a dense cytoplasmic F-actin meshwork seems more likely to promote an increase in cortical tension. Furthermore previous lab member Jessica Azoury had observed a thickening of the cortical actin was observed during meiotic maturation which also pointed towards an increase in cortical tension. She had finally observed that this F-actin thickening was not present in *mos -/-* oocytes.

The work I conducted during my PhD addressed these questions by identifying the links between a newly described Arp2/3 nucleated structure, the Mos/MAPK pathway, the drop in cortical tension and spindle migration and proposes a biophysical model to explain the first asymmetric division in these acentriolar cells. This work also developed biophysical tools to study mechanical properties in mouse oocytes.

RESULTS

Meiotic divisions are highly asymmetric in size as they produce a big cell, the oocyte, and two small polar bodies. During Meiosis I, the microtubule spindle migrates to the cortex in an actin dependent fashion, allowing this asymmetric division in size. During spindle migration, cortical tension drops, which is counter-intuitive since oocytes are round cells stable in shape that actively position their spindle and since a very dense Spire1/2 and Formin-2 F-actin meshwork is progressively nucleated. In this paper, we set out to understand the origin and the role of the drop in cortical tension during mouse first meiotic division (Meiosis I).

We demonstrated that during Meiosis I, concomitant with spindle migration, a thickening of the F-actin cortex is detectable around NEBD+ 3 hours. This F-actin subcortex is thickening homogeneously under the cortex until the end of spindle migration where it measures around 4 μm. In addition, it is deformed above the spindle. The branched actin nucleator Arp2/3 is responsible for the nucleation of this cortical actin thickening as shown by chemical inhibition. The actin subcortex is required for spindle migration since its absence leads to symmetrical divisions due to impaired off-center positioning of the spindle.

The Mos/MAPK pathway is necessary and sufficient for the nucleation of the F-actin cortical thickening since it is absent in *mos-/-* oocytes and that expressing Mos is sufficient to nucleate it *de novo*. The link between the Mos/MAPK pathway and Arp2/3 is probably the NPF Wave2, which is phosphorylated during Meiosis I in control cells but only partially in *mos-/-* oocytes. This suggests that the Mos/MAPK pathway might activate Arp2/3 dependent nucleation by regulation of its NPF Wave2, as suggested in other models *in vitro* and *in vivo* ((Nakanishi et al., 2006; Mendoza et al., 2011). In accordance with Mos and Arp2/3 being in the same molecular pathway, Arp2/3, Wave2 and Mos inhibitions all lead to similar phenotypes (Verlhac et al., 2000; Sun et al., 2011a, 2011d), namely the absence of spindle migration.

Spindle positioning in mouse Meiosis I thus depends on two different actin networks. We decided to investigate their relative contribution to cell mechanics to understand how they regulate spindle migration. By micropipette aspiration techniques, I confirmed that cortical tension drops during Meiosis I (Larson et al., 2010), concomitantly to cortical F-actin thickening. I showed that this drop in cortical tension is due to Myosin-II cortical displacement. Similarly, the Mos/MAPK is also necessary and sufficient for removal of Myosin-II from the cortex. Contrary to what was published in the Li lab (Li et al., 2008), we

confirmed that Myosin-II is the force generator for spindle migration (Schuh and Ellenberg, 2008; Simerly et al., 1998) since its chemical inhibition abolishes spindle migration. Furthermore, the F-actin thickening promotes cortical plasticity. Thus the Mos/MAPK pathway controls both Myosin-II cortical exclusion and the F-actin thickening nucleation. The consequence in terms of mechanics is that cortical tension drops and cortical plasticity increases, leading to a softening of the cortex.

Finally, I demonstrated that the drop in cortical tension is required for spindle migration since artificially stiffening the cortex leads to impaired spindle off-centering.

In conclusion, the Mos/MAPK pathway is responsible for spindle migration by inducing a softening of the cortex, via a drop of cortical tension and an increase of cortical plasticity mediated respectively by Myosin-II cortical exclusion and F-actin subcortical nucleation. Mathematical modeling suggests that a soft cortex would allow the amplification of an initial unbalance of forces coming from the fact that the spindle does not form at the exact center of the cell, but a little bit off-centered (Brunet and Maro, 2007). Myosin-II spindle pulling would be amplified by the F-actin subcortex deformation and thus accelerate the speed of spindle migration towards the closest cortex (Verlhac et al., 2000)

Authors contribution:

A.C., M-H.V. and M-E.T. designed the experiments, interpreted the results and wrote the manuscript. A.C., C.U-D. and M.E.T. carried out most of the experiments. J.A. performed the preliminary observations that started the project. M.A. assisted in the photoactivation experiments. I.Q. assisted in genotyping the animals. A.C. and C.C. carried out the micropipette experiments. C.C., P.N. and C.S. designed the micropipette experiments and interpreted the results. N.S.G. and R.V. designed the physical model. M.E.T. and M.H.V. conceived and supervised the project.

nature cell biology

A soft cortex is essential for asymmetric spindle positioning in mouse oocytes

Agathe Chaigne[1,2], Clément Campillo[3,8], Nir S. Gov[4,9], Raphaël Voituriez[5,9], Jessica Azoury[1,2], Claudia Umaña-Diaz[1,2], Maria Almonacid[1,2], Isabelle Queguiner[1,2], Pierre Nassoy[3,6,7,8], Cécile Sykes[3,6,7], Marie-Hélène Verlhac[1,2,10] and Marie-Emilie Terret[1,2,10]

At mitosis onset, cortical tension increases and cells round up, ensuring correct spindle morphogenesis and orientation. Thus, cortical tension sets up the geometric requirements of cell division. On the contrary, cortical tension decreases during meiotic divisions in mouse oocytes, a puzzling observation because oocytes are round cells, stable in shape, that actively position their spindles. We investigated the pathway leading to reduction in cortical tension and its significance for spindle positioning. We document a previously uncharacterized Arp2/3-dependent thickening of the cortical F-actin essential for first meiotic spindle migration to the cortex. Using micropipette aspiration, we show that cortical tension decreases during meiosis I, resulting from myosin-II exclusion from the cortex, and that cortical F-actin thickening promotes cortical plasticity. These events soften and relax the cortex. They are triggered by the Mos–MAPK pathway and coordinated temporally. Artificial cortex stiffening and theoretical modelling demonstrate that a soft cortex is essential for meiotic spindle positioning.

The development of pluricellular organisms requires a balance between proliferation and differentiation. This equilibrium is regulated in part by asymmetric cell divisions. Positioning of the microtubule spindle with respect to the polarity axis of the mother cell specifies the geometry of cell division (for review, see ref. 1). Mitotic spindle positioning depends on astral microtubules emanating from centrosomes at spindle poles (reviewed by ref. 2). In addition, mitotic cell rounding, a consequence of increased cortical tension, regulates spindle orientation[3–6].

In female meiosis, oocytes divide twice asymmetrically forming two small degenerating polar bodies and a big unique round haploid oocyte. Oocytes are arrested in prophase of the first meiotic division (prophase I) in the ovary. Following hormonal stimulation, meiosis resumes, characterized by nuclear envelope breakdown (NEBD) followed by the formation of the first meiotic spindle. In mouse oocytes, the asymmetry of the first meiotic division (meiosis I) is ensured by off-centre positioning of the spindle, which forms more or less in the centre of the cell and 4 to 5 h after NEBD migrates towards the closest cortex[7]. Then anaphase occurs followed by extrusion of the first polar body. The spindle axis forms randomly, not influenced by cortical cues[7], because at this stage oocytes show no sign of polarization[8–10]. As meiotic spindles lack true centrosomes and astral microtubules[11], spindle positioning does not depend on microtubules as in mitosis. Instead, meiosis I spindle migration is supported by a dynamic cytoplasmic filamentous actin (F-actin) meshwork, nucleated by formin-2 (refs 12–16) and spire 1/2 (ref. 17). Contrary to mitosis, cortical tension decreases during meiotic divisions in mouse oocytes[18], a surprising observation because oocytes remain round and actively position their spindles. We investigated the molecular basis for this reduction in cortical tension and its significance in spindle positioning.

We describe an Arp2/3-dependent cortical F-actin thickening detectable 3 h after NEBD and reaching its maximum thickness at polar body extrusion 4 h later, required for spindle positioning to the cortex. Using micropipette aspiration, we show that cortical tension decreases during meiosis I, resulting from myosin-II exclusion from the cortex, and that cortical F-actin thickening promotes cortical plasticity. These two events soften the cortex and are triggered by Mos–MAPK, signalling and are thus coordinated temporally. Softening of the cortex

[1]CIRB, Collège de France, and CNRS-UMR7241 and INSERM-U1050, Equipe Labellisée Ligue Contre le Cancer, Paris F-75005, France. [2]Memolife Laboratory of Excellence and Paris Science Lettre, Paris F-75005, France. [3]Institut Curie, Centre de Recherche, Laboratoire Physico-Chimie, Paris F-75248, France. [4]Department of Chemical Physics, Weizmann Institute of Science, Rehovot 76100, Israel. [5]UMR7600-CNRS/UPMC, 4 Place Jussieu, Paris F-75005, France. [6]CNRS-UMR168, Paris F-75248, France. [7]UPMC, 4 Place Jussieu, Paris F-75248, France. [8]Present addresses: Institut Lumière Matière, UMR5306 CNRS/UCBL, Villeurbanne 69622, France (C.C.); LP2N, Institut d'Optique, CNRS UMR 5298 & Université de Bordeaux 1, F-33405 Talence, France (P.N.). [9]These authors contributed equally to this work.
[10]Correspondence should be addressed to M-H.V. or M-E.T. (e-mail: marie-helene.verlhac@college-de-france.fr or marie-emilie.terret@college-de-france.fr)

Received 2 January 2013; accepted 3 June 2013; published online 14 July 2013; DOI: 10.1038/ncb2799

© 2013 Macmillan Publishers Limited. All rights reserved.

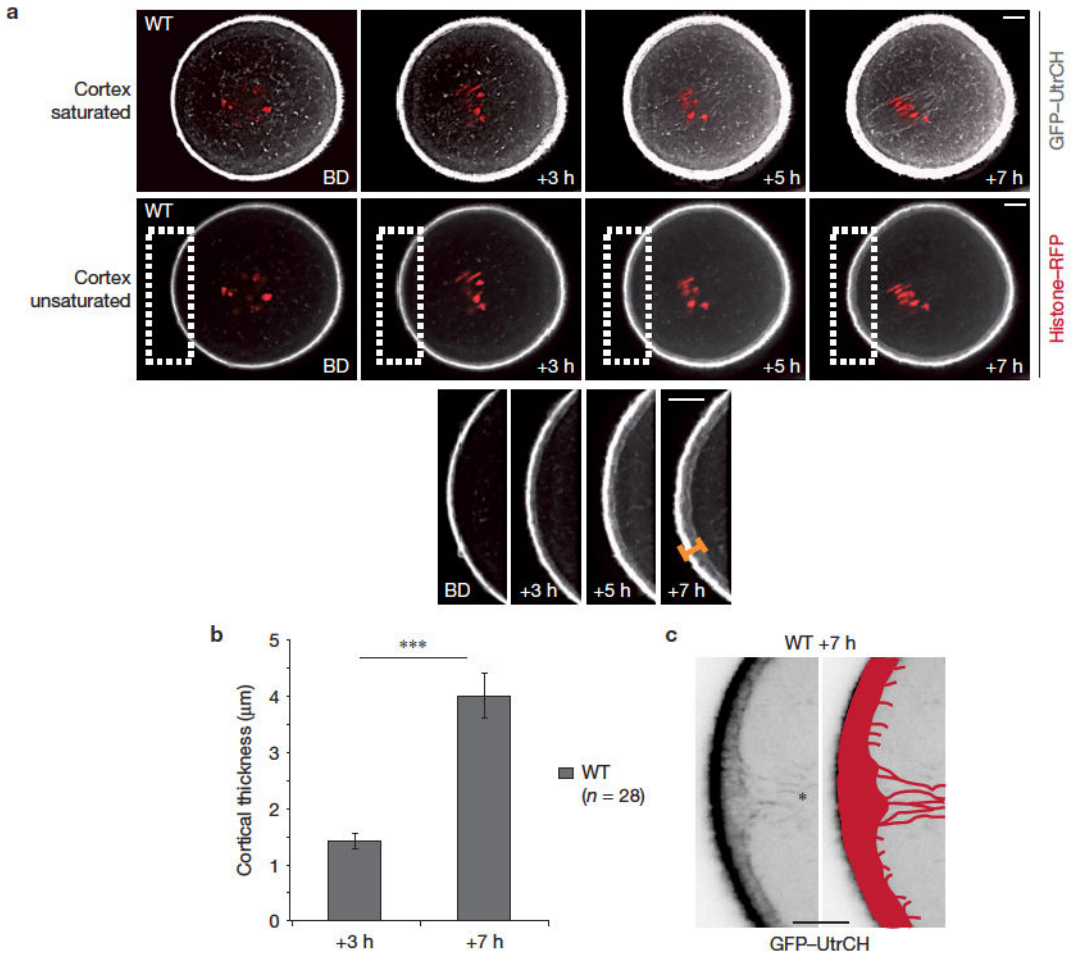


Figure 1 Cortical F-actin thickening appears during meiosis. (**a**) Time-lapse spinning disc confocal microscopy of a WT oocyte expressing GFP–UtrCH (white) and histone–RFP (red) observed from NEBD (BD) until NEBD+7 h. Eighty-four oocytes were imaged. One *Z* plane is shown. The upper panel corresponds to saturated images, the lower panels to unsaturated images. The orange bar indicates cortical F-actin thickness, referred to as the subcortex. Scale bars, 10 µm. (**b**) Bar graph showing measures of the subcortex in micrometres at NEBD+3 h and NEBD+7 h in WT oocytes. Mean of $n=28$ oocytes, assessed over 3 independent experiments. Standard deviation is plotted on each bar. The statistical significance of differences was assessed with a *t*-test with Welch correction, ***P value <0.0001. (**c**) Time-lapse spinning disc confocal microscopy of a WT oocyte expressing GFP–UtrCH (black) observed at NEBD+7 h. The black asterisk marks the spindle pole. One *Z* plane is shown. In the right panel, the subcortex is coloured in red and the red lines overlay F-actin filaments connecting it to the cytoplasmic actin meshwork and the actin cage. Scale bar, 10 µm.

promotes spindle positioning because artificial stiffening prevents it. Cortical softening might allow amplification of a slight initial imbalance of forces contributing to spindle off-centring, as suggested by the development of a mathematical model.

RESULTS

A cortical F-actin thickening appears during meiosis I

Wild-type (WT) oocytes expressing an F-actin probe (GFP–UtrCH; ref. 19) were imaged by live spinning-disc microscopy during meiosis I. An outer very bright layer of cortical F-actin is present at all stages of meiotic maturation. In addition, an inner dimmer layer can be detected around 3 h after NEBD, which expands during meiosis I. To assess cortical actin thickness, we measured the overall thickness of the outer bright layer and the inner dimmer layer (Fig. 1a orange dash, referred to as the subcortex). The subcortex reaches its maximum thickness close to polar body extrusion (from 1.4 µm at NEBD+3 h, up to 4 µm at NEBD+7 h, Fig. 1a,b and Supplementary Video S1). It is uniform except in the region overhanging the spindle in late meiosis I where it is connected to cytoplasmic F-actin (Fig. 1c short red lines) and to the actin cage surrounding the meiotic spindle (Fig. 1c long red lines and Supplementary Video S2).

Cortical and cytoplasmic F-actin define two distinct compartments

We used the dynamics of the PA-GFP–UtrCH probe as a proxy to compare the structure and dynamics of actin filaments[19] in the cytoplasm and subcortex (Fig. 2a red dots). The fluorescence decay is faster in the cytoplasm than in the subcortex (Fig. 2b,c and Supplementary Video S3), suggesting that filaments have different dynamics and/or structure depending on their location, consistent with FRAP (fluorescence recovery after photobleaching) experiments using actin–YFP in mouse oocytes[14].

To further analyse the border between cortical and cytoplasmic actin, we analysed the directionality of fluorescence decay. In the subcortex, the fluorescence decay is slow and identical between the left and right side of the photoactivated area (Fig. 2d). However, the decay towards

© 2013 Macmillan Publishers Limited. All rights reserved.

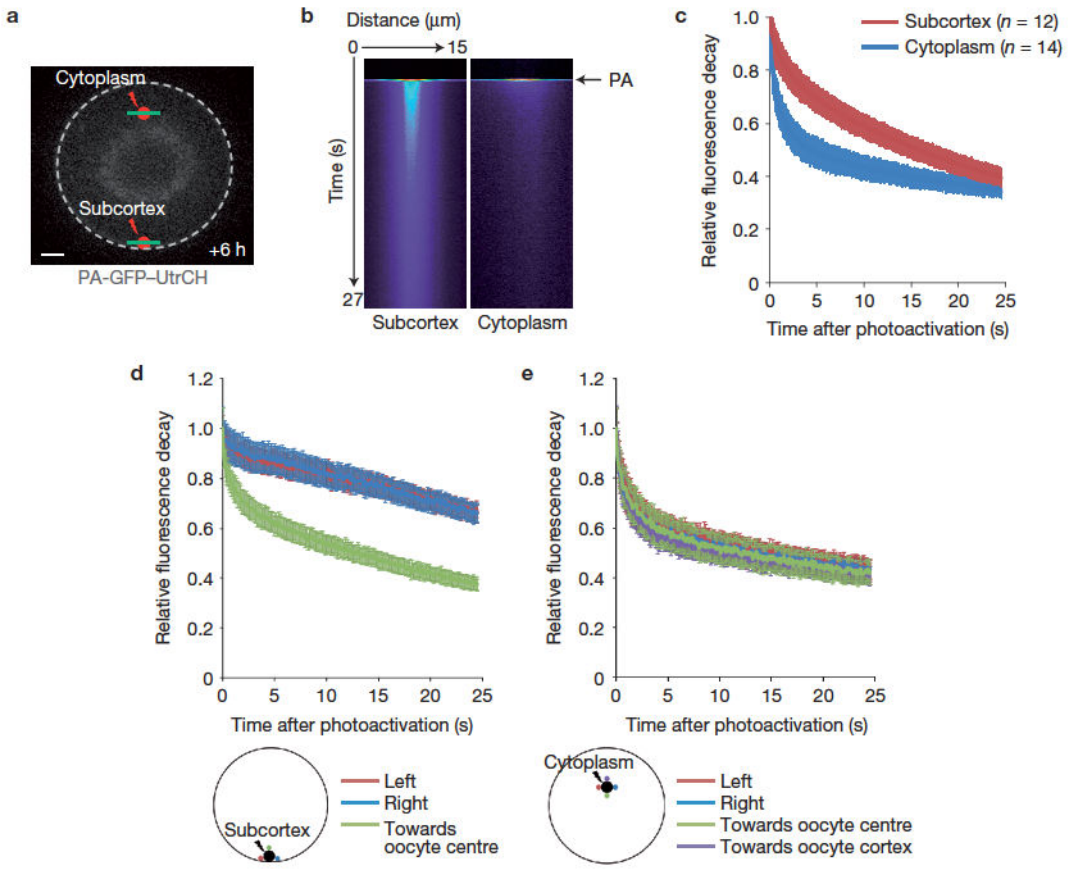


Figure 2 Cortical and cytoplasmic F-actin define two distinct compartments. (**a**) Confocal spinning disc image of a NEBD + 6 h oocyte expressing PA-GFP–UtrCH before photoactivation. The red dots correspond to the region of photoactivation in the cytoplasm or subcortex (more precisely in the cortical inner dimmer layer). Scale bar, 10 μm. (**b**) Kymographs generated along the green lines shown in **a**. The movie duration is 27 s and the width is 15 μm centred around the region of photoactivation (PA). Black, lowest intensity; white, highest intensity. (**c**) Profiles of PA-GFP–UtrCH fluorescence decay after photoactivation over time in the subcortex and cytoplasm of NEBD + 6 h oocytes. Mean of $n = 12$ oocytes in the subcortex and $n = 14$ oocytes in the cytoplasm, assessed over 3 independent experiments. Standard errors are plotted on each curve. See Methods for photoactivation analysis. The curves are statistically different using a t-test performed for each time point. (**d**) Profiles of PA-GFP–UtrCH fluorescence decay in regions adjacent to the photoactivated subcortical region of NEBD + 6 h oocytes over time. The left and right regions are in the subcortex (more precisely in the cortical inner dimmer layer) whereas towards the oocyte centre is a cytoplasmic region. Mean of $n = 12$ oocytes, assessed over 3 independent experiments. Standard errors are plotted on each curve. Statistical differences were assessed for each time point using a t-test. The left and right curves are not statistically different, whereas the left and right curves are statistically different from the towards oocyte centre curve just after photoactivation (1.4 s after photoactivation $P < 0.05$). (**e**) Profiles of PA-GFP–UtrCH fluorescence decay in regions adjacent to the photoactivated cytoplasmic region of NEBD + 6 h oocytes over time. Left, right, towards oocyte centre and towards oocyte cortex are all cytoplasmic regions. Mean of $n = 14$ oocytes, assessed over 3 independent experiments. Standard errors are plotted on each curve. Statistical differences were assessed for each time point using a t-test. All curves are not statistically different from each other.

the centre of the oocyte is fast, showing that filaments in the subcortex have very different dynamics and/or structure from cytoplasmic ones (Fig. 2d). In the cytoplasm, the fluorescence decay is isotropic around the photoactivated region (Fig. 2e), suggesting that filaments in the cytoplasm are homogeneously distributed. Importantly, the diffusion of PA-GFP is comparable in the subcortex versus cytoplasm (Supplementary Fig. S1a–c and Video S3), arguing that differences in behaviour between these two regions do not originate from a diffusion hindrance. Oocytes then present at least two F-actin compartments, whose organization and/or dynamics are notably different, maybe owing to distinct nucleators.

The Arp2/3 complex nucleates the subcortex

Formin-2 is an essential nucleator of cytoplasmic F-actin[14,15]. In *fmn2*$^{-/-}$ oocytes[12] the cytoplasmic meshwork is absent at all stages whereas the subcortex is present (Fig. 3a). It is slightly thinner than in controls (3.4 μm versus 4 μm, Fig. 3b) indicating that formin-2 is a minor nucleator of the subcortex. On the basis of previous work[20,21], the Arp2/3 complex was a good candidate for subcortex nucleation. Inhibition of the Arp2/3 complex using CK666 (ref. 22) does not affect cytoplasmic F-actin (Fig. 3c). However, thickening of cortical F-actin does not occur (1.6 μm versus 4 μm, Fig. 3c,d). The Arp2/3 complex is thus a main nucleator of the subcortex.

Mos–MAPK signalling triggers nucleation of the Arp2/3-dependent subcortex

The subcortex is detectable 3 h after NEBD when the MAPKs ERK1 and ERK2 (extracellular signal-regulated kinases 1 and 2) are activated by Mos[23–25]. Cytoplasmic F-actin is present in *mos*$^{-/-}$ oocytes; however

© 2013 Macmillan Publishers Limited. All rights reserved.

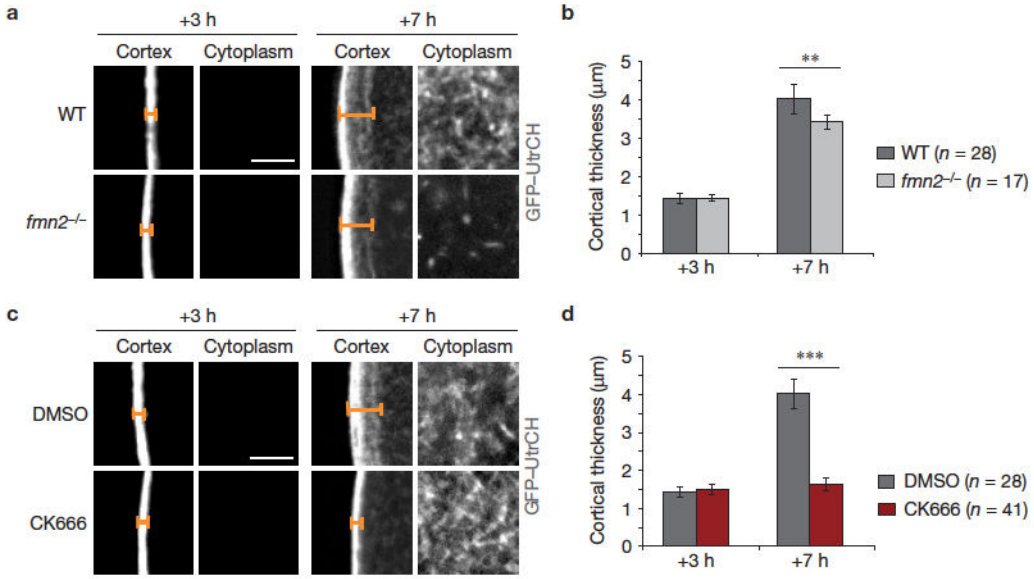


Figure 3 The Arp2/3 complex nucleates the subcortex. (**a**) Confocal spinning disc images of WT and *fmn2*$^{-/-}$ oocytes expressing GFP–UtrCH at NEBD+3 h and 7 h. One *Z* plane is shown. The orange bars indicate the subcortex. Scale bar, 5 μm. (**b**) Bar graph showing measures of the subcortex in micrometres at NEBD+3 h and NEBD+7 h in WT and *fmn2*$^{-/-}$ oocytes. Mean of $n=28$ WT oocytes and $n=17$ *fmn2*$^{-/-}$ oocytes, assessed over 5 independent experiments. Standard deviation is plotted on each bar. The statistical significance of differences was assessed with a *t*-test with Welch correction, $^{**}P$ value = 0.004. (**c**) Confocal spinning disc images of DMSO- and CK666-treated oocytes expressing GFP–UtrCH at NEBD+3 h and 7 h. To measure cortical thickness in CK666-treated oocytes, we scored only the oocytes with centrally located spindles at NEBD+7 h (see Supplementary Fig. S3). One *Z* plane is shown. The orange bars indicate the subcortex. Scale bar, 5 μm. (**d**) Bar graph showing measures of the subcortex in micrometres at NEBD+3 h and NEBD+7 h in DMSO- and CK666-treated oocytes. Mean of $n=28$ DMSO-treated oocytes and $n=41$ CK666-treated oocytes, assessed over 5 independent experiments. Standard deviation is plotted on each bar. The statistical significance of differences was assessed with a *t*-test with Welch correction, $^{***}P$ value <0.0001.

cortical F-actin thickening does not occur (1.6 μm versus 4 μm, Fig. 4a,b) as in oocytes treated with U0126, an inhibitor of the MEK1/2 kinases that mimics a *mos*$^{-/-}$ phenotype[26,27] (Supplementary Fig. S2a), showing that Mos–MAPK signalling is required for subcortex formation. We further tested whether it was sufficient for its appearance. We expressed Mos in prophase I oocytes where it is not normally expressed[23,24], leading to precocious MAPK activation and NEBD in non-permissive conditions[23–25]. At NEBD in controls, MAPK is not active, cytoplasmic F-actin is dismantled[28] and cortical F-actin thickening is not yet detectable (Figs 1a and 4c,d). On the contrary, in Mos-expressing oocytes, cytoplasmic F-actin is dismantled but a subcortex forms *de novo* (3.3 μm versus 1 μm in controls, Fig. 4c,d). Hence, the Mos–MAPK pathway is both necessary and sufficient for the nucleation of the Arp2/3-dependent subcortex.

Mos–MAPK signalling could act either directly on the Arp2/3 complex or through one of its nucleation-promoting factors. Wave2 seemed a good candidate, being phosphorylated by ERK2 leading to Arp2/3 activation[29,30] and participating in spindle migration in mouse oocytes[31]. In Prophase I WT oocytes (GV), Wave2 migrates to an apparent relative molecular mass of 80,000 (Fig. 4e). At NEBD, Wave2 migrates more slowly (Fig. 4e). Later, after MAPK activation (active ERKs migrate more slowly[23–25], Fig. 4e), Wave2 migration is further delayed, arguing for additional post-translational modifications, corresponding mostly to phosphorylations, being reversed after phosphatase treatment (Fig. 4e). In *mos*$^{-/-}$ oocytes where MAPK is not activated, ERKs migrate faster and Wave2 has a higher electrophoretic mobility when compared with controls (Fig. 4f). This MAPK-dependent phosphorylation of Wave2 could activate the Arp2/3 complex to promote cortical F-actin nucleation in mouse oocytes as it does at the leading edge of migrating cells[29].

The subcortex is essential for spindle migration in meiosis I

In *mos*$^{-/-}$ oocytes, cortical actin thickening is absent and spindle migration does not occur[7]. We thus investigated whether this subcortex played a role in spindle positioning. Compared with control dimethylsulphoxide (DMSO)-treated oocytes where more than 95% of oocytes undergo an asymmetric division, 50% of oocytes inhibited for Arp2/3 achieve a complete symmetric division (Supplementary Fig. S3a). In these symmetrically dividing oocytes, chromosome segregation occurs on time yet the spindle does not migrate to the cortex (Supplementary Fig. S3b), as observed previously[20]. Therefore, we establish a strong correlation between the presence of a thick subcortex and off-centre positioning of the meiotic spindle.

Myosin-II exclusion from the cortex decreases cortical tension during meiosis I

When mitotic cells enter M-phase, the increase in cortical tension is essential to control spindle orientation[32]. Mouse oocytes undergoing meiosis I exhibit a cortical F-actin thickening, yet cortical tension decreases[18]. We investigated further these two paradoxical observations. Using micropipette aspiration[18] (Methods and Fig. 5a and Supplementary Video S4), we measured cortical tension in different conditions: WT, *fmn2*$^{-/-}$ or *mos*$^{-/-}$ oocytes at early (NEBD+1 h) and late stages (NEBD+6 h) of meiosis I. At early stages, cytoplasmic F-actin and subcortex are absent in all cases, whereas at later stages they are both present in WT oocytes, only the subcortex in *fmn2*$^{-/-}$ oocytes and only

© 2013 Macmillan Publishers Limited. All rights reserved.

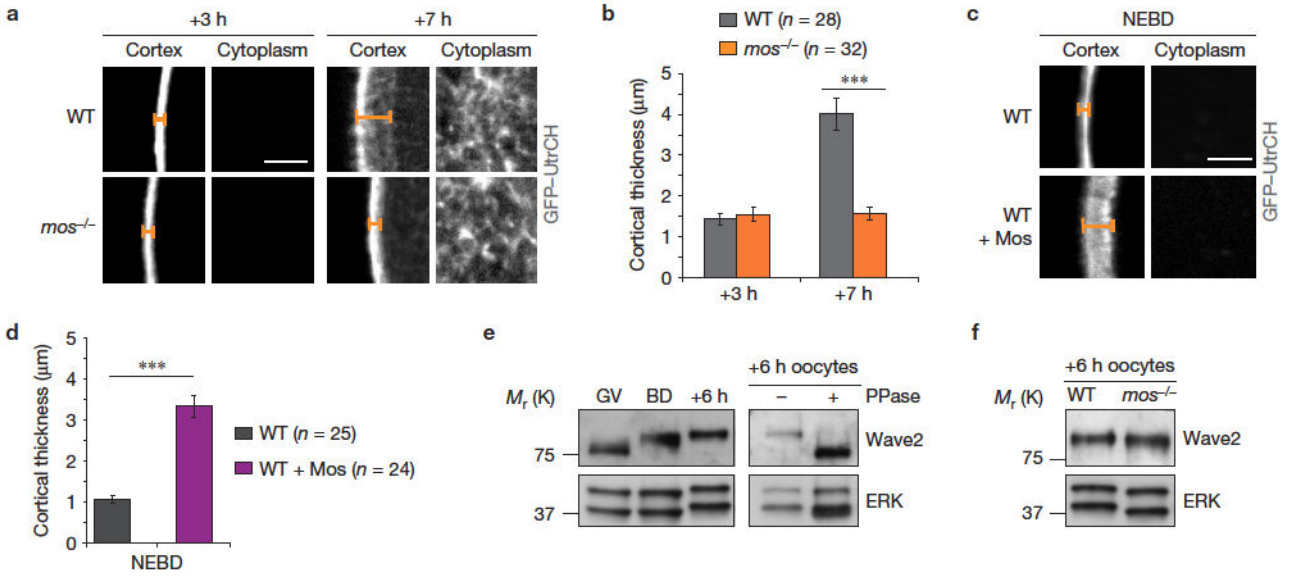


Figure 4 Mos–MAPK triggers nucleation of the Arp2/3-dependent subcortex. **(a)** Confocal spinning disc images of WT and $mos^{-/-}$ oocytes expressing GFP–UtrCH at NEBD+3 h and 7 h. One *Z* plane is shown. The orange bars indicate the subcortex. Scale bar, 5 µm. **(b)** Bar graph showing measures of the subcortex in micrometres at NEBD+3 h and NEBD+7 h in WT and $mos^{-/-}$ oocytes. Mean of $n = 28$ WT oocytes and $n = 32$ $mos^{-/-}$ oocytes, assessed over 6 independent experiments. Standard deviation is plotted on each bar. The statistical significance of differences was assessed with a *t*-test with Welch correction, $^{***}P$ value <0.0001. **(c)** Confocal spinning disc images of WT oocytes expressing either GFP–UtrCH alone or GFP–UtrCH and Mos at NEBD. Oocytes expressing GFP–UtrCH and Mos were kept in a medium non-permissive for meiotic resumption. One *Z* plane is shown. The orange bars indicate the subcortex. Scale bar, 5 µm. **(d)** Bar graph showing measures of the subcortex in micrometres at NEBD in WT oocytes expressing or not Mos. Mean of $n = 25$ WT oocytes and $n = 24$ Mos-expressing oocytes, assessed over 3 independent experiments. Standard deviation is plotted on each bar. The statistical significance of differences was assessed with a *t*-test with Welch correction, $^{***}P$ value <0.0001. **(e)** Expression of endogenous Wave2 (upper panels) and ERK (lower panels) in WT prophase I (GV), NEBD and NEBD+6 h oocytes. Where written, oocyte lysates were incubated with arctic phosphatase (PPase+). Each lane contains 30 oocytes. **(f)** Expression of endogenous Wave2 (upper panels) and ERK (lower panels) in NEBD+6 h oocytes from WT or $mos^{-/-}$ oocytes. Each lane contains 30 oocytes. Uncropped images of blots are shown in Supplementary Fig. S7. Data of **e**,**f** are representative of 6 independent experiments.

the cytoplasmic mesh in $mos^{-/-}$ oocytes (Fig. 5b). At early stages, the absolute values of cortical tension for WT, $fmn2^{-/-}$ and $mos^{-/-}$ oocytes are in the same order of magnitude (0.92, 0.72 and 0.64 nN µm^{-1} respectively) and not statistically different. They can reflect a genetic background difference. As a result, the comparison of absolute values in these three conditions might not be relevant, but rather their evolution during meiosis progression. We thus normalized the data using values of cortical tension of early stages for each condition.

As observed previously[18], in WT oocytes, cortical tension decreases between early and late stages (Fig. 5c). Myosin-II mediates cortical tension and cell shaping of mitotic cells (for review, see ref. 33). Therefore, we investigated whether myosin-II contributes to the drop in cortical tension observed. We followed endogenous myosin-II localization using a specific GFP-coupled intrabody directed against myosin-II (ref. 34) and measured the ratio between the average fluorescence signal intensity in the cortex versus the cytoplasm. If the ratio is above 1, then myosin-II is enriched cortically whereas if it is below 1, it is enriched in the cytoplasm. Myosin-II is clearly cortically enriched in prophase I oocytes (Fig. 5d,e) and then gradually disappears from the cortex ending up mostly cytoplasmic in late meiosis I (Fig. 5d,e). In $fmn2^{-/-}$ oocytes, cortical tension also decreases during meiosis I (Fig. 5c) and myosin-II gradually disappears from the cortex as for WT oocytes (Fig. 5d,e). Conversely, cortical tension remains high in $mos^{-/-}$ oocytes (Fig. 5c) and myosin-II remains cortically enriched at all stages (Fig. 5d,e) as in U0126-treated oocytes (Supplementary Fig. S2b). Myosin-II at the cortex correlates with a high cortical tension and its displacement is associated with the decrease in cortical tension occurring during meiosis I.

Mos–MAPK signalling triggers myosin-II exclusion from the cortex and cortical F-actin thickening

Myosin-II cortical displacement and cortical F-actin thickening occur concomitantly. In other cells, MAPK can phosphorylate and activate MLCK (myosin light-chain kinase), a myosin-II activator, inducing changes in actin dynamics[35–37]. To determine whether Mos–MAPK controls myosin-II localization, we measured the ratio between cortical and cytoplasmic myosin-II in oocytes expressing Mos at NEBD. In controls, myosin-II is cortically enriched (Figs 5d,e and 6a,b) whereas precocious Mos expression induces myosin-II cortical exclusion at NEBD (Fig. 6a,b). Hence, Mos–MAPK is necessary and sufficient for myosin-II cortical displacement.

Myosin-II is displaced from the cortex when the subcortex is nucleated. Therefore we examined whether the reduction of myosin-II activity at the cortex contributes to cortex thickening. We reduced myosin-II activity using ML-7 (ref. 38), which prevents spindle relocation to the cortex[15,39] (Fig. 6c) and measured cortex thickness at NEBD. Oocytes with reduced myosin-II activity, like controls, do not exhibit a thickening of their cortex (1 µm versus 1 µm, Fig. 6d,e). Reduction in cortical myosin-II activity is not sufficient to induce cortex thickening, unlike precocious MAPK activation.

© 2013 Macmillan Publishers Limited. All rights reserved.

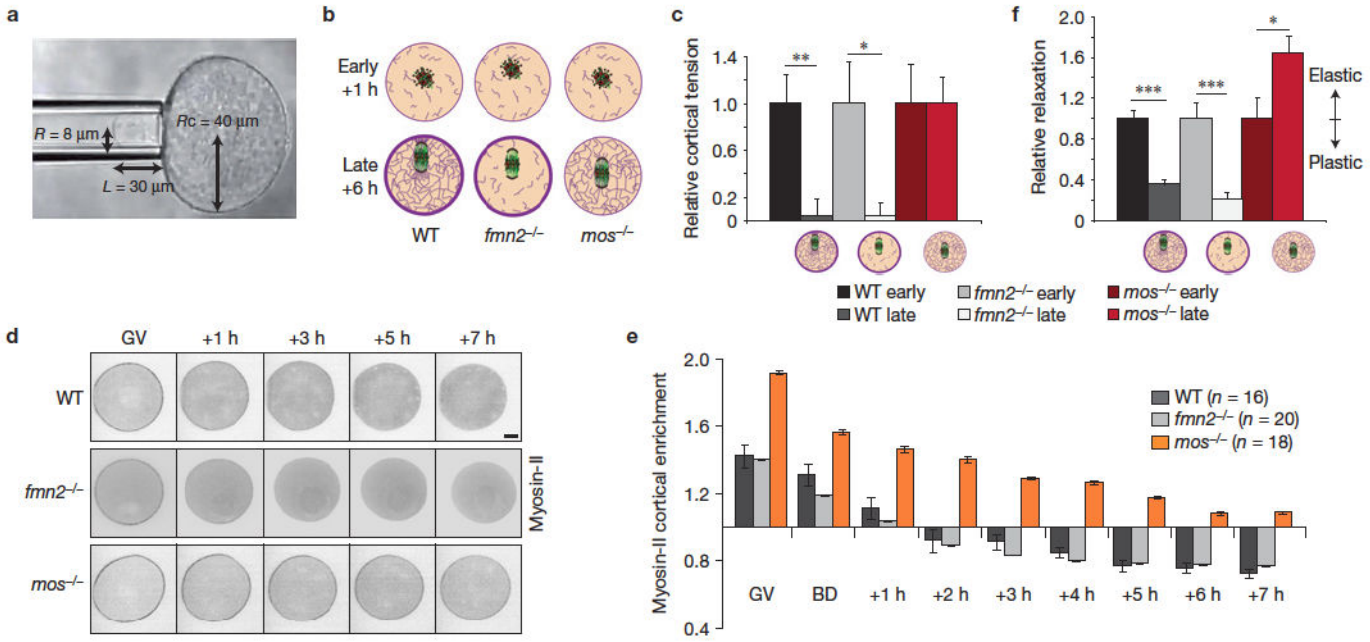


Figure 5 The cortex softens in meiosis I owing to myosin-II exclusion from the cortex that decreases cortical tension and to the the subcortex that promotes cortical plasticity. (**a**) Image of a micropipette aspiration experiment ($P_{pipet} - P_{ext} = 600$ Pa). (**b**) Schematic representation of the oocyte stages and types at which micropipette aspiration experiments were conducted. Chromosomes are shown in red, microtubules in green and actin in violet. (**c**) Bar graph showing normalized values of cortical tension at NEBD+1 h (early stage) and NEBD+6 h (late stage) in the three types of oocyte: WT, *fmn2*$^{-/-}$ and *mos*$^{-/-}$. Mean of $n = 13$ WT early stage oocytes, $n = 11$ WT late stage, $n = 11$ *fmn2*$^{-/-}$ early stage, $n = 10$ *fmn2*$^{-/-}$ late stage, $n = 9$ *mos*$^{-/-}$ early and late stages, assessed over 3 independent experiments. Standard error is plotted on each bar. The statistical significance of differences between early and late stages was assessed with a *t*-test with Welch correction (P value = 0.0043 for WT (**), 0.028 for *fmn2*$^{-/-}$ (*) and 0.96 for *mos*$^{-/-}$). (**d**) Time-lapse spinning disc confocal microscopy of WT, *fmn2*$^{-/-}$ and *mos*$^{-/-}$ oocytes expressing SF9–GFP (myosin-II intrabody, black) observed every 2 h from GV until NEBD+7 h. One *Z* plane is shown. Scale bar, 10 µm. (**e**) Bar graph showing the ratio between the average intensities of cortical and cytoplasmic myosin-II at different stages in WT, *fmn2*$^{-/-}$ and *mos*$^{-/-}$ oocytes. For each oocyte, 6 measurements were taken in the cortex and 6 in the cytoplasm. Mean of $n = 16$ WT oocytes, $n = 20$ *fmn2*$^{-/-}$ oocytes and $n = 18$ *mos*$^{-/-}$ oocytes, assessed over 3 independent experiments. Standard error is plotted on each bar. The statistical significance of differences presented in Supplementary Table S1 was assessed with a *t*-test with Welch correction. (**f**) Bar graph showing normalized relaxation ratio at NEBD+1 h (early stage) and NEBD+6 h (late stage) in WT, *fmn2*$^{-/-}$ and *mos*$^{-/-}$ oocytes. Mean of $n = 23$ WT early stage oocytes, $n = 11$ WT late stage, $n = 15$ *fmn2*$^{-/-}$ early stage, $n = 14$ *fmn2*$^{-/-}$ late stage, $n = 11$ *mos*$^{-/-}$ early stage and $n = 21$ *mos*$^{-/-}$ late stage, assessed over 3 independent experiments. Standard error is plotted on each bar. The statistical significance of differences between early and late stages was assessed with a *t*-test with Welch correction (P value < 0.0001 for WT (***), =0.0003 for *fmn2*$^{-/-}$ (***) and =0.0267 for *mos*$^{-/-}$ (*)).

The subcortex promotes cortical plasticity

To better characterize the mechanical properties of this subcortical layer, we measured the ability of oocytes to recover from their deformation after micropipette aspiration. Oocytes that go back from their original spherical shape exhibit an elastic behaviour whereas those remaining deformed after pressure release exhibit a plastic behaviour (Supplementary Video S5). At early stages, the deformation ratio (see Methods) for the WT, *fmn2*$^{-/-}$ and *mos*$^{-/-}$ oocytes is different but in the same order of magnitude (0.63, 0.4 and 0.38 respectively). Thus, we normalized the data setting the ratio value to 1 for all cases at early stages (Fig. 5f). In this scenario, an increase of the normalized ratio corresponds to a more elastic behaviour whereas a decrease reveals a plastic behaviour.

WT late stage oocytes have a more plastic behaviour when compared with early stages (Fig. 5f). *fmn2*$^{-/-}$ oocytes, like WT cells, are more plastic at late stages when compared with early stages (Fig. 5f). On the contrary, *mos*$^{-/-}$ oocytes are more elastic at later stages when compared with earlier stages (Fig. 5f), suggesting that the cytoplasmic mesh increases elasticity. On the contrary, cortical F-actin thickening promotes cortical plasticity.

A soft cortex is required for spindle migration in meiosis I

Cortex mechanics depend both on myosin-II cortical exclusion that decreases cortical tension and on the subcortex that promotes cortical plasticity. Myosin-II activity[15,39] (Fig. 6c) and cortical F-actin thickening[20] (Supplementary Fig. S3b) are both required for spindle migration; we hence tested whether cortex softening was required for spindle positioning. We artificially stiffened the cortex using concanavalin A (ConA), a tetravalent lectin that crosslinks the cell surface through binding to membrane glycosylated proteins[5,18,40–43]. The spindle remains central in 80% of ConA-treated cells whereas it does so only in 5% of the controls (Fig. 6f,g). Eventually, a division occurs at the right time in ConA-treated oocytes (Supplementary Fig. S4a) but with blebbing (Supplementary Fig. S4b–c), arguing that ConA treatment does affect cortical tension[44]. Actin architecture and myosin-II localization are similar with or without ConA (Supplementary Fig. S4d–e), suggesting that the phenotype induced by ConA treatment is not due to aberrant actin structures. Furthermore, only 13% of oocytes present a central spindle (Fig. 6f,g) and 27% bleb when dividing (Supplementary Fig. S4b–c) after treatment with Succinyl-ConA (SuccConA), a lectin

© 2013 Macmillan Publishers Limited. All rights reserved.

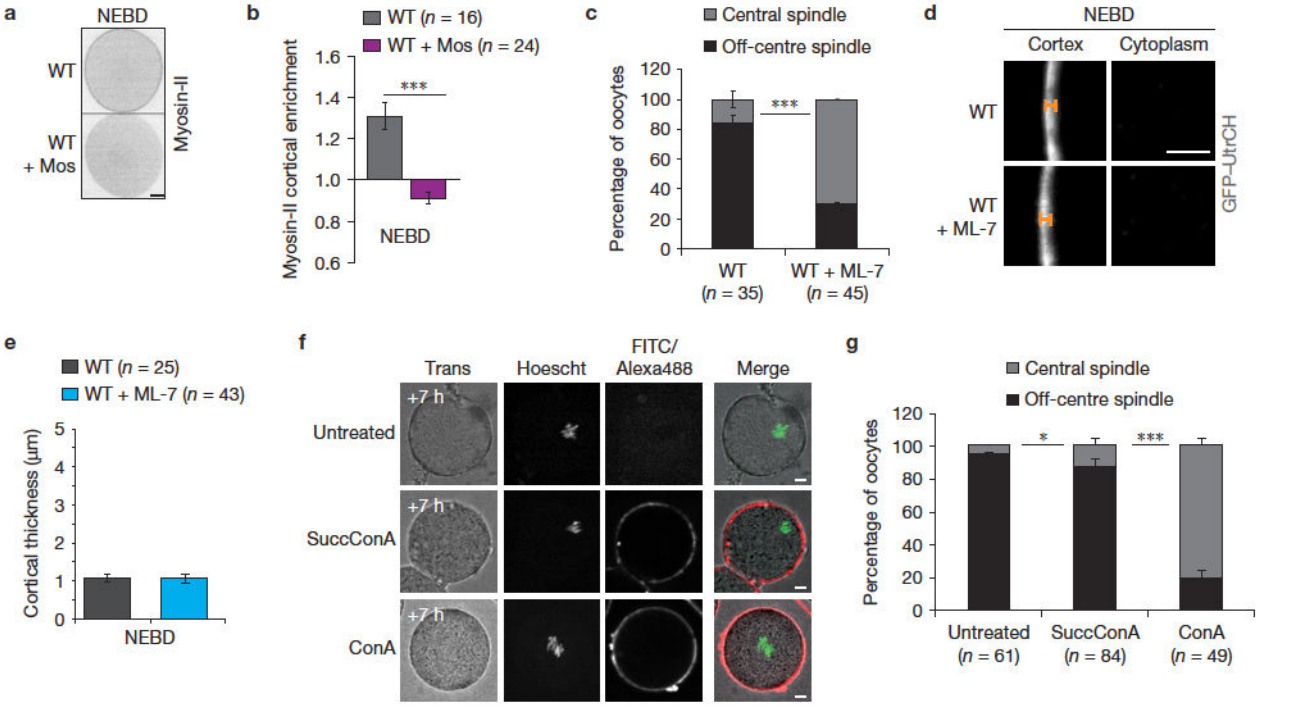


Figure 6 Mos–MAPK triggers myosin-II exclusion from the cortex and nucleation of the subcortex resulting in cortex softening, required for spindle migration in meiosis I. **(a)** Confocal spinning disc images of WT oocytes expressing a myosin-II intrabody alone or together with Mos at NEBD. One *Z* plane is shown. Scale bar, 10 µm. **(b)** Bar graph showing the ratio between the average intensities of cortical and cytoplasmic myosin-II at different stages. For each oocyte, 6 measurements were taken in the cortex and in the cytoplasm. Mean of $n = 16$ WT and $n = 24$ WT Mos-expressing oocytes, assessed over 3 independent experiments. Standard error is plotted on each bar. The statistical significance of differences was assessed with a *t*-test with Welch correction, $^{***}P$ value <0.0001. **(c)** Bar graph showing the percentage of central and off-centre meiotic I spindles at NEBD + 7 h in WT oocytes treated or not with ML-7. Mean of $n = 35$ WT oocytes and $n = 45$ WT oocytes treated with ML-7, assessed over 3 independent experiments. Standard deviation is plotted on each bar. The statistical significance of differences was assessed with a *t*-test with Welch correction, $^{***}P$ value <0.0001. **(d)** Higher magnification of confocal spinning disc images of NEBD WT oocytes expressing GFP–UtrCH treated or not with ML-7. One *Z* plane is shown. The orange bars indicate the subcortex. Scale bar, 5 µm. **(e)** Bar graph showing measures of the subcortex in micrometres at NEBD in oocytes treated or not with ML-7. Mean of $n = 25$ WT oocytes and $n = 43$ WT oocytes treated with ML-7, assessed over 4 independent experiments. Standard deviation is plotted on each bar. The values are not statistically different using a *t*-test. **(f)** Confocal spinning disc images of untreated, SuccConA- and ConA-treated oocytes at NEBD + 7 h. SuccConA is coupled to Alexa488 whereas ConA is coupled to FITC. Chromosomes are marked with Hoechst live. Scale bar, 10 µm. **(g)** Bar graph showing the percentage of central and off-centre meiotic I spindles in untreated, SuccConA- and ConA-treated oocytes at NEBD + 7 h. Mean of $n = 61$ untreated oocytes, $n = 84$ SuccConA-treated oocytes and $n = 49$ ConA-treated oocytes, assessed over 3 independent experiments. Standard deviation is plotted on each bar. The statistical significance of differences was assessed with a *t*-test, $^{*}P$ value = 0.042 untreated versus SuccConA and $^{***}P$ value <0.0001 SuccConA versus ConA.

with reduced crosslinking capacity[43,45]. In conclusion, the cortex has to become softer during meiosis I to allow spindle migration.

Mathematical modelling of meiosis I spindle motion and impact of cortical tension on velocity

We converted our observations into a theoretical model (Supplementary Fig. S5 and Methods). Our model shows the following. First, the cortex needs to have a minimum stiffness, otherwise the spindle will never make it to the cortex. Second, the most favourable situation (WT cells) corresponds to an intermediate stiffness. In this case the cortex does induce acceleration of spindle movement. Third, if the cortex is too stiff ($mos^{-/-}$ oocytes), the velocity of spindle motion decays owing to weaker pulling forces. The cell having a finite time to achieve meiosis I, a too slow spindle motion will prevent spindle asymmetric positioning before anaphase.

DISCUSSION

We document an Arp2/3-dependent cortical F-actin thickening required for spindle migration to the cortex. We show that cortical tension decreases during meiosis I owing to myosin-II exclusion from the cortex and that cortical F-actin thickening provides cortical plasticity. These two events are triggered by Mos–MAPK signalling and soften the cortex. Finally, a soft cortex is required for spindle positioning to the oocyte cortex (Supplementary Fig. S6).

It is interesting to consider why a soft cortex would be important for spindle positioning. In mouse oocytes, the asymmetry is set by a slight off-centring of the nucleus in prophase I. At NEBD cytoplasmic F-actin is dismantled; thus, the spindle can bipolarize in the absence of physical constraints[28]. It takes 3 h for the spindle to bipolarize[46,47], during which both cytoplasmic and subcortical F-actin start to form. The spindle is then progressively embedded in an elastic mesh connected to the subcortex through actin filaments emanating from the actin cage poles[14,15] (Fig. 1c and Supplementary Fig. S6a). The cytoplasmic mesh does not contract isotropically as in starfish oocytes[48]. Instead, the forces at play for spindle migration are generated at spindle poles where active myosin-II (ref. 15) is localized (Fig. 6c), from overlapping filaments pulling the poles towards the cortex. The amount of force depends on the spindle–cortex distance, such that the smaller the distance, the

© 2013 Macmillan Publishers Limited. All rights reserved.

more overlapping filaments and the larger the pulling force. As the spindle always forms slightly off-centre[7], the pulling forces are more important at the pole closest to the cortex (Supplementary Fig. S6a). This small imbalance of forces is sufficient to break the symmetry but not amplify it. However, as the spindle moves in the direction of the closest cortex and the subcortex thickens, the force in that direction increases, whereas the force opposing the motion decreases, thereby the spindle accelerates towards the cortex[15,49] amplifying the imbalance of forces. In *mos*$^{-/-}$ oocytes the cortex remains stiff and is not able to deform in response to the pulling forces (Supplementary Fig. S6b and Fig. 5c,f). In such oocytes, the pulling force necessary to move the spindle would have to be much higher than in WT oocytes, the original imbalance of forces lacking amplification (Supplementary Fig. S5).

Eventually reduction in cortical tension might favour oocytes extrusion from the ovary during ovulation. Strikingly, *mos*$^{-/-}$ oocytes are not extruded from the ovary but fail to arrest in metaphase II and activate parthenogenetically, inducing ovarian teratomas[50,51]. Whereas most normal cells undergoing mitosis present a stiff cortex, mouse oocytes soften their cortex, like malignant cells do. The softening of invasive tumour cells enhances their capacity to escape primary tumours[52–54]. Oocytes might use the same strategy to break free from the ovaries, a process coordinated by the Mos–MAPK pathway. Mos–MAPK signalling could act as a quality control mechanism to ensure that only oocytes that have undergone asymmetric division are extruded from the ovary. □

METHODS

Methods and any associated references are available in the online version of the paper.

Note: Supplementary Information is available in the online version of the paper

ACKNOWLEDGEMENTS

We thank T. Pollard (Yale University, USA) for providing the CK666 and F. Perez (Curie Institute, France) for providing SF9-expressing plasmids. We thank J. Teillon for helping set up the photoactivation experiments. We thank C. Klein for his help with the analysis of the photoactivation data. We also thank A. Roux, M. Piel, A. Echard, A. Gautreau, E. Derivery and R. Li for helpful discussions. This work was supported by grants from the Ligue Nationale Contre le Cancer (EL2009-EL2012/LNCC/MHV) and from the Agence Nationale pour la Recherche (ANR-08-BLAN-0136-01 to MHV and ANR-08-BLAN-0012-12 to CS). A. Chaigne is a recipient of a fellowship from the Ecole Normale Supérieure (ENS) Paris. C. Campillo acknowledges financial support from the Association pour la Recherche contre le Cancer (ARC). N. S. Gov wishes to thank the Mayent-Rothschild Foundation for the Visiting Professor grant at the Curie Institute.

AUTHOR CONTRIBUTIONS

A.C., M-H.V. and M-E.T. designed the experiments, interpreted the results and wrote the manuscript. A.C., C.U-D. and M.E.T. carried out most of the experiments. J.A. performed the preliminary observations that started the project. M.A. assisted in the photoactivation experiments. I.Q. assisted in genotyping the animals. A.C. and C.C. carried out the micropipette experiments. C.C., P.N. and C.S. designed the micropipette experiments and interpreted the results. N.S.G. and R.V. designed the physical model. M.E.T. and M.H.V. conceived and supervised the project.

COMPETING FINANCIAL INTERESTS

The authors declare no competing financial interests.

Published online at www.nature.com/doifinder/10.1038/ncb2799
Reprints and permissions information is available online at www.nature.com/reprints

1. Gillies, T. E. & Cabernard, C. Cell division orientation in animals. *Curr. Biol* **21,** R599–R609 (2011).
2. Moore, J. K. & Cooper, J. A. Coordinating mitosis with cell polarity: molecular motors at the cell cortex. *Semin. Cell. Dev. Biol.* **21,** 283–289 (2010).
3. Thery, M. & Bornens, M. Cell shape and cell division. *Curr. Opin. Cell. Biol.* **18,** 648–657 (2006).
4. Carreno, S. *et al.* Moesin and its activating kinase Slik are required for cortical stability and microtubule organization in mitotic cells. *J. Cell. Biol.* **180,** 739–746 (2008).
5. Kunda, P., Pelling, A. E., Liu, T. & Baum, B. Moesin controls cortical rigidity, cell rounding, and spindle morphogenesis during mitosis. *Curr. Biol.* **18,** 91–101 (2008).
6. Kunda, P. & Baum, B. The actin cytoskeleton in spindle assembly and positioning. *Trends Cell. Biol.* **19,** 174–179 (2009).
7. Verlhac, M. H., Lefebvre, C., Guillaud, P., Rassinier, P. & Maro, B. Asymmetric division in mouse oocytes: with or without Mos. *Curr. Biol.* **10,** 1303–1306 (2000).
8. FitzHarris, G., Marangos, P. & Carroll, J. Changes in endoplasmic reticulum structure during mouse oocyte maturation are controlled by the cytoskeleton and cytoplasmic dynein. *Dev. Biol.* **305,** 133–144 (2007).
9. Halet, G. & Carroll, J. Rac activity is polarized and regulates meiotic spindle stability and anchoring in mammalian oocytes. *Dev. Cell.* **12,** 309–317 (2007).
10. Brunet, S. & Verlhac, M. H. Positioning to get out of meiosis: the asymmetry of division. *Hum. Reprod. Update.* **1,** 68–75 (2011).
11. Szollosi, D., Calarco, P. & Donahue, R. P. Absence of centrioles in the first and second meiotic spindles of mouse oocytes. *J. Cell. Sci.* **11,** 521–541 (1972).
12. Leader, B. *et al.* Formin-2, polyploidy, hypofertility and positioning of the meiotic spindle in mouse oocytes. *Nat. Cell. Biol.* **4,** 921–928 (2002).
13. Dumont, J. *et al.* Formin-2 is required for spindle migration and for the late steps of cytokinesis in mouse oocytes. *Dev. Biol.* **301,** 254–265 (2007).
14. Azoury, J. *et al.* Spindle positioning in mouse oocytes relies on a dynamic meshwork of actin filaments. *Curr. Biol.* **18,** 1514–1519 (2008).
15. Schuh, M. & Ellenberg, J. A new model for asymmetric spindle positioning in mouse oocytes. *Curr. Biol.* **18,** 1986–1992 (2008).
16. Li, H., Guo, F., Rubinstein, B. & Li, R. Actin-driven chromosomal motility leads to symmetry breaking in mammalian meiotic oocytes. *Nat. Cell. Biol.* **10,** 1301–1308 (2008).
17. Pfender, S., Kuznetsov, V., Pleiser, S., Kerkhoff, E. & Schuh, M. Spire-type actin nucleators cooperate with formin-2 to drive asymmetric oocyte division. *Curr. Biol.* **21,** 955–960 (2011).
18. Larson, S. M. *et al.* Cortical mechanics and meiosis II completion in mammalian oocytes are mediated by myosin-II and Ezrin-Radixin-Moesin (ERM) proteins. *Mol. Biol. Cell* **21,** 3182–3192 (2010).
19. Burkel, B. M., von Dassow, G. & Bement, W. M. Versatile fluorescent probes for actin filaments based on the actin-binding domain of utrophin. *Cell. Motil. Cytoskeleton.* **64,** 822–832 (2007).
20. Sun, S. C. *et al.* Arp2/3 complex regulates asymmetric division and cytokinesis in mouse oocytes. *PLoS One* **6,** e18392 (2011).
21. Yi, K. *et al.* Dynamic maintenance of asymmetric meiotic spindle position through Arp2/3-complex-driven cytoplasmic streaming in mouse oocytes. *Nat. Cell. Biol.* **13,** 1252–1258 (2011).
22. Nolen, B. J. *et al.* Characterization of two classes of small molecule inhibitors of Arp2/3 complex. *Nature* **460,** 1031–1034 (2009).
23. Verlhac, M. H., de Pennart, H., Maro, B., Cobb, M. H. & Clarke, H. J. MAP kinase becomes stably activated at metaphase and is associated with microtubule-organizing centers during meiotic maturation of mouse oocytes. *Dev. Biol.* **158,** 330–340 (1993).
24. Verlhac, M. H. *et al.* Mos is required for MAP kinase activation and is involved in microtubule organization during meiotic maturation in the mouse. *Development* **122,** 815–822 (1996).
25. Verlhac, M. H. *et al.* Mos activates MAP kinase in mouse oocytes through two opposite pathways. *EMBO J.* **19,** 6065–6074 (2000).
26. Phillips, K. P. *et al.* Inhibition of MEK or cdc2 kinase parthenogenetically activates mouse eggs and yields the same phenotypes as Mos(-/-) parthenogenotes. *Dev. Biol.* **247,** 210–223 (2002).
27. Tong, C. *et al.* Effects of MEK inhibitor U0126 on meiotic progression in mouse oocytes: microtuble organization, asymmetric division and metaphase II arrest. *Cell. Res.* **13,** 375–383 (2003).
28. Azoury, J., Lee, K. W., Georget, V., Hikal, P. & Verlhac, M. H. Symmetry breaking in mouse oocytes requires transient F-actin meshwork destabilization. *Development* **138,** 2903–2908 (2011).
29. Mendoza, M. C. *et al.* ERK-MAPK drives lamellipodia protrusion by activating the WAVE2 regulatory complex. *Mol. Cell.* **41,** 661–671 (2011).
30. Nakanishi, O., Suetsugu, S., Yamazaki, D. & Takenawa, T. Effect of WAVE2 phosphorylation on activation of the Arp2/3 complex. *J. Biochem.* **141,** 319–325 (2007).
31. Sun, S. C. *et al.* WAVE2 regulates meiotic spindle stability, peripheral positioning and polar body emission in mouse oocytes. *Cell. Cycle* **10,** 1853–1860 (2011).
32. Fink, J. *et al.* External forces control mitotic spindle positioning. *Nat. Cell. Biol.* **13,** 771–778 (2011).
33. Lecuit, T., Lenne, P. F. & Munro, E. Force generation, transmission, and integration during cell and tissue morphogenesis. *Annu. Rev. Cell. Dev. Biol.* **27,** 157–184 (2011).
34. Nizak, C. *et al.* Recombinant antibodies against subcellular fractions used to track endogenous Golgi protein dynamics *in vivo*. *Traffic* **4,** 739–753 (2003).
35. Klemke, R. L. *et al.* Regulation of cell motility by mitogen-activated protein kinase. *J. Cell. Biol.* **137,** 481–492 (1997).

© 2013 Macmillan Publishers Limited. All rights reserved.

36. Nguyen, D. H. *et al.* Myosin light chain kinase functions downstream of Ras/ERK to promote migration of uro kinase-type plasminogen activator-stimulated cells in an integrin-selective manner. *J. Cell. Biol.* **146,** 149–64 (1999).
37. Deng, M., Williams, C. J. & Schultz, R. M. Role of MAP kinase and myosin light chain kinase in chromosome-induced development of mouse egg polarity. *Dev. Biol.* **278,** 358–366 (2005).
38. Saitoh, M., Ishikiwa, T., Matsushima, S., Naka, M. & Hidaka, H. Selective inhibition of catalytic activity of smooth muscle myosin light chain kinase. *J. Biol. Chem.* **262,** 7796–7801 (1987).
39. Simerly, C., Nowak, G., de Lanerolle, P. & Schatten, G. Differential expression and functions of cortical myosin IIA and IIB isotypes during meiotic maturation, fertilization, and mitosis in mouse oocytes and embryos. *Mol. Biol. Cell.* **9,** 2509–2525 (1998).
40. Pasternak, C. & Elson, E. L. Lymphocyte mechanical response triggered by cross-linking surface receptors. *J. Cell. Biol.* **100,** 860–872 (1985).
41. Pasternak, C., Spudich, J. A. & Elson, E. L. Capping of surface receptors and concomitant cortical tension are generated by conventional myosin. *Nature* **341,** 549–551 (1989).
42. Dai, J., Ting-Beall, H. P., Hochmuth, R. M., Sheetz, M. P. & Titus, M. A. Myosin I contributes to the generation of resting cortical tension. *Biophys. J.* **77,** 1168–1176 (1999).
43. Rosenblatt, J., Cramer, L. P., Baum, B. & McGee, K. M. Myosin II-dependent cortical movement is required for centrosome separation and positioning during mitotic spindle assembly. *Cell* **117,** 361–372 (2004).
44. Sedzinski, J. *et al.* Polar actomyosin contractility destabilizes the position of the cytokinetic furrow. *Nature* **476,** 462–466 (2011).
45. Canman, J. C. & Bement, W. M. Microtubules suppress actomyosin-based cortical flow in *Xenopus* oocytes. *J. Cell. Sci.* **110,** 1907–1917 (1997).
46. Dumont, J. *et al.* A centriole- and RanGTP-independent spindle assembly pathway in meiosis I of vertebrate oocytes. *J. Cell. Biol.* **176,** 295–305 (2007).
47. Breuer, M. *et al.* HURP permits MTOC sorting for robust meiotic spindle bipolarity, similar to extra centrosome clustering in cancer cells. *J. Cell. Biol.* **191,** 1251–1260 (2010).
48. Mori, M. *et al.* Intracellular transport by an anchored homogeneously contracting F-actin meshwork. *Curr. Biol.* **21,** 606–611 (2011).
49. Yi, K. *et al.* Sequential actin-based pushing forces drive meiosis I chromosome migration and symmetry breaking in oocytes. *J. Cell. Biol.* **200,** 567–576 (2013).
50. Colledge, W. H., Carlton, M. B., Udy, G. B. & Evans, M. J. Disruption of c-mos causes parthenogenetic development of unfertilized mouse eggs. *Nature* **370,** 65–68 (1994).
51. Hashimoto, N. *et al.* Parthenogenetic activation of oocytes in c-mos-deficient mice. *Nature.* **370,** 68–71 (1994).
52. Guck, J. *et al.* Optical deformability as an inherent cell marker for testing malignant transformation and metastatic competence. *Biophysical. J.* **88,** 3689–3698 (2005).
53. Suresh, S. *et al.* Connections between single-cell biomechanics and human disease states: gastrointestinal cancer and malaria. *Acta. Biomaterialia* **1,** 15–30 (2005).
54. Hou, H. *et al.* Deformability study of breast cancer cells using microfluidics. *Biomedical. Microdev.* **11,** 557–564 (2009).

© 2013 Macmillan Publishers Limited. All rights reserved.

METHODS

Oocyte collection, culture and micro-injection. Oocytes were collected from 11-week-old OF1 (WT), *fmn2*$^{-/-}$ or *mos*$^{-/-}$ female mice as previously described[55] and maintained in prophase I arrest (GV stage) in M2+BSA medium supplemented with 1 μM milrinone[56]. At this stage, they were micro-injected with cRNAs using an Eppendorf Femtojet micro-injector. GV stage oocytes were kept for 2–3 h in prophase I arrest to allow expression of fusion proteins. Meiosis resumption was triggered by releasing oocytes into milrinone-free M2+BSA medium. All live culture and imaging were carried out under oil at 37 °C.

Plasmids and *in vitro* transcription of cRNAs. We used the following constructs: pspe3–GFP–UtrCH (ref. 14), pCS2–PaGfp–UtrCH (ref. 19), pRN3–histone–RFP (ref. 57), pRN3–Mos (ref. 25) and pRN3–SF9–GFP (derived from ref. 34). *In vitro* synthesis of capped cRNAs was performed as previously described[58]. cRNAs were centrifuged at 4 °C for 45 min at 20,000*g* before micro-injection.

Drug treatments. The stock solution of CK666 (gift from T. Pollard and Calbiochem, Ref. 182515) was diluted at 100 mM in DMSO and stored at −80 °C. It was used on oocytes at 200 μM starting from NEBD + 3 h. Control experiments were performed in M2 + BSA medium with equivalent dilutions of DMSO or with an inactive analogue of CK666, CK689 (Calbiochem, Ref. 182517), in separate dishes (the drug diffuses in the oil).

U0126 (Calbiochem, Ref. 662005) was diluted at 10 mM in DMSO and stored at −20 °C. It was used on oocytes at 20 μM from prophase I.

ML-7 (Sigma, Ref. I2764) was diluted at 10 mM in DMSO and stored at −20°C. It was used on oocytes at 30 μM from prophase I.

Live imaging. Spinning disc images were acquired at 37 °C in M2 + BSA medium using a Plan-APO ×40/1.25 NA objective on a Leica DMI6000B microscope enclosed in a thermostatic chamber (Life Imaging Service) equipped with a CoolSnap HQ2/CCD (charge-coupled device) camera (Princeton Instruments) coupled to a Sutter filter wheel (Roper Scientific) and a Yokogawa CSU-X1-M1 spinning disc. Metamorph software (Universal Imaging) was used to collect data and ImageJ (NIH) to analyse and process data.

Photoactivation experiments. The photoactivation experiments were conducted at 37 °C in M2 + BSA medium using a Plan-APO ×60/1.4 NA objective on a Nikon Eclipse TL microscope enclosed in a thermostatic chamber equipped with an Evolve EMCCD camera (Photometrics) coupled to a Sutter filter wheel (Roper Scientific) and a Yokogawa CSUX1-A1 spinning disc. Photoactivation measurements were performed on oocytes expressing PA-GFP–UtrCH or PA-GFP using the following routine: 20 pre-bleach scans every 100 ms with full power of the 491 nm laser line, point-bleach function with full power of the 405 nm laser line for 200 ms and then 250 post-bleach scans every 100 ms with full power of the 491 nm laser line. The diameter of the photoactivated region is 5 μm. The fluorescence intensity quantification was performed using the Metamorph software (Universal Imaging). PA data were analysed as described below.

Analysis of the photoactivation experiments. Normalization of the measured fluorescence intensities was performed using the Microsoft Excel software. The statistical analysis was performed using the GraphPad Prism software. As the expression levels of PA-GFP–UtrCH and PA-GFP vary from one experiment to another, we normalized every point in each experiment by the first post-bleach point.

Cortical thickness measurements. The overall thickness (referred as the subcortex) of both the cortical outer bright layer (which is constant throughout meiosis) and the cortical inner dimmer layer (which increases during meiosis I) was measured manually in Metamorph (Fig. 1a orange bar). All measures were taken on one focal plane corresponding to the oocyte's biggest diameter to avoid projection artefacts. At least four measurements were taken per cell at various locations excluding the region overhanging the spindle. The contrast between cytoplasmic and cortical actin is strong and cytoplasmic F-actin is less apparent in conditions of subcortex visualization (Fig. 1a upper and lower panels).

Immunoblotting and antibodies. Immunoblotting of mouse oocytes was performed as described previously[58]. We used the following antibodies: the anti-ERK antibody (sc-94; Santa Cruz Biotechnology, 1:1000) and the anti-Wave2 antibody (D2C8; Cell Signaling, 1:750).

Dephosphorylation assay. Just after collection and lysis, oocytes were incubated with or without 5 U of antarctic phosphatase (New England Biolabs) at 37 °C for 1 h and then processed for immunoblotting.

Micropipette aspiration experiments. The zona pellucida of oocytes was removed using acid tyrod (pH = 2.3), and oocytes were analysed at desired stages. Oocytes were loaded onto a chamber equilibrated with M2 + BSA medium. A glass micropipette of a diameter 5 times smaller than the oocyte diameter (Fig. 5a and Supplementary Video S4) was connected to a water reservoir of adjustable height to apply a defined aspiration pressure. Zero aspiration pressure was set before each experiment by checking the absence of visible flow inside the pipette. Observations were made through an inverted microscope (Axiovert 200, Zeiss) equipped with a ×40 immersion oil objective (Neofluar 1.3 NA) and connected to a CCD camera (XC-ST70CE, Sony). For every applied pressure, we monitored the length L of the oocyte portion aspirated in the pipette as a function of time and derived the speed dL/dt at which the oocyte cortex enters the pipette. Then, we extrapolated the critical aspiration pressure ΔP_c at which $dL/dt = 0$ from the plot dL/dt versus the aspiration pressure. To obtain the cortical tension T_c, we used the viscous drop model previously used for cells[59],

$$T_c = \frac{R\Delta P_c}{2(1-\frac{R}{R_c})}$$

where R is the pipette radius and R_c is the cell radius.

At early stages, the absolute values of cortical tension for WT, *fmn2*$^{-/-}$ and *mos*$^{-/-}$ oocytes are 0.92, 0.72 and 0.64 nN μm^{-1} respectively and 0.034, 0.03 and 0.65 nN μm^{-1} at late stages.

For relaxation measurements, quantitative description was achieved by measuring the deformation ratio between the change in length (before pressure release and 1 min after pressure release) and the initial tongue length (before pressure release). If the tongue disappears after pressure release, the system is elastic and the ratio is 1. If the tongue remains, the ratio is 0.

At early stages, the absolute values of the deformation ratio for WT, *fmn2*$^{-/-}$ and *mos*$^{-/-}$ oocytes are 0.63, 0.4 and 0.38 respectively and 0.22, 0.09 and 0.63 at late stages.

Concanavalin A and succinyl-concanavalin A treatments. Concanavalin A–FITC (Sigma, Ref. C7642) and succinyl-concanavalin A–Alexa488 (Invitrogen, Ref. C211401) were diluted in M2 + PVP medium at a final concentration of 100 μg ml^{-1}. Oocytes were incubated in these solutions at NEBD + 1 h on glass slides previously sonicated in a solution containing 1.8 M NaOH in 57% ethanol and coated with 0.067% agarose to avoid oocyte sticking. The glass slides were extensively rinsed after sonication. Hoechst 33342 (Invitrogen, Ref. H3570) was added at NEBD + 6 h 30 at a concentration of 5 ng ml^{-1} to label the chromosomes.

Modelling the motion of the spindle. We describe here a theoretical model for the motion of the spindle during meiosis I in mouse oocytes. The spindle moves in one dimension along its long axis, which we call axis $(0,x)$, 0 being the centre of the oocyte and x the position of the centre of gravity of the spindle at a given time. L represents the distance between the closest spindle pole and the cortex before the spindle starts migrating (Supplementary Fig. S5a). We model the spindle motion on the basis of the following main ingredients. First, the spindle is connected to the cortex of the oocyte through actin filaments that emanate from the actin cage surrounding the spindle. Second, the force is produced when these actin filaments overlap with the actin network at the cortex, allowing myosin-II contractility to produce tension in the filaments and induce a pulling force from the spindle towards the cortex, because myosin-II is localized at spindle poles.

With these assumptions, it is clear that the force pulling the spindle in one particular direction is proportional to the overlap between the filaments that connect the spindle and the cortex along that direction. The amount of overlap depends on the spindle–cortex distance, such that the smaller this separation, the more filaments reach from the spindle to the cortex, and the larger the pulling force. When the spindle is at the cell centre, the forces pulling it along opposite directions almost balance, and only a small fluctuation can break the symmetry. However, as the spindle moves off-centre in the direction of the original small deviation, the force in that direction increases, whereas the force opposing the motion decreases, thereby the spindle accelerates towards the cortex.

We can convert the above scenario into a mathematical model, as follows. The balance of forces acting on the spindle (at position x) is simply:

$$\gamma v = F_+ - F_- \quad (1)$$

where v is the speed of the spindle, F are the forces in the two opposing directions and γ is the effective friction coefficient of the spindle as it moves through the cytoplasm.

© 2013 Macmillan Publishers Limited. All rights reserved.

DOI: 10.1038/ncb2799

The spindle starts close to the centre of the oocyte $x \approx 0$, and is then pulled towards the cortex, which is placed at a distance L.

The same force pulls the cortical layer and deforms it, as a simple elastic response:

$$k\delta h_{\pm} = F_{\pm} \tag{2}$$

where k describes the elastic stiffness of the cortex and δh are the local deformations of the cortex.

The total force on the spindle is therefore simply:

$$F_{\text{tot}} = F_{+} - F_{-} = k(\delta h_{+} - \delta h_{-}) \tag{3}$$

In this model we assume that there are filaments starting at the spindle and that they have an exponential distribution of the form:

$$P(l) = \frac{1}{l_0} e^{-\frac{l}{l_0}}$$

where l_0 is the average filament (or bundle) length.

The overlap of this distribution with the cortical layer can be calculated as the integral of $P(l)$ for l greater or equal to the spindle–cortex distance. This overlap determines the force that the myosin-II motors can exert, as they act when anti-parallel filaments overlap:

$$F_{\pm} = \beta e^{-\frac{(L \pm x - \delta h_{\pm})}{l_0}} \tag{4}$$

where β is some proportionality factor that describes the overall myosin-II motor activity.

We see that the force increases as the spindle approaches the cortex, and as the cortex is deformed towards the pulling spindle.

Using equations (2) and (4) we get:

$$\delta h_{\pm} = -l_0 W\left[-\frac{\beta}{kl_0} e^{-\frac{L \pm x}{l_0}}\right] \tag{5}$$

where W is the product log or Lambert W function.

This function is defined only when the argument becomes equal to $-1/e^1$, so there is a minimal value of k (for example) below which there is no solution even for $x \to 0$, given by:

$$k_{\min} = \frac{\beta}{l_0} e^{1-\frac{L}{l_0}} \tag{6}$$

The deformation δh counterbalances the force applied on the cortex. If $k < k_{\min}$, there is no linear δh big enough to counterbalance the force applied on the cortex; therefore, the connection between the cortex and the spindle is lost (Supplementary Fig. S5b). Of course we may consider that when the cortex is pulled, it might be stabilized by nonlinear processes that we have not investigated, thus preventing this loss of connection between the spindle and the cortex.

At any $k > k_{\min}$ there is no solution to equations (2) and (4) when the spindle reaches the position given by:

$$x_{\max} = l_0 \ln \frac{kl_0}{\beta e^1} + L \tag{7}$$

Using the solution for δh given by equation (5) we can calculate the total force using equation (3), which we find to be linearly increasing with x only for small values of x. If the value of $x_{\max}$ is larger than L, the spindle can move successfully all the way to the cortex. Above a critical stiffness given by $k_L = \beta / l_0 e^1$ the force balance can always be satisfied and the spindle can reach the cortex without being disconnected.

However, the speed of the spindle motion decreases as the stiffness is increased beyond k_L because the total force pulling the spindle, near the origin, has the linear form: $F_{\text{tot}} = \alpha x$, where for a stiff cortex α has the following form:

$$\alpha = \alpha_0 + \frac{(\alpha_0)^2 -}{k} \tag{8}$$

Therefore, if the motion is limited to occur over a finite time duration, set by the internal clock of the cell, then it may not complete if it is too slow (Supplementary Fig. S5b). We therefore predict from our model that the spindle will successfully reach the cortex within a window of cortex stiffness: $k_L < k < k_{\max}$. Above $k_{\max}$ the spindle will not move fast enough to complete the repositioning to the cortex during the time over which this process can take place.

Given that WT cells successfully position their spindle to the cortex, it means that their cortical tension k is larger than the minimal value $k_{\min}$, and that their cortex is located at most at $x_{\max}$ or below ($x_{\max} > L$). The average length of actin filaments (l_0) is roughly 6 µm and the shortest distance from the closest spindle pole to the cortex (L) is around 17 µm(ref. 15). Choosing $k = 0.034\ \text{nN}\,\mu\text{m}^{-1}$ (k measured experimentally in WT cells, see the Results section) and $x_{\max} = L$, we can extract from equation (7) an upper bound on $\beta \geq 0.075$ nN (because in WT cells $x_{\max} > L$). Using this upper bound of β in equation (6), we get $k_{\min} \approx 0.002\ \text{nN}\,\mu\text{m}^{-1}$. This value is indeed much lower than the value for the WT cortex ($0.034\ \text{nN}\,\mu\text{m}^{-1}$): k is an order of magnitude greater than the minimal value $k_{\min}$, at which the cortex would be disconnected from the spindle. Therefore, the mechanism proposed is consistent with the experimental data, confirming the validity of our model.

In WT oocytes, k measured experimentally is $0.034\ \text{nN}\,\mu\text{m}^{-1}$ (Supplementary Fig. S5b red curve). In *mos*$^{-/-}$ oocytes, k measured experimentally is $0.65\ \text{nN}\,\mu\text{m}^{-1}$ (Supplementary Fig. S5b green curve). One can see that the speed of spindle migration is consistently slower in *mos*$^{-/-}$ when compared with WT oocytes. However, the spindle is able to migrate all the way to the cortex in *mos*$^{-/-}$ oocytes, whereas it cannot for k values smaller than $k_L = 0023\ \text{nN}\,\mu\text{m}^{-1}$ (Supplementary Fig. S5b first blue curve).

Statistical analysis. The statistical analysis was performed using the GraphPad Prism software. Student's t-tests were used (with Welch correction where indicated) with a confidence interval of 95%. In all figures, * corresponds to a P value <0.05, ** to a P value <0.005 and *** to a P value <0.0005.

55. Verlhac, M. H., Kubiak, J. Z., Clarke, H. J. & Maro, B. Microtubule and chromatin behavior follow MAP kinase activity but not MPF activity during meiosis in mouse oocytes. *Development* **120,** 1017–1025 (1994).
56. Reis, A., Chang, H. Y., Levasseur, M. & Jones, K. T. APCcdh1 activity in mouse oocytes prevents entry into the first meiotic division. *Nat. Cell. Biol.* **8,** 539–540 (2006).
57. Tsurumi, C., Hoffmann, S., Geley, S., Graeser, R. & Polanski, Z. The spindle assembly checkpoint is not essential for CSF arrest of mouse oocytes. *J. Cell. Biol.* **167,** 1037–1050 (2004).
58. Terret, M. E. *et al.* DOC1R: a MAP kinase substrate that control microtubule organization of metaphase II mouse oocytes. *Development* **130,** 5169–5177 (2003).
59. Evans, E. & Yeung, A. Apparent viscosity and cortical tension of blood granulocytes determined by micropipet aspiration. *Biophys. J.* **56,** 151–160 (1989).

© 2013 Macmillan Publishers Limited. All rights reserved.

DOI: 10.1038/ncb2799

nature cell biology

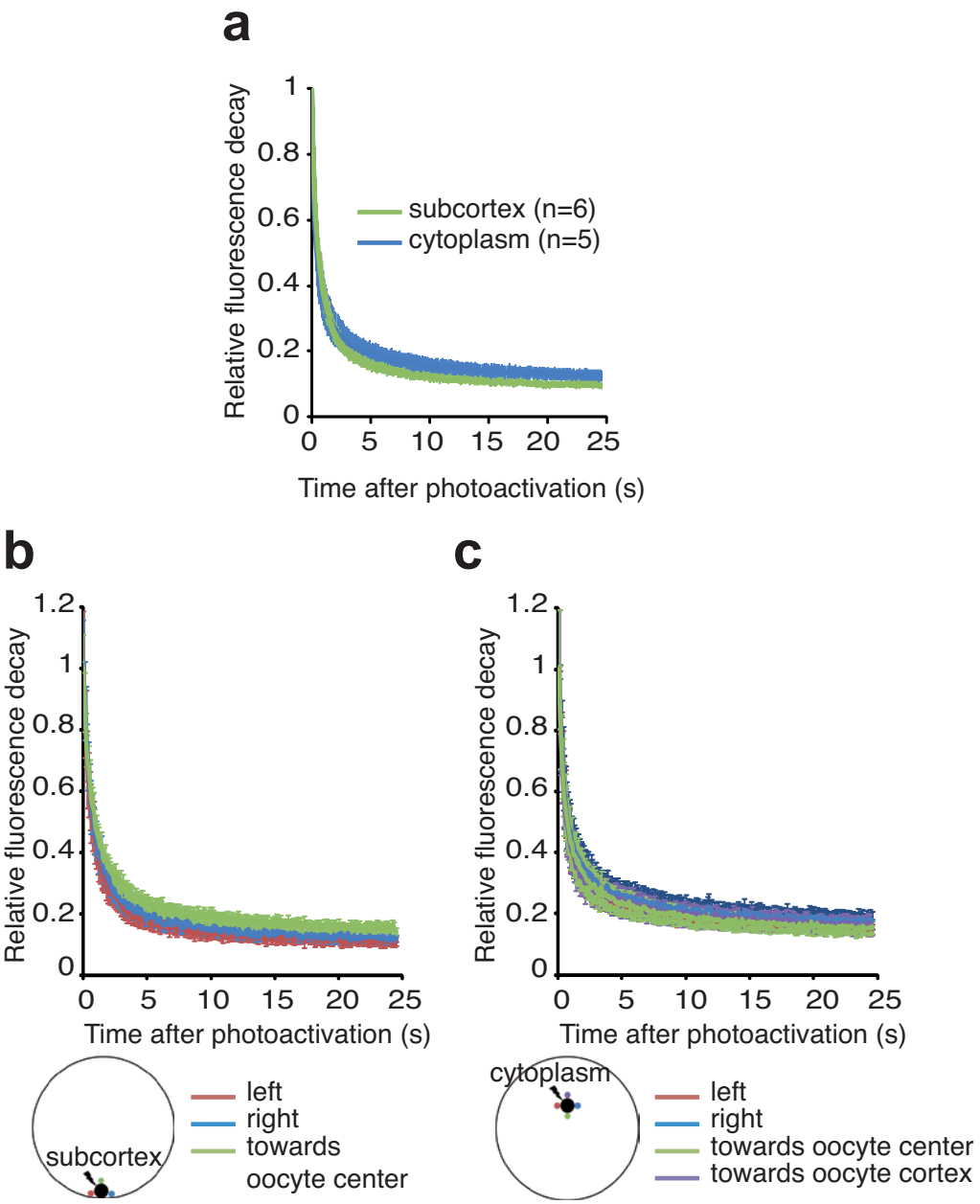


Figure S1 Spatial analysis of PA-GFP dynamics in mouse oocytes. (a) Profiles of PA-GFP fluorescence decay after photoactivation over time in the subcortex and cytoplasm of NEBD+6h oocytes. Mean of n=6 *wt* oocytes photoactivated in the subcortex and n=5 *wt* oocytes photoactivated in the cytoplasm, assessed over 2 independent experiments. Standard errors are plotted on each curve. See methods section for photoactivation analysis. The curves are are not statistically different using a t test for each timepoint. (b) Profiles of PA-GFP fluorescence decay in regions adjacent to the photoactivated subcortical region of NEBD+6h oocytes over time. Mean of n=6 *wt* oocytes, assessed over 2 independent experiments. Standard errors are plotted on each curve. Statistical differences were assessed for each timepoint using a t test. All curves are not statistically different from each other. (c) Profiles of PA-GFP fluorescence decay in regions adjacent to the photoactivated cytoplasmic region of NEBD+6h oocytes over time. Mean of n=5 *wt* oocytes, assessed over 2 independent experiments. Standard errors are plotted on each curve. Statistical differences were assessed for each timepoint using a t test. All curves are not statistically different from each other.

© 2013 Macmillan Publishers Limited. All rights reserved.

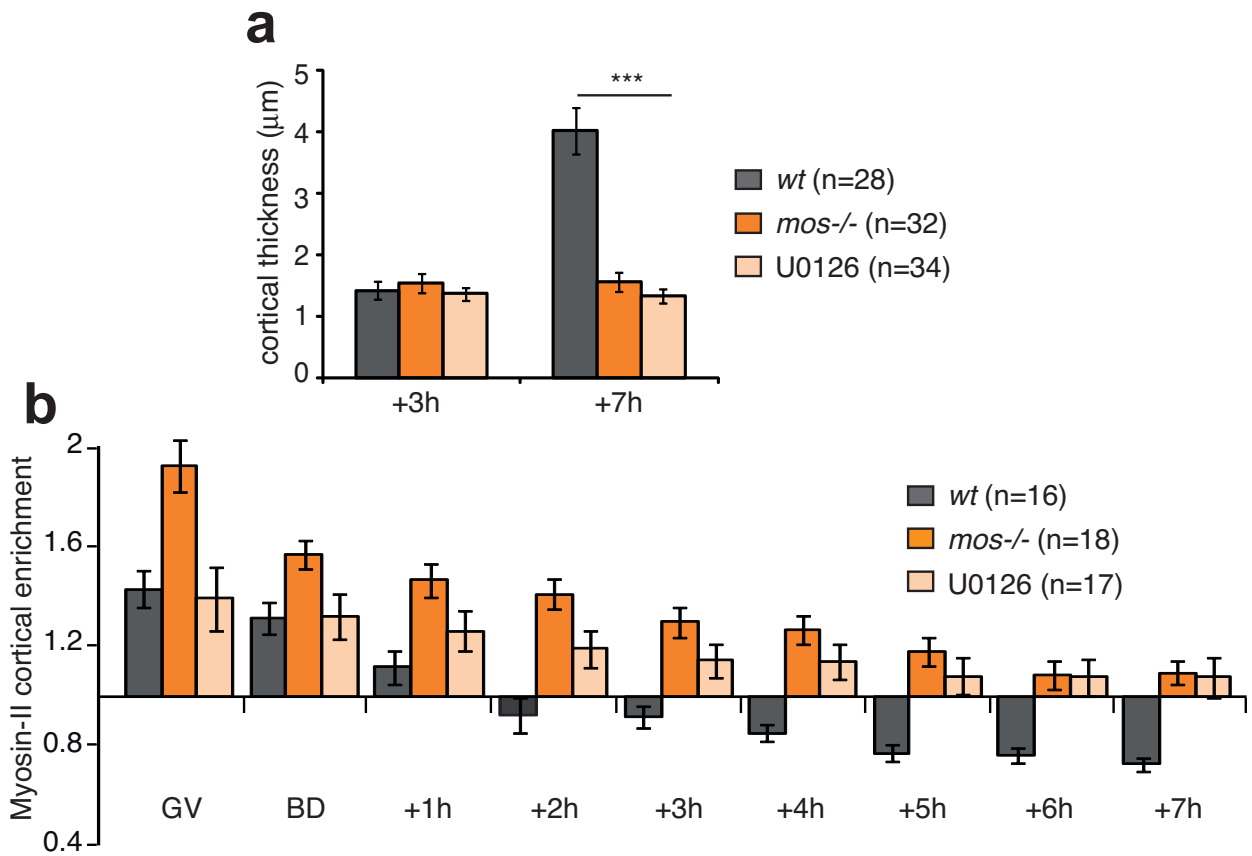


Figure S2 U0126 mimics *mos-/-* phenotype on the cortical actin thickening and Myosin-II cortical localization. (a) Bar graph showing measures of the subcortex in mm at NEBD+3h and NEBD+7h in *wt*, *mos-/-* or U0126 treated oocytes expressing GFP-UtrCH. Mean of n=28 *wt* oocytes, n=32 *mos-/-* oocytes and n=34 U0126 treated oocytes, assessed over 8 independent experiments. Standard deviation is plotted on each bar. The statistical significance of differences was assessed with a t test with Welch correction, p value < 0.0001. (b) Bar graph showing the ratio between the average intensities of cortical and cytoplasmic Myosin-II at different stages in *wt*, *mos-/-* or U0126 treated oocytes expressing SF9-GFP. Mean of n=16 *wt* oocytes, n=18 *mos-/-* oocytes and n=17 U0126 treated oocytes, assessed over 3 independent experiments. For each oocyte, 6 measurements were taken in the cortex and in the cytoplasm. Standard error is plotted on each bar. The statistical significance of differences presented in Supplementary Table 1 was assessed with a t test with Welch correction.

© 2013 Macmillan Publishers Limited. All rights reserved.

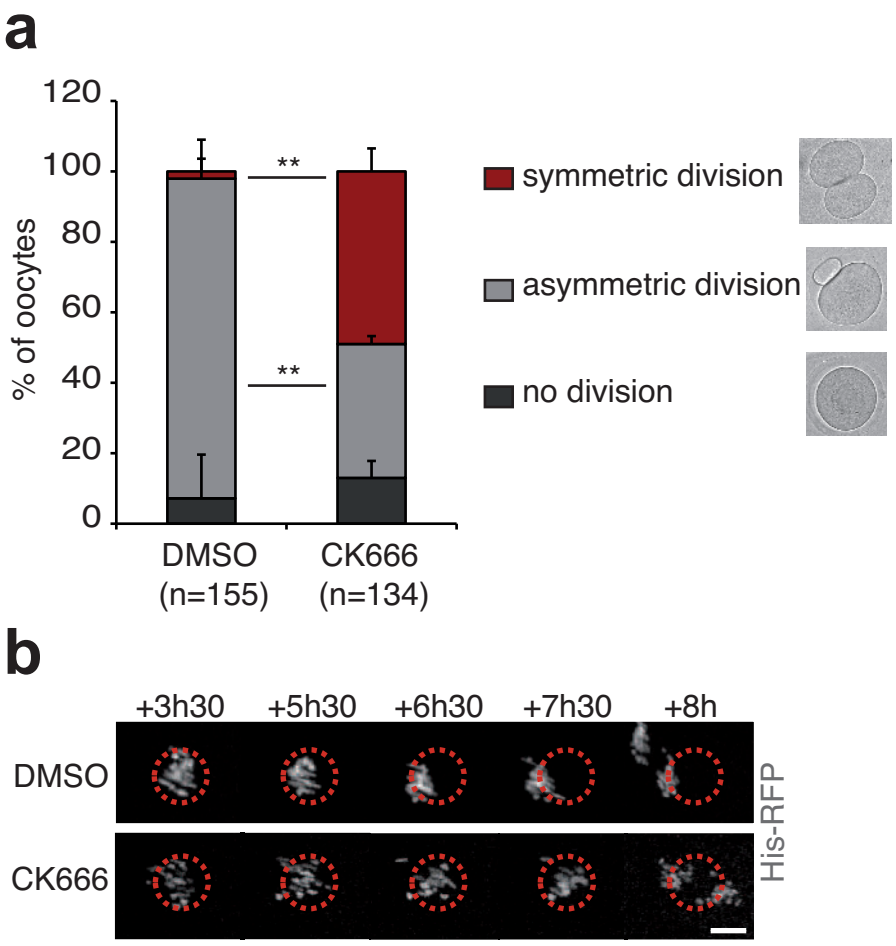


Figure S3 The cortical F-actin thickening is essential for spindle migration in meiosis I. (a) Bar graph showing the percentage of symmetric, asymmetric and absence of division in DMSO and CK666 treated oocytes. Mean of n=155 DMSO treated oocytes and n=134 CK666 treated oocytes, assessed over 4 independent experiments. Standard deviation is plotted on each bar. The statistical significance of differences was assessed with a t test, p values = 0.0007 for symmetric division and 0.0041 for asymmetric division. (b) Time-lapse spinning disk confocal microscopy of Histone-RFP expressing oocytes followed during meiotic maturation. The upper panel corresponds to a DMSO treated oocyte while the lower panel shows a CK666 treated one. The red dotted circle highlights the initial position of chromosomes. A projection of 3 Z planes is shown. Times from NEBD are indicated in hours. Scale bar, 10 μm.

© 2013 Macmillan Publishers Limited. All rights reserved.

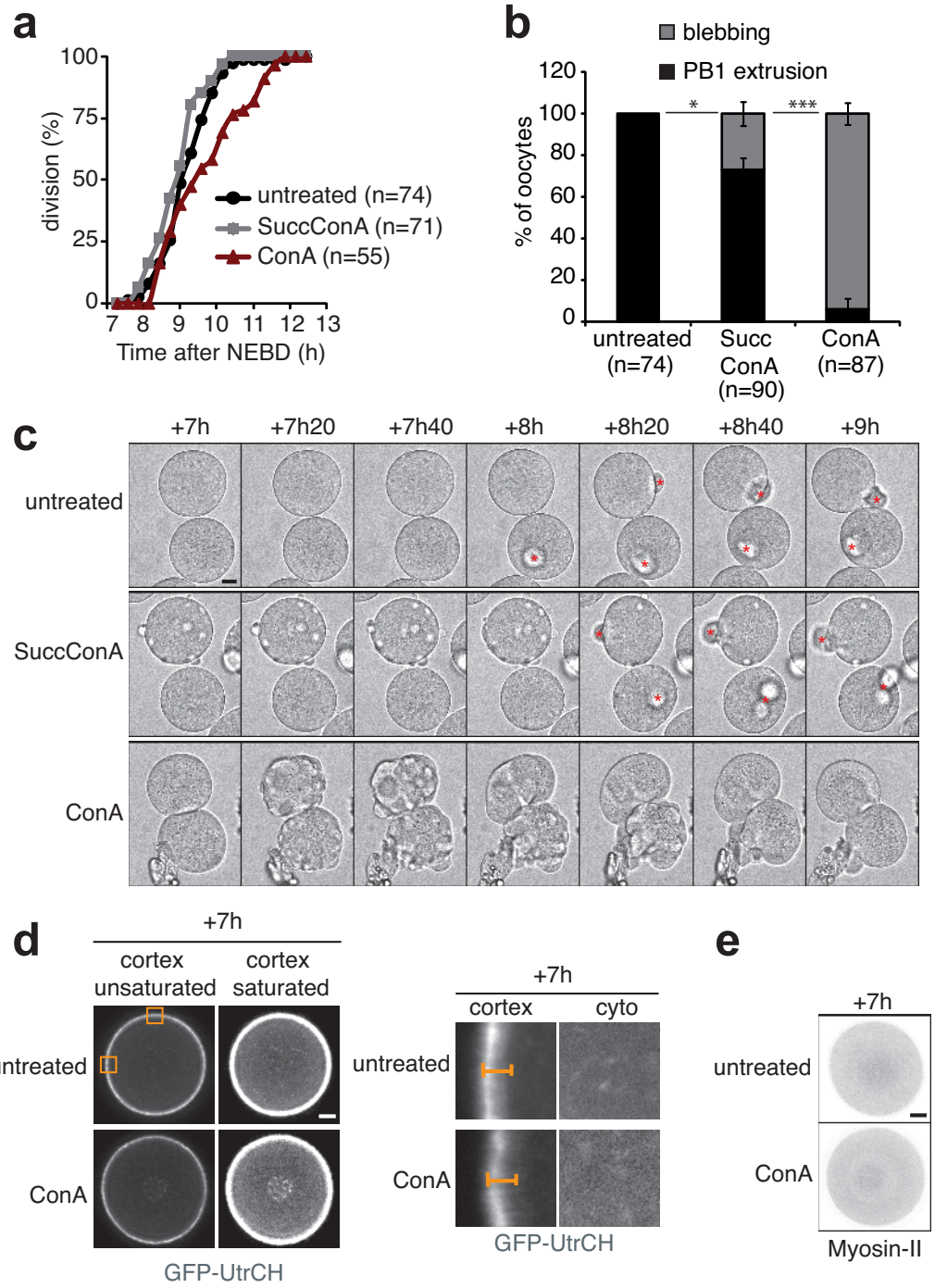


Figure S4 ConA effects on meiosis I division, actin meshworks organization and Myosin-II localization. (a) Graph representing the kinetics of division in *untreated*, SuccConA treated and ConA treated oocytes. For all kinetics, the percentage of division is calculated only from the population of oocytes that actually undergo a division. (b) Bar graph showing the percentage of oocytes undergoing blebbing and polar body extrusion (PB1) in untreated, SuccConA treated and ConA treated conditions at NEBD+7h. Mean of n=74 untreated oocytes, n=90 SuccConA treated oocytes and n=87 ConA treated oocytes, assessed over 4 independent experiments. Standard deviation is plotted on each bar. The statistical significance of differences was assessed with a t test with welch correction, p values = 0.0951 for untreated versus SuccConA and 0.0009 for SuccConA versus ConA. (c) Time-lapse spinning disk confocal microscopy of untreated, SuccConA treated and ConA treated oocytes observed every 20 minutes starting from NEBD+7h until NEBD+9h. The red asterisks mark the first polar bodies. Scale bar, 10 μm. (d) Confocal spinning disk images of NEBD+7h oocytes expressing GFP-UtrCH treated or not with ConA. The left panels correspond to unsaturated images, the right panels to saturated images. One Z plane is shown. On the right are magnified regions of these oocytes outlined by the orange squares. Due to culture conditions on agarose coated glass slides, the stainings appear blurry. Scale bar, 10 μm. (e) Time-lapse spinning disk confocal microscopy of NEBD+7h oocytes expressing a Myosin-II intrabody (black) treated or not with ConA. One Z plane is shown. Scale bar, 10 μm.

© 2013 Macmillan Publishers Limited. All rights reserved.

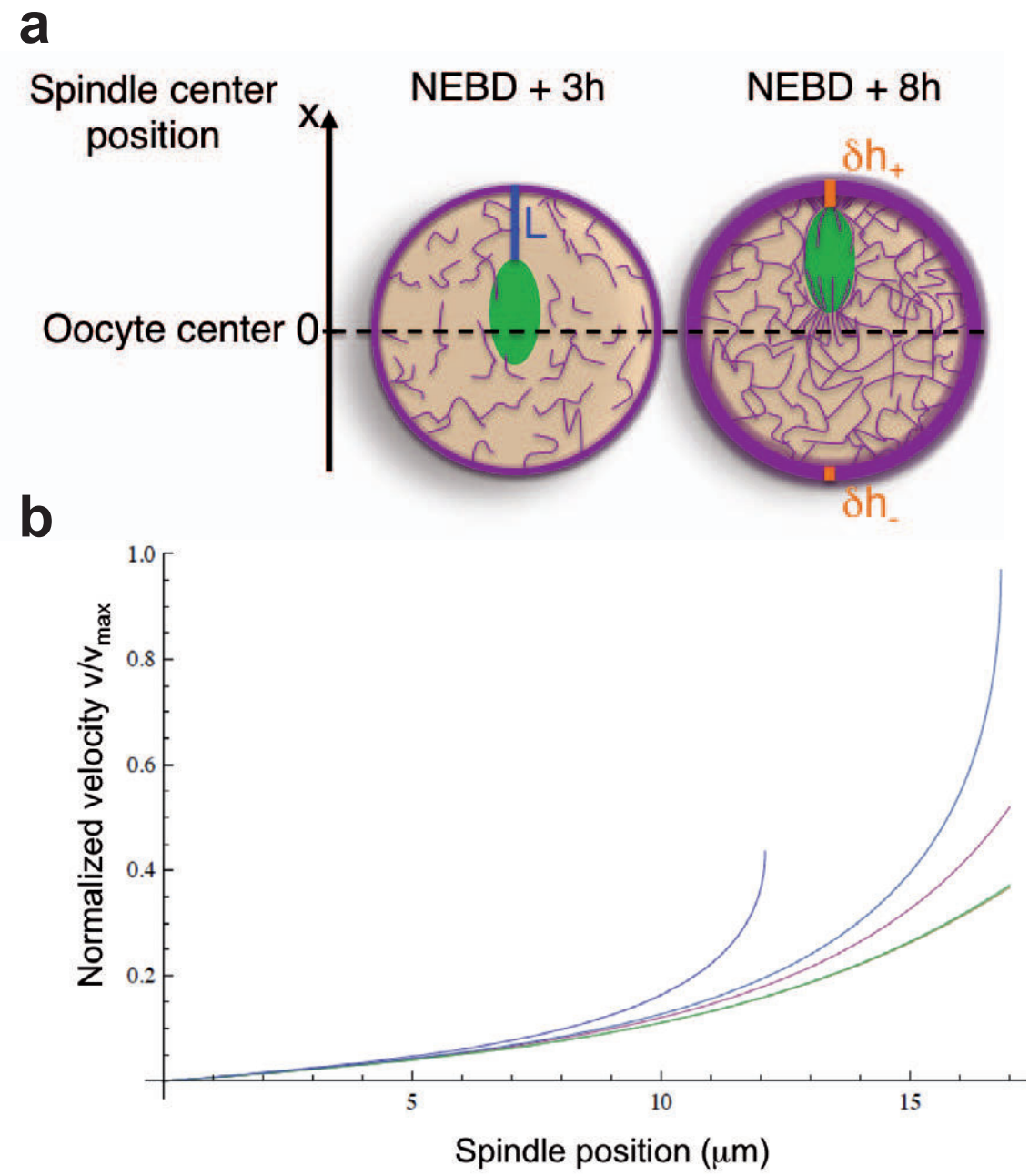


Figure S5 Theoretical model of spindle motion. (a) The spindle moves in one dimension along its long axis, which we call axis (0,x), 0 being the center of the oocyte and x the position of the center of gravity of the spindle at a given time. L represents the distance between the closest spindle pole and the cortex before the spindle starts migrating. The origin (x=0) is at the cell center. The spindle is shown with a finite size, while in the model only its center is described, not its spatial extent. (b) Velocity of the spindle along its long axis as a function of cortex stiffness (k). From top to bottom k=0,01; 0,023; 0,034; 0,65; 10 nN/μm (using L=17 μm, b= 0,05 nN, l_0=6 μm). The velocity is plotted normalized by the value of the maximal velocity v_{max}, defined when the spindle reaches the cortex for k=k_L=0,023 nN/μm. The curves for k=0,65 and 10 nN/μm are indistinguishable.

© 2013 Macmillan Publishers Limited. All rights reserved.

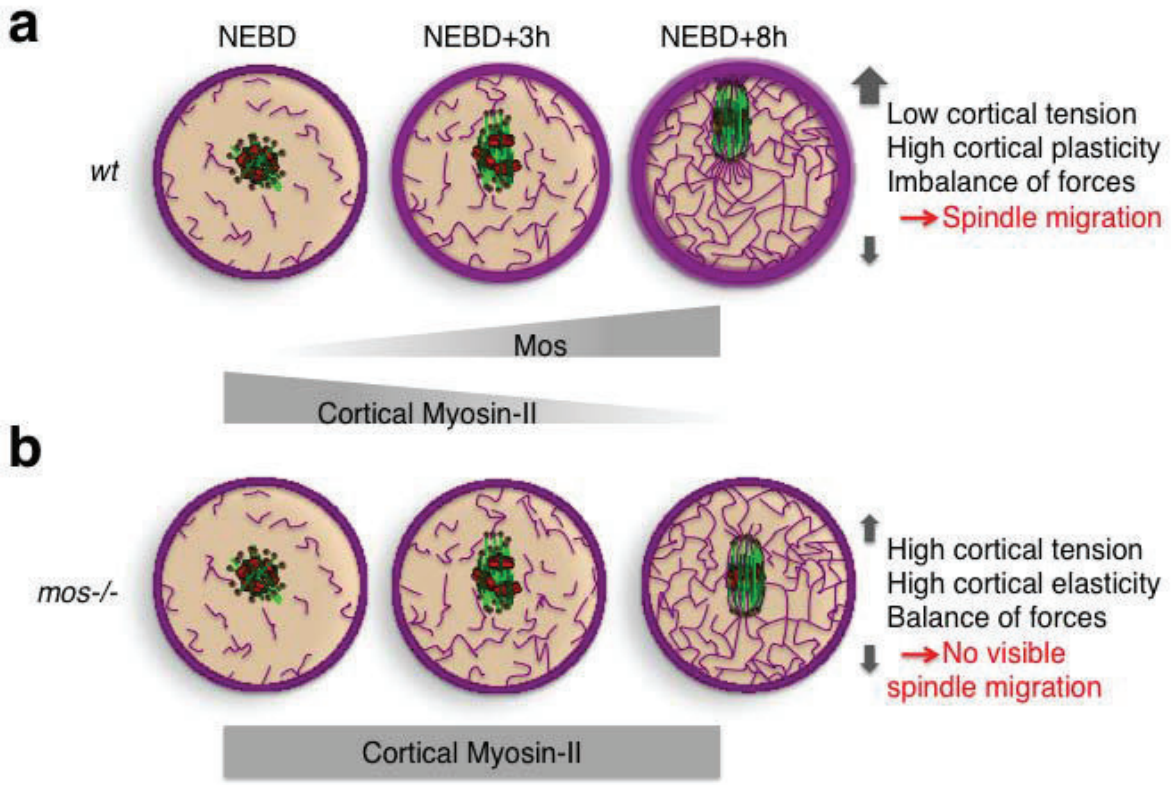


Figure S6 Spindle positioning in mouse oocytes is the result of an imbalance of forces favored by a soft cortex. A schematic showing the relationship between Mos expression, cortical Myosin-II enrichment, cortical thickening, cortical mechanics and spindle positioning during meiotic maturation in *wt* and *mos-/-* oocytes. Chromosomes are shown in red, microtubules in green and actin in violet.

© 2013 Macmillan Publishers Limited. All rights reserved.

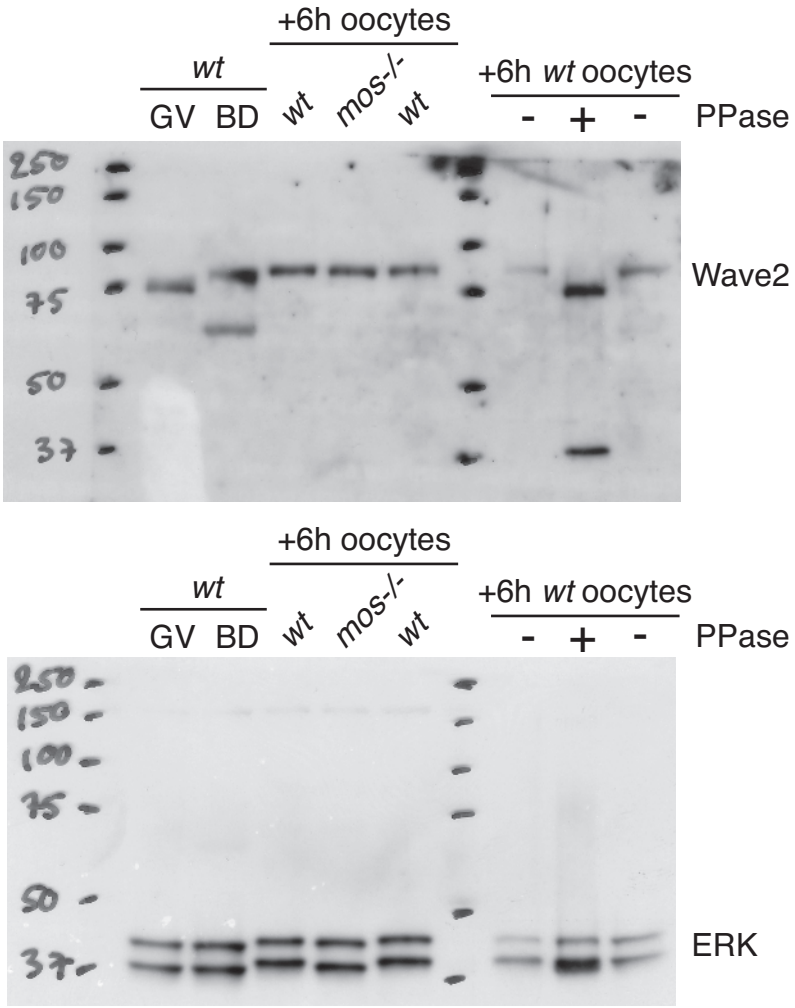


Figure S7 Full scans of the blots from Fig. 4e-f

© 2013 Macmillan Publishers Limited. All rights reserved.

Supplementary Table and Video legends

Supplementary Table 1: Statistical analysis of Fig. 5e and Supplementary Fig. S2b. NS: not statistically different.

Video S1: Time-lapse movie showing a *wt* oocyte expressing GFP-UtrCH (gray) and histone-RFP (red). Frames were 1h apart. The movie starts at NEBD and stops at NEBD+7h. One Z plane is shown.

Video S2: Time-lapse movie showing a *wt* oocyte expressing GFP-UtrCH. Frames were 5 seconds apart. The movie starts at NEBD+7h and lasts 5 minutes. One Z plane is shown.

Video S3: Pseudocolored time-lapse movies showing *wt* NEBD+6h oocytes expressing PA-GFP-UtrCH (upper cells) and PA-GFP (lower cells) photoactivated in the subcortex (cells on the left) or in the cytoplasm (cells on the right). Black, lowest intensity; white highest intensity. Frames were 100 milliseconds apart. The movies start at NEBD+6h and lasts 25 seconds. One Z plane is shown.

Video S4: 13 seconds movie showing micropipette aspiration of a *wt* NEBD+1h mouse oocyte. Note that the plasma membrane does not detach from the cytoplasm, as cytoplasmic particles can be seen flowing into the micropipette.

Video S5: 31 seconds movies showing the relaxation after suction of a NEBD+6h *mos-/-* oocyte (left cell, elastic behavior) and a NEBD+6h *wt* oocyte (right cell, plastic behavior).

© 2013 Macmillan Publishers Limited. All rights reserved.

Mouse first meiotic division (Meiosis I) is a very asymmetric division in size because of F-actin dependent off-center spindle positioning. We have demonstrated that a cortical F-actin thickening was nucleated during spindle migration. Concomitantly, Myosin-II is removed from the cortex. The Mos/MAPK pathway controls both these events. Myosin-II cortical displacement is responsible for a drop in cortical tension required for spindle migration (Chaigne et al., 2013). Based on these previous observations, we established a model for spindle migration. Since the spindle forms slightly off-centered (Maro and Verlhac, 2002; Verlhac et al., 2000), one pole is closer from the cortex than the other. The postulates of the model are the following assumptions:

- The spindle is pulled by interactions between F-actin connecting the spindle and the cortex and Myosin-II which is present at spindle poles (Simerly et al., 1998; Schuh and Ellenberg, 2008).
- The actin filaments emanate from the cortex and the spindle. From these two points, the density of actin filaments decrease exponentially. Thus the density of filaments depends on the position of the spindle.
- The pulling force exerted at the pole closer to the cortex is bigger that at the other pole.
- The cortex, by being soft and deformable, drives spindle migration by modulating F-actin filaments distribution.

The goal of this work was to test our model and its predictions to confirm or disprove these assumptions.

The forces exerted by Actin-Myosin on the spindle are transmitted to the cortex, explaining the final deformation of the F-actin thickening at the end of Meiosis I (Chaigne et al., 2013). To constrain the model, we measured this deformation and found that indeed it is bigger on the side of the spindle pole closer to the cortex. From this measurement we could deduce the total force applied on the spindle, which is in the order of 10 pN.

This force translates into spindle motion. However the oocyte viscosity slows spindle migration. Thus, we measured the viscosity of the cell by micropipette experiments and the speed of the spindle motion to calculate the force applied on the spindle using a different equation. We could find a value of forces in the same range as with the previous calculation.

The model predicts that the cortical tension must be intermediate for spindle migration, i.e a too high or too low cortical tension would not allow off-center spindle positioning. We showed previously that a too high cortical tension leads to impaired spindle migration, in the case of *mos-/-* oocytes (Chaigne et al., 2013). We designed a tool to study the opposite, namely the consequences of a reduced cortical tension. To do so, we fused Ezrin, an ERM protein that goes to the cortex throughout Meiosis I (Louvet et al., 1996) and the VCA common to all Arp2/3 NPFs. We showed that this fusion is targeted at the cortex at all stages of Meiosis I and demonstrated that it is sufficient to nucleate an F-actin thickening independently of the Mos/MAPK pathway. This VCA induced F-actin thickening is similar to the one present during Meiosis I, strengthening the hypothesis that the F-actin thickening in Meiosis I is indeed dependent on NPF activated Arp2/3 nucleation. Furthermore, the cortical VCA is also sufficient to induce Myosin-II cortical displacement from the cortex in the absence of the Mos/MPAK pathway. Lastly, it leads to a decrease in cortical tension in Prophase I arrested oocytes. This probably elucidates the mechanism for tension drop in mouse oocytes: the MAPKs, activated after Mos synthesis, directly or indirectly phosphorylate and activate Wave2 (Chaigne et al., 2013), which induces Arp2/3 dependent F-actin nucleation at the cortex. By a completely unknown mechanism, F-actin nucleation is necessary and sufficient to remove Myosin-II from the cortex, which causes cortical tension to drop. Eventually, we used the VCA targeted at the membrane to test the effect of a reduced cortical tension and found that it impairs spindle migration. Furthermore, when expressed in *mos-/-* oocytes that harbor a high tension incompatible with spindle migration, we observed a partial rescue of spindle motion. Thus, the cortical tension needs to be neither too high nor too low to allow spindle migration.

To conclude, this work thoroughly explains how the drop of cortical tension is achieved in Meiosis I, as the result of F-actin mediated Myosin-II delocalization. Moreover, all of the results predicted by the model are consistent with live measurements. Thus, we conclude that the postulates we took accurately describe spindle migration in mouse oocyte Meiosis I: spindle migration is mediated by Myosin-II pulling on the actin cage surrounding the microtubule spindle, the forces being stronger at one pole because of the initial asymmetry of nuclear position (Brunet and Maro, 2007). The motion is very slow but is amplified by the deformation of the cortex, which is made possible because Mos triggers F-actin nucleation at the cortex, allowing recruitment of more F-actin between the cortex and the spindle and

therefore amplification of the forces.

Author contributions:

A.C, M.H.V and M.E.T designed the experiments, interpreted the results and wrote the manuscript. A.C and M.E.T carried out most of the experiments. A.C and C.C carried out the micropipette experiments. A.C, C.C and C.S designed the micropipette experiments and interpreted the results. N.S.G and R.V designed the mathematical model. M.E.T and M.H.V supervised the project.

Force amplification driven motion of mouse meiosis I spindle is tightly regulated by cortical tension

Chaigne A[1,2], Campillo C [3], Gov NS[4,9], Voituriez R[5,9], Sykes C[6,7,8], Verlhac MH[1,2,10], Terret ME[1,2,10].

[1]CIRB, Collège de France, and CNRS-UMR7241 and INSERM-U1050, Equipe Labellisée Ligue Contre le Cancer, Paris F-75005, France. [2]Memolife Laboratory of Excellence and Paris Science Lettre, Paris F-75005, France. [3]LAMBE UMR 8587, Evry, France. [4]Department of Chemical Physics, Weizmann Institute of Science, Rehovot 76100, Israel. [5]UMR7600-CNRS/UPMC, 4 Place Jussieu, Paris F-75005, France. [6]CNRS-UMR168, Paris F-75248, France. [7]UPMC, 4 Place Jussieu, Paris F-75248, France. [8]Institut Curie, Centre de Recherche, Laboratoire Physico-Chimie, Paris F-75248, France. [9] These authors contributed equally to this work.

[10] Correspondence should be addressed to MHV or MET (e-mail: marie-helene.verlhac@college-de-france.fr or marie-emilie.terret@college-de-france.fr)

Abstract

Cell mechanics are crucial for successful cell division. During mitosis, external forces applied on the cortex by the cell environment can control spindle orientation [1,2], but the cell itself can increase its cortical tension at the onset of mitosis ensuring correct spindle morphogenesis and positioning. In mouse oocytes on the contrary, off-center positioning of the spindle following its migration, allowing the asymmetry in size of the first meiotic division, depends on a decrease of cortical tension, correlated with increased cortical actin nucleation and myosin-II delocalization from the cortex [3]. However, how these changes in cortex organization induce a drop in cortical tension has not been established. Furthermore, how precisely cortical tension has to be gated to allow spindle migration has not been addressed. Here, using artificial manipulation of mouse oocyte cortical tension and modeling, we show that cortical tension has to be tightly regulated to allow off-center spindle positioning. Indeed, a too soft or too stiff cortex leads to unsuccessful spindle migration. We clearly demonstrate that the decrease in cortical tension required for spindle migration is fine-tuned by a branched F-actin network that trigger the delocalization of myosin-II from the cortex, which sheds new light on the interplay between actin networks architecture and cortex tension.

Results and discussion

Mouse oocytes are arrested in Prophase I of the first meiotic division (Meiosis I) in the ovary. Upon hormonal stimulation meiosis resumes, triggering Nuclear Envelope BreakDown (NEBD) and the two consecutive meiotic divisions. Rapidly, the first meiotic spindle forms where the nucleus was, never at the perfect center of the oocyte but always a little bit off-centered [4,5]. At that stage, the oocyte bears no apparent sign of polarization [6–8]. The spindle then migrates along its long axis towards the closest cortex [4]. This migration does not depend on microtubules [4], in accordance with the fact that mouse oocytes lack true centrosomes and thus astral microtubules at spindle poles which in mitosis connect the spindle to the cortex to position it within the cell [9]. Spindle positioning in Meiosis I instead depends on two actin networks that assemble progressively: a cytoplasmic F-actin meshwork nucleated by Formin-2 [10–13] and Spire1/2 [14] and an Arp2/3 nucleated actin thickening at the cortex [3]. Mos, a MAPKKK (MAP Kinase Kinase Kinase) expressed specifically in oocytes after NEBD and activating MAPKs around NEBD+3h [4,15,16] controls both the nucleation of this actin thickening and the removal of myosin-II from the cortex, two events responsible for the drop in cortical tension required for spindle migration [17,3]. Interestingly, the situation is very different in mitotic cells where, at the onset of cell division, cells round up [18] following an increase of osmotic pressure [19] and a change in cortical tension mediated by the cell cortex [18,20]. This global increase in cell stiffness is essential to allow proper spindle formation, stability and positioning as it creates an optimal volume for chromosome capture and allows interactions between the cell cortex and astral microtubules [20–22]. How and to which extend cortical tension needs to decrease in mouse oocyte in order to promote spindle migration have thus remained elusive so far.

To investigate how the regulation of cortical tension could affect spindle migration, we artificially manipulated oocyte cortical tension and turned to theoretical modeling. First, we needed to describe the force generator. During spindle migration, F-actin forms an actin cage that surrounds the microtubule spindle and connects it to the actin thickening [12,13] (Figure 1a). At the end of Meiosis I, the cortical thickening gets deformed above the spindle where the filaments emanating from the actin cage connect with the cortical filaments (Figure 1a, d-e: δh_+ on the side where the spindle is migrating, δh_- on the opposite side) [3], suggesting pulling forces at play between the actin cage and the cortical actin that stretch the cortical thickening towards the migrating spindle and pull the migrating spindle towards the cortex by

an action reaction mechanism. Furthermore, when the actin motor myosin-II, localized at the spindle in late Meiosis I [13,23], is inhibited, the spindle does not migrate [3,13]. Thus, we postulate that myosin-II pulls the spindle towards the cortex from both poles, the force depending on the overlap between the cortical and cytoplasmic filaments. This overlap seemed to be more important on the side where the spindle is migrating (Figure 1a). To confirm this, we measured the fluorescence intensity of an F-actin probe (GFP-UtrCH)[24] as a proxy for filaments density and found that it is indeed larger between the closest pole and the cortex than between the pole further away from the cortex and the cortex (Figure 1c, black bar), suggesting that the overlap is indeed larger between the pole approaching the cortex and the cortex above it. Furthermore, when the Arp2/3 complex is inhibited in oocytes using CK666[25], the spindle does not migrate to the cortex but stays centrally located [3,26] and in that case the density of actin filaments is similar on both sides of the spindle (Figure 1b and Figure 1c, white bar). To account for these observations, we model the spindle as an object represented by its center of mass moving along its long axis (0l) under traction forces exerted at each pole (F_+ and F_-) (Figure 1d). We postulate that actin filaments emanate from the actin cage tips (see Methods section) and from the cortex, creating an overlap [3]. L, the distance between the spindle and the closest cortex when it starts migrating, was measured in ref 13. We obtain a density of actin filaments at a position l (N(l)) depending on the position x of the spindle (Figure 1e), such that the closer the spindle the more important the overlap gets (Figure 1a-c, Figure 1e compare left and right panels).

Since the spindle does not form at the exact center of the oocyte [4,5] the pulling force should be stronger on the side closer to the cortex (F_+) where the overlap is more important, thus explaining why the spindle migrates towards the closest cortex [4,5]. Conversely, by an action reaction mechanism, the force applied on the cortical actin thickening (h_0) should be larger at the closest cortex than on the other side producing an extra-deformation δh_+ larger than δh_-. This is indeed the case as shown in Figure 2a-b. The cortical actin thickening $h_- = h_0+\delta h_-$ stays constant after NEBD+6h whereas $h_+ = h_0+\delta h_+$ increases up to 6 µm when the spindle reaches the cortex at NEBD+8h. The force applied on each side of the spindle (F_+ and F_-) is opposite of the force deforming the same side of the cortex, which depends on the elastic response of the cortex (k') that itself depends on the cortical tension k, and cortical deformation (δh) such as $F_\pm = k'\delta h_\pm$. The total force F_{tot} is then the difference between these two forces ($F_{tot} = F_+ - F_-$). Since the cortical tension of *wt* oocytes previously measured during late Meiosis I is 0.034nN/µm [3], we can deduce an estimate of the forces applied on the spindle

in late Meiosis I when x = 17μm: $F_+ \approx 0.051$nN and $F_- = 0$nN. Thus the total force exerted on the spindle in late Meiosis I is in the range of 0.051nN. This is a weak force but very satisfactory since the spindle moves very slowly towards the cortex inside the cell, with a speed of 0.15 μm/min in late Meiosis I [13]; as a comparison, a moving keratocyte develops a force in the range of 10 nN [27] and harbors a speed in the range of 10 μm/min [28] which leads a comparable ratio speed produced/force exerted.

Assuming that the filaments emanating from the spindle tip grow slower when they penetrate inside the cortex than in the cytoplasm, consistent with the fact that the cortical actin and the cytoplasmic actin define two different compartments in terms of dynamics [3], we can postulate that the mean length of the filaments in the cortex is shorter than in the cytoplasm, depending on the cortical tension, such as: $l_c = l_0 e^{-\frac{k}{k_s}}$, with k the cortical tension, k_s the stall tension at which the filaments cannot penetrate the cortex anymore because it is too stiff, l_0 the mean length of the filaments in the cytoplasm and l_c the mean length of filaments penetrating the cortex. Thus, the overlap responsible for the pulling force should be smaller if the cortex is stiffer. Using the equation for the actin distribution previously established (see Method section and Figure 1e), we can now solve it numerically for δh_+ and δh_- (Figure 2b). The overall fit is reasonable using these values: $h_0 = 3$μm (as measured in Figure 2a-b), L = 17μm (as measured in ref 13), k = 0.03nN/μm (as measured in ref 3). It yields values for $l_0 =$ 7μm, very close from what was measured in ref 12, and $l_c = 0.5$μm which is the proper range for cortical filaments, h_o measuring around 3μm (Figure 2a-b). This supports the validity of the model. Furthermore, using this fit, $\beta = 0.065$nN/μm which is an acceptable value since in structures very rich in myosin-II such as the growth cone it was estimated that $\beta \approx 1$nN/μm [29]. Here, since the spindle motion is very slow, one would expect a small contractility. We can also extract $k_s = 0.01$nN/μm from the fitting, which means that above a cortical tension in this range, the cytoplasmic actin filaments cannot enter the cortex. Hence, when the tension is too high, the overlap between cortical and cytoplasmic filaments is impaired and the spindle will not migrate, which is indeed the case [3].

The forces exerted on the spindle lead to its movement inside the oocyte. Thus we can use the force balance to describe the total force F_{tot} as a function of the spindle speed $\dot{x}$ tempered by the viscous drag γ exerted by the cytoplasm of the cell: $\gamma\dot{x} = F_+ - F_-$. The speed of spindle migration $\dot{x}$ was measured and plotted as a function of spindle position x (Figure 2c-d). Using the same parameters as obtained before (Figure 2b), we fitted the speed as a

function of time (Figure 2d), and obtained a friction parameter γ = 2nN.min/μm, which, for a spindle length of roughly 30μm [30] gives a total viscosity of 4.10^3Pa.s. We then measured the viscosity η in late Meiosis I oocytes using micropipette aspiration (see Methods section) and obtained a value of $1.6.10^2$+/-0,5Pa.s which is in the same range as other cell types measured with the same techniques [31] and not very different from the calculated value, thus we find a relatively good fit between the measured and calculated parameters. This reinforces the validity of the model.

A very strong prediction of the model is that a low cortical tension would also impair spindle migration since in that case, the cortex would not be strong enough to sustain the pulling forces exerted by the cytoplasmic filaments (Figure 4a, blue curve) [3]. In order to test this prediction, we wanted to further decrease cortical tension during Meiosis I. We have shown previously that the drop in cortical tension required in Meiosis I for spindle migration was correlated to myosin-II displacement from the cortex and to a cortical actin thickening dependent of Arp2/3 [3]. We thus fused the VCA domain of Wave2, a Nucleating Promoting Factor of Arp2/3 [32], to Ezrin (Ez), a member of the ERM (Ezrin-Radixin-Moesin) family that is located at the cortex of mouse oocyte [33] (whole construct referred below as cVCA for cortical VCA). This allowed us to target the VCA domain, and thus activate Arp2/3 [34] at the oocyte cortex. The cVCA was mostly enriched at the cortex throughout Meiosis I (Supplemental Figure 1a-d). We then visualized cortical actin in Prophase I at a stage where MAPKs are not activated since Mos is not yet expressed [35,15]. Targeting the VCA to the plasma membrane was sufficient to nucleate *de novo* an actin thickening independently of the Mos/MAPK pathway (Figure 3a and quantification in Figure 3b). Furthermore and very surprisingly, it was also sufficient to chase myosin-II from the cortex (Figure 3c and quantification in Figure 3d). Thus, the nucleation of cortical actin filaments by Arp2/3 is sufficient to trigger by itself the delocalization of myosin-II from the cortex. None of these effects were due to Ezrin expression itself since oocytes overexpressing it (Supplemental Figure 1g) did not trigger an ectopic actin thickening (Figure 3b grey curve) and did not induce myosin-II removal from the cortex (Figure 3d grey bar). Moreover, the expression of the cVCA in Prophase I oocytes impaired neither the overall architecture of the cytoplasmic actin meshwork present at that stage [14,36,37] (Supplemental Figure 1e) nor its dynamics since the vesicles present at the crossing points of actin filaments were found to move at 12.4 +/-3.8 μm/min (Supplemental Movies 1-2) which is very similar to what was previously described [37]. Cell cycle progression was not deeply affected by expression of the cVCA or Ez since

anaphase occurred in both cases around the same time (Supplemental Figure 2a). Interestingly, most cVCA expressing oocytes attempted to extrude a polar body with sometimes bleb-like polar bodies or secondary retraction of the polar body (Figure 3f, lower panel) suggesting that the huge deformation of the oocyte could provoke a spatial proximity between the oocyte cortex and the chromosomes which would be sufficient to induce polar body extrusion.

The expression of the cVCA was sufficient to induce a huge decrease in cortical tension, measured at 0.03nN/μm in Prophase I oocytes expressing the cVCA versus 0.9nN/μm minimum (see Method section) in *wt* oocytes in Prophase I (Figure 3e red bar). As a consequence, oocytes were deformed and no longer round nor stable in shape like controls (Figure 3f, Movies 1-2), suggesting also that cortical tension keeps decreasing as Meiosis I proceeds. This was not due to the presence of Ezrin since oocytes overexpressing it harbor a minimal tension of 1.3nN/μm in Prophase I, comparable to the controls (Figure 3e grey bar). To test the prediction of the model that a very low cortical tension should prevent spindle migration (Figure 4a, blue curve), we expressed the cVCA in *wt* oocytes and let them progress into Meiosis I. This led to an incomplete or lack of spindle migration in 92% of the cases compared to 15% of the cases in non-injected *wt* oocytes (Figure 4b-c, Movies 1-2). This again was not due to Ezrin since oocytes overexpressing it harbor an incomplete of absent spindle migration in only 29% of the cases, not statistically different from the controls (Figure 4c). Furthermore, the level of expression of Ezrin was higher than the one of cVCA (Supplemental Figure 1g). The dismantlement of the cytoplasmic actin meshwork, which normally occurs at NEBD [36], did take place in oocytes expressing the cVCA (Figure 4d, Supplementary Movie 1-2), excluding any stabilization effect of F-actin at NEBD to explain the absence of spindle migration [36]. The absence of spindle migration was then clearly due to a very low cortical tension throughout Meiosis I, which is consistent with the predictions from the model.

In *mos*-/- oocytes, the spindle does not migrate [4] and the cortical tension stays high throughout Meiosis I [3]. Our model postulates that a stiff cortex should prevent spindle migration (Figure 4a, red curve), which is indeed the case [3]. We thus tested if we could rescue spindle migration in *mos*-/- oocytes by expressing the cVCA. Because this construct is very potent in decreasing cortical tension (Figure 3e), we used extremely low doses of the construct (see Methods section). This was sufficient to partially rescue spindle migration in 56% of the cases compared to 9% in non-injected *mos*-/- oocytes (Figure 4e-f, Movies 3-4).

We could not obtain a complete rescue, certainly due to the variability in the level of expression of the cRNAs injected. The oocytes displaying a lack of spindle movement could either express less cVCA (too high tension, no spindle migration) or more cVCA (too low tension, no spindle migration) (see Figure 4a). Thus we clearly demonstrate that cortical tension regulates spindle migration in mouse oocyte Meiosis I and that the window allowing spindle migration is quite narrow.

Since the model fits well with the experimental data, it validates the postulates that we took and its predictions, namely that the force generator for spindle migration is myosin-II pulling on the actin cage surrounding the microtubule spindle. The motor pulls when filaments emanating from the cortex and the actin cage overlap, creating a deformation of the cortical actin thickening. This deformation is amplified when the spindle approaches the cortex (as shown in Figure 2a-b), leading to a high asymmetry in actin filaments distribution (as shown in Figure 1a-c), with more filaments between the pole and the closest cortex than on the other side, increasing the pulling force created by this overlap. When the cortical tension is too high, the actin filaments cannot penetrate a too stiff cortex and the cortex cannot deform to increase the overlap (as shown in Figure 1b-c, CK666 treated oocytes), thus the spindle speed is null. On the contrary, when the cortical tension is too low, myosin-II cannot properly pull on the cortex leading to impaired spindle migration (Figure 4b-c). Here, we show that the boundary value for cortical tension is k_s which is around 0.01 nN/μm, very close to 0.034 nN/μm, the value measured in control oocytes [3]. Thus cortical tension has to be fine-tuned around this value in order to promote spindle migration. It is interesting to wonder why such a narrow window of cortical tension has been conserved throughout evolution, as any variation around the appropriate value gives rise to a symmetric division or no division at all, possibly leading to oogenesis failure. One possibility is that it could be used as a quality control for a suitable environment for further embryo development. Indeed, a defect in osmotic regulation or in temperature in the female genitalia, a potential threat for embryo development, would probably impair cortical tension early on. Therefore, an impaired Meiosis I would lead to the absence of fertilization, which could be less costly than further embryonic development eventually leading to the loss of the embryo. Another possibility is that cortical tension plays an additional role after Meiosis I. For example, above the arrested Metaphase II spindle, cortical tension is higher that in the rest of the oocyte [17]. It is possible that the decrease in cortical tension helps building an asymmetry between this region and the

rest of the oocyte, preventing sperm entry where the tension is the highest and thus avoiding precocious DNA fusion between the sperm and the oocyte.

At meiosis resumption, oocytes are isolated cells, implying that changes inside the oocyte can only come from within compared to mitotic cells which are able to read external constraints and respond to them [1]. Indeed, the precise regulation of cortex stiffness comes from the fact that the oocyte is able to trigger itself the decrease of cortical tension needed for spindle migration by nucleating an actin thickening that removes myosin-II from the cortex. This could be important to allow myosin-II to relocate at the poles of the actin cage and act as a force generator. To our knowledge, this is the first description of an F-actin network that is able to actively change the localization of myosin-II. The mechanism involved is completely unknown. One possibility is that the nucleation of the cortical F-actin thickening creates an environment that is not favorable for myosin-II attachment to actin filaments. The cortical filaments indeed seem to create a very dense environment (Figure 1a-e). Furthermore, photoactivation experiments point to the fact that the cortical actin network is far less dynamic than the cytoplasmic actin meshwork [3]. It is also possible that the actin networks structure play a role in the localization of myosin-II: straight filaments nucleated by Formin-2 and Spire1/2 could have a better affinity for myosin-II than Arp2/3 nucleated branched filaments. Alternatively, it is possible that the physical stress experimented by the actin filaments plays a part in myosin-II recruitment. Indeed, in the amoeba *Dictyostelium discoideum*, myosin-II is preferentially localized to actin filaments under tension [38]. Here, one could imagine that the filaments connecting the actin cage and the cortex, pulled by myosin-II, are under more stress than the other cortical filaments and hence recruit more myosin-II, in an auto-amplificatory mechanism, thus depleting myosin-II from the cortex. One argument in this direction is that the so called “actin cap” above the Metaphase II spindle harbors a higher cortical tension than the rest of the cortex [17] and is enriched is myosin-II [39].

Finally, this work paves the way for future clinical applications, as finding simple tools (for example measurement of cortical tension, as used for cancer cells metastatic prognosis [40]) to rate the quality of an oocyte to achieve meiosis successfully is critical for the success of *in vitro* fertilization, a technique more and more used in modern societies where women tend to postpone childbearing.

Methods

Oocyte collection, culture, micro-injection and drug treatment.

Oocytes were collected from 11-week-old OF1 (*wt*) or *mos*-/- female mice as previously described [41] and maintained in Prophase I arrest in M2+BSA medium supplemented with 1mM milrinone [42]. At this stage, they were micro-injected with cRNAs using an Eppendorf Femtojet micro-injector. For rescue experiments in *mos*-/- oocytes, cRNAs encoding the cVCA were injected at a dilution of 50ng/μL. Prophase I oocytes were kept for 2-3h in Prophase I arrest to allow expression of fusion proteins. Meiosis resumption was triggered by releasing oocytes into milrinone-free M2+BSA medium. All live culture and imaging were carried out under oil at 37 °C.

The stock solution of CK666 (gift from T. Pollard and Calbiochem, Ref. 182515) was diluted at 100 mM in DMSO and stored at –80 ° C. It was used on oocytes at 200 μM starting from NEBD+3h. Control experiments were performed in M2+BSA medium with equivalent dilutions of DMSO in separate dishes (the drug diffuses in the oil).

Plasmids and *in vitro* transcription of cRNAs.

We used the following constructs: pspe3-GFP-UtrCH [12], pRN3-histone-RFP [43] or pRN3-histone-GFP, pRN3-SF9-GFP [44].

We constructed pRN3-Ez-mCherry-VCA by cloning the VCA domain of Wave2 into a pRN3-EzTD-mCherry [33] construct.

In vitro synthesis of capped cRNAs was performed as previously described [45]. cRNAs were centrifuged at 4°C for 45min at 20,000g before micro-injection.

Live imaging.

Spinning disc images were acquired at 37°C in M2+BSA medium using a Plan-APO x40/1.25NA objective on a Leica DMI6000B microscope enclosed in a thermostatic chamber (Life Imaging Service) equipped with a CoolSnap HQ2/CCD (charge-coupled device) camera (Princeton Instruments) coupled to a Sutter filter wheel (Roper Scientific) and a Yokogawa CSU-X1-M1spinning disc. Metamorph software (Universal Imaging) was used to collect data and ImageJ (NIH) to analyse and process data.

Modeling of actin distribution in the oocyte.

We assume that actin filaments emanate from the actin cage tip and have an exponential distribution. The filaments grow in the cytoplasm and penetrate the cortex. We call N(l) the density of filaments at a given length l.

Then:

$N_{cyto}(l) \propto e^{-(\frac{l}{l_0})}$, with l_0 the mean length of filaments in the cytoplasm, and $N_c(l) \propto e^{-(\frac{l}{l_c})}$ with l_c the mean length of the cortical part of the filaments.

The density of filaments is thus given by:

$$N(l,x) = \begin{cases} e^{-\frac{(l-x)}{l_0}}, L \mp x + \delta h_{\pm} \geq l \geq 0 \\ e^{(-\frac{L \mp x - \delta h_{\pm}}{l_0} - \frac{l - L \pm x + \delta h_{\pm}}{l_c})}, l \geq L \mp x - \delta h_{\pm} \end{cases}$$

The force is produced when the filaments emanating from the spindle tip overlap with the cortex, and the overlap is given by the mean length of overlap multiplied by the density of filaments.

$L_{overlap,\pm} = l_c e^{-(\frac{L \mp x - \delta h_{\pm}}{l_0})}$.

Thus the force is given by: $F_{\pm} = \beta L_{overlap,\pm}$, with β a parameter describing myosin-II activity.

Vesicle speed analysis.

Stream movies were acquired at a frequency of 500ms for five minutes. Movies were then denoised using the Safir plugin for the Metamorph software (Universal Imaging), aligned and corrected for the bleaching using Fiji (NIH). Vesicles were then tracked using the Trackmate plugin for Fiji. The tracks were considered relevant when they exceeded 25 seconds.

Cortical tension and viscosity measurements.

Measurements of cortical tension in Prophase I oocytes were performed as previously described [3]. For Prophase I *wt* oocytes and Prophase I Ezrin overexpressing oocytes, the cortical tension was so high that the critical pressure could not be reached. Thus, in order to

access a minimum value for critical pressure, we looked at which pressure we first saw bleb forming during cortex aspiration. The critical pressure would necessarily be smaller than this value, thus we used this pressure value as “minimal” critical pressure value. This allowed us to calculate a minimum value for cortical tension.

For viscosity measurements, the zona pellucida of oocytes was removed using acid tyrod (pH = 2,3). Oocytes were aspirated in a 50μm diameter micropipette until they were completely inside the pipette. Great care was taken that all oocytes stay inside the pipette for the same duration. They were then released and the shape recovery was recorded. The curve representing the evolution of the flattened diameter was plotted as a function of time and fitted as an exponential. The characteristic time τ was extracted and the viscosity η was deduced from the formula: $\tau = \frac{\eta Rc}{k}$, with Rc the cell radius and k the cortical tension.

Statistical analysis.

The statistical analysis was performed using GraphPad Prism version 6.00 for MacOS, GraphPad Software, La Jolla California USA, www.graphpad.com. Student's t-tests (with Welch correction where indicated), χ^2 and one-way Anova were used with a confidence interval of 95%. In all figures, * corresponds to a P value <0 ,05, ** to a P value <0, 005, *** to a P value <0,0005 and **** to a P value <0,0001. NS: Not statistically Significant.

Acknowledgments :

We thank G. Halet for providing the pRN3-histone-GFP plasmid, S. Louvet for providing the pRN3-EzTD-mCherry plasmid, A. Gautreau for providing the pCS2-Wave2 plasmid, F. Perez for providing SF9-expressing plasmids. We also thank M. Piel, A. Echard, and A. Gautreau for helpful discussions.

This work was supported by grants from the Ligue Nationale Contre le Cancer (EL2009-EL2012/LNCC/MHV) and from the Agence Nationale pour la Recherche (ANR-08-BLAN-0136-01 to MHV). A. Chaigne is a recipient of a fellowship from the Ecole Normale Supérieure (ENS) Paris.

Author contributions

A.C, M.H.V and M.E.T designed the experiments, interpreted the results and wrote the manuscript. A.C and M.E.T carried out most of the experiments. A.C and C.C carried out the micropipette experiments. A.C, C.C and C.S designed the micropipette experiments and interpreted the results. N.S.G and R.V designed the mathematical model. M.E.T and M.H.V supervised the project.

Competing Financial interests

The authors declare no competing financial interests.

References:

1. Fink, J. *et al.* External forces control mitotic spindle positioning. *Nat. Cell Biol.* **13,** 771–778 (2011).
2. Théry, M. *et al.* The extracellular matrix guides the orientation of the cell division axis. *Nat. Cell Biol.* **7,** 947–953 (2005).
3. Chaigne, A. *et al.* A soft cortex is essential for asymmetric spindle positioning in mouse oocytes. *Nat. Cell Biol.* **15,** 958–966 (2013).
4. Verlhac, M.-H., Lefebvre, C., Guillaud, P., Rassinier, P. & Maro, B. Asymmetric division in mouse oocytes: with or without Mos. *Curr. Biol.* **10,** 1303–1306 (2000).
5. Maro, B. & Verlhac, M.-H. Polar body formation: new rules for asymmetric divisions. *Nat. Cell Biol.* **4,** E281–E283 (2002).
6. Halet, G. & Carroll, J. Rac Activity Is Polarized and Regulates Meiotic Spindle Stability and Anchoring in Mammalian Oocytes. *Dev. Cell* **12,** 309–317 (2007).
7. FitzHarris, G., Marangos, P. & Carroll, J. Changes in endoplasmic reticulum structure during mouse oocyte maturation are controlled by the cytoskeleton and cytoplasmic dynein. *Dev. Biol.* **305,** 133–144 (2007).
8. Dalton, C. M. & Carroll, J. Biased inheritance of mitochondria during asymmetric cell division in the mouse oocyte. *J. Cell Sci.* **126,** 2955–2964 (2013).
9. Szollosi, D., Calarco, P. & Donahue, R. P. Absence of centrioles in the first and second meiotic spindles of mouse oocytes. *J. Cell Sci.* **11,** 521–541 (1972).
10. Leader, B. *et al.* Formin-2, polyploidy, hypofertility and positioning of the meiotic spindle in mouse oocytes. *Nat. Cell Biol.* **4,** 921–928 (2002).

11. Dumont, J. *et al.* Formin-2 is required for spindle migration and for the late steps of cytokinesis in mouse oocytes. *Dev. Biol.* **301,** 254–265 (2007).
12. Azoury, J. *et al.* Spindle Positioning in Mouse Oocytes Relies on a Dynamic Meshwork of Actin Filaments. *Curr. Biol.* **18,** 1514–1519 (2008).
13. Schuh, M. & Ellenberg, J. A New Model for Asymmetric Spindle Positioning in Mouse Oocytes. *Curr. Biol.* **18,** 1986–1992 (2008).
14. Pfender, S., Kuznetsov, V., Pleiser, S., Kerkhoff, E. & Schuh, M. Spire-Type Actin Nucleators Cooperate with Formin-2 to Drive Asymmetric Oocyte Division. *Curr. Biol.* **21,** 955–960 (2011).
15. Verlhac, M. H. *et al.* Mos is required for MAP kinase activation and is involved in microtubule organization during meiotic maturation in the mouse. *Development* **122,** 815 – 822 (1996).
16. Verlhac, M.-H. Mos activates MAP kinase in mouse oocytes through two opposite pathways. *EMBO J.* **19,** 6065–6074 (2000).
17. Larson, S. M. *et al.* Cortical Mechanics and Meiosis II Completion in Mammalian Oocytes Are Mediated by Myosin-II and Ezrin-Radixin-Moesin (ERM) Proteins. *Mol. Biol. Cell* **21,** 3182–3192 (2010).
18. Matthews, H. K. *et al.* Changes in Ect2 Localization Couple Actomyosin-Dependent Cell Shape Changes to Mitotic Progression. *Dev. Cell* **23,** 371–383 (2012).
19. Stewart, M. P. *et al.* Hydrostatic pressure and the actomyosin cortex drive mitotic cell rounding. *Nature* **469,** 226–230 (2011).
20. Kunda, P., Pelling, A. E., Liu, T. & Baum, B. Moesin Controls Cortical Rigidity, Cell Rounding, and Spindle Morphogenesis during Mitosis. *Curr. Biol.* **18,** 91–101 (2008).
21. Lancaster, O. M. *et al.* Mitotic rounding alters cell geometry to ensure efficient bipolar spindle formation. *Dev. Cell* **25,** 270–283 (2013).
22. Cadart, C., Zlotek-Zlotkiewicz, E., Le Berre, M., Piel, M. & Matthews, H. K. Exploring the Function of Cell Shape and Size during Mitosis. *Dev. Cell* **29,** 159–169 (2014).
23. Simerly, C., Nowak, G., de Lanerolle, P. & Schatten, G. Differential expression and functions of cortical myosin IIA and IIB isotypes during meiotic maturation, fertilization, and mitosis in mouse oocytes and embryos. *Mol. Biol. Cell* **9,** 2509–2525 (1998).
24. Burkel, B. M., von Dassow, G. & Bement, W. M. Versatile fluorescent probes for actin filaments based on the actin-binding domain of utrophin. *Cell Motil. Cytoskeleton* **64,** 822–832 (2007).
25. Nolen, B. J. *et al.* Characterization of two classes of small molecule inhibitors of

Arp2/3 complex. *Nature* **460,** 1031–1034 (2009).

26. Sun, S.-C. *et al.* Arp2/3 Complex Regulates Asymmetric Division and Cytokinesis in Mouse Oocytes. *PLoS ONE* **6,** e18392 (2011).

27. Prass, M. Direct measurement of the lamellipodial protrusive force in a migrating cell. *J. Cell Biol.* **174,** 767–772 (2006).

28. Dang, I. *et al.* Inhibitory signalling to the Arp2/3 complex steers cell migration. *Nature* **503,** 281–284 (2013).

29. Craig, E. M., Van Goor, D., Forscher, P. & Mogilner, A. Membrane Tension, Myosin Force, and Actin Turnover Maintain Actin Treadmill in the Nerve Growth Cone. *Biophys. J.* **102,** 1503–1513 (2012).

30. Kolano, A., Brunet, S., Silk, A. D., Cleveland, D. W. & Verlhac, M.-H. Error-prone mammalian female meiosis from silencing the spindle assembly checkpoint without normal interkinetochore tension. *Proc. Natl. Acad. Sci.* **109,** E1858–E1867 (2012).

31. Lam, J., Herant, M., Dembo, M. & Heinrich, V. Baseline Mechanical Characterization of J774 Macrophages. *Biophys. J.* **96,** 248–254 (2009).

32. Campellone, K. G. & Welch, M. D. A nucleator arms race: cellular control of actin assembly. *Nat. Rev. Microbiol.* **11,** 237–251 (2010).

33. Dard, N., Louvet-Vallée, S., Santa-Maria, A. & Maro, B. Phosphorylation of ezrin on threonine T567 plays a crucial role during compaction in the mouse early embryo. *Dev. Biol.* **271,** 87–97 (2004).

34. Goley, E. D. & Welch, M. D. The ARP2/3 complex: an actin nucleator comes of age. *Nat Rev Mol Cell Biol* **7,** 713–726 (2006).

35. Verlhac, M. H., de Pennart, H., Maro, B., Cobb, M. H. & Clarke, H. J. MAP kinase becomes stably activated at metaphase and is associated with microtubule-organizing centers during meiotic maturation of mouse oocytes. *Dev. Biol.* **158,** 330–340 (1993).

36. Azoury, J., Lee, K. W., Georget, V., Hikal, P. & Verlhac, M.-H. Symmetry breaking in mouse oocytes requires transient F-actin meshwork destabilization. *Development* **138,** 2903–2908 (2011).

37. Schuh, M. An actin-dependent mechanism for long-range vesicle transport. *Nat. Cell Biol.* **13,** 1431–1436 (2011).

38. Uyeda, T. Q. P., Iwadate, Y., Umeki, N., Nagasaki, A. & Yumura, S. Stretching Actin Filaments within Cells Enhances their Affinity for the Myosin II Motor Domain. *PLoS ONE* **6,** e26200 (2011).

39. Longo, F. & Chen, D. Development of cortical polarity in mouse eggs: Involvement of

the meiotic apparatus. *Dev. Biol.* **107,** 382–394 (1985).

40. Guck, J. *et al.* Optical Deformability as an Inherent Cell Marker for Testing Malignant Transformation and Metastatic Competence. *Biophys. J.* **88,** 3689–3698 (2005).

41. Verlhac, M. H., Kubiak, J. Z., Clarke, H. J. & Maro, B. Microtubule and chromatin behavior follow MAP kinase activity but not MPF activity during meiosis in mouse oocytes. *Dev. Camb. Engl.* **120,** 1017–1025 (1994).

42. Reis, A., Chang, H.-Y., Levasseur, M. & Jones, K. T. APCcdh1 activity in mouse oocytes prevents entry into the first meiotic division. *Nat. Cell Biol.* **8,** 539–540 (2006).

43. Tsurumi, C. The spindle assembly checkpoint is not essential for CSF arrest of mouse oocytes. *J. Cell Biol.* **167,** 1037–1050 (2004).

44. Nizak, C. *et al.* Recombinant Antibodies Against Subcellular Fractions Used to Track Endogenous Golgi Protein Dynamics in Vivo: Recombinant Antibodies for Cell Biology. *Traffic* **4,** 739–753 (2003).

45. Terret, M. E. *et al.* DOC1R: a MAP kinase substrate that control microtubule organization of metaphase II mouse oocytes. *Dev. Camb. Engl.* **130,** 5169–5177 (2003).

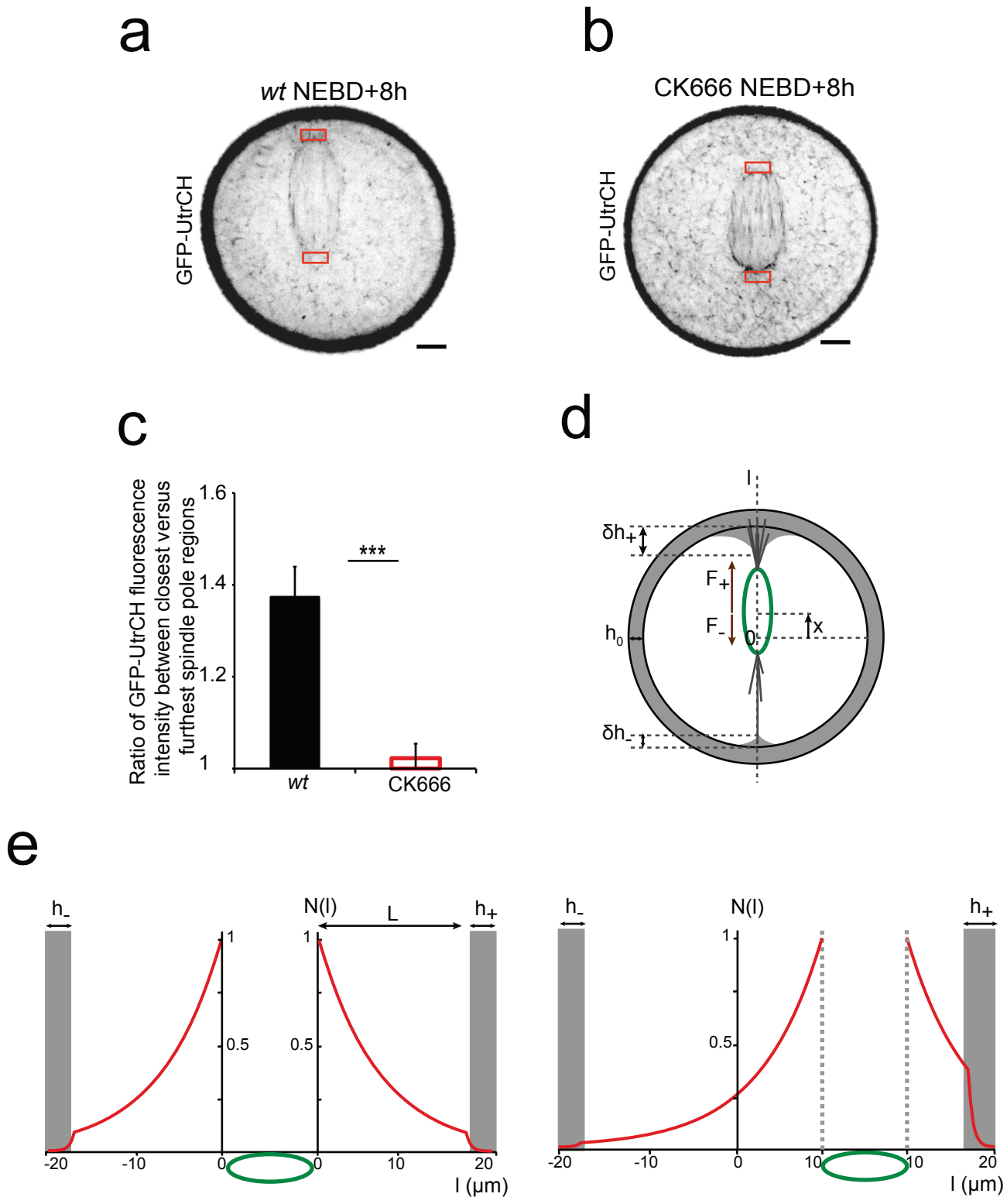
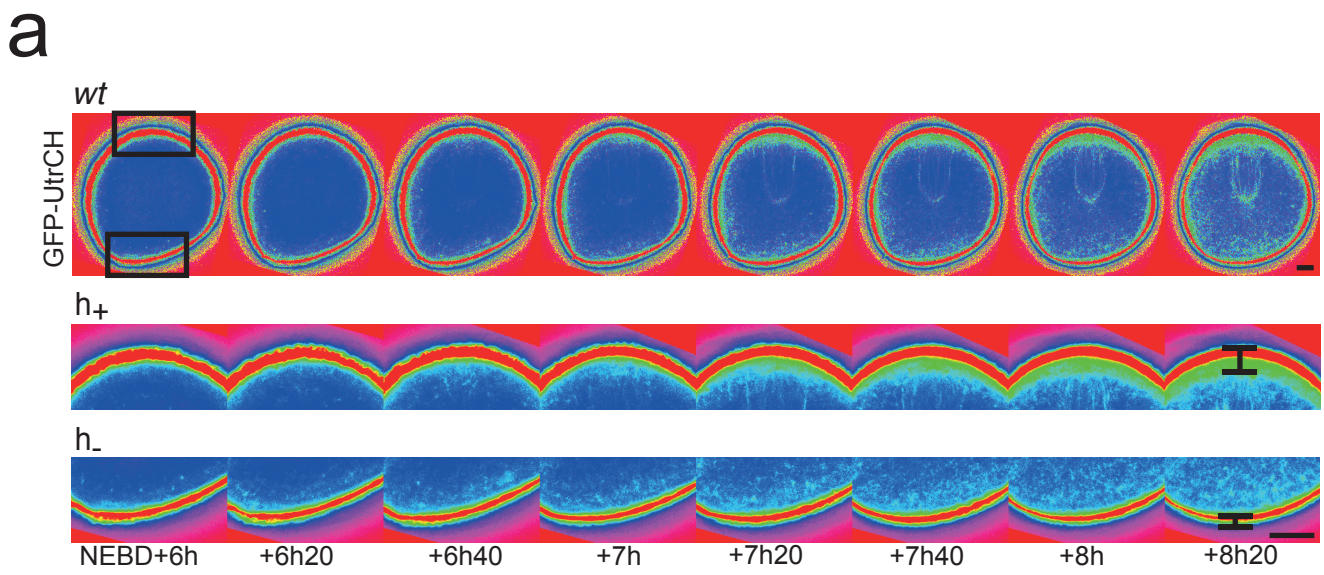
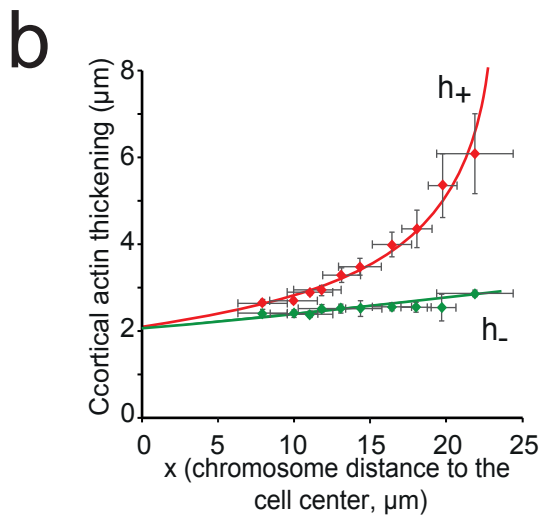
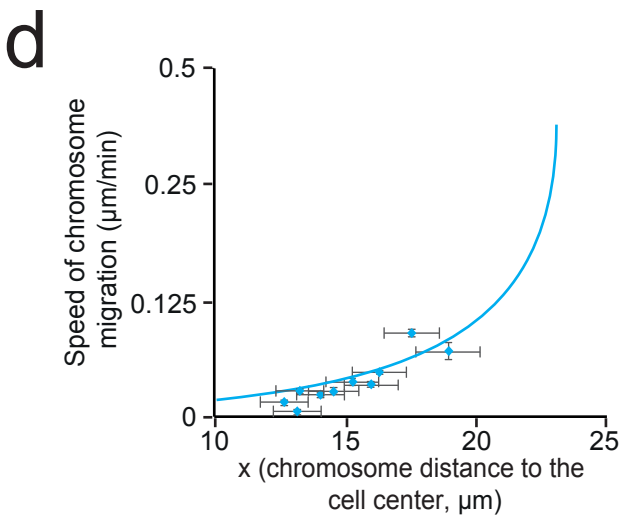

a
wt NEBD+8h
GFP-UtrCH
b
CK666 NEBD+8h
GFP-UtrCH
c
Ratio of GFP-UtrCH fluorescence intensity between closest versus furthest spindle pole regions
1.6
1.4
1.2
1
***
wt
CK666
d
l
δh+
F+
F-
h0
0
x
δh-
e
h-
N(l)
L
h+
1
0.5
-20
-10
0
10
20
l (μm)

Figure 1


a
wt
GFP-UtrCH
h+
h-
NEBD+6h
+6h20
+6h40
+7h
+7h20
+7h40
+8h
+8h20


b
Ccortical actin thickening (µm)
h+
h-
x (chromosome distance to the cell center, µm)


d
Speed of chromosome migration (µm/min)
x (chromosome distance to the cell center, µm)

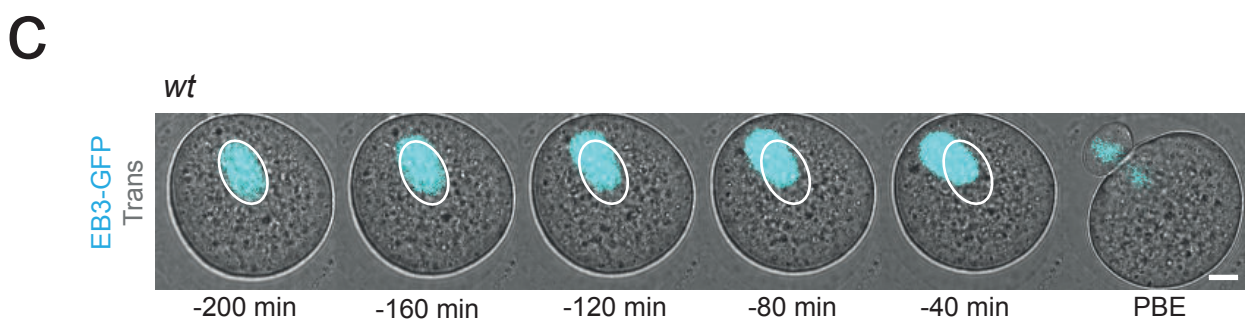

c
wt
EB3-GFP
Trans
-200 min
-160 min
-120 min
-80 min
-40 min
PBE

Figure 2

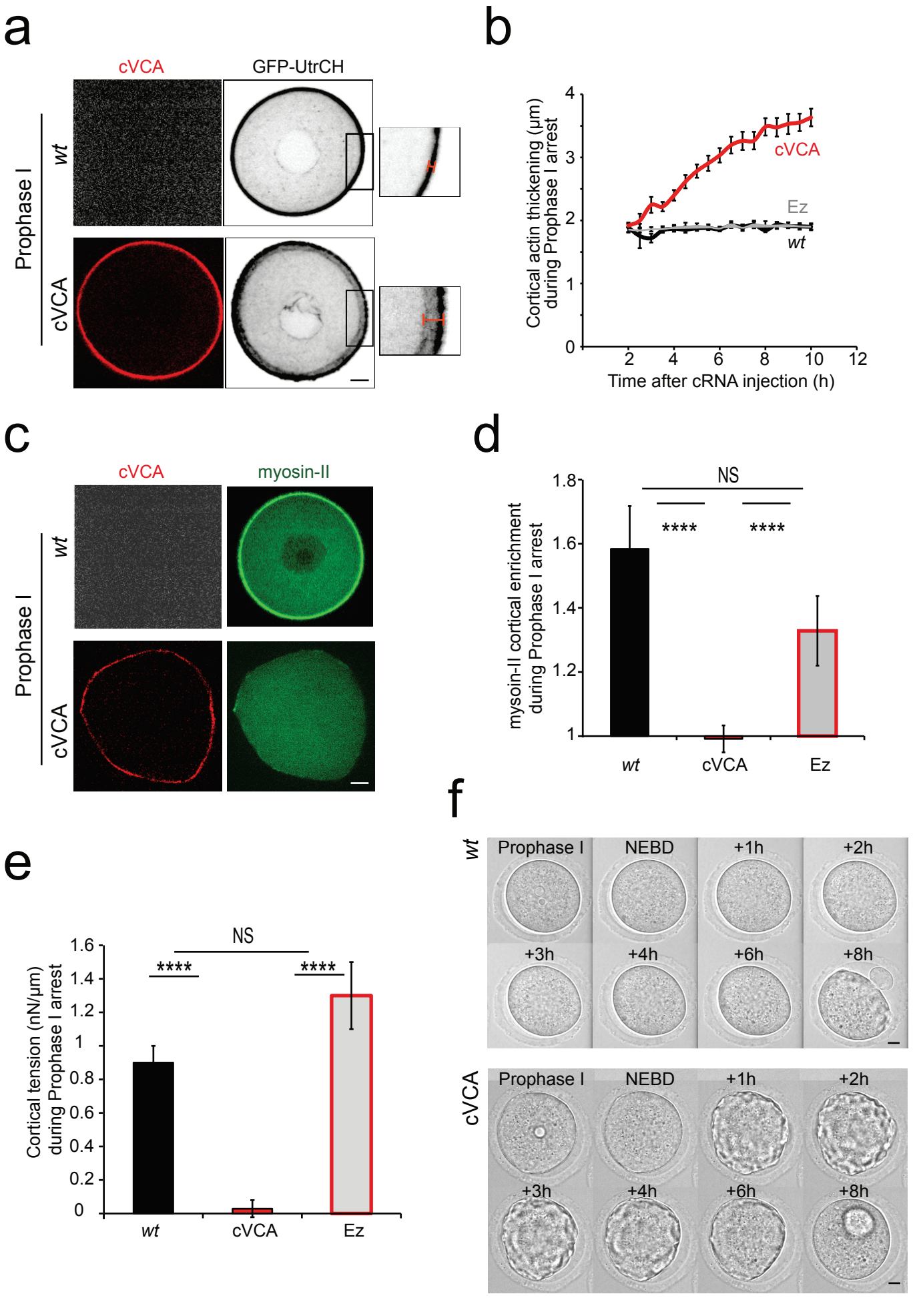

a
cVCA
GFP-UtrCH
Prophase I
wt
cVCA
b
Cortical actin thickening (µm) during Prophase I arrest
cVCA
Ez
wt
Time after cRNA injection (h)
c
cVCA
myosin-II
Prophase I
wt
cVCA
d
mysoin-II cortical enrichment during Prophase I arrest
NS
****
****
wt
cVCA
Ez
e
Cortical tension (nN/µm) during Prophase I arrest
NS
****
****
wt
cVCA
Ez
f
wt
Prophase I
NEBD
+1h
+2h
+3h
+4h
+6h
+8h
cVCA
Prophase I
NEBD
+1h
+2h
+3h
+4h
+6h
+8h

Figure 3

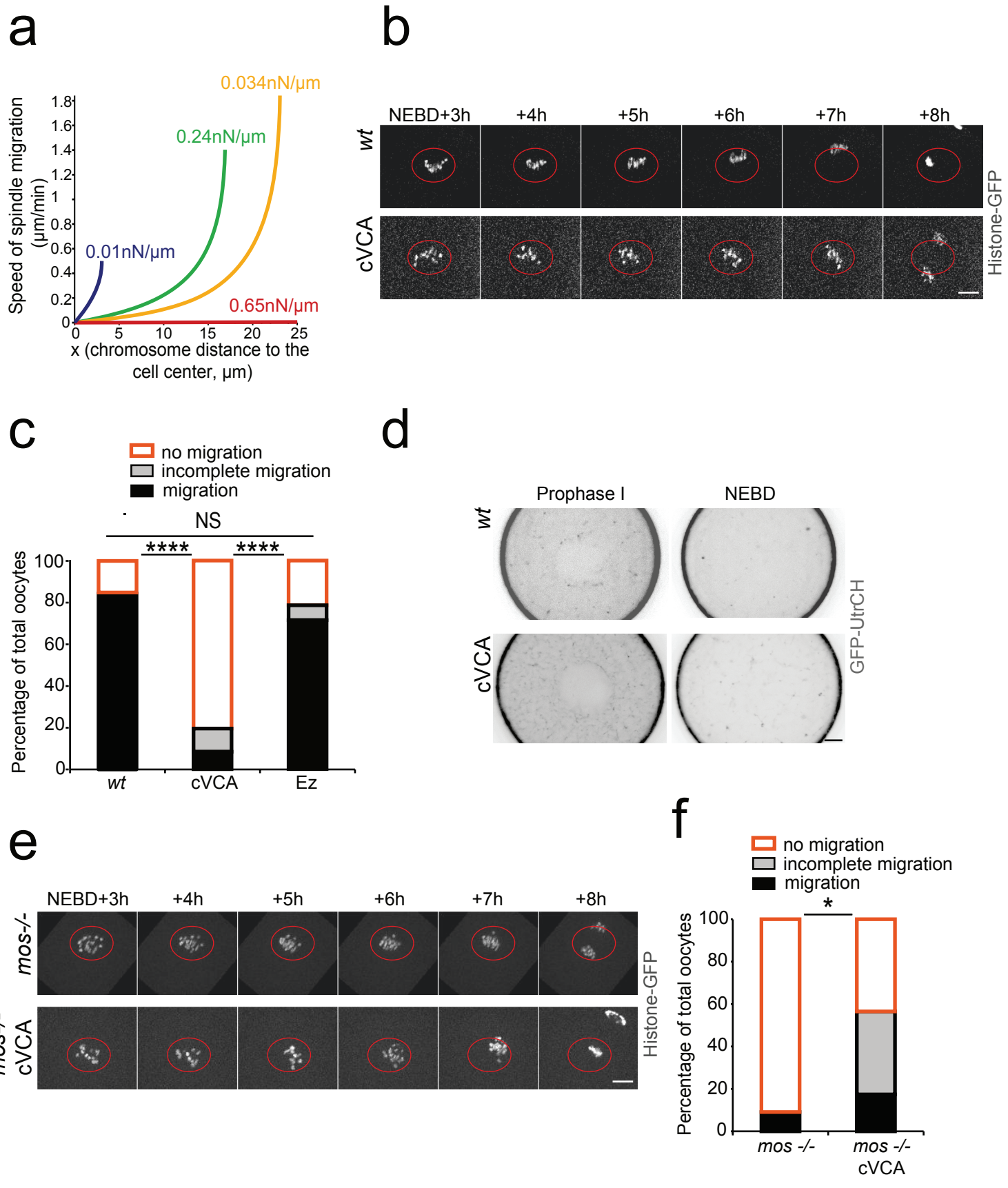
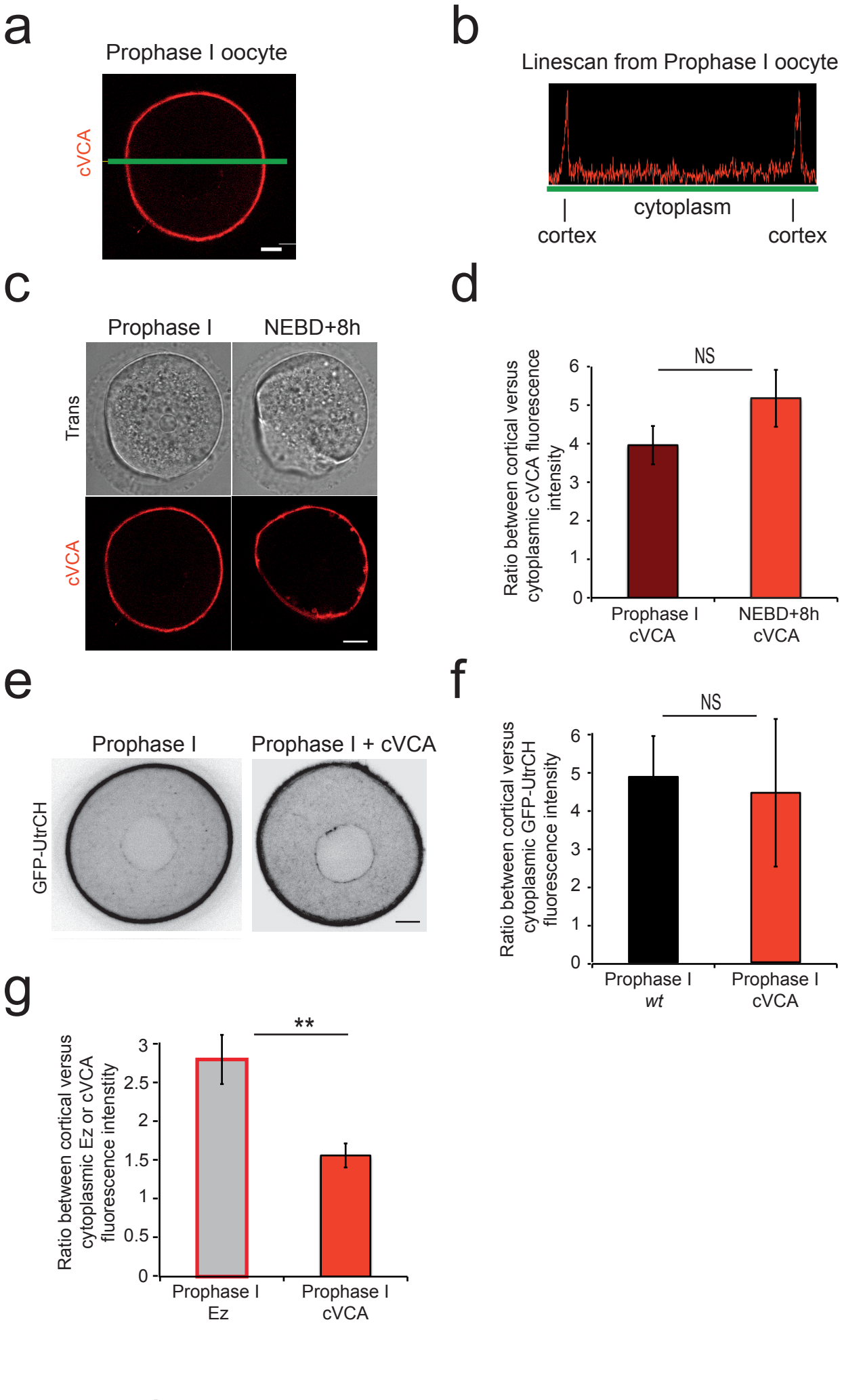
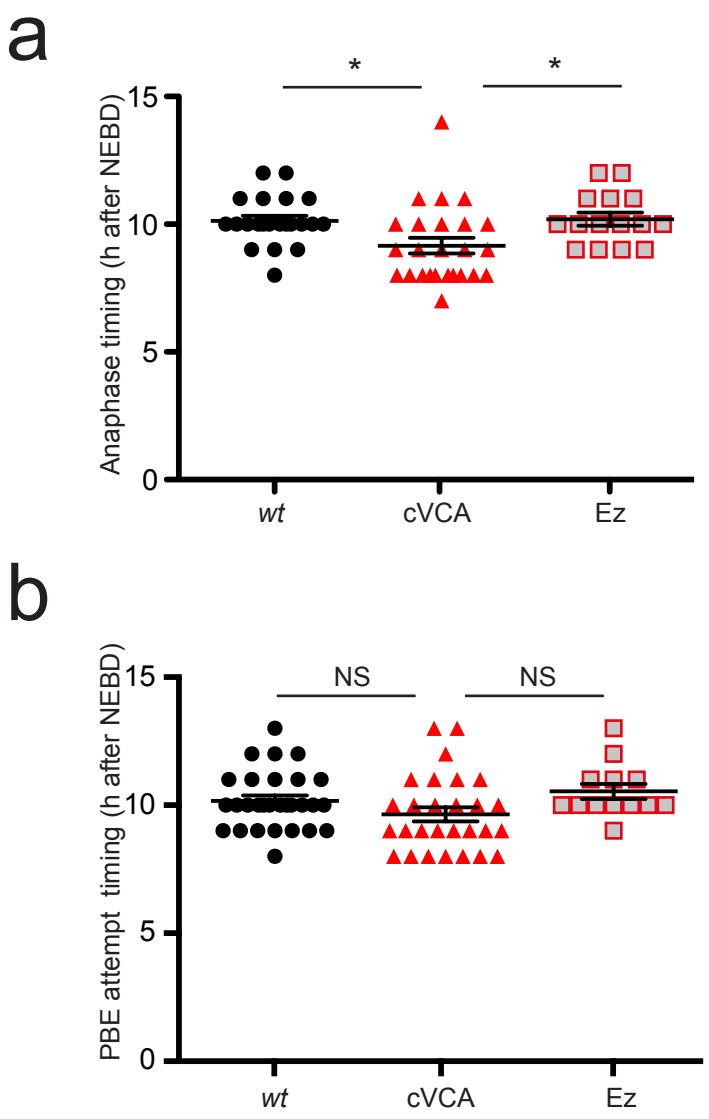

a
0.034nN/µm
0.24nN/µm
0.01nN/µm
0.65nN/µm
Speed of spindle migration (µm/min)
x (chromosome distance to the cell center, µm)
b
NEBD+3h
+4h
+5h
+6h
+7h
+8h
wt
cVCA
Histone-GFP
c
no migration
incomplete migration
migration
NS
****
****
Percentage of total oocytes
wt
cVCA
Ez
d
Prophase I
NEBD
wt
cVCA
GFP-UtrCH
e
NEBD+3h
+4h
+5h
+6h
+7h
+8h
mos-/-
mos-/- cVCA
Histone-GFP
f
no migration
incomplete migration
migration
*
Percentage of total oocytes
mos -/-
mos -/- cVCA

Figure 4



Supplemental Figure 1



Supplemental Figure 2

Figure legend:

Figure 1: myosin-II pulls the actin cage towards the cortex during Meiosis I. a) Confocal spinning disc image of a *wt* oocyte in late Meiosis I (NEBD+8h) expressing GFP-UtrCH (black). One Z-plane is shown. The red boxes highlight the regions taken to measure the density of actin filaments in c). Scale bar: 10μm. b) Confocal spinning disc image of a *wt* oocyte treated with 200 μM of CK666 in late Meiosis I (NEBD+8h) expressing GFP-UtrCH (black). One Z-plane is shown. The red boxes highlight the regions taken to measure the density of actin filaments in c). Scale bar: 10μm. c) Ratio of GFP-UtrCH fluorescence intensity between regions taken at the closest and furthest spindle poles from the cortex (red boxes in a)) in *wt* oocytes (black bar) and *wt* oocytes treated with CK666 (white bar) in late Meiosis I. Mean of 10 *wt* oocytes and 7 *wt* oocytes treated with CK666 is shown over 2 independent experiments. Standard error of the mean is plotted on each bar. Statistical difference is assessed with a t-test with Welch correction (pvalue = 0.0002). d) Model of spindle migration. The green object represents the spindle, (0l) the migration axis and x the position of the spindle at a given time t. Actin is in grey. The spindle tip is source of actin polymerization (dark grey lines). h_0 represents the cortical actin thickening, δh_+ the extra deformation where the spindle reaches the cortex and δh_- on the other side. F_+ and F_- are the pulling forces exerted on the spindle poles by myosin-II. e) Model of F-actin density as a function of spindle position. The cortical actin thickening is figured in grey and referred as h_- (representing $h_o + \delta h_+$) or h_+ (representing $h_o + \delta h_{+)}$. The parameters used are L = 17μm, l_0 = 7μm, l_c = 0.5μm, h_0 = 3μm. The left panel represents the distribution for a spindle that would be in the exact center of the cell thus x = 0μm and in that case $\delta h_+ = \delta h_- = 0$μm. The right panel represents the distribution during spindle migration for x = 10μm and in that case δh_+ = 0.5μm and $\delta h_- = 0$μm.

Figure 2: The force exerted on the spindle is converted into a movement towards the cortex. a) Upper panel: confocal spinning disc images of a *wt* oocyte in late Meiosis I expressing GFP-UtrCH (Blue, lowest intensity; red, highest intensity). One Z-plane is shown. Scale bar: 10μm. Frames are 20 minutes apart. Lower panel: magnifications of the black boxes presented in upper panel. The black bars indicate h_+ (top) and h_- (bottom). Scale bar: 3μm. b) Quantification of the deformation of the cortex (h_+: red, h_-: green) in μm as a function of

chromosome position x in μm and fitting curves. Quantification starts at NEBD+6h. Mean of 10 oocytes over 3 different experiments is shown. Standard error of the mean is shown. c) Confocal spinning disc images of a *wt* oocyte in late Meiosis I expressing EB3-GFP (blue). A Z-projection over 25μm is shown. Time is given as time in minutes before Polar Body Extrusion (PBE). The white circle highlights the initial position of the spindle. Scale bar: 10μm. d) Speed of the spindle as a function of chromosome position (x) and fitting curve. Mean of 12 oocytes is shown from 4 independent experiments. Standard error of the mean is plotted.

Figure 3: The cortical actin thickening is responsible for myosin-II exclusion from the cortex and decrease in cortical tension in Meiosis I. a) Confocal spinning disc images of a Prophase I oocyte expressing GFP-UtrCH (black) (top panel) or cVCA (red) and GFP-UtrCH (black) (bottom panel) 4 hours after cRNA injection. Boxes represent magnification of the cortex region. One Z-plane is shown. Scale bar: 10μm. b) Curves showing the cortical actin thickening as a function of time after cRNA injection. Mean is shown of 11 oocytes expressing GFP-UtrCH (black curve), 20 oocytes expressing cVCA and GFP-UtrCH (red curve) and 15 oocytes expressing Ez and GFP-UtrCH (grey curve) assessed over 2 independent experiments. Oocytes are kept in Prophase I. Standard error of the mean is shown. c) Confocal spinning disc images of a Prophase I oocyte expressing SF9-GFP (myosin-II intrabody, green) (upper panel) or cVCA (red) and SF9-GFP (green) (lower panel) 3 hours after cRNA injection. One Z-plane is shown. Scale bar: 10μm. d) Bar graph showing the ratio between the average intensities of cortical versus cytoplasmic myosin-II in Prophase I oocytes expressing for 3 hours SF9-GFP (black bar), SF9-GFP and cVCA (red bar), or SF9-GFP and Ez (grey bar). For each oocyte, 6 measurements were taken in the cortex and 6 in the cytoplasm. Mean of 12 SF9-GFP expressing oocytes, 17 SF9-GFP and cVCA expressing oocytes and 10 SF9-GFP and Ez expressing oocytes is shown assessed over 3 independent experiments. Standard error is plotted on each bar. The statistical significance of differences is assessed with a t-test or a t-test with Welch correction (pvalues: SF9-GFP expressing oocytes versus SF9-GFP and cVCA expressing oocytes 0.0002; SF9-GFP expressing oocytes versus SF9-GFP and Ez expressing oocytes 0.609; SF9-GFP and Ez expressing oocytes versus SF9-GFP and cVCA expressing oocytes 0.0145). e) Bar graph showing values of cortical tension in Prophase I oocytes (black bar, minimum value see Method section), Prophase I oocytes expressing cVCA (red bar) or Prophase I oocytes expressing Ez (grey bar,

minimum value see Method section). Mean of 20 *wt* oocytes, 11 oocytes expressing cVCA and 14 oocytes expressing Ez is shown, assessed over 2 independent experiments. Standard error is plotted on each bar. Statistical differences were assessed with a t-test with Welch correction (pvalues: *wt* oocytes versus cVCA expressing oocytes <0.0001; *wt* oocytes versus Ez expressing oocytes 0.0892; Ez expressing oocytes versus cVCA expressing oocytes <0.0001). f) Confocal spinning disc transmitted light images of a *wt* oocyte or a *wt* oocyte expressing cVCA during Meiosis I. Scale bar: 10μm.

Figure 4: Cortical tension has to be tightly regulated to allow spindle migration. a) Model prediction of spindle velocity $\dot{x}$ as a function of spindle position for different values of cortical tension k (blue curve: k = 0.01nN/μm; green curve k = 0.024nN/μm; yellow curve k = 0.034nN/μm; red curve k = 0.65nN/μm). b) Confocal spinning disc images of *wt* oocytes in Meiosis I expressing Histone-GFP (upper panel) or Histone-GFP and cVCA (lower panel). Frames are 1 hour apart. A Z-projection over 25μm is shown. The red circle highlights the initial position of the chromosomes before migration. Scale bar: 10μm. c) Bar graph representing the percentage of oocytes out of 33 Prophase I oocytes, 36 Prophase I oocytes expressing cVCA or 14 Prophase I oocytes expressing Ez undergoing normal spindle migration (black bar), incomplete spindle migration (grey bar) or no spindle migration (white bar) over four independent experiments. Statistical difference of repartition was assessed using a χ^2 test (pvalues: *wt* oocytes versus cVCA expressing oocytes <0.0001; *w*t oocytes versus Ez expressing oocytes 0.2849; Ez expressing oocytes versus cVCA expressing oocytes <0.0001). d) Confocal spinning disc images of a *wt* oocyte expressing GFP-UtrCH (black) (upper panel) or GFP-UtrCH (black) and cVCA (lower panel) in Prophase I two hours after injection, when the actin thickening is not yet formed (see Figure 3b)) and at NEBD. Scale bar: 10μm. e) Confocal spinning disc images of *mos-/-* oocytes in Meiosis I expressing Histone-GFP (upper panel) or Histone-GFP and cVCA (lower panel). Frames are 1 hour apart. A Z-projection over 25μm is shown. The red circle highlights the initial position of the chromosomes before migration. Scale bar: 10μm. f) Bar graph representing the percentage of oocytes out of 11 *mos-/-* oocytes or 23 *mos-/-* oocytes expressing cVCA undergoing normal spindle migration (black bar), incomplete spindle migration (grey bar) or no spindle migration (white bar) over 3 independent experiments. Statistical difference of repartition was assessed using a χ^2 test (pvalue = 0.0235).

Movie 1: Time-lapse movie showing a *wt* oocyte expressing Histone-GFP (red) and cVCA from Prophase I to NEBD+10h. Frames are 1 hour apart. A Z-projection over 25μm is shown.

Movie 2: Time-lapse movie showing a *wt* oocyte expressing Histone-GFP (red) from Prophase I to NEBD+10h. Frames are 1 hour apart. A Z-projection over 25μm is shown.

Movie 3: Time-lapse movie showing a *mos-/-* oocyte expressing Histone-GFP (red) and cVCA from Prophase I to NEBD+10h. Frames are 1 hour apart. A Z-projection over 25μm is shown.

Movie 4: Time-lapse movie showing a *mos-/-* oocyte expressing Histone-GFP (red) from Prophase I to NEBD+10h. Frames are 1 hour apart. A Z-projection over 25μm is shown

Supplemental figure legend:

Supplemental Figure 1: cVCA is stably restricted to the oocyte membrane and does not perturb actin in the cytoplasm. a) Confocal spinning disc image of a Prophase I *wt* oocyte expressing cVCA (red). One Z-plane is shown. Scale bar: 10μm. b) Linescan along the green line presented in a) showing cVCA fluorescence intensity in arbitrary units. c) Confocal spinning disc images of a *wt* oocyte expressing cVCA (red) in Prophase I (left) or at NEBD+8h (right). Upper panel: transmitted light. One Z-plane is shown. Scale bar: 10μm. d) Bar graph showing the ratio between cortical versus cytoplasmic cVCA fluorescence intensity of *wt* oocytes expressing cVCA in Prophase I (dark red) or at NEBD+8h (red). Mean of 12 oocytes is shown. Standard error of the mean is plotted on each bar. Statistical difference was assessed using a t-test (pvalue = 0.1860). e) Confocal spinning disc images of a Prophase I oocyte expressing GFP-UtrCH (black) (left) or GFP-UtrCH (black) and cVCA (right) 2 hours after cRNA injection when the actin thickening has not formed yet (see Figure 3b)). One Z-plane is shown. Scale bar: 10μm. f) Bar graph showing the ratio between cortical versus cytoplasmic GFP-UtrCH fluorescence intensity of Prophase I oocytes (black bar) or Prophase

I oocytes expressing cVCA (red bar) 2 hours after cRNA injection. Mean of 14 *wt* oocytes and 26 oocytes expressing cVCA assessed over 2 independent experiments is shown. Standard deviation is plotted on each bar. Statistical difference was assessed using a t-test with Welch correction (pvalue = 0.3846). g) Bar graph showing the ratio between cortical versus cytoplasmic Ez or cVCA fluorescence intensity of Ez (grey bar) or cVCA (red bar) expressing oocytes in Prophase I, 2 hours after cRNA injection. Mean of 12 *wt* oocytes expressing Ez and 12 oocytes expressing cVCA assessed over 2 independent experiments is shown. Standard deviation is plotted on each bar. Statistical difference was assessed using a t-test with Welch correction (pvalue = 0.0029).

Supplemental Figure 2: cVCA does not perturb drastically cell cycle progression. a) Scatter plot showing the timing of anaphase for *wt* oocytes (black), *wt* oocytes expressing cVCA (red), or *wt* oocytes expressing Ez (grey). Mean of 22 *wt* oocytes, 25 cVCA expressing oocytes and 15 Ez expressing oocytes is shown from 4 independent experiments. Standard error of the mean is shown. Statistical difference was assessed using a t-test with Welch correction (pvalues: *wt* oocytes versus cVCA expressing oocytes 0.0106; *wt* oocytes versus Ez expressing oocytes 0.8459; Ez expressing oocytes versus cVCA expressing oocytes 0.0241). b) Scatter plot showing the timing of polar body extrusion or polar body extrusion attempt for *wt* oocytes (black), *wt* oocytes expressing cVCA (red), or *wt* oocytes expressing Ez (grey). Mean of 29 *wt* oocytes, 28 cVCA expressing oocytes and 13 Ez expressing oocytes is shown from 4 independent experiments. Standard error of the mean is shown. Statistical differences were assessed using a one-way Anova (pvalue = 0.0871).

Supplemental Movie 1: Time-lapse movie showing a *wt* oocyte expressing GFP-UtrCH (white) from Prophase I to NEBD+1h. Frames are 15 minutes apart. One Z-plane is shown.

Supplemental Movie 2: Time-lapse movie showing a *wt* oocyte expressing GFP-UtrCH (white) and cVCA from Prophase I to NEBD+1h. Frames are 15 minutes apart. One Z-plane is shown.

DISCUSSION AND PERSPECTIVES

A) Cooperation of two actin networks in positioning the Meiosis I spindle

1) Relationships between the two actin networks

The migration of the spindle during Meiosis I in mouse oocytes depends on a cytoplasmic F-actin meshwork Formin-2 and Spire1/2 dependent (Azoury et al., 2008; Dumont et al., 2007a; Leader et al., 2002; Pfender et al., 2011; Schuh and Ellenberg, 2008). This F-actin network is progressively nucleated after NEBD and is composed of a very dynamic cytoplasmic meshwork and an actin cage surrounding the microtubule spindle. It is not known whether the two structures are connected. It is possible that they are linked via Myosin-X, a Myosin able to interact with actin and microtubules (Weber et al., 2004), since in Xenopus embryos Myosin-X is responsible for F-actin association with the microtubule spindle (Woolner et al., 2008). The role of Myosin-X in mouse oocytes remains elusive, but the gene is expressed (Evsikov et al., 2006; Chen et al., 2011). It could be interesting to test this hypothesis by imaging the cytoplasmic F-actin meshwork and especially the actin cage in oocytes injected with a dominant negative made of tail truncates for Myosin-X, similar to the approach used in Xenopus oocytes (Weber et al., 2004). This approach is likely to work since it has been used to study the role of Myosin-V and Myosin-VI in mouse oocytes (Holubcová et al., 2013). Alternatively, it could be interesting to generate a conditional invalidation of Myosin-X in oocytes by crossing mice engineered with a floxed exon of Myosin-X with transgenic mice possessing the Cre recombinase under the control of ZP3 (Zona Pellucida 3, a protein expressed during the growth phase of the oocyte) promoter.

Arp2/3 and many of its NPFs (Wave2, JMY, WHAMM) have been implicated in spindle migration in Meiosis I (Huang et al., 2013; Liu et al., 2012, 2009; Sun et al., 2011b, 2011c). However, no actin network had been observed in these studies so it was not clear what F-actin network they were nucleating and how it could relate to spindle migration. In my work, I have identified a progressive thickening of the F-actin cortex, detectable around three hours after NEBD and reaching a maximum thickness (4 μm) prior to the first polar body extrusion. This F-actin thickening depends on Arp2/3 and the Mos/MAPK pathway. Since Mos downstream kinases ERK1/2 have been shown to phosphorylate Wave2 *in vitro* and *in vivo* (Nakanishi et al., 2006; Mendoza et al., 2011), since Wave2 is also phosphorylated at the time of ERK1/2 activation in mouse oocytes but not in *mos*-/- occytes and since Mos knock-down or ERK1/2 inhibition leads to the same phenotype as Arp2/3 inhibition, we propose that the nucleation of this F-actin thickening is controlled by Mos-dependent phosphorylation of Wave2 (Chaigne et al., 2013). Its progressive nucleation could be due to the fact that Wave2

seems to be phosphorylated also by the MPF, whose activity raises slowly in Meiosis I (Chaigne et al., 2013).

It is interesting to notice that the two F-actin networks are detectable at the same time, around NEBD+3 hours. This suggests that they are temporally coordinated. The cortical actin thickening is nucleated under the dependence of the Mos/MAPK pathway. In *mos-/-* oocytes, the F-actin meshwork is still present, thus Mos does not control the nucleation of the F-actin cytoplasmic meshwork. The nucleation of the cytoplasmic actin meshwork after NEBD is not controlled by Formin-2 activation but by its resynthesis (Azoury et al., 2011). The nucleation of these two networks, indispensible for the migration of the spindle (ERK1/2 activation following Mos synthesis and Formin-2 resynthesis), requires protein synthesis. Since mouse oocytes are transcriptionally inactive (Bouniol-Baly et al., 1999; Moore et al., 1974), it means that there are strong mechanisms controlling translation, possibly coordinating Mos and Formin-2 synthesis shortly after NEBD. Hence, it could be very interesting to investigate the control of Mos and Formin-2 RNA stability and translation, for example by manipulation of translation pathways.

The two F-actin networks are needed for spindle migration. How the cytoplasmic F-actin meshwork promotes spindle migration is not clear, because it is not a contracting meshwork as in Starfish oocytes (Lénárt et al., 2005; Mori et al., 2011). We and others have shown that the main motor for spindle migration is Myosin-II producing pulling forces at spindle poles (Chaigne et al., 2013; Schuh and Ellenberg, 2008; Simerly et al., 1998). What could be the role of the cytoplasmic actin meshwork? One possibility could be a simple mechanical role, in embedding the microtubule spindle into an actin cage that is itself connected to the cortex. It could then transmit the forces exerted by Myosin-II on the actin cage to the cortex, thus promoting efficient pulling.

2) Cortical tension: a catalyst for forces unbalance

What is then the role of the cortical F-actin thickening? We have shown that its nucleation correlates with the drop in cortical tension observed during Meiosis I (Larson et al., 2010). This was very puzzling because an increase in cortically nucleated actin should lead to an increase in cortical tension. However, in mitotic cells, a decrease in cortical F-actin thickness has been correlated to an increase in cortical tension (Clark and Paluch, communication at the 2013 ASCB meeting), which is the exact opposite situation. We

demonstrated that nucleating F-actin at the cortex was sufficient to remove Myosin-II from the cortex (see below), which is, in fact, responsible for the drop in cortical tension.

What is the biological significance for this drop in cortical tension? We have shown that the drop in cortical tension is required for proper spindle migration, since when cortical tension is artificially increased, the spindle stays centrally located. We postulated that the drop in cortical tension could amplify the unbalance of forces initially created by the fact that the nucleus is slightly off-centered when meiosis resumes. Indeed at NEBD the spindle forms slightly off-centered as well, where the nucleus was. Thus, if the motor driving spindle migration is Myosin-II, the force should be stronger at the pole closest to the cortex and the spindle should migrate in that direction, which is indeed the case (Verlhac et al., 2000). A soft cortex could then be deformed (Chaigne et al. 2013), bringing together more F-actin and Myosin-II and thus amplifying the pulling strength. What happens in oocytes with a stiff cortex such as *mos-/-* oocytes? The slight initial unbalance of forces is still present and Myosin-II is also present along the actin cage as in control oocytes (unpublished data), arguing that the absence of spindle migration is not due to motor mislocalization. The motion however cannot get amplified since the cortex is stiff and not deformable, thus our model predicts that the motion should be null, which is what we observe.

To test this hypothesis, we created a mathematical model taking into account the observations that we and others have made on spindle migration. This model gave us a few predictions that we could numerically test; for example, we calculated the forces exerted on the spindle using the spindle speed and the oocyte viscosity on one hand, and the deformation of the actin thickening on the other hand. These two approaches led to very close numerical results. Furthermore, the model predicted that a too low cortical tension would also lead to defects in spindle migration. We designed a tool to artificially decrease cortical tension (see below) and showed that this prediction was also correct. This got us to conclude that our model is overall representative, hence it validates our hypothesis: the drop in cortical tension is an amplificatory mechanism to the initial unbalance of forces.

During the growth phase, the nucleus is actively centralized, but ends up not perfectly at the exact cell center (Brunet and Maro, 2007). The initial imbalance of forces, capital for spindle migration, is due to the fact that the spindle forms where the nucleus was, which is a little bit off-centered. How the centering of the nucleus is mediated is currently unknown, however it is very possible that it is an actin-mediated phenomenon since Prophase I oocytes harbor a very dense F-actin meshwork that resembles the one present at the end of Meiosis I

and since in *fmn2-/-* oocytes the nucleus is frequently off-centered (Azoury et al., 2011). This F-actin meshwork has to be dismantled at NEBD in order to allow proper spindle migration during Meiosis I (Azoury et al., 2011). At NEBD, the network is dismantled concomitantly to Formin-2 degradation, allowing the formation of the spindle in absence of mechanical constraints, thus maybe amplifying the fact that it is not formed exactly at the center. Then the cytoplasmic meshwork reforms at the same time that cortical F-actin thickens, allowing a drop in cortical tension by removing Myosin-II from the cortex. Myosin-II then pulls stronger on the closest side, amplified by cortex deformation.

It is interesting to notice that during the growth phase the nucleus is positioned at the center whereas in the following Meiosis I the spindle needs to be off-centered. In simple words, why not leave the nucleus where it is? One possible explanation is that the spindle cannot form too close to the cortex, maybe because it is not very robust and takes a long time to form and thus cannot form to close to a very stiff cortex (Chaigne et al., 2013; Larson et al., 2010). However in *fmn2-/-* oocytes which harbor an off-centered nucleus the spindle seems to form normally (unpublished data) arguing that the spindle can form close to the cortex. It could also prevent the early-on polarization of the oocyte and avoid meiotic drive, which is the preferential selection for one or several alleles during meiosis. Indeed, if the spindle is formed off-centered, one could imagine that the way chromosomes are positioned inside the nucleus in Prophase I could bias their segregation later on.

B) Actin network architecture influences Myosin-II activity

As mentioned above, to investigate the role of cortical tension, we developed a tool to induce a decrease in cortical tension. This construct is a fusion between the ERM protein Ezrin which is at the cortex throughout meiotic maturation (Dard et al., 2004; Louvet et al., 1996) and the VCA domain common to all Arp2/3 NPFs (referred as Ez-mCherry-VCA or cVCA). As described in the result section, this construct is targeted to the cortex of the oocyte in Prophase I and during meiotic maturation. It is sufficient to nucleate an F-actin thickening at the cortex of the oocyte in the absence of the Mos/MAPK pathway, which is the physiological trigger for it during meiotic maturation. This F-actin thickening is then sufficient to remove Myosin-II from the cortex, even without the Mos/MAPK pathway.

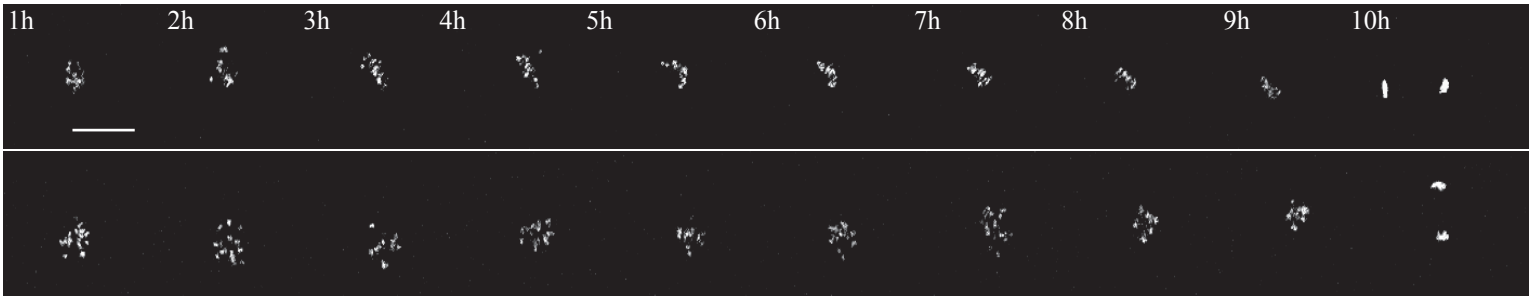
This is a very intriguing observation because it was never shown before that F-actin

nucleation per se could relocate Myosin-II. However, in mitosis, the increase in cortical tension observed at NEBD depends on Myosin-II localized at the cortex and is concomitant with a decrease in cortical F-actin thickness (Clark and Paluch, communication at the 2013 ASCB meeting). Controlling the nucleation of F-actin at the cortex could then be a conserved mechanism to induce either a Myosin-II dependent increase or decrease in cortical tension.

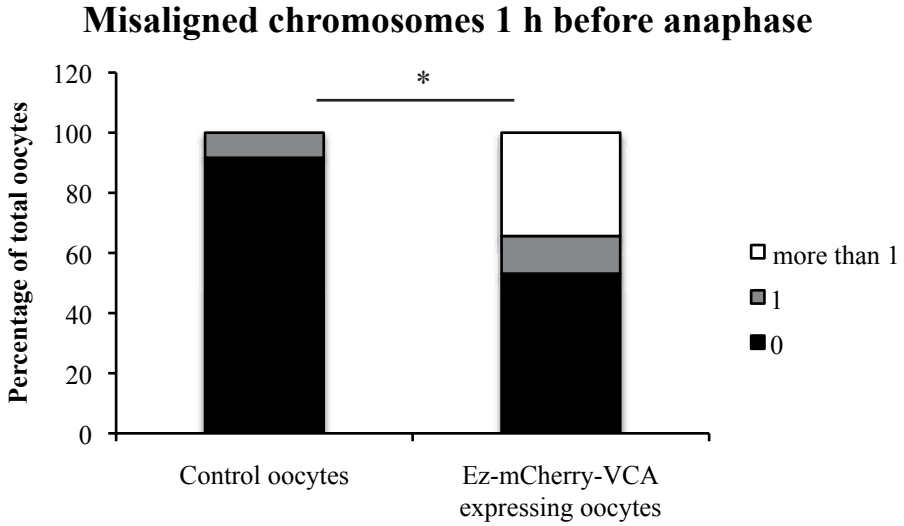
How does F-actin mediate Myosin-II delocalization from the cortex? The first hypothesis is simply that the way filaments are organized with respect to each other in this Arp2/3 nucleated F-actin thickening does not allow the fixation of Myosin-II; in other words, this could only be a steric blockage. This is possible because the cortical F-actin thickening seems to be a very dense actin network, composed of many layers. Furthermore, our photoactivation experiments point to the fact that it is a very static network compared to the cytoplasmic actin meshwork: this could also be due to the fact that the filaments are packed very close to each other. To test this hypothesis, it could be interesting to gain more resolution into cortical actin filaments dynamics. This could be achieved by using a photoconvertible probe fused to UtrCH: this probe emits a fluorescent signal at one particular wavelength and when illuminated with a laser at another wavelength it irreversibly converts into a protein that emits a fluorescent signal at yet another wavelength, thus it is possible to follow in live the evolution of a photoconverted region. We have tried to use EOS-UtrCH, however this is very difficult to use for two reasons. First, as UtrCH, overexpressing this probe leads to stabilization of actin filaments (Holubcová et al., 2013). Second, it takes for the probe around 8h to fold, so getting a decent signal inside the oocyte implies to keep them arrested in Prophase I for several hours, which can affect meiotic maturation. So far, we have not achieved proper monitoring of F-actin filaments dynamics using this tool.

The second hypothesis is that Myosin-II does not have the same affinity for the two F-actin networks. This could be due to the way that they are nucleated (unbranched versus branched filaments). Indeed, in mouse oocytes, the cytoplasmic F-actin meshwork is an unbranched network nucleated by Formin-2 and Spire1/2. The cortical F-actin thickening however is branched and nucleated by Arp2/3. How the affinity of Myosin-II for branched or unbranched networks could be regulated is at the moment completely unknown. Alternatively, Myosin-II could be targeted to actin filaments depending on the stress that they are under; for example, in Dictyostelium, Myosin-II localizes preferentially to F-actin under stress (Uyeda et al., 2011). Myosin-II is localized at the cortex at the onset of meiotic maturation and at the actin cage during spindle migration. Since the actin cage is actively

A. Ooyctes with a low cortical tension harbor defects in chromosomes alignement during Meiosis I. Histone-GFP in white. Upper panel, control oocyte; lower panel, Ez-mCherry-VCA expressing oocyte. Frames are 1 hour apart. Scale bar: 10 µm



B. Number of misaligned chromosomes 1 hour before anaphase in control oocytes or oocytes expressing Ez-mCherry-VCA. The percentage of total oocytes is shown assessed over 2 independent experiments. Statistical difference of the repartition is assessed with a Fisher test (pvalue= 0,0429).



C. Progression of chromosomes alignement in Meiosis I. The percentage of oocytes harboring aligned chromosomes is shown as a function of time, assessed over 2 independent experiments. PBE: Polar Body Extrusion

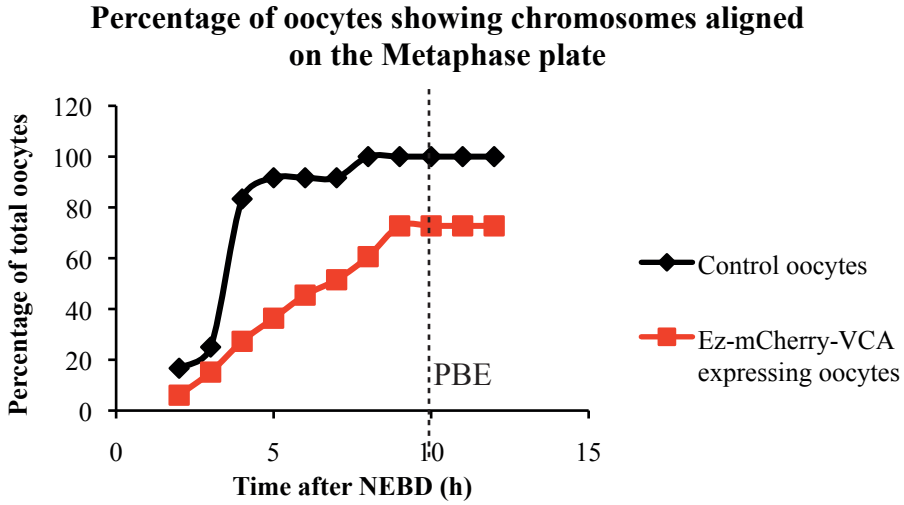


Figure 28: Spindle defects in Meiosis I oocytes harboring a low cortical tension

pulled, it is possible that Myosin-II is preferentially recruited to these stretched filaments. Myosin-II delocalization from the cortex could therefore be a passive mechanism in response to stretching of the F-actin filaments surrounding the microtubule spindle. In that case, since Myosin-II is enriched at the actin cap in late meiosis I, it would mean that another input is needed in order to recruit it back at the cortex, for example through Ran-dependent Rac-GTP and Cdc42-GTP accumulation at the cortex which in turn could activate MLCK for example (Dehapiot et al., 2013; Deng et al., 2007; Halet and Carroll, 2007). Alternatively, it could mean that the level of stretching of F-actin is different at the actin cage versus the rest of the cortex, which is possible since cortical tension is higher above the actin cap than everywhere else (Larson et al., 2010).

C) Multiple roles for cortical tension?

1) A role for cortical tension in spindle formation?

The Ez-mCherry-VCA efficiently nucleates an Arp2/3 dependent F-actin network at the cortex, and this is sufficient in Prophase I oocyte to induce a major drop in cortical tension. We assume that this tool also drops cortical tension when it is expressed during Meiosis I, as suggested by the shape of the oocytes (see results) and supported by the fact that expressing Ez-mCherry-VCA leads to impaired spindle migration which is predicted by our model to occur when the cortical tension is too low and rescues migration in *mos -/-* oocytes which have a high cortical tension.

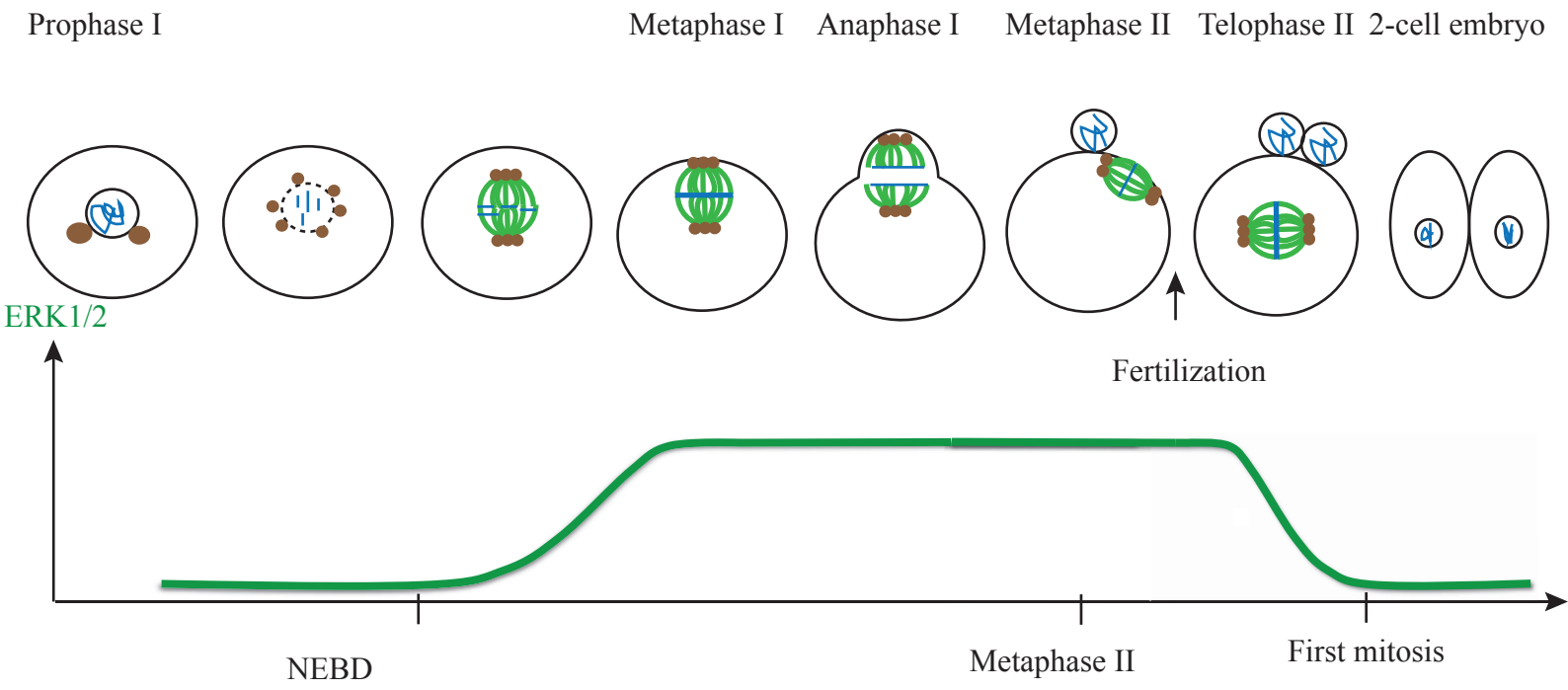
When we expressed Ez-mCherry-VCA, we could observe that many oocytes showed defects in chromosomes alignment during Meiosis I (Figure 28A, unpublished results). More precisely just before anaphase, 50% of the oocytes had one or more chromosomes lagging outside the metaphase plate, compared to less than 10% in controls (Figure 28B). In addition, in oocytes expressing Ez-mCherry-VCA, it took more than 8 hours after NEBD for all the chromosomes to align and in 30% of the cases the chromosomes were never fully aligned, whereas in control oocytes chromosomes were fully aligned at NEBD+5 hours in most cases (Figure 28C). This is a very interesting observation suggesting that lowering the cortical tension impairs chromosome alignment on the metaphase plate.

How could cortical tension play a role in chromosome alignment during mouse Meiosis I? One hypothesis is that cortex stifness plays a role in spindle morphogenesis. To test this, it is possible to follow microtubules organization during meiotic maturation by co-

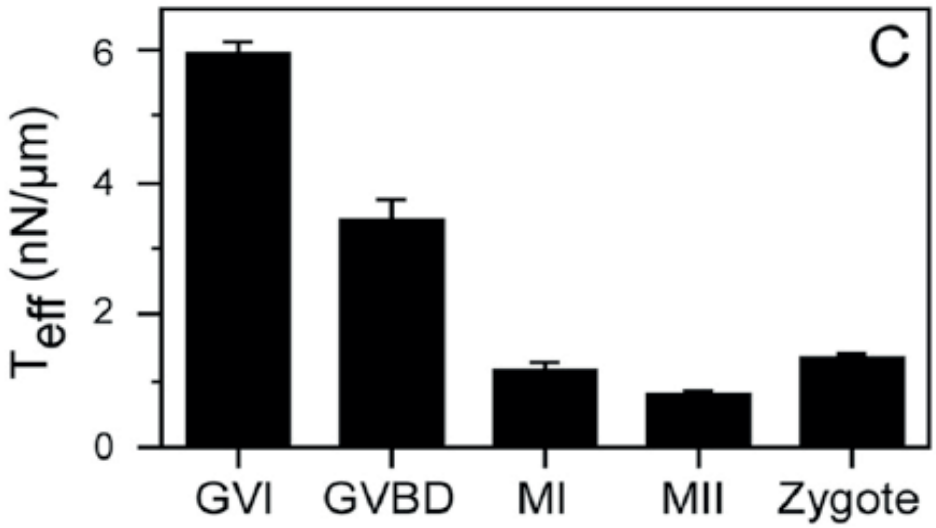
injecting Ez-mCherry-VCA to decrease cortical tension and Tubulin-GFP or EB3-GFP, a protein that binds to the plus end of the microtubules. As discussed before (Figure 16), the spindle is built from inside out, microtubules being first nucleated around the chromosomes via the RAN-GTP gradient supported by the chromosomes (Dumont et al., 2007b). Then MTOCs are sorted and clustered, forming the spindle poles. What could be the role of cortical tension in spindle architecture? One possibility is that the spindle, probably because of its peculiar formation, is not a robust structure and needs to be surrounded and guided by F-actin. In mitotic cells, the presence of F-actin colocalized with the spindle is well described in plants but still controversial in animal cells (for review see (Sandquist et al., 2011)). In mouse oocytes, when the spindle starts to be built, the cytoplasmic meshwork is reforming, notably forming an actin cage surrounding the microtubule spindle. A high cortical tension could be transmitted by this meshwork and in particular by the actin cage to the spindle and somehow help it to be shaped. If the spindle and the actin cage are indeed connected, for example by Myosin-X, a decrease in cortical tension could impair the shape of the actin cage and thus the shape of the microtubule spindle. However we detected no obvious differences between the shape of the actin cages in oocytes expressing Ez-mCherry-VCA compared to control oocytes. Alternatively, the cytoplasmic actin meshwork, by connecting the actin cage and the microtubule spindle to the cortex, could help put the chromosomes under tension. Hence, the cytoplasmic meshwork would play the role that astral microtubules and dynein play in mitotic cells (reviewed in (Kunda and Baum, 2009)). In that case, *fmn2-/-* oocytes lacking a cytoplasmic meshwork should also display similar defects in chromosomes alignment, but this remains to be tested. In the absence of F-actin, microtubules are able to form a well-shaped spindle in mitotic cells (Wilbur and Heald, 2013). However it might not be the case in meiotic cells where spindles are formed in the absence of true centrosomes, lack dominant poles and therefore are less robust than their mitotic counterparts.

Moreover, it was shown in mitotic cells that cortical tension driven rounding was essential for spindle formation (Kunda et al., 2008; Lancaster et al., 2013). In these studies, cells that were not round had defects in spindle formation because the microtubules were too short to properly reach and capture the chromosomes (Lancaster et al., 2013). This is probably not the case in mouse oocyte since the spindle is formed around the chromosomes. Flattened mitotic cells also harbored pole instability and underwent pole splitting at anaphase (Lancaster et al., 2013). To test here if it is the case in mouse oocytes with decreased cortical tension, it could be possible to follow the poles in live microscopy by injecting a fluorescent

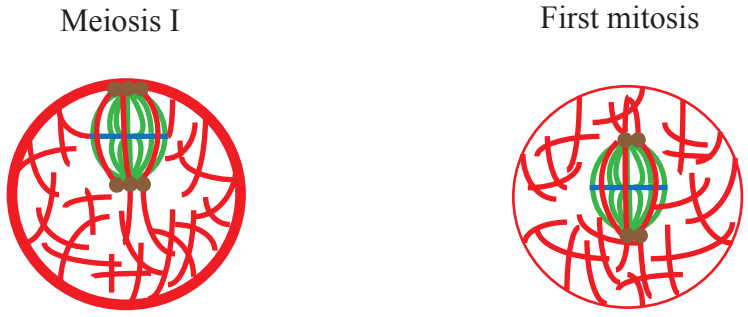
A: Symmetric and asymmetric divisions during early mouse development



B: Cortical tension in mouse oocyte and 1-cell embryo (from Larson et al. 2010)



C: Model for cortical tension switch between symmetric and asymmetric division in acentriolar cells



F-actin thickening
Low cortical tension
Unbalance of forces
Asymmetric division

No F-actin thickening
High cortical tension
Balance of forces
Symmetric division

Figure 29: A role for cortical tension in mediating the switch between symmetric and asymmetric divisions in acentriolar cells?

probe labeling the MTOCs. Interestingly, flattened cells with extra centrosomes that usually have to cluster their centrosomes to achieve proper chromosome segregation had more defects than cells with only two centrosomes (Lancaster et al., 2013). As the mechanism of MTOCs clustering in Meiosis I is similar to extra-centrosome clustering of cancer cells (Breuer et al., 2010), this suggests that impaired cortical tension could be more important in a cell with less symmetrical or robust spindles. Overall, following the morphogensis and function of the microtubule spindle and spindle poles in oocytes with a low cortical tension could be useful to understand the differences between centriolar and acentriolar pole shaping and stability.

Interestingly, most oocytes with decreased cortical tension undergo anaphase and attempt to extrude a polar body even with misaligned chromosomes (Figure 1A-C). This suggests that the SAC is not activated by these misaligned chromosomes. If indeed the tension exerted on the chromosomes is lowered by cortex stiffness decrease, this would also suggest that the SAC is less sensitive to tension defects than the mitotic SAC (Kolano et al., 2012).

2) A role for cortical tension in the switch between symmetric and asymmetric acentriolar division?

Mouse Meiosis I is a very asymmetrical division in size that happens in the absence of canonical centrosomes. As shown previously, this is due to the cooperation of two F-actin networks mediating spindle migration, one network providing the "capture" mechanism for the microtubule spindle, and the other accelerating the movement by decreasing cortical tension. Interestingly, following fertilization, the first mitosis happens also in the absence of true centrosomes, since centrioles will be synthesized de novo at the 64-cell stage (Calarco-Gillam et al., 1983; Courtois et al., 2012; Gueth-Hallonet et al., 1993). Contrary to meiotic divisions, this first mitosis is a symmetric division (Figure 29A). Concomitantly, it seems that cortical tension re-increases just after fertilization (Figure 29B) (Larson et al., 2010) at the time of MAPK inactivation (Figure 29A) (Kalab et al., 1996). Furthermore, it seems that the symmetry of the division requires F-actin since when it is chemically inhibited, the division becomes asymmetric (Chew et al., 2012). This leads to the very seducing hypothesis that in cells where there are no true centrosomes and where spindle positioning is F-actin-dependent, a low cortical tension would lead to an asymmetric division as described previously in the model and a high cortical tension would lead to a symmetric division as it is the case in *mos-/-* oocytes that have a high cortical tension throughout meiotic maturation (Figure 29C). This of course needs to be properly demonstrated. A first step would be to accurately measure cortical

tension during the first mitosis and not just after fertilization. The second step would be to describe the actin networks present during this first embryonic division and a third step would be to inject the Ez-mCherry-VCA prior to the first mitotic division and test whether decreasing cortical tension would lead to an asymmetric division.

To conclude, this could indicate that cell mechanics, mediated by protein synthesis and activation, are key in the process of acentriolar cell division, and that cells have developed ways to bypass the lack of astral microtubules to undergo asymmetric division. However, it is interesting to notice that cortical tension mediated spindle positioning always requires F-actin whether it is during mitosis or meiosis, arguing that this is a conserved mechanism. In bacteria, isolated cells as well, there are no centrosomes. We could then imagine that acentriolar divisions were actually an ancestral mechanism. From that point of view, F-actin mediated cortical tension would be the ancestral way to position a mitotic spindle. Why then would it be important for Eukaryotic cells to possess canonical centrosome during their division? One possibility is that many Eukaryotes are multicellular, thus cell division needs to be much more controlled in space and centrosomes could be a back-up mechanism to make sure that the spindle is properly positioned. Plant cells have no true centrosomes and undergo acentriolar mitosis; however, these cells are surrounded by a very thick and rigid cell wall maybe very efficient at ensuring that the divisions are symmetrical, reinforcing the hypothesis that the absence of centrioles would be ancestral. Therefore, the only cells where the centrioles would actually be needed would be animal mitotic cells requiring a very precise spindle localization and cells that develop ciliae, a process requiring centrosome. Indeed, flies lacking centrosomes harbor a normal development but die at adulthood because of defects in ciliated cells (Basto et al., 2006). Furthermore, in these mutant flies, mitosis is slowed but not perturbed (Basto et al., 2006), which suggests that indeed centrosomes are not essential for the division but maybe help speed up the process; this hypothesis could also explain why Meiosis I is such a long division in mouse oocytes.

Centriolar loss in vertebrate meiosis could thus be a secondary loss: since centrioles would not be needed, we can imagine that it is less costly to lose them than to maintain them throughout a process where they are not required. This is of course completely speculative, but could be an answer to the still very elusive question of why the centrioles are lost during oogenesis.

REFERENCES

Ahuja, R., Pinyol, R., Reichenbach, N., Custer, L., Klingensmith, J., Kessels, M.M., and Qualmann, B. (2007). Cordon-bleu is an actin nucleation factor and controls neuronal morphology. Cell *131*, 337–350.

Ai, J.-S., Wang, Q., Li, M., Shi, L.-H., Ola, S.I., Xiong, B., Yin, S., Chen, D.-Y., and Sun, Q.-Y. (2008). Roles of microtubules and microfilaments in spindle movements during rat oocyte meiosis. J. Reprod. Dev. *54*, 391–396.

Almonacid, M., Terret, M.-É., and Verlhac, M.-H. (2014). Actin-based spindle positioning: new insights from female gametes. J. Cell Sci. *127*, 477–483.

Amiel, A., Leclère, L., Robert, L., Chevalier, S., and Houliston, E. (2009). Conserved Functions for Mos in Eumetazoan Oocyte Maturation Revealed by Studies in a Cnidarian. Curr. Biol. *19*, 305–311.

Azoury, J., Lee, K.W., Georget, V., Rassinier, P., Leader, B., and Verlhac, M.-H. (2008). Spindle Positioning in Mouse Oocytes Relies on a Dynamic Meshwork of Actin Filaments. Curr. Biol. *18*, 1514–1519.

Azoury, J., Lee, K.W., Georget, V., Hikal, P., and Verlhac, M.-H. (2011). Symmetry breaking in mouse oocytes requires transient F-actin meshwork destabilization. Development *138*, 2903–2908.

Bamburg, J.R., Harris, H.E., and Weeds, A.G. (1980). Partial purification and characterization of an actin depolymerizing factor from brain. FEBS Lett. *121*, 178–182.

Basto, R., Lau, J., Vinogradova, T., Gardiol, A., Woods, C.G., Khodjakov, A., and Raff, J.W. (2006). Flies without centrioles. Cell *125*, 1375–1386.

Blanchoin, L., Pollard, T.D., and Mullins, R.D. (2000a). Interactions of ADF/cofilin, Arp2/3 complex, capping protein and profilin in remodeling of branched actin filament networks. Curr. Biol. *10*, 1273–1282.

Blanchoin, L., Amann, K.J., Higgs, H.N., Marchand, J.-B., Kaiser, D.A., and Pollard, T.D. (2000b). Direct observation of dendritic actin filament networks nucleated by Arp2/3 complex and WASP/Scar proteins. Nature *404*, 1007–1011.

Bloemink, M.J., and Geeves, M.A. (2011). Shaking the myosin family tree: Biochemical kinetics defines four types of myosin motor. Semin. Cell Dev. Biol. *22*, 961–967.

Bouniol-Baly, C., Hamraoui, L., Guibert, J., Beaujean, N., Szöllösi, M.S., and Debey, P. (1999). Differential transcriptional activity associated with chromatin configuration in fully grown mouse germinal vesicle oocytes. Biol. Reprod. *60*, 580–587.

Breitsprecher, D., Jaiswal, R., Bombardier, J.P., Gould, C.J., Gelles, J., and Goode, B.L. (2012). Rocket Launcher Mechanism of Collaborative Actin Assembly Defined by Single-

Molecule Imaging. Science *336*, 1164–1168.

Bretscher, A., Edwards, K., and Fehon, R.G. (2002). ERM proteins and merlin: integrators at the cell cortex. Nat. Rev. Mol. Cell Biol. *3*, 586–599.

Breuer, M., Kolano, A., Kwon, M., Li, C.-C., Tsai, T.-F., Pellman, D., Brunet, S., and Verlhac, M.-H. (2010). HURP permits MTOC sorting for robust meiotic spindle bipolarity, similar to extra centrosome clustering in cancer cells. J. Cell Biol. *191*, 1251–1260.

Brunet, S., and Maro, B. (2007). Germinal vesicle position and meiotic maturation in mouse oocyte. Reproduction *133*, 1069–1072.

Brunet, S., and Verlhac, M.H. (2010). Positioning to get out of meiosis: the asymmetry of division. Hum. Reprod. Update *17*, 68–75.

Brunet, S., Maria, A.S., Guillaud, P., Dujardin, D., Kubiak, J.Z., and Maro, B. (1999). Kinetochore fibers are not involved in the formation of the first meiotic spindle in mouse oocytes, but control the exit from the first meiotic M phase. J. Cell Biol. *146*, 1–12.

Brunet, S., Dumont, J., Lee, K.W., Kinoshita, K., Hikal, P., Gruss, O.J., Maro, B., and Verlhac, M.-H. (2008). Meiotic Regulation of TPX2 Protein Levels Governs Cell Cycle Progression in Mouse Oocytes. PLoS ONE *3*, e3338.

Burkel, B.M., von Dassow, G., and Bement, W.M. (2007). Versatile fluorescent probes for actin filaments based on the actin-binding domain of utrophin. Cell Motil. Cytoskeleton *64*, 822–832.

Calarco-Gillam, P.D., Siebert, M.C., Hubble, R., Mitchison, T., and Kirschner, M. (1983). Centrosome development in early mouse embryos as defined by an autoantibody against pericentriolar material. Cell *35*, 621–629.

Campellone, K.G., and Welch, M.D. (2010). A nucleator arms race: cellular control of actin assembly. Nat. Rev. Microbiol. *11*, 237–251.

Campellone, K.G., Webb, N.J., Znameroski, E.A., and Welch, M.D. (2008). WHAMM is an Arp2/3 complex activator that binds microtubules and functions in ER to Golgi transport. Cell *134*, 148–161.

Campinho, P., Behrndt, M., Ranft, J., Risler, T., Minc, N., and Heisenberg, C.-P. (2013). Tension-oriented cell divisions limit anisotropic tissue tension in epithelial spreading during zebrafish epiboly. Nat. Cell Biol. *15*, 1405–1414.

Carazo-Salas, R.E., and Karsenti, E. (2003). Long-range communication between chromatin and microtubules in Xenopus egg extracts. Curr. Biol. CB *13*, 1728–1733.

Carlier, M.F., Didry, D., Erk, I., Lepault, J., Van Troys, M.L., Vandekerckhove, J., Perelroizen, I., Yin, H., Doi, Y., and Pantaloni, D. (1996). Tbeta 4 is not a simple G-actin

sequestering protein and interacts with F-actin at high concentration. J. Biol. Chem. *271*, 9231–9239.

Carreno, S., Kouranti, I., Glusman, E.S., Fuller, M.T., Echard, A., and Payre, F. (2008). Moesin and its activating kinase Slik are required for cortical stability and microtubule organization in mitotic cells. J. Cell Biol. *180*, 739–746.

Casella, J.F., Craig, S.W., Maack, D.J., and Brown, A.E. (1987). Cap Z(36/32), a barbed end actin-capping protein, is a component of the Z-line of skeletal muscle. J. Cell Biol. *105*, 371–379.

Chaigne, A., Campillo, C., Gov, N.S., Voituriez, R., Azoury, J., Umaña-Diaz, C., Almonacid, M., Queguiner, I., Nassoy, P., Sykes, C., et al. (2013). A soft cortex is essential for asymmetric spindle positioning in mouse oocytes. Nat. Cell Biol. *15*, 958–966.

Charras, G.T., Hu, C.-K., Coughlin, M., and Mitchison, T.J. (2006). Reassembly of contractile actin cortex in cell blebs. J. Cell Biol. *175*, 477–490.

Chen, J., Melton, C., Suh, N., Oh, J.S., Horner, K., Xie, F., Sette, C., Blelloch, R., and Conti, M. (2011). Genome-wide analysis of translation reveals a critical role for deleted in azoospermia-like (Dazl) at the oocyte-to-zygote transition. Genes Dev. *25*, 755–766.

Chereau, D., Boczkowska, M., Skwarek-Maruszewska, A., Fujiwara, I., Hayes, D.B., Rebowski, G., Lappalainen, P., Pollard, T.D., and Dominguez, R. (2008). Leiomodin is an actin filament nucleator in muscle cells. Science *320*, 239–243.

Chesarone, M.A., DuPage, A.G., and Goode, B.L. (2010). Unleashing formins to remodel the actin and microtubule cytoskeletons. Nat. Rev. Mol. Cell Biol. *11*, 62–74.

Chew, T.G., Lorthongpanich, C., Ang, W.X., Knowles, B.B., and Solter, D. (2012). Symmetric cell division of the mouse zygote requires an actin network. Cytoskeleton *69*, 1040–1046.

Choi, T., Fukasawa, K., Zhou, R., Tessarollo, L., Borror, K., Resau, J., and Vande Woude, G.F. (1996). The Mos/mitogen-activated protein kinase (MAPK) pathway regulates the size and degradation of the first polar body in maturing mouse oocytes. Proc. Natl. Acad. Sci. *93*, 7032 –7035.

Colledge, W.H., Carlton, M.B.L., Udy, G.B., and Evans, M.J. (1994). Disruption of c-mos causes parthenogenetic development of unfertilized mouse eggs. Nature *370*, 65–68.

Colombo, K., Grill, S.W., Kimple, R.J., Willard, F.S., Siderovski, D.P., and Gönczy, P. (2003). Translation of polarity cues into asymmetric spindle positioning in Caenorhabditis elegans embryos. Science *300*, 1957–1961.

Conti, M., Andersen, C.B., Richard, F.J., Shitsukawa, K., and Tsafriri, A. (1998). Role of

cyclic nucleotide phosphodiesterases in resumption of meiosis. Mol. Cell. Endocrinol. *145*, 9–14.

Courtois, A., Schuh, M., Ellenberg, J., and Hiiragi, T. (2012). The transition from meiotic to mitotic spindle assembly is gradual during early mammalian development. J. Cell Biol. *198*, 357–370.

Dahlgaard, K., Raposo, A.A.S.F., Niccoli, T., and St Johnston, D. (2007). Capu and Spire Assemble a Cytoplasmic Actin Mesh that Maintains Microtubule Organization in the Drosophila Oocyte. Dev. Cell *13*, 539–553.

Dalton, C.M., and Carroll, J. (2013). Biased inheritance of mitochondria during asymmetric cell division in the mouse oocyte. J. Cell Sci. *126*, 2955–2964.

Dang, I., Gorelik, R., Sousa-Blin, C., Derivery, E., Guérin, C., Linkner, J., Nemethova, M., Dumortier, J.G., Giger, F.A., Chipysheva, T.A., et al. (2013). Inhibitory signalling to the Arp2/3 complex steers cell migration. Nature *503*, 281–284.

Dard, N., Louvet-Vallée, S., Santa-Maria, A., and Maro, B. (2004). Phosphorylation of ezrin on threonine T567 plays a crucial role during compaction in the mouse early embryo. Dev. Biol. *271*, 87–97.

Von Dassow, G., and Schubiger, G. (1994). How an actin network might cause fountain streaming and nuclear migration in the syncytial Drosophila embryo. J. Cell Biol. *127*, 1637–1653.

Dayel, M.J., Holleran, E.A., and Mullins, R.D. (2001). Arp2/3 complex requires hydrolyzable ATP for nucleation of new actin filaments. Proc. Natl. Acad. Sci. *98*, 14871–14876.

Dehapiot, B., and Halet, G. (2013). Ran GTPase promotes oocyte polarization by regulating ERM (Ezrin/Radixin/Moesin) inactivation. Cell Cycle Georget. Tex *12*, 1672–1678.

Dehapiot, B., Carrière, V., Carroll, J., and Halet, G. (2013). Polarized Cdc42 activation promotes polar body protrusion and asymmetric division in mouse oocytes. Dev. Biol. *377*, 202–212.

Deng, M., Suraneni, P., Schultz, R.M., and Li, R. (2007). The Ran GTPase Mediates Chromatin Signaling to Control Cortical Polarity during Polar Body Extrusion in Mouse Oocytes. Dev. Cell *12*, 301–308.

Duan, X., Liu, J., Dai, X.-X., Liu, H.-L., Cui, X.-S., Kim, N.-H., Wang, Z.-B., Wang, Q., and Sun, S.-C. (2014). Rho-GTPase effector ROCK phosphorylates cofilin in actin-meditated cytokinesis during mouse oocyte meiosis. Biol. Reprod. *90*, 37.

Ducibella, T. (1988). Quantitative studies of changes in cortical granule number and distribution in the mouse oocyte during meiotic maturation. Dev. Biol. *130*, 184–197.

Dumont, S. (2011). Chromosome Segregation: Spindle Mechanics Come To Life. Curr. Biol. *21*, R688–R690.

Dumont, J., Umbhauer, M., Rassinier, P., Hanauer, A., and Verlhac, M.-H. (2005). p90Rsk is not involved in cytostatic factor arrest in mouse oocytes. J. Cell Biol. *169*, 227–231.

Dumont, J., Million, K., Sunderland, K., Rassinier, P., Lim, H., Leader, B., and Verlhac, M.-H. (2007a). Formin-2 is required for spindle migration and for the late steps of cytokinesis in mouse oocytes. Dev. Biol. *301*, 254–265.

Dumont, J., Petri, S., Pellegrin, F., Terret, M.-E., Bohnsack, M.T., Rassinier, P., Georget, V., Kalab, P., Gruss, O.J., and Verlhac, M.-H. (2007b). A centriole- and RanGTP-independent spindle assembly pathway in meiosis I of vertebrate oocytes. J. Cell Biol. *176*, 295–305.

Duncan, F., Moss, S., Schultz, R., and Williams, C. (2005). PAR-3 defines a central subdomain of the cortical actin cap in mouse eggs. Dev. Biol. *280*, 38–47.

Elbaz, J., Reizel, Y., Nevo, N., Galiani, D., and Dekel, N. (2009). Epithelial Cell Transforming Protein 2 (ECT2) Depletion Blocks Polar Body Extrusion and Generates Mouse Oocytes Containing Two Metaphase II Spindles. Endocrinology *151*, 755–765.

Evans, E., and Yeung, A. (1989). Apparent viscosity and cortical tension of blood granulocytes determined by micropipet aspiration. Biophys. J. *56*, 151–160.

Evsikov, A.V., Graber, J.H., Brockman, J.M., Hampl, A., Holbrook, A.E., Singh, P., Eppig, J.J., Solter, D., and Knowles, B.B. (2006). Cracking the egg: molecular dynamics and evolutionary aspects of the transition from the fully grown oocyte to embryo. Genes Dev. *20*, 2713–2727.

Field, C.M., and Lénárt, P. (2011). Bulk Cytoplasmic Actin and Its Functions in Meiosis and Mitosis. Curr. Biol. *21*, R825–R830.

Field, C.M., Wühr, M., Anderson, G.A., Kueh, H.Y., Strickland, D., and Mitchison, T.J. (2011). Actin behavior in bulk cytoplasm is cell cycle regulated in early vertebrate embryos. J. Cell Sci. *124*, 2086–2095.

Fink, J., Carpi, N., Betz, T., Bétard, A., Chebah, M., Azioune, A., Bornens, M., Sykes, C., Fetler, L., Cuvelier, D., et al. (2011). External forces control mitotic spindle positioning. Nat. Cell Biol. *13*, 771–778.

FitzHarris, G., Marangos, P., and Carroll, J. (2007). Changes in endoplasmic reticulum structure during mouse oocyte maturation are controlled by the cytoskeleton and cytoplasmic dynein. Dev. Biol. *305*, 133–144.

Gilula, N.B., Epstein, M.L., and Beers, W.H. (1978). Cell-to-cell communication and ovulation. A study of the cumulus-oocyte complex. J. Cell Biol. *78*, 58–75.

Goh, W.I., Lim, K.B., Sudhaharan, T., Sem, K.P., Bu, W., Chou, A.M., and Ahmed, S. (2012). mDia1 and WAVE2 proteins interact directly with IRSp53 in filopodia and are involved in filopodium formation. J. Biol. Chem. *287*, 4702–4714.

Goley, E.D., and Welch, M.D. (2006). The ARP2/3 complex: an actin nucleator comes of age. Nat. Rev. Mol. Cell Biol. *7*, 713–726.

Goley, E.D., Rodenbusch, S.E., Martin, A.C., and Welch, M.D. (2004). Critical conformational changes in the Arp2/3 complex are induced by nucleotide and nucleation promoting factor. Mol. Cell *16*, 269–279.

Gueth-Hallonet, C., Antony, C., Aghion, J., Santa-Maria, A., Lajoie-Mazenc, I., Wright, M., and Maro, B. (1993). gamma-Tubulin is present in acentriolar MTOCs during early mouse development. J. Cell Sci. *105*, 157–166.

Gui, L., and Homer, H. (2012). Spindle assembly checkpoint signalling is uncoupled from chromosomal position in mouse oocytes. Dev. Camb. Engl. *139*, 1941–1946.

Halet, G., and Carroll, J. (2007). Rac Activity Is Polarized and Regulates Meiotic Spindle Stability and Anchoring in Mammalian Oocytes. Dev. Cell *12*, 309–317.

Hammer, J.A., 3rd, and Sellers, J.R. (2012). Walking to work: roles for class V myosins as cargo transporters. Nat. Rev. Mol. Cell Biol. *13*, 13–26.

Hashimoto, N., Watanabe, N., Furuta, Y., Tamemoto, H., Sagata, N., Yokoyama, M., Okazaki, K., Nagayoshi, M., Takedat, N., Ikawatll, Y., et al. (1994). Parthenogenetic activation of oocytes in c-mos-deficient mice. Nature *370*, 68–71.

Hochmuth, R. (2000). Micropipette aspiration of living cells. J. Biomech. *33*, 15–22.

Holt, J.E., Lane, S.I.R., and Jones, K.T. (2013). The control of meiotic maturation in mammalian oocytes. Curr. Top. Dev. Biol. *102*, 207–226.

Holubcová, Z., Howard, G., and Schuh, M. (2013). Vesicles modulate an actin network for asymmetric spindle positioning. Nat. Cell Biol. *15*, 937–947.

Homer, H.A., McDougall, A., Levasseur, M., Yallop, K., Murdoch, A.P., and Herbert, M. (2005). Mad2 prevents aneuploidy and premature proteolysis of cyclin B and securin during meiosis I in mouse oocytes. Genes Dev. *19*, 202–207.

Hong, F., Haldeman, B.D., Jackson, D., Carter, M., Baker, J.E., and Cremo, C.R. (2011). Biochemistry of smooth muscle myosin light chain kinase. Arch. Biochem. Biophys. *510*, 135–146.

Huang, X., Ding, L., Pan, R., Ma, P.-F., Cheng, P.-P., Zhang, C.-H., Shen, Y.-T., Xu, L., Liu, Y., He, X.-Q., et al. (2012). WHAMM is required for meiotic spindle migration and asymmetric cytokinesis in mouse oocytes. Histochem. Cell Biol.

Huang, X., Ding, L., Pan, R., Ma, P.-F., Cheng, P.-P., Zhang, C.-H., Shen, Y.-T., Xu, L., Liu, Y., He, X.-Q., et al. (2013). WHAMM is required for meiotic spindle migration and asymmetric cytokinesis in mouse oocytes. Histochem. Cell Biol. *139*, 525–534.

Irobi, E., Aguda, A.H., Larsson, M., Guerin, C., Yin, H.L., Burtnick, L.D., Blanchoin, L., and Robinson, R.C. (2004). Structural basis of actin sequestration by thymosin-beta4: implications for WH2 proteins. EMBO J. *23*, 3599–3608.

Jaffe, A.B., and Hall, A. (2005). RHO GTPASES: Biochemistry and Biology. Annu. Rev. Cell Dev. Biol. *21*, 247–269.

Jones, K.T., and Lane, S.I.R. (2012). Chromosomal, metabolic, environmental, and hormonal origins of aneuploidy in mammalian oocytes. Exp. Cell Res. *318*, 1394–1399.

Kaksonen, M., Toret, C.P., and Drubin, D.G. (2006). Harnessing actin dynamics for clathrin-mediated endocytosis. Nat. Rev. Mol. Cell Biol. *7*, 404–414.

Kalab, P., Kubiak, J.Z., Verlhac, M.H., Colledge, W.H., and Maro, B. (1996). Activation of p90rsk during meiotic maturation and first mitosis in mouse oocytes and eggs: MAP kinase-independent and -dependent activation. Dev. Camb. Engl. *122*, 1957–1964.

Kalab, P., Pu, R.T., and Dasso, M. (1999). The ran GTPase regulates mitotic spindle assembly. Curr. Biol. CB *9*, 481–484.

Kelleher, J.F., Atkinson, S.J., and Pollard, T.D. (1995). Sequences, structural models, and cellular localization of the actin-related proteins Arp2 and Arp3 from Acanthamoeba. J. Cell Biol. *131*, 385–397.

Kitajima, T.S., Ohsugi, M., and Ellenberg, J. (2011). Complete kinetochore tracking reveals error-prone homologous chromosome biorientation in mammalian oocytes. Cell *146*, 568–581.

Kolano, A., Brunet, S., Silk, A.D., Cleveland, D.W., and Verlhac, M.-H. (2012). Error-prone mammalian female meiosis from silencing the spindle assembly checkpoint without normal interkinetochore tension. Proc. Natl. Acad. Sci. *109*, E1858–E1867.

Krause, M., Dent, E.W., Bear, J.E., Loureiro, J.J., and Gertler, F.B. (2003). E NA /VASP P ROTEINS : Regulators of the Actin Cytoskeleton and Cell Migration. Annu. Rev. Cell Dev. Biol. *19*, 541–564.

Kubiak, J.Z., Ciemerych, M.A., Hupalowska, A., Sikora-Polaczek, M., and Polanski, Z. (2008). On the transition from the meiotic to mitotic cell cycle during early mouse development. Int. J. Dev. Biol. *52*, 201–217.

Kunda, P., and Baum, B. (2009). The actin cytoskeleton in spindle assembly and positioning. Trends Cell Biol. *19*, 174–179.

Kunda, P., Pelling, A.E., Liu, T., and Baum, B. (2008). Moesin Controls Cortical Rigidity, Cell Rounding, and Spindle Morphogenesis during Mitosis. Curr. Biol. *18*, 91–101.

Kunda, P., Rodrigues, N.T.L., Moeendarbary, E., Liu, T., Ivetic, A., Charras, G., and Baum, B. (2012). PP1-Mediated Moesin Dephosphorylation Couples Polar Relaxation to Mitotic Exit. Curr. Biol. *22*, 231–236.

Kwiatkowski, D.J., Stossel, T.P., Orkin, S.H., Mole, J.E., Colten, H.R., and Yin, H.L. (1986). Plasma and cytoplasmic gelsolins are encoded by a single gene and contain a duplicated actin-binding domain. Nature *323*, 455–458.

Lafaurie-Janvore, J., Maiuri, P., Wang, I., Pinot, M., Manneville, J.-B., Betz, T., Balland, M., and Piel, M. (2013). ESCRT-III Assembly and Cytokinetic Abscission Are Induced by Tension Release in the Intercellular Bridge. Science *339*, 1625–1629.

Lam, J., Herant, M., Dembo, M., and Heinrich, V. (2009). Baseline Mechanical Characterization of J774 Macrophages. Biophys. J. *96*, 248–254.

Lancaster, O.M., Le Berre, M., Dimitracopoulos, A., Bonazzi, D., Zlotek-Zlotkiewicz, E., Picone, R., Duke, T., Piel, M., and Baum, B. (2013). Mitotic rounding alters cell geometry to ensure efficient bipolar spindle formation. Dev. Cell *25*, 270–283.

Lane, S.I.R., Yun, Y., and Jones, K.T. (2012). Timing of anaphase-promoting complex activation in mouse oocytes is predicted by microtubule-kinetochore attachment but not by bivalent alignment or tension. Dev. Camb. Engl. *139*, 1947–1955.

Larson, S.M., Lee, H.J., Hung, P. -h., Matthews, L.M., Robinson, D.N., and Evans, J.P. (2010). Cortical Mechanics and Meiosis II Completion in Mammalian Oocytes Are Mediated by Myosin-II and Ezrin-Radixin-Moesin (ERM) Proteins. Mol. Biol. Cell *21*, 3182–3192.

Leader, B., Lim, H., Carabatsos, M.J., Harrington, A., Ecsedy, J., Pellman, D., Maas, R., and Leder, P. (2002). Formin-2, polyploidy, hypofertility and positioning of the meiotic spindle in mouse oocytes. Nat. Cell Biol. *4*, 921–928.

Lecuit, T., and Lenne, P.-F. (2007). Cell surface mechanics and the control of cell shape, tissue patterns and morphogenesis. Nat. Rev. Mol. Cell Biol. *8*, 633–644.

Ledan, E., Polanski, Z., Terret, M.E., and Maro, B. (2001). Meiotic maturation of the mouse oocyte requires an equilibrium between cyclin B synthesis and degradation. Dev. Biol. *232*, 400–413.

Lefebvre, C., Terret, M.E., Djiane, A., Rassinier, P., Maro, B., and Verlhac, M.-H. (2002). Meiotic spindle stability depends on MAPK-interacting and spindle-stabilizing protein (MISS), a new MAPK substrate. J. Cell Biol. *157*, 603–613.

Lénárt, P., Bacher, C.P., Daigle, N., Hand, A.R., Eils, R., Terasaki, M., and Ellenberg, J.

(2005). A contractile nuclear actin network drives chromosome congression in oocytes. Nature *436*, 812–818.

Li, H., Guo, F., Rubinstein, B., and Li, R. (2008). Actin-driven chromosomal motility leads to symmetry breaking in mammalian meiotic oocytes. Nat. Cell Biol. *10*, 1301–1308.

Lieber, A.D., Yehudai-Resheff, S., Barnhart, E.L., Theriot, J.A., and Keren, K. (2013). Membrane Tension in Rapidly Moving Cells Is Determined by Cytoskeletal Forces. Curr. Biol. *23*, 1409–1417.

Linardopoulou, E.V., Parghi, S.S., Friedman, C., Osborn, G.E., Parkhurst, S.M., and Trask, B.J. (2007). Human subtelomeric WASH genes encode a new subclass of the WASP family. PLoS Genet. *3*, e237.

Liu, J., Wang, Q.-C., Wang, F., Duan, X., Dai, X.-X., Wang, T., Liu, H.-L., Cui, X.-S., Kim, N.-H., and Sun, S.-C. (2012). Nucleation promoting factors regulate the expression and localization of Arp2/3 complex during meiosis of mouse oocytes. PloS One *7*, e52277.

Liu, R., Abreu-Blanco, M.T., Barry, K.C., Linardopoulou, E.V., Osborn, G.E., and Parkhurst, S.M. (2009). Wash functions downstream of Rho and links linear and branched actin nucleation factors. Development *136*, 2849–2860.

Longo, F., and Chen, D. (1985). Development of cortical polarity in mouse eggs: Involvement of the meiotic apparatus. Dev. Biol. *107*, 382–394.

Louvet, S., Aghion, J., Santa-Maria, A., Mangeat, P., and Maro, B. (1996). Ezrin becomes restricted to outer cells following asymmetrical division in the preimplantation mouse embryo. Dev. Biol. *177*, 568–579.

Lu, M.S., and Johnston, C.A. (2013). Molecular pathways regulating mitotic spindle orientation in animal cells. Dev. Camb. Engl. *140*, 1843–1856.

Luksza, M., Queguigner, I., Verlhac, M.-H., and Brunet, S. (2013). Rebuilding MTOCs upon centriole loss during mouse oogenesis. Dev. Biol. *382*, 48–56.

Machesky, L.M., Atkinson, S.J., Ampe, C., Vandekerckhove, J., and Pollard, T.D. (1994). Purification of a cortical complex containing two unconventional actins from Acanthamoeba by affinity chromatography on profilin-agarose. J. Cell Biol. *127*, 107–115.

Machesky, L.M., Mullins, R.D., Higgs, H.N., Kaiser, D.A., Blanchoin, L., May, R.C., Hall, M.E., and Pollard, T.D. (1999). Scar, a WASp-related protein, activates nucleation of actin filaments by the Arp2/3 complex. Proc. Natl. Acad. Sci. *96*, 3739–3744.

Marchand, J.-B., Kaiser, D.A., Pollard, T.D., and Higgs, H.N. (2001). Interaction of WASP/Scar proteins with actin and vertebrate Arp2/3 complex. Nat Cell Biol *3*, 76–82.

Maro, B., and Verlhac, M.-H. (2002). Polar body formation: new rules for asymmetric

divisions. Nat. Cell Biol. *4*, E281–E283.

Martin, A.C., Welch, M.D., and Drubin, D.G. (2006). Arp2/3 ATP hydrolysis-catalysed branch dissociation is critical for endocytic force generation. Nat. Cell Biol. *8*, 826–833.

Matthews, H.K., Delabre, U., Rohn, J.L., Guck, J., Kunda, P., and Baum, B. (2012). Changes in Ect2 Localization Couple Actomyosin-Dependent Cell Shape Changes to Mitotic Progression. Dev. Cell *23*, 371–383.

May, R.C., Caron, E., Hall, A., and Machesky, L.M. (2000). Involvement of the Arp2/3 complex in phagocytosis mediated by FcgammaR or CR3. Nat. Cell Biol. *2*, 246–248.

McGuinness, B.E., Anger, M., Kouznetsova, A., Gil-Bernabé, A.M., Helmhart, W., Kudo, N.R., Wuensche, A., Taylor, S., Hoog, C., Novak, B., et al. (2009). Regulation of APC/C activity in oocytes by a Bub1-dependent spindle assembly checkpoint. Curr. Biol. CB *19*, 369–380.

McNally, F.J. (2013). Mechanisms of spindle positioning. J. Cell Biol. *200*, 131–140.

Mendoza, M.C. (2013). Phosphoregulation of the WAVE regulatory complex and signal integration. Semin. Cell Dev. Biol. *24*, 272–279.

Mendoza, M.C., Er, E.E., Zhang, W., Ballif, B.A., Elliott, H.L., Danuser, G., and Blenis, J. (2011). ERK-MAPK Drives Lamellipodia Protrusion by Activating the WAVE2 Regulatory Complex. Mol. Cell *41*, 661–671.

Millard, T.H., Behrendt, B., Launay, S., Fütterer, K., and Machesky, L.M. (2003). Identification and characterisation of a novel human isoform of Arp2/3 complex subunit p16-ARC/ARPC5. Cell Motil. Cytoskeleton *54*, 81–90.

Mitchison, T., Evans, L., Schulze, E., and Kirschner, M. (1986). Sites of microtubule assembly and disassembly in the mitotic spindle. Cell *45*, 515–527.

Montaville, P., Jégou, A., Pernier, J., Compper, C., Guichard, B., Mogessie, B., Schuh, M., Romet-Lemonne, G., and Carlier, M.-F. (2014). Spire and Formin 2 Synergize and Antagonize in Regulating Actin Assembly in Meiosis by a Ping-Pong Mechanism. PLoS Biol. *12*, e1001795.

Moore, J.K., and Cooper, J.A. (2010). Coordinating mitosis with cell polarity: Molecular motors at the cell cortex. Semin. Cell Dev. Biol. *21*, 283–289.

Moore, G.P., Lintern-Moore, S., Peters, H., and Faber, M. (1974). RNA synthesis in the mouse oocyte. J. Cell Biol. *60*, 416–422.

Mori, M., Monnier, N., Daigle, N., Bathe, M., Ellenberg, J., and Lénárt, P. (2011). Intracellular Transport by an Anchored Homogeneously Contracting F-Actin Meshwork. Curr. Biol. *21*, 606–611.

Munsie, L.N., Caron, N., Desmond, C.R., and Truant, R. (2009). Lifeact cannot visualize some forms of stress-induced twisted F-actin. Nat. Methods *6*, 317.

Musacchio, A., and Salmon, E.D. (2007). The spindle-assembly checkpoint in space and time. Nat. Rev. Mol. Cell Biol. *8*, 379–393.

Na, J., and Zernicka-Goetz, M. (2006). Asymmetric Positioning and Organization of the Meiotic Spindle of Mouse Oocytes Requires CDC42 Function. Curr. Biol. *16*, 1249–1254.

Nakanishi, O., Suetsugu, S., Yamazaki, D., and Takenawa, T. (2006). Effect of WAVE2 Phosphorylation on Activation of the Arp2/3 Complex. J. Biochem. (Tokyo) *141*, 319–325.

Nance, J., and Zallen, J.A. (2011). Elaborating polarity: PAR proteins and the cytoskeleton. Development *138*, 799–809.

Neisch, A.L., and Fehon, R.G. (2011). Ezrin, Radixin and Moesin: key regulators of membrane-cortex interactions and signaling. Curr. Opin. Cell Biol. *23*, 377–382.

Niault, T., Hached, K., Sotillo, R., Sorger, P.K., Maro, B., Benezra, R., and Wassmann, K. (2007). Changing Mad2 Levels Affects Chromosome Segregation and Spindle Assembly Checkpoint Control in Female Mouse Meiosis I. PLoS ONE *2*, e1165.

Norris, R.P., Freudzon, M., Mehlmann, L.M., Cowan, A.E., Simon, A.M., Paul, D.L., Lampe, P.D., and Jaffe, L.A. (2008). Luteinizing hormone causes MAP kinase-dependent phosphorylation and closure of connexin 43 gap junctions in mouse ovarian follicles: one of two paths to meiotic resumption. Dev. Camb. Engl. *135*, 3229–3238.

Padrick, S.B., Doolittle, L.K., Brautigam, C.A., King, D.S., and Rosen, M.K. (2011). Arp2/3 complex is bound and activated by two WASP proteins. Proc. Natl. Acad. Sci. *108*, E472–E479.

Paterson, H.F., Self, A.J., Garrett, M.D., Just, I., Aktories, K., and Hall, A. (1990). Microinjection of recombinant p21rho induces rapid changes in cell morphology. J. Cell Biol. *111*, 1001–1007.

Pechlivanis, M., Samol, A., and Kerkhoff, E. (2009). Identification of a short Spir interaction sequence at the C-terminal end of formin subgroup proteins. J. Biol. Chem. *284*, 25324–25333.

Perelroizen, I., Marchand, J.B., Blanchoin, L., Didry, D., and Carlier, M.F. (1994). Interaction of profilin with G-actin and poly(L-proline). Biochemistry (Mosc.) *33*, 8472–8478.

Perrin, B.J., and Ervasti, J.M. (2010). The actin gene family: Function follows isoform. Cytoskeleton *67*, 630–634.

Pfender, S., Kuznetsov, V., Pleiser, S., Kerkhoff, E., and Schuh, M. (2011). Spire-Type Actin Nucleators Cooperate with Formin-2 to Drive Asymmetric Oocyte Division. Curr. Biol. *21*,

955–960.

Pinot, M., Steiner, V., Dehapiot, B., Yoo, B.-K., Chesnel, F., Blanchoin, L., Kervrann, C., and Gueroui, Z. (2012). Confinement induces actin flow in a meiotic cytoplasm. Proc. Natl. Acad. Sci. *109*, 11705–11710.

Powell, A.E., Shung, C.-Y., Saylor, K.W., Müllendorf, K.A., Weiss, J.B., and Wong, M.H. (2010). Lessons from development: A role for asymmetric stem cell division in cancer. Stem Cell Res. *4*, 3–9.

Proctor, S.A., Minc, N., Boudaoud, A., and Chang, F. (2012). Contributions of Turgor Pressure, the Contractile Ring, and Septum Assembly to Forces in Cytokinesis in Fission Yeast. Curr. Biol. *22*, 1601–1608.

Propst, F., Rosenberg, M.P., Iyer, A., Kaul, K., and Vande Woude, G.F. (1987). c-mos proto-oncogene RNA transcripts in mouse tissues: structural features, developmental regulation, and localization in specific cell types. Mol. Cell. Biol. *7*, 1629–1637.

Pruyne, D., Evangelista, M., Yang, C., Bi, E., Zigmond, S., Bretscher, A., and Boone, C. (2002). Role of formins in actin assembly: nucleation and barbed-end association. Science *297*, 612–615.

Pullikuth, A., and Catling, A. (2007). Scaffold mediated regulation of MAPK signaling and cytoskeletal dynamics: A perspective. Cell. Signal. *19*, 1621–1632.

Quinlan, M.E., Heuser, J.E., Kerkhoff, E., and Mullins, R.D. (2005). Drosophila Spire is an actin nucleation factor. Nature *433*, 382–388.

Quinlan, M.E., Hilgert, S., Bedrossian, A., Mullins, R.D., and Kerkhoff, E. (2007). Regulatory interactions between two actin nucleators, Spire and Cappuccino. J. Cell Biol. *179*, 117–128.

Rai, A.K., Rai, A., Ramaiya, A.J., Jha, R., and Mallik, R. (2013). Molecular adaptations allow dynein to generate large collective forces inside cells. Cell *152*, 172–182.

Dos Remedios, C.G., Chhabra, D., Kekic, M., Dedova, I.V., Tsubakihara, M., Berry, D.A., and Nosworthy, N.J. (2003). Actin binding proteins: regulation of cytoskeletal microfilaments. Physiol. Rev. *83*, 433–473.

Reymann, A.-C., Boujemaa-Paterski, R., Martiel, J.-L., Guerin, C., Cao, W., Chin, H.F., De La Cruz, E.M., Thery, M., and Blanchoin, L. (2012). Actin Network Architecture Can Determine Myosin Motor Activity. Science *336*, 1310–1314.

Riedl, J., Crevenna, A.H., Kessenbrock, K., Yu, J.H., Neukirchen, D., Bista, M., Bradke, F., Jenne, D., Holak, T.A., Werb, Z., et al. (2008). Lifeact: a versatile marker to visualize F-actin. Nat. Methods *5*, 605–607.

Robinson, R.C., Mejillano, M., Le, V.P., Burtnick, L.D., Yin, H.L., and Choe, S. (1999). Domain movement in gelsolin: a calcium-activated switch. Science *286*, 1939–1942.

Rocca, D.L., Martin, S., Jenkins, E.L., and Hanley, J.G. (2008). Inhibition of Arp2/3-mediated actin polymerization by PICK1 regulates neuronal morphology and AMPA receptor endocytosis. Nat. Cell Biol. *10*, 259–271.

Rosales-Nieves, A.E., Johndrow, J.E., Keller, L.C., Magie, C.R., Pinto-Santini, D.M., and Parkhurst, S.M. (2006). Coordination of microtubule and microfilament dynamics by Drosophila Rho1, Spire and Cappuccino. Nat. Cell Biol. *8*, 367–376.

Rosenblatt, J., Cramer, L.P., Baum, B., and McGee, K.M. (2004). Myosin II-dependent cortical movement is required for centrosome separation and positioning during mitotic spindle assembly. Cell *117*, 361–372.

Rotty, J.D., Wu, C., and Bear, J.E. (2013). New insights into the regulation and cellular functions of the ARP2/3 complex. Nat. Rev. Mol. Cell Biol. *14*, 7–12.

Sagata, N., Watanabe, N., Vande Woude, G.F., and Ikawa, Y. (1989). The c-mos proto-oncogene product is a cytostatic factor responsible for meiotic arrest in vertebrate eggs. Nature *342*, 512–518.

Sagot, I., Rodal, A.A., Moseley, J., Goode, B.L., and Pellman, D. (2002). An actin nucleation mechanism mediated by Bni1 and profilin. Nat. Cell Biol. *4*, 626–631.

Sandquist, J.C., Kita, A.M., and Bement, W.M. (2011). And the Dead Shall Rise: Actin and Myosin Return to the Spindle. Dev. Cell *21*, 410–419.

Sato, N., Funayama, N., Nagafuchi, A., Yonemura, S., Tsukita, S., and Tsukita, S. (1992). A gene family consisting of ezrin, radixin and moesin. Its specific localization at actin filament/plasma membrane association sites. J. Cell Sci. *103 (Pt 1)*, 131–143.

Schuh, M. (2011). An actin-dependent mechanism for long-range vesicle transport. Nat. Cell Biol. *13*, 1431–1436.

Schuh, M., and Ellenberg, J. (2007). Self-Organization of MTOCs Replaces Centrosome Function during Acentrosomal Spindle Assembly in Live Mouse Oocytes. Cell *130*, 484–498.

Schuh, M., and Ellenberg, J. (2008). A New Model for Asymmetric Spindle Positioning in Mouse Oocytes. Curr. Biol. *18*, 1986–1992.

Schutt, C.E., Myslik, J.C., Rozycki, M.D., Goonesekere, N.C., and Lindberg, U. (1993). The structure of crystalline profilin-beta-actin. Nature *365*, 810–816.

Sebestova, J., Danylevska, A., Novakova, L., Kubelka, M., and Anger, M. (2012). Lack of response to unaligned chromosomes in mammalian female gametes. Cell Cycle Georget. Tex *11*, 3011–3018.

Sedzinski, J., Biro, M., Oswald, A., Tinevez, J.-Y., Salbreux, G., and Paluch, E. (2011). Polar actomyosin contractility destabilizes the position of the cytokinetic furrow. Nature *476*, 462–466.

Sela-Abramovich, S., Edry, I., Galiani, D., Nevo, N., and Dekel, N. (2006). Disruption of gap junctional communication within the ovarian follicle induces oocyte maturation. Endocrinology *147*, 2280–2286.

Shimamoto, Y., Maeda, Y.T., Ishiwata, S., Libchaber, A.J., and Kapoor, T.M. (2011). Insights into the Micromechanical Properties of the Metaphase Spindle. Cell *145*, 1062–1074.

Shoji, S., Yoshida, N., Amanai, M., Ohgishi, M., Fukui, T., Fujimoto, S., Nakano, Y., Kajikawa, E., and Perry, A.C.F. (2006). Mammalian Emi2 mediates cytostatic arrest and transduces the signal for meiotic exit via Cdc20. EMBO J. *25*, 834–845.

Simerly, C., Nowak, G., de Lanerolle, P., and Schatten, G. (1998). Differential expression and functions of cortical myosin IIA and IIB isotypes during meiotic maturation, fertilization, and mitosis in mouse oocytes and embryos. Mol. Biol. Cell *9*, 2509–2525.

Smith, B.A., Daugherty-Clarke, K., Goode, B.L., and Gelles, J. (2013). Pathway of actin filament branch formation by Arp2/3 complex revealed by single-molecule imaging. Proc. Natl. Acad. Sci. *110*, 1285–1290.

Stewart, M.P., Helenius, J., Toyoda, Y., Ramanathan, S.P., Muller, D.J., and Hyman, A.A. (2011). Hydrostatic pressure and the actomyosin cortex drive mitotic cell rounding. Nature *469*, 226–230.

Suizu, F., Ueda, K., Iwasaki, T., Murata-Hori, M., and Hosoya, H. (2000). Activation of actin-activated MgATPase activity of myosin II by phosphorylation with MAPK-activated protein kinase-1b (RSK-2). J. Biochem. (Tokyo) *128*, 435–440.

Sun, S.-C., Wang, Z.-B., Xu, Y.-N., Lee, S.-E., Cui, X.-S., and Kim, N.-H. (2011a). Arp2/3 Complex Regulates Asymmetric Division and Cytokinesis in Mouse Oocytes. PLoS ONE *6*, e18392.

Sun, S.-C., Sun, Q.-Y., and Kim, N.-H. (2011b). JMY is required for asymmetric division and cytokinesis in mouse oocytes. Mol. Hum. Reprod. *17*, 296–304.

Sun, S.-C., Xu, Y.-N., Li, Y.-H., Lee, S.-E., Jin, Y.-X., Cui, X.-S., and Kim, N.-H. (2011c). WAVE2 regulates meiotic spindle stability, peripheral positioning and polar body emission in mouse oocytes. Cell Cycle Georget. Tex *10*, 1853–1860.

Sun, S.-C., Xu, Y.-N., Li, Y.-H., Lee, S.-E., Jin, Y.-X., Cui, X.-S., and Kim, N.-H. (2011d). WAVE2 regulates meiotic spindle stability, peripheral positioning and polar body emission in mouse oocytes. Cell Cycle Georget. Tex *10*.

Szollosi, D., Calarco, P., and Donahue, R.P. (1972). Absence of centrioles in the first and second meiotic spindles of mouse oocytes. J. Cell Sci. *11*, 521–541.

Terret, M.-E., Chaigne, A., and Verlhac, M.-H. (2013). Mouse oocyte, a paradigm of cancer cell. Cell Cycle *12*, 0–6.

Terret, M.E., Wassmann, K., Waizenegger, I., Maro, B., Peters, J.-M., and Verlhac, M.-H. (2003a). The Meiosis I-to-Meiosis II Transition in Mouse Oocytes Requires Separase Activity. Curr. Biol. *13*, 1797–1802.

Terret, M.E., Lefebvre, C., Djiane, A., Rassinier, P., Moreau, J., Maro, B., and Verlhac, M.-H. (2003b). DOC1R: a MAP kinase substrate that control microtubule organization of metaphase II mouse oocytes. Dev. Camb. Engl. *130*, 5169–5177.

Théry, M., and Bornens, M. (2006). Cell shape and cell division. Curr. Opin. Cell Biol. *18*, 648–657.

Théry, M., Racine, V., Pépin, A., Piel, M., Chen, Y., Sibarita, J.-B., and Bornens, M. (2005). The extracellular matrix guides the orientation of the cell division axis. Nat. Cell Biol. *7*, 947–953.

Tinevez, J.-Y., Schulze, U., Salbreux, G., Roensch, J., Joanny, J.-F., and Paluch, E. (2009). Role of cortical tension in bleb growth. Proc. Natl. Acad. Sci. U. S. A. *106*, 18581–18586.

Toyoshima, F., and Nishida, E. (2007). Integrin-mediated adhesion orients the spindle parallel to the substratum in an EB1- and myosin X-dependent manner. EMBO J. *26*, 1487–1498.

Tremoleda, J.L., Schoevers, E.J., Stout, T.A., Colenbrander, B., and Bevers, M.M. (2001). Organisation of the cytoskeleton during in vitro maturation of horse oocytes. Mol. Reprod. Dev. *60*, 260–269.

Tsukita, S., Oishi, K., Sato, N., Sagara, J., Kawai, A., and Tsukita, S. (1994). ERM family members as molecular linkers between the cell surface glycoprotein CD44 and actin-based cytoskeletons. J. Cell Biol. *126*, 391–401.

Urbanek, A.N., Smith, A.P., Allwood, E.G., Booth, W.I., and Ayscough, K.R. (2013). A Novel Actin-Binding Motif in Las17/WASP Nucleates Actin Filaments Independently of Arp2/3. Curr. Biol. *23*, 196–203.

Uruno, T., Liu, J., Zhang, P., Fan, Y., Egile, C., Li, R., Mueller, S.C., and Zhan, X. (2001). Activation of Arp2/3 complex-mediated actin polymerization by cortactin. Nat Cell Biol *3*, 259–266.

Uyeda, T.Q.P., Iwadate, Y., Umeki, N., Nagasaki, A., and Yumura, S. (2011). Stretching Actin Filaments within Cells Enhances their Affinity for the Myosin II Motor Domain. PLoS ONE *6*, e26200.

Valentine, M.T., Perlman, Z.E., Mitchison, T.J., and Weitz, D.A. (2005). Mechanical Properties of Xenopus Egg Cytoplasmic Extracts. Biophys. J. *88*, 680–689.

Vavylonis, D., Kovar, D.R., O'Shaughnessy, B., and Pollard, T.D. (2006). Model of Formin-Associated Actin Filament Elongation. Mol. Cell *21*, 455–466.

Verlhac, M.-H. (2000). Mos activates MAP kinase in mouse oocytes through two opposite pathways. EMBO J. *19*, 6065–6074.

Verlhac, M.-H., Lefebvre, C., Guillaud, P., Rassinier, P., and Maro, B. (2000). Asymmetric division in mouse oocytes: with or without Mos. Curr. Biol. *10*, 1303–1306.

Verlhac, M.H., de Pennart, H., Maro, B., Cobb, M.H., and Clarke, H.J. (1993). MAP kinase becomes stably activated at metaphase and is associated with microtubule-organizing centers during meiotic maturation of mouse oocytes. Dev. Biol. *158*, 330–340.

Verlhac, M.H., Kubiak, J.Z., Clarke, H.J., and Maro, B. (1994). Microtubule and chromatin behavior follow MAP kinase activity but not MPF activity during meiosis in mouse oocytes. Dev. Camb. Engl. *120*, 1017–1025.

Verlhac, M.H., Kubiak, J.Z., Weber, M., Geraud, G., Colledge, W.H., Evans, M.J., and Maro, B. (1996). Mos is required for MAP kinase activation and is involved in microtubule organization during meiotic maturation in the mouse. Development *122*, 815 –822.

Vinot, S., Le, T., Maro, B., and Louvet-Vallée, S. (2004). Two PAR6 Proteins Become Asymmetrically Localized during Establishment of Polarity in Mouse Oocytes. Curr. Biol. *14*, 520–525.

Wang, Z.-B., Jiang, Z.-Z., Zhang, Q.-H., Hu, M.-W., Huang, L., Ou, X.-H., Guo, L., Ouyang, Y.-C., Hou, Y., Brakebusch, C., et al. (2013). Specific deletion of Cdc42 does not affect meiotic spindle organization/migration and homologous chromosome segregation but disrupts polarity establishment and cytokinesis in mouse oocytes. Mol. Biol. Cell *24*, 3832–3841.

Wassmann, K., Niault, T., and Maro, B. (2003). Metaphase I arrest upon activation of the Mad2-dependent spindle checkpoint in mouse oocytes. Curr. Biol. CB *13*, 1596–1608.

Weaver, A.M., Karginov, A.V., Kinley, A.W., Weed, S.A., Li, Y., Parsons, J.T., and Cooper, J.A. (2001). Cortactin promotes and stabilizes Arp2/3-induced actin filament network formation. Curr. Biol. *11*, 370–374.

Weber, K.L., Sokac, A.M., Berg, J.S., Cheney, R.E., and Bement, W.M. (2004). A microtubule-binding myosin required for nuclear anchoring and spindle assembly. Nature *431*, 325–329.

Wilbur, J.D., and Heald, R. (2013). Mitotic spindle scaling during Xenopus development by kif2a and importin α. eLife *2*, e00290.

Woolner, S., and Papalopulu, N. (2012). Spindle Position in Symmetric Cell Divisions during Epiboly Is Controlled by Opposing and Dynamic Apicobasal Forces. Dev. Cell *22*, 775–787.

Woolner, S., O'Brien, L.L., Wiese, C., and Bement, W.M. (2008). Myosin-10 and actin filaments are essential for mitotic spindle function. J. Cell Biol. *182*, 77–88.

Yang, H.-C., and Pon, L.A. (2002). Actin cable dynamics in budding yeast. Proc. Natl. Acad. Sci. U. S. A. *99*, 751–756.

Yi, K., Unruh, J.R., Deng, M., Slaughter, B.D., Rubinstein, B., and Li, R. (2011). Dynamic maintenance of asymmetric meiotic spindle position through Arp2/3-complex-driven cytoplasmic streaming in mouse oocytes. Nat. Cell Biol. *13*, 1252–1258.

Yi, K., Rubinstein, B., Unruh, J.R., Guo, F., Slaughter, B.D., and Li, R. (2013). Sequential actin-based pushing forces drive meiosis I chromosome migration and symmetry breaking in oocytes. J. Cell Biol. *200*, 567–576.

Yun, C.H., Lamprecht, G., Forster, D.V., and Sidor, A. (1998). NHE3 kinase A regulatory protein E3KARP binds the epithelial brush border Na+/H+ exchanger NHE3 and the cytoskeletal protein ezrin. J. Biol. Chem. *273*, 25856–25863.

Zhong, Z.-S., Huo, L.-J., Liang, C.-G., Chen, D.-Y., and Sun, Q.-Y. (2005). Small GTPase RhoA is required for ooplasmic segregation and spindle rotation, but not for spindle organization and chromosome separation during mouse oocyte maturation, fertilization, and early cleavage. Mol. Reprod. Dev. *71*, 256–261.

Zhu, Z.-Y. (2002). Rotation of Meiotic Spindle Is Controlled by Microfilaments in Mouse Oocytes. Biol. Reprod. *68*, 943–946.

Zuchero, J.B., Coutts, A.S., Quinlan, M.E., Thangue, N.B.L., and Mullins, R.D. (2009). p53-cofactor JMY is a multifunctional actin nucleation factor. Nat. Cell Biol. *11*, 451–459.

ANNEXES

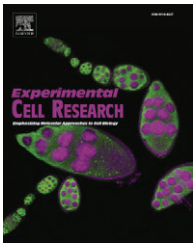
EXPERIMENTAL CELL RESEARCH 318 (2012) 1442–1447



Available online at www.sciencedirect.com

SciVerse ScienceDirect

www.elsevier.com/locate/yexcr



Review Article

Spindle positioning in mammalian oocytes

Agathe Chaigne, Marie-Hélène Verlhac, Marie-Emilie Terret**

Collège de France, Center for Interdisciplinary Research in Biology (CIRB), UMR-CNRS7241/INSERM-U1050, 11 place Marcelin Berthelot, 75005 Paris, France
Memolife Laboratory of Excellence and Paris Science Lettre, France

ARTICLE INFORMATION

Article Chronology:
Received 21 December 2011
Revised version received
21 February 2012
Accepted 22 February 2012
Available online 3 March 2012

Keywords:
Meiosis
Oocyte
Spindle positioning
F-actin

ABSTRACT

To preserve the maternal stores accumulated during oogenesis for further embryo development, oocytes divide asymmetrically which minimizes the volume of cytoplasm lost with each set of haploid genome. To ensure asymmetric division to occur, oocytes have to position their division spindle asymmetrically as well as tailor the size of daughter cells to the chromatin mass. In this review, we will discuss the recent advances in the field, with emphasis on the control mechanisms involved in meiotic spindle positioning in mammalian oocytes.

© 2012 Elsevier Inc. All rights reserved.

Contents

Introduction . . . 1443
Importance of spindle position . . . 1443
Role of spindle off-centering . . . 1443
Basis of spindle migration . . . 1443
Establishment of spindle position . . . 1444
Spindle migration to the cortex . . . 1444
Actin, a key player in spindle migration . . . 1444
Force generators . . . 1444
Pulling force . . . 1444
Pushing force . . . 1444
Cytoskeletal regulators involved in spindle migration . . . 1445
Maintenance of spindle position . . . 1445
Consequences of spindle migration . . . 1445
Conclusion . . . 1446

* *Corresponding authors at:* Collège de France, Center for Interdisciplinary Research in Biology (CIRB), UMR-CNRS7241/INSERM-U1050, 11 place Marcelin Berthelot, 75005 Paris, France.
E-mail addresses: marie-helene.verlhac@college-de-france.fr (M.-H. Verlhac), marie-emilie.terret@college-de-france.fr (M.-E. Terret).

0014-4827/$ – see front matter © 2012 Elsevier Inc. All rights reserved.
doi:10.1016/j.yexcr.2012.02.019

Acknowledgments 1446
References 1446

Introduction

Female meiotic maturation is the last event of oogenesis and involves genetic reduction from a replicated diploid cell to a haploid gamete, the oocyte. It consists of two highly asymmetric divisions in size without an intervening DNA replication, resulting in the formation of a big oocyte and two small polar bodies. These two tiny polar bodies will eventually degenerate in species that do not reproduce parthenogenetically.

All oocytes are arrested in prophase of the first meiotic division (prophase I) in the ovary. The nucleus of prophase I-arrested oocytes is slightly off-center. Upon hormonal stimulation, meiosis resumption occurs. It is characterized by the event of nuclear envelope breakdown (NEBD) followed by the formation of the first meiotic (MI) spindle. In mouse oocytes, the first meiotic division lasts from 8 to 10 h. Late after meiosis resumption (3–5 h depending on the strain), the MI spindle migrates along its long axis towards the closest cortex and attaches to it. The migration takes about 4 h, then anaphase occurs followed by the first asymmetric meiotic division, which results in the extrusion of the first polar body (PBE) [1]. The second meiotic (MII) spindle reforms parallel to the cortex after PBE. In vertebrates, oocytes are blocked once again in metaphase of the second meiotic division until the extrusion of the second polar body triggered by fertilization. In mouse oocytes, the MII spindle rotates 90° before extrusion of the second polar body. The process of meiotic maturation is schematized in Fig. 1.

Hence, positioning and anchoring of the meiotic spindles to the cortex are essential for the success of asymmetric divisions and subsequent egg polarization.

Importance of spindle position

Role of spindle off-centering

One of the roles of meiosis is to produce a haploid gamete from a diploid cell, thus to divide the total amount of DNA by four. In all species, the first and second oocyte divisions are extremely asymmetric resulting in very different sizes of the daughter cells, polar bodies being much smaller than the oocyte (diameter 10 µm versus 80 µm respectively, in the mouse). In species reproducing by spawning, it is essential for the oocyte to keep the maternal RNA and protein stock, accumulated during oocyte growth, to support embryo development outside the female body. Despite the fact that in mammals the embryo develops inside the female reproductive track, it is generally accepted that asymmetric meiotic divisions favor the maintenance of maternal reserves, sustaining embryo development until the implantation of the blastocyst in the uterus 5 days post-fertilization. On the other hand, this asymmetry might ensure that the sperm fertilizes only the large oocyte but not the tiny first polar body, and thus allow the production of unique gamete [2].

Basis of spindle migration

In many model systems such as the one-cell stage embryo of the worm *C. elegans*, mitotic spindle positioning is achieved through astral microtubule–cortex interactions. Astral microtubules emanate from the centrosomes and anchor to the cortex, asserting pulling forces on the spindle poles [3].

However, in oocytes and in particular in mammalian models, there are no true centrosomes after the pachytene stage [4,5] and therefore no astral microtubules. Instead, microtubules emanate from multiple microtubule organizing centers (MTOCs) devoid of centrioles [4]. In correlation, the positioning of the meiotic spindle has been shown to be microtubule-independent but actin-dependent [6]. However it is only recently, through the development of F-actin binding probes [7,8] that actin organization in mouse oocytes could be visualized and the spindle migration mechanisms unraveled. These past few years, it has been shown that both straight (Formin-2, Spire 1/2) and branched (Arp2/3) actin nucleators play a role in controlling spindle positioning in mouse oocytes [9–12]. Their precise role will be discussed below.

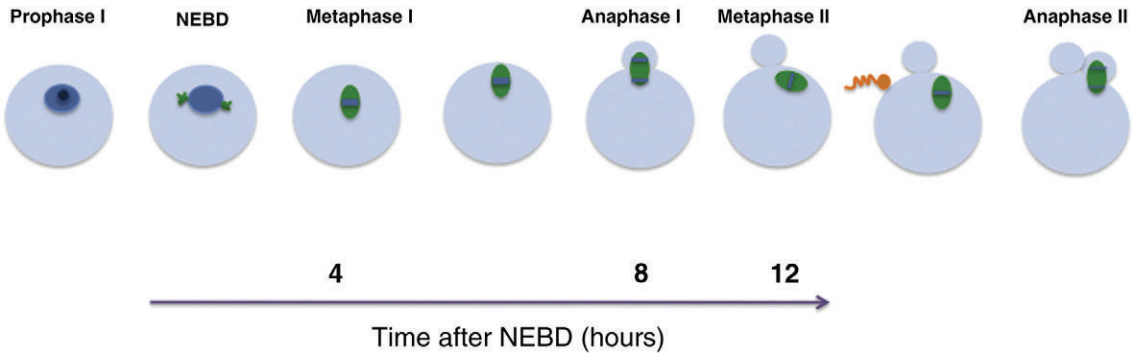


Fig. 1 – Scheme representing meiotic maturation of a mouse oocyte (DNA in blue, microtubule in green, sperm in orange). NEBD: nuclear envelope breakdown (characterizes meiosis resumption).

Establishment of spindle position

Spindle migration to the cortex

The position of the prophase I nucleus varies among mammalian species. In mouse oocytes, it is slightly off-center [13] while it is more eccentric in horse and human oocytes [14,15].

After NEBD, the microtubule spindle forms progressively at the original position of the nucleus (Fig. 1). The spindle axis, which defines the spindle migration direction, is random and the spindle always migrates along its long axis towards the closest cortex [1]. Apparently, there is no pre-determined cytoplasmic or cortical polarity [16,17] so there is no pre-determined site in the cortex able to attract the spindle [1].

Actin, a key player in spindle migration

In mouse oocytes, spindle migration is independent of microtubules. Moreover, microtubules seem to slow down the movement as treatment of oocytes with nocodazole, a drug that depolymerizes microtubules leads to chromosomes moving faster than in controls [1,18]. Surprisingly this is not the case in another rodent species, the rat oocyte, where a higher dose of nocodazole inhibits spindle migration [19].

As mentioned above, spindle migration is an F-actin-dependent event. The implication of actin was shown using various pharmacological agents. The treatment with actin polymerization inhibitors, cytochalasin B [5] and latrunculin [18,20] prevents chromosome migration. On the other hand, an inhibitor of actin depolymerization, jasplakinolide, also impedes on chromosome migration to the cortex [18,21]. Moreover, oocytes from mice lacking Formin-2 (Fmn2 −/−) harbor defects in spindle migration showing the importance of this actin nucleator [9,10]. It appears that not only the presence but also the turnover of F-actin is required for spindle migration.

In the past few years, the F-actin structure involved in spindle migration was eventually visualized by different groups [22,23] using a novel F-actin specific probe based on the actin-binding domain of Utrophin [7]. This probe binds to F- but not G-actin and does not stabilize actin filaments, allowing live imaging of actin filaments during meiotic maturation. A dense and dynamic cytoplasmic F-actin meshwork forms during meiotic maturation. It is required for proper migration of the spindle to the cortex [22,23]. Besides, the microtubule spindle is surrounded by an F-actin cage, which migrates towards the cortex along with the spindle [22,23]. This meshwork is nucleated partly by Formin-2, as it is absent in Fmn2 −/− oocytes [22,23]. Formin-2 is present both at the cortex [24] and in the cytoplasm [25] of the cell. Furthermore Spire1/2, straight actin filaments nucleators, cooperate with Formin-2 to nucleate the cytoplasmic F-actin meshwork [11] as it is the case in *Drosophila* oocytes [26,27]. Spire1/2 seem to act redundantly with each other and form a functional unit with Formin-2 [11]. In prophase I, these three nucleators co-localize at the surface of vesicles positioned at crossing-points of the cytoplasmic actin meshwork; they move towards the plasma membrane in an F-actin- and myosin-Vb-dependent manner [25]. From this latest study, it seems that, at least in prophase I, the cytoplasmic meshwork is nucleated from vesicles.

The branched actin nucleator, Arp2/3 complex, is also involved in spindle migration. In oocytes treated with an Arp2/3 specific inhibitor [28], the spindle does not migrate to the cortex, which results in symmetric division [12]. Interestingly, siRNAs and antibody injections against Wave2 also lead to the absence of spindle migration [29]. Wave2 belongs to the Scar (Suppressor of cAMP repressor) family of type I nucleating promoting factors (NPF). These proteins are known to activate the Arp2/3 complex via their highly conserved carboxyl-terminal, WCA domain [30]. In addition, junction mediating and regulatory protein (JMY), another Arp2/3 complex activator, also participates in spindle migration in mouse oocytes [31]. Although the precise role of the Arp2/3 complex in meiosis I remains unknown, it is a key player in the positioning of the second meiotic spindle as discussed below [32].

Latest results show that the regulation of the F-actin meshwork and of its nucleators is itself instrumental in the translocation of the meiotic spindle to the cortex. Indeed, the density of the meshwork is very high in prophase I, drops at NEBD and progressively increases while the spindle migrates, correlated with the endogenous levels of Formin-2 [24]. Overexpression of Formin-2 results in the stabilization of the meshwork at NEBD and subsequently prevents spindle migration. The destruction of the F-actin meshwork at NEBD allows the formation of a new asymmetric mesh (and thus forces) that is required for spindle migration. How are the forces transduced by this meshwork to the meiotic spindle?

Force generators

Pulling force

When the spindle approaches the cortex, in some cases, the cortex invaginates, suggesting that pulling forces might be exerted via the spindle onto the cortex [23]. Moreover, the phospho-activated form of the non-muscle myosin II (MyoII) has been detected at both poles of the first meiotic spindle [23] and its inhibition impairs spindle migration [23,33] consistent with the presence of MyoII-dependent pulling forces. However, the involvement of MyoII is still under debate: oocytes treated with the same MyoII inhibitor at a similar concentration harbor opposite phenotype on spindle migration [18]. Similarly, different groups have reported different localization for MyoII: (1) metaphase I spindle [33]; (2) one or both ends of the spindle [23]; and (3) cleavage furrow [10].

Pushing force

On the other hand, overexpression of Formin-2 stabilizes the meshwork and induces nucleus invaginations suggesting that the meshwork is also able to exert pushing forces [24]. It is tempting to propose that pushing forces might also account for the migration of the spindle. In contrast, using Lifeact [8], another F-actin labeling probe, Li et al. have shown the presence of an actin cloud behind the chromosomes that mediates the pushing of the first meiotic spindle [18]. Therefore, the use of different F-actin probes may account for the discrepancy in the actin structure visualized, as the latest study of Yi and collaborators reported that Lifeact may label only cortical F-actin but not the cytoplasmic actin meshwork [32].

As a conclusion, it is still entirely possible that both pulling and pushing mechanisms exist in this model system in order to position the first meiotic spindle precisely.

Cytoskeletal regulators involved in spindle migration

Cdc42, a small GTPase of the Rho-family, is involved in the control of actin organization and dynamics. It activates the Myosin Light Chain Kinase (MLCK), which phosphorylates the myosin regulatory light chain (RLC) and subsequently induces actin–myosin movement [34]. It activates type I NPFs such as WASP (Wiskott–Aldrich syndrome protein), N-WASP (Neuronal WASP) and proteins of the Scar family [35]. Using an inactive mutant of Cdc42, it has been shown that this effector is required for spindle migration [36]. Interestingly, Cdc42 is also involved in spindle morphogenesis probably acting through aPKCζ (atypical protein kinase C ζ) [36], showing that it could be a key player linking the structure of the spindle and its proper localization. aPKCζ normally co-localizes with the spindle poles and is known to function with several PARs (PARtitioning defective protein) and mediate cell polarity [37] in other systems.

Kinases also participate in spindle positioning. Mos is a MAPKKK (MAP kinase kinase kinase) expressed in oocytes that activates two MAPKs, ERK1 and ERK2. Mos is essential for spindle migration since in its absence the spindle does not migrate. Instead, the pole closest to the cortex elongates at anaphase leading to the extrusion of a large polar body [1,38]. MEK1/2, a MAPKK (MAP kinase kinase) downstream of Mos, is activated after NEBD. Its inactivation leads to the extrusion of bigger polar bodies and subsequent formation of more centralized MII spindles [39]. Thus the Mos/…/MAPK pathway controls the position of the spindle and this role has been conserved through evolution since it also does so in jellyfish oocytes [40].

Maintenance of spindle position

After extrusion of the first polar body, the meiosis II spindle forms underneath the cortex and remains anchored until second polar body extrusion is triggered by fertilization. Interestingly, the metaphase II spindles of aging oocytes do not stay anchored to the cortex [41], which may account for the observed decrease in fertility, suggesting that anchoring of meiotic spindles might be essential for the success of female gametogenesis.

The small GTPase Rac participates in spindle anchoring. Indeed, the active form Rac (Rac-GTP) accumulates in the cortical region overlying the MI and MII spindles (see Consequences of spindle migration section) whereas Rac is present throughout the entire cortex. Furthermore, overexpression of an inactive form of Rac in MII oocytes leads to partial or total detachment of the spindle from the cortex [17].

Very recently, Yi et al. [32] have shown that the Arp2/3 complex is involved in the maintenance of the spindle position in MII. Inhibition of Arp2/3 with a specific drug [28] leads to the detachment of the metaphase II spindle. Arp2/3 also localizes in the cortical region overlying the spindle (but only in MII) and can initiate an actin flow. This flow seems to generate a cytoplasmic retrograde flow that pushes the spindle towards the cortex and thus maintains its position [32]. On the contrary, MyoII seems to mediate a backward flow when Arp2/3 is inhibited [32]. However, it is not clear how Arp2/3 could mediate a cytoplasmic flow throughout the entire oocyte simply via actin nucleation [42]. Interestingly enough, while playing antagonistic roles in maintaining the cortical positioning of the spindle in MII, Arp2/3 and MyoII seem to cooperate to pull the MI spindle to the cortex.

Consequences of spindle migration

Before spindle migration, the oocyte has no obvious polarity. In particular, the cortex is uniformly covered with microvilli and a dense actin layer [6]. Underlying the cortex, cortical granules are evenly distributed [6]. The positioning of the spindle to the cortex in meiosis I induces cortical differentiation. Overhanging the closest spindle pole, a cortical domain devoid of microvilli and very rich in actin, the “actin cap”, is formed [6] (Fig. 2). The actin cap is the first sign of oocyte polarization. Thus, oocyte polarization is directly dependent upon spindle migration [1]. The actin cap is also characterized by a local accumulation of Rac-GTP [17], MyoII [33] and an isoform a of Par6 (mPar6a) [43] and by the absence of cortical granules below it [44].

The precise signaling pathways initiating the formation of the actin cap remain to be discovered. Nevertheless, as mentioned above, it has been shown that chromosomes are key players of this reorganization. Chromosomes artificially dispersed in the cytoplasm underlying the cortex are able to induce actin caps above them [45]. Moreover, beads coated with DNA mediate actin cap formation with a size corresponding to the amount of DNA coated on the beads and their distance to the cortex: the more DNA and the closer to the cortex, the bigger the size of the cap [46]. These elegant experiments demonstrated that chromosomes directly induce cortical polarization. Furthermore, it was shown that the effect of chromosomes is mediated by the small GTPase Ran [46]. The active form of Ran, Ran-GTP, forms a gradient centered on the chromosomes at all stages of meiotic maturation [47]. This gradient is broad in mouse oocytes and migrates towards the cortex concomitantly with chromosome movement. When chromosomes reach the cortex, the associated Ran-GTP activity induces cortical differentiation. Indeed, the actin cap formation is impaired when the Ran-GTP gradient is disrupted [46].

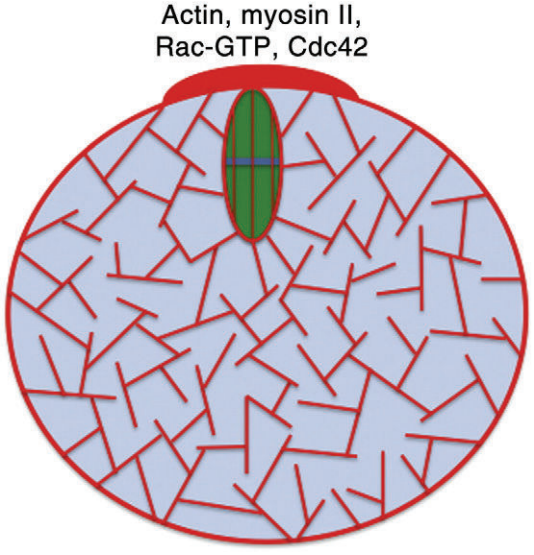


Fig. 2 – Cortical polarization above an anchored spindle (F-actin in red, DNA in blue, microtubules in green).

The Rac-GTPase also participates in cortical reorganization. As discussed before, Rac-GTP accumulates in the actin cap in a chromatin-dependent manner. Inhibiting Rac in meiosis II leads to the loss of the actin cap [17]. Accumulation of Rac-GTP would occur downstream of Ran-GTP, maybe promoting the stabilization of the cap. Indeed, overexpression of a dominant negative form of Rac perturbs metaphase II spindle anchoring to the cortex [17]. Rac-GTP, through activation of N-Wasp [32,35], could be in a positive feedback loop which reinforces the effect of the chromosomes and the associated Ran-GTP gradient in promoting spindle anchorage via a cortically F-actin enriched structures.

At last, the role of this actin cap reorganization is not fully understood. Microvilli are required for sperm entry. One hypothesis suggests that the absence of microvilli in the cap reduces the chance of fusion of the sperm in this region to avoid the extrusion of sperm chromosomes together with the haploid DNA of the oocyte [48]. Another hypothesis is that the actin cap restricts the size of the polar bodies to the cortical region above the chromosomes. Indeed, disrupting the actin cap by the expression of a constitutively active Ran mutant leads to the extrusion of bigger polar bodies [46,47].

Conclusion

Spindle migration during meiosis I is a long process that lasts 4 h and is a pre-requisite for the symmetry breaking of the first meiotic division and polarization of the oocyte. It is controlled by a very dense and dynamic cytoplasmic actin meshwork nucleated by Formin-2 and Spire1/2 that pulls and/or pushes on the microtubule spindle. Concomitant with spindle positioning, a differentiated cortical actin cap forms above the region where the spindle will finish its migration. It is a region devoid of cortical granules and microvilli but rich in actin and several other proteins such as MyoII, mPar6a, Rac-GTP and Cdc42. The anchoring of the MII spindle to the cortex and its rotation for the extrusion of the second polar body also depend on actin filaments. The branched actin nucleator Arp2/3 has been involved in the maintenance of the MII spindle position in mouse oocyte. Thus, actin filaments are key players of spindle movements in this model system.

Even though microtubules are the main spindle positioning machinery in many cell types, there is growing evidence that F-actin is also involved (for review, see [49]). In mitotic cells, actin is involved in the sensing of the substrate and the orientation of the spindle according to the adhesion pattern [50]. In cultured cells, a dynamic subcortical actin structure has been shown to control the positioning of the mitotic spindle [51]. Oocytes are non-adherent cells. The asymmetry is not controlled by external cues as in other model systems. On the contrary, the asymmetry comes from within the cell. How these events are initiated, how the symmetry is broken is still under intense investigations. Nevertheless, the loss of asymmetry, as in aging oocytes, is often linked to a decrease in the fertilization rate [41].

Acknowledgments

We thank Karen Lee for critical reading of the manuscript. AC is a recipient of a fellowship from the Ecole Normale Supérieure (ENS) Paris. This work was supported by grants from the *Ligue Nationale Contre le Cancer* (EL/2009/LNCC/MHV) and from the *Agence Nationale pour la Recherche* (ANR08-BLAN-0136-01 to MHV).

REFERENCES

[1] M.-H. Verlhac, C. Lefebvre, P. Guillaud, P. Rassinier, B. Maro, Asymmetric division in mouse oocytes: with or without Mos, Curr. Biol. 10 (2000) 1303–1306.
[2] S. Brunet, M.H. Verlhac, Positioning to get out of meiosis: the asymmetry of division, Hum. Reprod. Update 17 (2010) 68–75.
[3] C.R. Cowan, A.A. Hyman, Asymmetric cell division in *C. elegans*: cortical polarity and spindle positioning, Annu. Rev. Cell Dev. Biol. 20 (2004) 427–453.
[4] D. Szollosi, P. Calarco, R.P. Donahue, Absence of centrioles in the first and second meiotic spindles of mouse oocytes, J. Cell Sci. 11 (1972) 521–541.
[5] A.H. Sathananthan, K. Selvaraj, M.L. Girijashankar, V. Ganesh, P. Selvaraj, A.O. Trounson, From oogonia to mature oocytes: inactivation of the maternal centrosome in humans, Microsc. Res. Tech. 69 (2006) 396–407.
[6] F. Longo, D. Chen, Development of cortical polarity in mouse eggs: involvement of the meiotic apparatus, Dev. Biol. 107 (1985) 382–394.
[7] B.M. Burkel, G. von Dassow, W.M. Bement, Versatile fluorescent probes for actin filaments based on the actin-binding domain of utrophin, Cell Motil. Cytoskeleton 64 (2007) 822–832.
[8] J. Riedl, A.H. Crevenna, K. Kessenbrock, J.H. Yu, D. Neukirchen, M. Bista, F. Bradke, D. Jenne, T.A. Holak, Z. Werb, M. Sixt, R. Wedlich-Soldner, Lifeact: a versatile marker to visualize F-actin, Nat. Methods 5 (2008) 605–607.
[9] B. Leader, H. Lim, M.J. Carabatsos, A. Harrington, J. Ecsedy, D. Pellman, R. Maas, P. Leder, Formin-2, polyploidy, hypofertility and positioning of the meiotic spindle in mouse oocytes, Nat. Cell Biol. 4 (2002) 921–928.
[10] J. Dumont, K. Million, K. Sunderland, P. Rassinier, H. Lim, B. Leader, M.H. Verlhac, Formin-2 is required for spindle migration and for the late steps of cytokinesis in mouse oocytes, Dev. Biol. 301 (2007) 254–265.
[11] S. Pfender, V. Kuznetsov, S. Pleiser, E. Kerkhoff, M. Schuh, Spire-type actin nucleators cooperate with Formin-2 to drive asymmetric oocyte division, Curr. Biol. 21 (2011) 955–960.
[12] S.-C. Sun, Z.-B. Wang, Y.-N. Xu, S.-E. Lee, X.-S. Cui, N.-H. Kim, Arp2/3 complex regulates asymmetric division and cytokinesis in mouse oocytes, PLoS One 6 (2011) e18392.
[13] S. Brunet, B. Maro, Germinal vesicle position and meiotic maturation in mouse oocyte, Reproduction 133 (2007) 1069–1072.
[14] J.L. Tremoleda, E.J. Schoevers, T.A. Stout, B. Colenbrander, M.M. Bevers, Organisation of the cytoskeleton during in vitro maturation of horse oocytes, Mol. Reprod. Dev. 60 (2001) 260–269.
[15] N.H. Kim, H.M. Chung, K.Y. Cha, K.S. Chung, Microtubule and microfilament organization in maturing human oocytes, Hum. Reprod. 13 (1998) 2217–2222.
[16] G. FitzHarris, P. Marangos, J. Carroll, Changes in endoplasmic reticulum structure during mouse oocyte maturation are controlled by the cytoskeleton and cytoplasmic dynein, Dev. Biol. 305 (2007) 133–144.
[17] G. Halet, J. Carroll, Rac activity is polarized and regulates meiotic spindle stability and anchoring in mammalian oocytes, Dev. Cell 12 (2007) 309–317.
[18] H. Li, F. Guo, B. Rubinstein, R. Li, Actin-driven chromosomal motility leads to symmetry breaking in mammalian meiotic oocytes, Nat. Cell Biol. 10 (2008) 1301–1308.
[19] J.-S. Ai, Q. Wang, M. Li, L.-H. Shi, S.I. Ola, B. Xiong, S. Yin, D.-Y. Chen, Q.-Y. Sun, Roles of microtubules and microfilaments in spindle movements during rat oocyte meiosis, J. Reprod. Dev. 54 (2008) 391–396.

[20] G. Schatten, H. Schatten, I. Spector, C. Cline, N. Paweletz, C. Simerly, C. Petzelt, Latrunculin inhibits the microfilament-mediated processes during fertilization, cleavage and early development in sea urchins and mice, Exp. Cell Res. 166 (1986) 191–208.
[21] Y. Terada, C. Simerly, G. Schatten, Microfilament stabilization by jasplakinolide arrests oocyte maturation, cortical granule exocytosis, sperm incorporation cone resorption, and cell-cycle progression, but not DNA replication, during fertilization in mice, Mol. Repro. Dev. 56 (2000) 89–98.
[22] J. Azoury, K.W. Lee, V. Georget, P. Rassinier, B. Leader, M.-H. Verlhac, Spindle positioning in mouse oocytes relies on a dynamic meshwork of actin filaments, Curr. Biol. 18 (2008) 1514–1519.
[23] M. Schuh, J. Ellenberg, A new model for asymmetric spindle positioning in mouse oocytes, Curr. Biol. 18 (2008) 1986–1992.
[24] J. Azoury, K.W. Lee, V. Georget, P. Hikal, M.-H. Verlhac, Symmetry breaking in mouse oocytes requires transient F-actin meshwork destabilization, Development 138 (2011) 2903–2908.
[25] M. Schuh, An actin-dependent mechanism for long-range vesicle transport, Nat. Cell Biol. 13 (2011) 1431–1436.
[26] K. Dahlgaard, A.A.S.F. Raposo, T. Niccoli, D. St Johnston, Capu and Spire assemble a cytoplasmic actin mesh that maintains microtubule organization in the *Drosophila* oocyte, Dev. Cell 13 (2007) 539–553.
[27] A.E. Rosales-Nieves, J.E. Johndrow, L.C. Keller, C.R. Magie, D.M. Pinto-Santini, S.M. Parkhurst, Coordination of microtubule and microfilament dynamics by *Drosophila* Rho1, Spire and Cappuccino, Nat. Cell Biol. 8 (2006) 367–376.
[28] B.J. Nolen, N. Tomasevic, A. Russell, D.W. Pierce, Z. Jia, C.D. McCormick, J. Hartman, R. Sakowicz, T.D. Pollard, Characterization of two classes of small molecule inhibitors of Arp2/3 complex, Nature 460 (2009) 1031–1034.
[29] S.-C. Sun, Y.-N. Xu, Y.-H. Li, S.-E. Lee, Y.-X. Jin, X.-S. Cui, N.-H. Kim, WAVE2 regulates meiotic spindle stability, peripheral positioning and polar body emission in mouse oocytes, Cell Cycle 10 (2011) 1853–1860.
[30] K.G. Campellone, M.D. Welch, A nucleator arms race: cellular control of actin assembly, Nat. Rev. Mol. Cell Biol. 11 (2010) 237–251.
[31] S.-C. Sun, Q.-Y. Sun, N.-H. Kim, JMY is required for asymmetric division and cytokinesis in mouse oocytes, Mol. Hum. Repro. 17 (2011) 296–304.
[32] K. Yi, J.R. Unruh, M. Deng, B.D. Slaughter, B. Rubinstein, R. Li, Dynamic maintenance of asymmetric meiotic spindle position through Arp2/3-complex-driven cytoplasmic streaming in mouse oocytes, Nat. Cell Biol. 13 (2011) 1252–1258.
[33] C. Simerly, G. Nowak, P. de Lanerolle, G. Schatten, Differential expression and functions of cortical myosin IIA and IIB isotypes during meiotic maturation, fertilization, and mitosis in mouse oocytes and embryos, Mol. Biol. Cell 9 (1998) 2509–2525.
[34] F. Matsumura, Regulation of myosin II during cytokinesis in higher eukaryotes, Trends Cell Biol. 15 (2005) 371–377.
[35] A.L. Bishop, A. Hall, Rho GTPases and their effector proteins, Biochem. J. 348 (2000) 241–255.
[36] J. Na, M. Zernicka-Goetz, Asymmetric positioning and organization of the meiotic spindle of mouse oocytes requires CDC42 function, Curr. Biol. 16 (2006) 1249–1254.
[37] S. Etienne-Manneville, A. Hall, Cell polarity: Par6, aPKC and cytoskeletal crosstalk, Curr. Opin. Cell Biol. 15 (2003) 67–72.
[38] T. Choi, K. Fukasawa, R. Zhou, L. Tessarollo, K. Borror, J. Resau, G.F. Vande Woude, The Mos/mitogen-activated protein kinase (MAPK) pathway regulates the size and degradation of the first polar body in maturing mouse oocytes, Proc. Natl. Acad. Sci. 93 (1996) 7032–7035.
[39] L.-Z. Yu, B. Xiong, W.-X. Gao, C.-M. Wang, Z.-S. Zhong, L.-J. Huo, Q. Wang, Y. Hou, K. Liu, J. Liu, H. Schatten, D.-Y. Chen, Q.-Y. Sun, MEK1/2 regulates microtubule organization, spindle pole tethering and asymmetric division during mouse oocyte meiotic maturation, Cell Cycle 6 (2007) 330–338.
[40] A. Amiel, L. Leclère, L. Robert, S. Chevalier, E. Houliston, Conserved functions for Mos in Eumetazoan oocyte maturation revealed by studies in a Cnidarian, Curr. Biol. 19 (2009) 305–311.
[41] M. Webb, S.K. Howlett, B. Maro, Parthenogenesis and cytoskeletal organization in ageing mouse eggs, J. Embryol. Exp. Morphol. 95 (1986) 131–145.
[42] M.-H. Verlhac, Spindle positioning: going against the actin flow, Nat. Cell Biol. 13 (2011) 1183–1185.
[43] S. Vinot, T. Le, B. Maro, S. Louvet-Vallée, Two PAR6 proteins become asymmetrically localized during establishment of polarity in mouse oocytes, Curr. Biol. 14 (2004) 520–525.
[44] T. Ducibella, Quantitative studies of changes in cortical granule number and distribution in the mouse oocyte during meiotic maturation, Dev. Biol. 130 (1988) 184–197.
[45] B. Maro, M.H. Johnson, M. Webb, G. Flach, Mechanism of polar body formation in the mouse oocyte: an interaction between the chromosomes, the cytoskeleton and the plasma membrane, J. Embryol. Exp. Morpho. 92 (1986) 11–32.
[46] M. Deng, P. Suraneni, R.M. Schultz, R. Li, The Ran GTPase mediates chromatin signaling to control cortical polarity during polar body extrusion in mouse oocytes, Dev. Cell 12 (2007) 301–308.
[47] J. Dumont, S. Petri, F. Pellegrin, M.-E. Terret, M.T. Bohnsack, P. Rassinier, V. Georget, P. Kalab, O.J. Gruss, M.-H. Verlhac, A centriole- and RanGTP-independent spindle assembly pathway in meiosis I of vertebrate oocytes, J. Cell Biol. 176 (2007) 295–305.
[48] K.E. Runge, J.E. Evans, Z.-Y. He, S. Gupta, K.L. McDonald, H. Stahlberg, P. Primakoffc, D.G. Mylesa, Oocyte CD9 is enriched on the microvillar membrane and required for normal microvillar shape and distribution, Dev. Biol. 304 (2007) 317–325.
[49] J.C. Sandquist, A.M. Kita, W.M. Bement, And the dead shall rise: actin and myosin return to the spindle, Dev. Cell 21 (2011) 410–419.
[50] M. Théry, V. Racine, A. Pépin, M. Piel, Y. Chen, J.-B. Sibarita, M. Bornens, The extracellular matrix guides the orientation of the cell division axis, Nat. Cell Biol. 7 (2005) 947–953.
[51] J. Fink, N. Carpi, T. Betz, A. Bétard, M. Chebah, A. Azioune, M. Bornens, C. Sykes, L. Felter, D. Cuvelier, M. Piel, External forces control mitotic spindle positioning, Nat. Cell Biol. 13 (2011) 771–778.

Cell Cycle 12:21, 3370–3376; November 1, 2013; © 2013 Landes Bioscience

Mouse oocyte, a paradigm of cancer cell

Marie-Emilie Terret[1,2,3,*], Agathe Chaigne[1,2,3], and Marie-Hélène Verlhac[1,2,3,*]

[1]CIRB; Collège de France and CNRS-UMR7241 and INSERM-U1050; Paris, France; [2]Equipe Labellisée Ligue Contre le Cancer; Paris, France; [3]Memolife Laboratory of Excellence and Paris Science Lettre; Paris, France

Oocytes undergo extremely asymmetric divisions in terms of size. Coordinating spindle assembly and positioning in the absence of canonical centrosomes appears to be a challenge for oocytes, which divide with an elevated rate of errors in chromosome segregation. Here we highlight recent work on the characteristics of oocyte meiotic divisions, giving special emphasis on MTOCs clustering, generation of aneuploidy, and cortex softening, properties shared by cancer cells. While the loss of canonical centrosomes in oocytes might favor the asymmetry in size of meiotic divisions by reducing the distance between spindle poles and the cortex, we propose that this acentrosomal pathway might also render meiotic spindles less robust and, so, be responsible for the high error rate of female meiosis.

Keywords: mouse, oocyte, asymmetric divisions, aneuploidy, cancer

Abbreviations: MTOC, microtubule organizing centers; APC, adenomatous polyposis coli; Lgl, lethal giant larvae; Brat, brain tumor; PCM, pericentriolar material; Mud, mushroom body defect; Pins, partner of inscuteable; NEBD, nuclear envelope breakdown; LH, luteinizing hormone; SAC, spindle assembly checkpoint; APC/C, anaphase-promoting complex/cyclosome; K-fibers, kinetochore fibers; NuMA, nuclear mitotic apparatus; MAP, microtubule-associated protein; HURP, hepatoma upregulated protein; HSET, human spleen embryonic tissue and testes, also known as KIFC1; Arp2/3, actin-related protein 2/3; MAPK, mitogen-activated protein kinase; PLCZ1, phospholipase C-zeta; MT, microtubule; PB1, polar body 1

Submitted: 09/19/2013

Accepted: 09/23/2013

http://dx.doi.org/10.4161/cc.26583

*Correspondence to: Marie-Emilie Terret; Email: marie-emilie.terret@college-de-france.fr; Marie-Hélène Verlhac; Email: marie-helene.verlhac@college-de-france.fr

Asymmetric Division in Mitotic Cells

The development of any given multicellular organism requires a fine equilibrium between proliferation and differentiation in order to promote cell diversity. This equilibrium can be regulated by the ratio between symmetric vs. asymmetric cell divisions. Whereas symmetric divisions are conservative and induce the formation of daughter cells identical to their mother, asymmetric divisions allow a mother cell to generate 2 daughter cells of distinct fates. In addition to their role in development, cell divisions are required for tissue homeostasis in adults, as stem cells can generate differentiated cells constituting the tissue via asymmetric divisions and, via symmetric divisions, undergo self-renewal, thus preserving their pool. In addition to their importance during normal development and adult life, asymmetric cell divisions can be involved in a variety of pathologies such as tumorigenesis, neurodevelopmental disorders, or polycystic kidney disease. Notably, the loss of asymmetric divisions following mutation of several tumor suppressors genes involved in mitotic spindle orientation, such as APC, Lgl, Brat, or p63, is associated with tumor initiation and progression, in particular in the brain and colon (for a review, see refs. 1 and 2). The positioning of the spindle along the polarity axis instructs the production of either symmetric or asymmetric division. Spindle positioning indeed specifies the geometry of cell division (for a review, see ref. 3). In most animal cells, centrosomes act as dominant microtubule-organizing centers and establish both the mitotic spindle axis[4] as well as indirectly control its orientation within the cell (**Fig. 1**; for a review, see ref. 5). Canonical centrosomes are composed of a pair of centrioles that recruit their surrounding pericentriolar material (PCM) necessary for microtubule nucleation. Mitotic spindle positioning depends on complexes of Dynein–Dynactin anchored on one side at the cell cortex and associated on the other side with plus-ends of astral microtubules that emanate from the 2 centrosomes. These complexes containing the minus-end-directed microtubule motor Dynein, which walks along astral microtubules, are therefore pulling on the 2 spindle poles (for a review, see ref. 6). In *Drosophila*, cortical adaptors such as Mud display a polarized localization following their association with cortical cues, such

as Pins. Mud associates with Dynein–Dynactin complexes, resulting in unequal pulling force at one spindle pole, since Mud is asymmetrically localized in the cell (for a review, see ref. 2). To generate efficient Dynein–Dynactin-dependent forces while preventing membrane invagination, the cell cortex stiffens at the beginning of mitosis. This stiffening is established following an increase in cortical tension, which leads to cell rounding (**Fig. 1**). A rigid cell cortex is thus essential for proper mitotic spindle positioning. The rigidity of the cortex, mediated by changes in the actin cytoskeleton at M-phase entry, also influences spindle morphogenesis and acts as an interface between the spindle and the cell environment (for a review, see refs. 7 and 8).

Asymmetric Division in Oocytes

Changes in the actin cytoskeleton are also instrumental during mouse female meiosis and are the main driving force in the control of meiotic spindle positioning, required in oocytes to produce extremely asymmetric divisions. Indeed, during female meiosis, 2 highly asymmetric divisions without an intermediate replicative phase produce a large functional haploid female gamete, the oocyte, and 2 small degenerating polar bodies (**Fig. 2**). The asymmetry in size and fate of those divisions is important for the production of a unique cell capable of being fertilized and preserving most of the maternal stores that will sustain embryo development[9] (for a review, see ref. 10). The asymmetry established during mouse oocyte divisions results mainly from 2 events: off-center positioning of the meiotic spindle and chromatin-induced polarization of the cortex (for a review, see ref. 11). Hence, whereas in mitotic cells, cortical cues influence spindle positioning to produce either symmetric or asymmetric divisions, in mouse female meiosis, cortical cues and cell polarity are both defined as a downstream consequence of spindle positioning. In mammals, oocytes arrest in prophase I of meiosis I in the ovaries with a slightly off-centered nucleus and no apparent sign of polarization, harboring both a uniform cytoplasm and cortex.[12,13] The resumption of meiosis will be triggered periodically by the LH (luteinizing hormone) surge after puberty. Meiosis resumption and exit from the block in prophase I is evidenced by nuclear envelope breakdown (NEBD). It is immediately followed by the formation of the first meiotic spindle at the exact location where the nucleus was, more or less in the center of the cell (**Fig. 2**). Most female meiotic spindles do not have centrioles and, thus, lack canonical centrosomes.[14] Instead, microtubules are nucleated by microtubule-organizing centers (MTOCs) composed only of pericentriolar material (PCM). In mouse and human oocytes, centrioles are lost at the beginning of follicle growth at puberty, imposing very peculiar modes of spindle morphogenesis and spindle positioning. In mouse oocytes, meiotic spindle axis forms randomly and is not influenced by cortical cues.[15] Late in meiosis I, the spindle migrates along its long axis toward the closest cortex[15,16] (**Fig. 2**). Since the meiotic spindle axis forms randomly, there is no predetermined direction of spindle migration. At the end of this migration process, the chromosomes are close to the cortex of the oocyte, and their Ran GTP-associated gradient specifies a cortical region above them where the fist polar body will be extruded.[17,18] This cortical region lacks microvilli, is enriched in actin filaments, and accumulates activated Rac-GTP;[13,19] after this specification the oocyte is polarized. Since oocytes lack canonical centrosomes, they also lack astral microtubules. Therefore their positioning does not depend on microtubules, as in mitosis, (**Fig. 1**) but depends on actin filaments.[15,20] Once the spindle reaches the cortex, anaphase takes place, with the segregation of homologous chromosomes and the formation of the first polar body. The meiosis II spindle reforms directly under the cortex and is maintained there by actin-mediated cytoplasmic streaming.[21] Mouse oocytes, like the majority of vertebrate oocytes, arrest in metaphase II (**Fig. 2**). Fertilization will trigger second anaphase and meiosis exit, the emission of a second polar body via another asymmetric division and will lead to embryo formation and development.

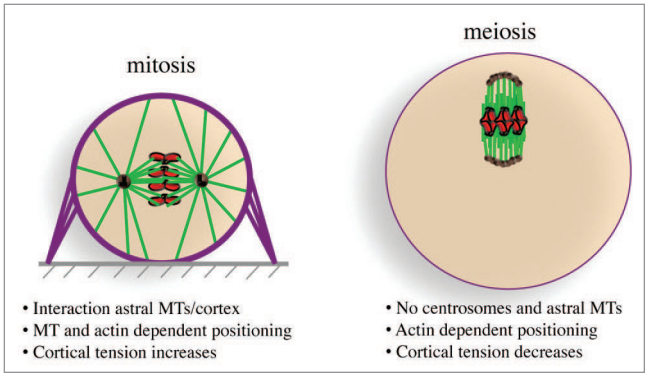


Figure 1. Spindle positioning in mitosis and meiosis. Chromosomes in red, microtubules (MTs) in green, actin in violet, and microtubule organizing centers (MTOCs) in brown.

Mouse Oocyte, a Paradigm of Cancer Cell

At least 10% of human pregnancies end up in the formation of aneuploid embryos (gain or loss of a whole chromosome—trisomy or monosomy). Aneuploidy frequently results from nondisjunction events that take place in the oocyte. The increase in maternal age further contributes to the occurrence of aneuploidy, a crucial phenomenom for modern societies, where women tend to post-pone child bearing.[22] Chromosome segregation in female meiosis is unusual in that meiotic spindle poles do not have centrioles, are not anchored to the cortex via astral microtubules, and therefore lack canonical centrosomes, imposing modes of spindle assembly and positioning that might be responsible for the high error rate of female meiosis. In that regard, oocytes share some common features with cancer cells, namely a certain degree of aneuploidy, the ability to sort and cluster MTOCs, and the importance of cortical softening for the division.

Cancer cells are aneuploid, gaining or losing whole chromosome sets. Even if the link between aneuploidy and tumorigenesis is far from being clear at present, it appears that cancer cells seem to be able to cope with high rates of aneuploidy and keep proliferating. Surprisingly, oocytes and early embryos also cope with a certain degree of aneuploidy. Meiosis I in human females is error-prone and is a leading cause of the occurrence of trisomies as well as other congenital defects due to the formation of aneuploid embryos.[23,24] In mitosis, the spindle assembly checkpoint (SAC) is essential to ensure accurate chromosome segregation by postponing anaphase onset until all the chromosomes are under tension, attached and correctly aligned onto the mitotic spindle. As a result, the SAC prevents chromosome mis-segregation and aneuploidy, and its dysfunction is implicated in tumorigenesis (for a review, see ref. 25). The SAC functions by preventing an ubiquitin ligase called the anaphase-promoting complex/cyclosome (APC/C) from ubiquitinating proteins whose degradation is required for anaphase onset and mitotic exit, namely Securin and Cyclin B (for a review, see ref. 26). In mitosis, a single unoccupied kinetochore can generate a Mad2-based diffusible "wait-anaphase" signal[27] sufficient to inhibit the APC/C. The SAC does act during meiosis I in mouse oocytes to ensure successful attachment of the kinetochores of homologously paired bivalent chromosomes.[28-31] However, despite being present and functional in meiosis I, it does not prevent errors from happening at a high rate. It has been recently established that during mammalian meiosis I, the SAC has a surprisingly low threshold for satisfaction.[32-35] In mitosis, Mad2 is displaced from the chromosomes when they are bi-oriented at the metaphase plate via kinetochore-microtubule attachment. In meiosis I, Mad2 is lost from kinetochores 3 to 4 h before anaphase, even when all K-fibers are not assembled and in the presence of chromosomes that have not become aligned at the metaphase plate and that are not bi-oriented.[33,34] These few free kinetochores or erroneous attachments of bivalent kinetochores are not able to generate a sufficient SAC "wait-anaphase" signal to inhibit the APC/C, but instead the SAC is silenced, predisposing to aneuploidy.[33-35] Furthermore, oocytes expressing a non-functional form of NuMA, a microtubule-associated protein (MAP), present major spindle pole defects. Interestingly, in these oocytes, the SAC is silenced even when tension between the kinetochores of homologs is reduced and accompanied by alignment defects.[32] These findings establish that in mammalian meiosis I, the SAC is unable to sustain meiotic arrest in the presence of one or few misaligned and/or misattached kinetochores with reduced inter-kinetochore tension, thereby offering an explanation for why meiosis I in mammals is so error-prone. In addition, it has been established that the rate of trisomy increases with maternal age, and this in a frightening exponential way starting at 35-y-old.[23] The age-dependent increase of errors during meiosis I could be due to the fact that the glue holding the bivalent chromosomes together, namely cohesins, becomes weaker with age, oocytes being arrested in prophase I for decades in human.[36,37] Such a defect would result in a decrease in inter-kinetochore tension, which would not be sensed by the meiotic SAC.[32] The origin for such an important rate of aneuploidy in oocytes could be due to the high volume of these cells and the low DNA/cytoplasm ratio inducing a strong dilution of the SAC signaling emitted from unattached or mis-attached kinetochores. Consistent with this hypothesis, in larger eggs, such as the ones from *Xenopus*, oocytes and embryos do not harbor any spindle assembly checkpoint until the mid-blastula transition, where in the early embryo, dividing only by cleavage with no increase in its total size, the ratio of DNA vs. cytoplasm increases, becoming closer to that encountered in mitotic cells.[38-43] Additionally, aneuploidy could be inherent to the less robust mode of

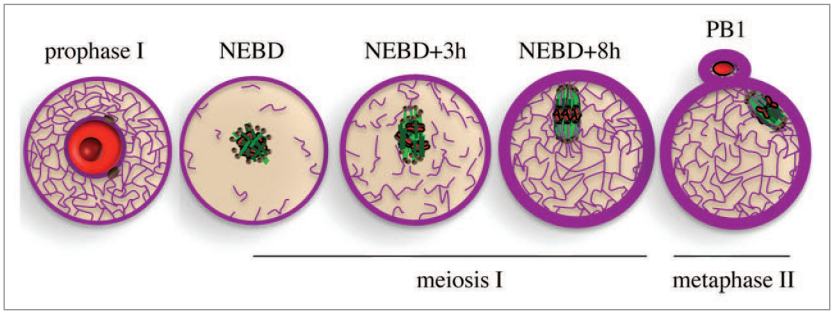


Figure 2. Meiotic maturation of mouse oocytes. NEBD, nuclear envelope breakdown; PB1, polar body 1. Chromosomes in red, microtubules in green, actin in violet, MTOCs in brown.

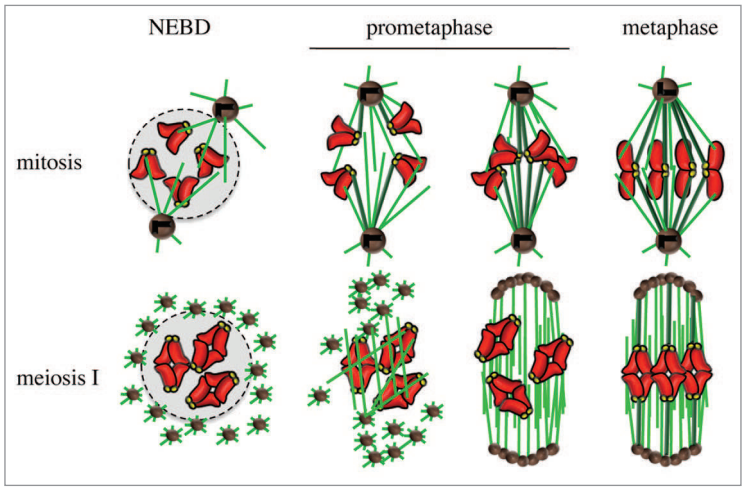


Figure 3. Spindle assembly in mitosis and meiosis. NEBD, nuclear envelope breakdown. Chromosomes in red, kinetochores in yellow, microtubules in green, K-fibers in dark green, centrioles in black, pericentriolar material (PCM) in brown, nucleus in light gray.

spindle assembly of female meiosis due to the absence of centrosomes.

Most healthy cells, with the exception of oocytes, possess 1 or 2 canonical centrosomes, depending on their cell cycle stage (centrosome duplication takes place in S phase). Extra centrosomes can induce multipolar spindle formation, resulting in chromosome mis-segregation and leading to cell death.[44] However, many cancer cells, as well as some healthy cells, do harbor an excess of centrosomes but manage to avoid cell death. They keep dividing, correlating with an increased rate of aneuploidy. The presence of extra-centrosomes can even induce tumorigenesis, as shown in *Drosophila*.[45] Cancer cells with extra centrosomes have developed a strategy to keep dividing and avoid multipolar spindle formation: they cluster their extra centrosomes prior to division.[46,47] Mouse oocytes also sort and cluster acentriolar MTOCs that are present in the egg at meiosis resumption. Following centriole loss at the beginning of follicle growth phase, oocytes reorganize their microtubule cytoskeleton by inducing the coalescence of few amorphous patches of PCM around the nuclear envelope by an unknown process.[48] Before entry into meiosis and NEBD, these discrete patches spread around the nuclear envelope via a microtubule-dependent process, such that they are evenly distributed around the chromatin when NEBD occurs.[48] The setup of spindle bipolarity is a slow process following NEBD and results from the sorting and coalescence of multiple MTOCs around the chromatin[49,50] (**Fig. 3**). The small GTPase Ran, present in a gradient around the chromosomes in the oocyte, locally activates spindle assembly factors to promote microtubule nucleation and stabilization.[17,51] Then the chromosomes congress toward the metaphase plate, showing highly oscillatory movements until the very end of prometaphase,[52] K-fibers being established only late in meiosis I[33,34,49,53] (**Fig. 3**). Interestingly, proper spindle assembly in oocytes requires the sorting and coalescence of multiple acentriolar MTOCs,[49] a process reminiscent centrosome clustering.[47] In particular, HURP, a MAP and Ran effector, is essential for the assembly of a robust central microtubule domain, acting as a scaffold for the sorting of MTOCs to spindle poles. HURP is essential in meiosis but dispensable for mitosis, since HURP-knockout mice are viable but female sterile. However, it is also required in cancer cells bearing multiple centrosomes to cluster them, suggesting that the pathway of acentriolar MTOC clustering in meiosis is also used by cancer cells to cluster their extra centrosomes.[49] HURP is not required for normal dividing cells; thus, like HSET, it would be a good therapeutic target to specifically slow down cancer cells but not somatic cell division, since cancer cells that do not cluster their extra centrosomes will eventually die.

Whereas most normal cells undergoing mitosis present a stiff cortex, which helps them read external constraints coming from their environing tissue, mouse oocytes soften their cortex, like malignant cells do, freeing them from external forces and allowing them to position their spindle off-center.[54] More precisely, meiosis I spindle migration to the cortex depends on the presence of a dynamic cytoplasmic F-actin meshwork (**Fig. 2**), nucleated by Formin-2[16,55-58] and Spire 1/2.[59] These nucleators are enriched in Rab11a- and Myosin-Vb-positive vesicles that drive the network dynamics and density.[60,61] This cytoplasmic F-actin meshwork is present in prophase I-arrested oocytes, then dismantled at NEBD, and reforms progressively during meiosis I.[62] It includes an actin cage surrounding the microtubule spindle, connected via straight actin filaments to the cortex.[16,57] In addition and contrary to what is observed during mitosis, cortical tension decreases during meiosis,[63] a puzzling observation, since oocytes are round cells stable in shape that actively position their spindles (**Fig. 1**). Softening of the cortex during meiosis I is due to cortical myosin II exclusion and to the nucleation of a cortical F-actin thickening by the Arp2/3 complex (**Fig. 4**). These 2 events are triggered by the Mos/MAPK pathway. Mos is a MAPKKK, which activates MAPKs ERK1 and ERK2 in oocytes after NEBD.[15] This pathway is required for the arrest of the cell cycle in metaphase II and for spindle migration in meiosis I[15] (**Fig. 2**). The softening of the cortex, absent from *mos*−/− oocytes, is essential for asymmetric positioning of the first meiotic spindle, since artificial stiffening of the cortex prevents spindle migration. Theoretical modeling of spindle migration as a function of cortical tension shows that a soft cortex amplifies a slight imbalance of forces generated at spindle poles by myosin II,[16] since the spindle does not form at the center of the cell after NEBD, but a little off-center[54] (**Fig. 4**). Toward the end of meiosis I, spindle migration is accelerated by actin-mediated cytoplasmic streaming.[64] Invasive tumor cells mechanically soften (up to 70% softer than their neighboring healthy cells) and modify their adhesion to the extracellular matrix, enhancing their capacity to escape the initial site of primary tumor growth. Cortex softening is a general feature of cancer cells and can be found in a variety of tumor cells from breast, gastrointestinal, ovarian, lungs, and pancreas cancers.[65-67] It has even been proposed that cell stiffness may be a useful biomarker to evaluate the relative metastatic potential of cancer cells.[65,68-71] In ovarian cancer, it has been shown that the reduced stiffness of cancer cells is associated with actin cytoskeleton remodeling.[71] In the neighboring stiffer healthy cells, the actin filaments are distributed through the cell body, with most

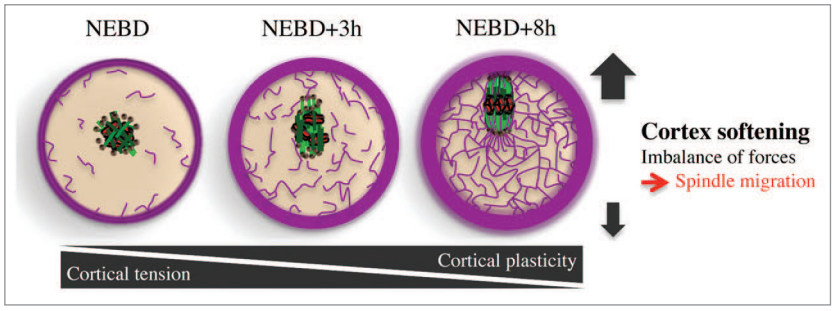


Figure 4. Spindle positioning in meiosis. Chromosomes in red, microtubules in green, actin in violet, and MTOCs in brown.

F-actin bundles aligned along the long axis of the cell with well-defined stress fibers and focal contacts. In contrast, F-actin in the softer ovarian cancer cells maintains a cortical structure, with most filaments lying in the peripheral region of the cell, but F-actin in the cytoplasm is less organized.[71] This cortical organization recalls the cortical actin thickening present in mouse oocytes that also soften their cortex.[54] Oocytes might use the same strategy of cancer cells to break free from the ovaries during ovulation. It is interesting that *mos*−/− oocytes, that keep a high cortical tension, fail to arrest in metaphase II and activate parthenogenetically in the absence of a sperm, inducing ovarian teratomas at a high frequency.[72,73] However, if the decrease in cortical tension may favor ovulation and extrusion from the ovary, it is certainly not the major driver of ovulation. Indeed females that overexpress the sperm protein PLCZ1 in oocytes show normal oocyte meiotic progression, yet induce parthenogenetic activation of their eggs and display even greater rates of teratocarninomas than *mos*−/− females.[74] Altogether, these results argue that it is mostly parthenogenetic activation and not increase in cortical tension that causes ovarian teratomas.

Conclusion

Oocytes development is strictly dependent on asymmetric divisions. In mouse oocytes, the asymmetry of the divisions relies mostly on actin and on a drop of cortical tension, an actin-dependent exclusive way to position the spindle, which may have evolved from the absence of canonical centrosomes and their associated astral microtubules. Both features make this model relevant to study processes used by cancer cells to divide, since they are the dominant mode in oocytes. Hence mouse oocytes may be used as test tubes to test new potential targets for therapies against cancer. Even though oocytes share features present in certain types of cancer cells, contrary to them, they also acquired the ability to stop dividing. Indeed the meiotic cell cycle is characterized by multiple arrests, i.e., in prophase I, in metaphase I or II, or even later in G_1, adapted to the reproductive pace specific to the species. It is puzzling that the same oncogenic pathway, namely the Mos/MAPK, actually controls both the asymmetry of meiotic divisions and actin-dependent cortex remodeling as well as the brake on the meiotic cell cycle. This unique feature has been conserved through evolution and is observed in species as distant as the jellyfish and the mouse, suggesting that the 2 functions may have been acquired simultaneously, avoiding gametes turning into teratomas.[72,73,75]

Disclosure of Potential Conflicts of Interest

No potential conflicts of interest were disclosed.

Acknowledgments

We thank Renata Basto for critical reading of this manuscript. This work was supported by grants from the *Ligue Nationale Contre le Cancer* (EL2012/LNCC/MHV). Agathe Chaigne is a recipient of a fellowship from the Ecole Normale Supérieure (ENS) Paris.

References

1. Powell AE, Shung CY, Saylor KW, Müllendorff KA, Weiss JB, Wong MH. Lessons from development: A role for asymmetric stem cell division in cancer. Stem Cell Res 2010; 4:3-9; PMID:19853549; http://dx.doi.org/10.1016/j.scr.2009.09.005
2. Lu MS, Johnston CA. Molecular pathways regulating mitotic spindle orientation in animal cells. Development 2013; 140:1843-56; PMID:23571210; http://dx.doi.org/10.1242/dev.087627
3. Gillies TE, Cabernard C. Cell division orientation in animals. Curr Biol 2011; 21:R599-609; PMID:21820628; http://dx.doi.org/10.1016/j.cub.2011.06.055
4. Toso A, Winter JR, Garrod AJ, Amaro AC, Meraldi P, McAinsh AD. Kinetochore-generated pushing forces separate centrosomes during bipolar spindle assembly. J Cell Biol 2009; 184:365-72; PMID:19204145; http://dx.doi.org/10.1083/jcb.200809055
5. Tanenbaum ME, Medema RH. Mechanisms of centrosome separation and bipolar spindle assembly. Dev Cell 2010; 19:797-806; PMID:21145497; http://dx.doi.org/10.1016/j.devcel.2010.11.011
6. Moore JK, Cooper JA. Coordinating mitosis with cell polarity: Molecular motors at the cell cortex. Semin Cell Dev Biol 2010; 21:283-9; PMID:20109571; http://dx.doi.org/10.1016/j.semcdb.2010.01.020
7. Théry M, Bornens M. Cell shape and cell division. Curr Opin Cell Biol 2006; 18:648-57; PMID:17046223; http://dx.doi.org/10.1016/j.ceb.2006.10.001
8. Kunda P, Baum B. The actin cytoskeleton in spindle assembly and positioning. Trends Cell Biol 2009; 19:174-9; PMID:19285869; http://dx.doi.org/10.1016/j.tcb.2009.01.006
9. Otsuki J, Nagai Y, Lopata A, Chiba K, Yasmin L, Sankai T. Symmetrical division of mouse oocytes during meiotic maturation can lead to the development of twin embryos that amalgamate to form a chimeric hermaphrodite. Hum Reprod 2012; 27:380-7; PMID:22147919; http://dx.doi.org/10.1093/humrep/der408
10. Brunet S, Verlhac MH. Positioning to get out of meiosis: the asymmetry of division. Hum Reprod Update 2011; 17:68-75; PMID:20833637; http://dx.doi.org/10.1093/humupd/dmq044
11. Chaigne A, Verlhac MH, Terret ME. Spindle positioning in mammalian oocytes. Exp Cell Res 2012; 318:1442-7; PMID:22406266; http://dx.doi.org/10.1016/j.yexcr.2012.02.019
12. FitzHarris G, Marangos P, Carroll J. Changes in endoplasmic reticulum structure during mouse oocyte maturation are controlled by the cytoskeleton and cytoplasmic dynein. Dev Biol 2007; 305:133-44; PMID:17368610; http://dx.doi.org/10.1016/j.ydbio.2007.02.006
13. Halet G, Carroll J. Rac activity is polarized and regulates meiotic spindle stability and anchoring in mammalian oocytes. Dev Cell 2007; 12:309-17; PMID:17276347; http://dx.doi.org/10.1016/j.devcel.2006.12.010
14. Szollosi D, Calarco P, Donahue RP. Absence of centrioles in the first and second meiotic spindles of mouse oocytes. J Cell Sci 1972; 11:521-41; PMID:5076360
15. Verlhac MH, Lefebvre C, Guillaud P, Rassinier P, Maro B. Asymmetric division in mouse oocytes: with or without Mos. Curr Biol 2000; 10:1303-6; PMID:11069114; http://dx.doi.org/10.1016/S0960-9822(00)00753-3
16. Schuh M, Ellenberg J. A new model for asymmetric spindle positioning in mouse oocytes. Curr Biol 2008; 18:1986-92; PMID:19062278; http://dx.doi.org/10.1016/j.cub.2008.11.022
17. Dumont J, Petri S, Pellegrin F, Terret ME, Bohnsack MT, Rassinier P, Georget V, Kalab P, Gruss OJ, Verlhac MH. A centriole- and RanGTP-independent spindle assembly pathway in meiosis I of vertebrate oocytes. J Cell Biol 2007a; 176:295-305; PMID:17261848; http://dx.doi.org/10.1083/jcb.200605199
18. Deng M, Suraneni P, Schultz RM, Li R. The Ran GTPase mediates chromatin signaling to control cortical polarity during polar body extrusion in mouse oocytes. Dev Cell 2007; 12:301-8; PMID:17276346; http://dx.doi.org/10.1016/j.devcel.2006.11.008
19. Maro B, Johnson MH, Webb M, Flach G. Mechanism of polar body formation in the mouse oocyte: an interaction between the chromosomes, the cytoskeleton and the plasma membrane. J Embryol Exp Morphol 1986; 92:11-32; PMID:3723057
20. Longo FJ, Chen DY. Development of cortical polarity in mouse eggs: involvement of the meiotic apparatus. Dev Biol 1985; 107:382-94; PMID:4038667; http://dx.doi.org/10.1016/0012-1606(85)90320-3
21. Yi K, Unruh JR, Deng M, Slaughter BD, Rubinstein B, Li R. Dynamic maintenance of asymmetric meiotic spindle position through Arp2/3-complex-driven cytoplasmic streaming in mouse oocytes. Nat Cell Biol 2011; 13:1252-8; PMID:21874009; http://dx.doi.org/10.1038/ncb2320
22. Nagaoka SI, Hassold TJ, Hunt PA. Human aneuploidy: mechanisms and new insights into an age-old problem. Nat Rev Genet 2012; 13:493-504; PMID:22705668; http://dx.doi.org/10.1038/nrg3245
23. Hassold T, Hunt P. To err (meiotically) is human: the genesis of human aneuploidy. Nat Rev Genet 2001; 2:280-91; PMID:11283700; http://dx.doi.org/10.1038/35066065
24. Hassold T, Hunt P. Maternal age and chromosomally abnormal pregnancies: what we know and what we wish we knew. Curr Opin Pediatr 2009; 21:703-8; PMID:19881348; http://dx.doi.org/10.1097/MOP.0b013e328332c6ab
25. Schvartzman JM, Sotillo R, Benezra R. Mitotic chromosomal instability and cancer: mouse modelling of the human disease. Nat Rev Cancer 2010; 10:102-15; PMID:20094045; http://dx.doi.org/10.1038/nrc2781

26. Musacchio A, Salmon ED. The spindle-assembly checkpoint in space and time. Nat Rev Mol Cell Biol 2007; 8:379-93; PMID:17426725; http://dx.doi.org/10.1038/nrm2163
27. Rieder CL, Cole RW, Khodjakov A, Sluder G. The checkpoint delaying anaphase in response to chromosome monoorientation is mediated by an inhibitory signal produced by unattached kinetochores. J Cell Biol 1995; 130:941-8; PMID:7642709; http://dx.doi.org/10.1083/jcb.130.4.941
28. Wassmann K, Niault T, Maro B. Metaphase I arrest upon activation of the Mad2-dependent spindle checkpoint in mouse oocytes. Curr Biol 2003; 13:1596-608; PMID:13678590; http://dx.doi.org/10.1016/j.cub.2003.08.052
29. Homer HA, McDougall A, Levasseur M, Herbert M. Restaging the spindle assembly checkpoint in female mammalian meiosis I. Cell Cycle 2005; 4:650-3; PMID:15846076; http://dx.doi.org/10.4161/cc.4.5.1677
30. Niault T, Hached K, Sotillo R, Sorger PK, Maro B, Benezra R, Wassmann K. Changing Mad2 levels affects chromosome segregation and spindle assembly checkpoint control in female mouse meiosis I. PLoS One 2007; 2:e1165; PMID:18043727; http://dx.doi.org/10.1371/journal.pone.0001165
31. McGuinness BE, Anger M, Kouznetsova A, Gil-Bernabé AM, Helmhart W, Kudo NR, Wuensche A, Taylor S, Hoog C, Novak B, et al. Regulation of APC/C activity in oocytes by a Bub1-dependent spindle assembly checkpoint. Curr Biol 2009; 19:369-80; PMID:19249208; http://dx.doi.org/10.1016/j.cub.2009.01.064
32. Kolano A, Brunet S, Silk AD, Cleveland DW, Verlhac MH. Error-prone mammalian female meiosis from silencing the spindle assembly checkpoint without normal interkinetochore tension. Proc Natl Acad Sci U S A 2012; 109:E1858-67; PMID:22552228; http://dx.doi.org/10.1073/pnas.1204686109
33. Lane SI, Yun Y, Jones KT. Timing of anaphase-promoting complex activation in mouse oocytes is predicted by microtubule-kinetochore attachment but not by bivalent alignment or tension. Development 2012; 139:1947-55; PMID:22513370; http://dx.doi.org/10.1242/dev.077040
34. Gui L, Homer H. Spindle assembly checkpoint signalling is uncoupled from chromosomal position in mouse oocytes. Development 2012; 139:1941-6; PMID:22513372; http://dx.doi.org/10.1242/dev.078352
35. Sebestova J, Danylevska A, Novakova L, Kubelka M, Anger M. Lack of response to unaligned chromosomes in mammalian female gametes. Cell Cycle 2012; 11:3011-8; PMID:22871737; http://dx.doi.org/10.4161/cc.21398
36. Chiang T, Duncan FE, Schindler K, Schultz RM, Lampson MA. Evidence that weakened centromere cohesion is a leading cause of age-related aneuploidy in oocytes. Curr Biol 2010; 20:1522-8; PMID:20817534; http://dx.doi.org/10.1016/j.cub.2010.06.069
37. Lister LM, Kouznetsova A, Hyslop LA, Kalleas D, Pace SL, Barel JC, Nathan A, Floros V, Adelfalk C, Watanabe Y, et al. Age-related meiotic segregation errors in mammalian oocytes are preceded by depletion of cohesin and Sgo2. Curr Biol 2010; 20:1511-21; PMID:20817533; http://dx.doi.org/10.1016/j.cub.2010.08.023
38. Gerhart J, Wu M, Kirschner MW. Cell cycle dynamics of an M-phase-specific cytoplasmic factor in *Xenopus laevis* oocytes and eggs. J Cell Biol 1984; 98:1247-55; PMID:6425302; http://dx.doi.org/10.1083/jcb.98.4.1247
39. Murray AW, Kirschner MW. Dominoes and clocks: the union of two views of the cell cycle. Science 1989; 246:614-21; PMID:2683077; http://dx.doi.org/10.1126/science.2683077
40. Clute P, Masui Y. Regulation of the appearance of division asynchrony and microtubule-dependent chromosome cycles in *Xenopus laevis* embryos. Dev Biol 1995; 171:273-85; PMID:7556912; http://dx.doi.org/10.1006/dbio.1995.1280
41. Taieb FE, Gross SD, Lewellyn AL, Maller JL. Activation of the anaphase-promoting complex and degradation of cyclin B is not required for progression from Meiosis I to II in *Xenopus* oocytes. Curr Biol 2001; 11:508-13; PMID:11413001; http://dx.doi.org/10.1016/S0960-9822(01)00145-2
42. Peter M, Castro A, Lorca T, Le Peuch C, Magnaghi-Jaulin L, Dorée M, Labbé JC. The APC is dispensable for first meiotic anaphase in *Xenopus* oocytes. Nat Cell Biol 2001; 3:83-7; PMID:11146630; http://dx.doi.org/10.1038/35050607
43. Shao H, Li R, Ma C, Chen E, Liu XJ. *Xenopus* oocyte meiosis lacks spindle assembly checkpoint control. J Cell Biol 2013; 201:191-200; PMID:23569212; http://dx.doi.org/10.1083/jcb.201211041
44. Ganem NJ, Godinho SA, Pellman D. A mechanism linking extra centrosomes to chromosomal instability. Nature 2009; 460:278-82; PMID:19506557; http://dx.doi.org/10.1038/nature08136
45. Basto R, Brunk K, Vinadogrova T, Peel N, Franz A, Khodjakov A, Raff JW. Centrosome amplification can initiate tumorigenesis in flies. Cell 2008; 133:1032-42; PMID:18555779; http://dx.doi.org/10.1016/j.cell.2008.05.039
46. Quintyne NJ, Reing JE, Hoffelder DR, Gollin SM, Saunders WS. Spindle multipolarity is prevented by centrosomal clustering. Science 2005; 307:127-9; PMID:15637283; http://dx.doi.org/10.1126/science.1104905
47. Kwon M, Godinho SA, Chandhok NS, Ganem NJ, Azioune A, Théry M, Pellman D. Mechanisms to suppress multipolar divisions in cancer cells with extra centrosomes. Genes Dev 2008; 22:2189-203; PMID:18662975; http://dx.doi.org/10.1101/gad.1700908
48. Łuksza M, Queguigner I, Verlhac M-H, Brunet S. Rebuilding MTOCs upon centriole loss during mouse oogenesis. Dev Biol 2013; In press; PMID:23954884.
49. Breuer M, Kolano A, Kwon M, Li CC, Tsai TF, Pellman D, Brunet S, Verlhac MH. HURP permits MTOC sorting for robust meiotic spindle bipolarity, similar to extra centrosome clustering in cancer cells. J Cell Biol 2010; 191:1251-60; PMID:21173113; http://dx.doi.org/10.1083/jcb.201005065
50. Schuh M, Ellenberg J. Self-organization of MTOCs replaces centrosome function during acentrosomal spindle assembly in live mouse oocytes. Cell 2007; 130:484-98; PMID:17693257; http://dx.doi.org/10.1016/j.cell.2007.06.025
51. Brunet S, Dumont J, Lee KW, Kinoshita K, Hikal P, Gruss OJ, Maro B, Verlhac MH. Meiotic regulation of TPX2 protein levels governs cell cycle progression in mouse oocytes. PLoS One 2008; 3:e3338; PMID:18833336; http://dx.doi.org/10.1371/journal.pone.0003338
52. Kitajima TS, Ohsugi M, Ellenberg J. Complete kinetochore tracking reveals error-prone homologous chromosome biorientation in mammalian oocytes. Cell 2011; 146:568-81; PMID:21854982; http://dx.doi.org/10.1016/j.cell.2011.07.031
53. Brunet S, Maria AS, Guillaud P, Dujardin D, Kubiak JZ, Maro B. Kinetochore fibers are not involved in the formation of the first meiotic spindle in mouse oocytes, but control the exit from the first meiotic M phase. J Cell Biol 1999; 146:1-12; PMID:10402455; http://dx.doi.org/10.1083/jcb.146.1.1
54. Chaigne A, Campillo C, Gov NS, Voituriez R, Azoury J, Umaña-Diaz C, Almonacid M, Queguiner I, Nassoy P, Sykes C, et al. A soft cortex is essential for asymmetric spindle positioning in mouse oocytes. Nat Cell Biol 2013; 15:958-66; PMID:23851486; http://dx.doi.org/10.1038/ncb2799
55. Leader B, Lim H, Carabatsos MJ, Harrington A, Ecsedy J, Pellman D, Maas R, Leder P. Formin-2, polyploidy, hypofertility and positioning of the meiotic spindle in mouse oocytes. Nat Cell Biol 2002; 4:921-8; PMID:12447394; http://dx.doi.org/10.1038/ncb880
56. Dumont J, Million K, Sunderland K, Rassinier P, Lim H, Leader B, Verlhac MH. Formin-2 is required for spindle migration and for the late steps of cytokinesis in mouse oocytes. Dev Biol 2007b; 301:254-65; PMID:16989804; http://dx.doi.org/10.1016/j.ydbio.2006.08.044
57. Azoury J, Lee KW, Georget V, Rassinier P, Leader B, Verlhac MH. Spindle positioning in mouse oocytes relies on a dynamic meshwork of actin filaments. Curr Biol 2008; 18:1514-9; PMID:18848445; http://dx.doi.org/10.1016/j.cub.2008.08.044
58. Li H, Guo F, Rubinstein B, Li R. Actin-driven chromosomal motility leads to symmetry breaking in mammalian meiotic oocytes. Nat Cell Biol 2008; 10:1301-8; PMID:18836438; http://dx.doi.org/10.1038/ncb1788
59. Pfender S, Kuznetsov V, Pleiser S, Kerkhoff E, Schuh M. Spire-type actin nucleators cooperate with Formin-2 to drive asymmetric oocyte division. Curr Biol 2011; 21:955-60; PMID:21620703; http://dx.doi.org/10.1016/j.cub.2011.04.029
60. Schuh M. An actin-dependent mechanism for long-range vesicle transport. Nat Cell Biol 2011; 13:1431-6; PMID:21983562; http://dx.doi.org/10.1038/ncb2353
61. Holubcová Z, Howard G, Schuh M. Vesicles modulate an actin network for asymmetric spindle positioning. Nat Cell Biol 2013; 15:937-47; PMID:23873150; http://dx.doi.org/10.1038/ncb2802
62. Azoury J, Lee KW, Georget V, Hikal P, Verlhac MH. Symmetry breaking in mouse oocytes requires transient F-actin meshwork destabilization. Development 2011; 138:2903-8; PMID:21653611; http://dx.doi.org/10.1242/dev.060269
63. Larson SM, Lee HJ, Hung PH, Matthews LM, Robinson DN, Evans JP. Cortical mechanics and meiosis II completion in mammalian oocytes are mediated by myosin-II and Ezrin-Radixin-Moesin (ERM) proteins. Mol Biol Cell 2010; 21:3182-92; PMID:20660156; http://dx.doi.org/10.1091/mbc.E10-01-0066
64. Yi K, Rubinstein B, Unruh JR, Guo F, Slaughter BD, Li R. Sequential actin-based pushing forces drive meiosis I chromosome migration and symmetry breaking in oocytes. J Cell Biol 2013; 200:567-76; PMID:23439682; http://dx.doi.org/10.1083/jcb.201211068
65. Guck J, Schinkinger S, Lincoln B, Wottawah F, Ebert S, Romeyke M, Lenz D, Erickson HM, Ananthakrishnan R, Mitchell D, et al. Optical deformability as an inherent cell marker for testing malignant transformation and metastatic competence. Biophys J 2005; 88:3689-98; PMID:15722433; http://dx.doi.org/10.1529/biophysj.104.045476
66. Suresh S, Spatz J, Mills JP, Micoulet A, Dao M, Lim CT, Beil M, Seufferlein T. Connections between single-cell biomechanics and human disease states: gastrointestinal cancer and malaria. Acta Biomater 2005; 1:15-30; PMID:16701777; http://dx.doi.org/10.1016/j.actbio.2004.09.001
67. Hou HW, Li QS, Lee GY, Kumar AP, Ong CN, Lim CT. Deformability study of breast cancer cells using microfluidics. Biomed Microdevices 2009; 11:557-64; PMID:19082733; http://dx.doi.org/10.1007/s10544-008-9262-8
68. Cross SE, Jin YS, Rao J, Gimzewski JK. Nanomechanical analysis of cells from cancer patients. Nat Nanotechnol 2007; 2:780-3; PMID:18654431; http://dx.doi.org/10.1038/nnano.2007.388

69. Lekka M, Laidler P. Applicability of AFM in cancer detection. Nat Nanotechnol 2009; 4:72-72, author reply 72-3; PMID:19197298; http://dx.doi.org/10.1038/nnano.2009.004
70. Lee GYH, Lim CT. Biomechanics approaches to studying human diseases. Trends Biotechnol 2007; 25:111-8; PMID:17257698; http://dx.doi.org/10.1016/j.tibtech.2007.01.005
71. Xu W, Mezencev R, Kim B, Wang L, McDonald J, Sulchek T. Cell stiffness is a biomarker of the metastatic potential of ovarian cancer cells. PLoS One 2012; 7:e46609; PMID:23056368; http://dx.doi.org/10.1371/journal.pone.0046609
72. Colledge WH, Carlton MB, Udy GB, Evans MJ. Disruption of c-mos causes parthenogenetic development of unfertilized mouse eggs. Nature 1994; 370:65-8; PMID:8015609; http://dx.doi.org/10.1038/370065a0
73. Hashimoto N, Watanabe N, Furuta Y, Tamemoto H, Sagata N, Yokoyama M, Okazaki K, Nagayoshi M, Takeda N, Ikawa Y, et al. Parthenogenetic activation of oocytes in c-mos-deficient mice. Nature 1994; 370:68-71; PMID:8015610; http://dx.doi.org/10.1038/370068a0
74. Yoshida N, Amanai M, Fukui T, Kajikawa E, Brahmajosyula M, Iwahori A, Nakano Y, Shoji S, Diebold J, Hessel H, et al. Broad, ectopic expression of the sperm protein PLCZ1 induces parthenogenesis and ovarian tumours in mice. Development 2007; 134:3941-52; PMID:17933795; http://dx.doi.org/10.1242/dev.007930
75. Amiel A, Leclère L, Robert L, Chevalier S, Houliston E. Conserved functions for Mos in eumetazoan oocyte maturation revealed by studies in a cnidarian. Curr Biol 2009; 19:305-11; PMID:19230670; http://dx.doi.org/10.1016/j.cub.2008.12.054

on T, Ehrlund A, *et al.* GPS2-
or/SUMO pathways govern anti-
s of LRH-1 and LXRbeta in the
response. *Genes Dev* 2010 ; 24 :

Fan R, *et al.* SMRT-GPS2
dysregulation coincides with
obesity-linked adipocyte inflammation. *J Clin Invest* 2013 ; 123 : 362-79.
11. Calay ES, Hotamisligil GS. Turning off the inflammatory, but not the metabolic, flames. *Nat Med* 2013 ; 19 : 265-7.
12. Liao X, Sharma N, Kapadia F, *et al.* Kruppel-like factor 4 regulates macrophage polarization. *J Clin Invest* 2011 ; 121 : 2736-49.
13. Stanley TL, Zanni MV, Johnsen S, *et al.* TNF-alpha antagonism with etanercept decreases glucose and increases the proportion of high molecular weight adiponectin in obese subjects with features of the metabolic syndrome. *J Clin Endocrinol Metab* 2011 ; 96 : E146-150.
14. Mack GS. Epigenetic cancer therapy makes headway. *J Natl Cancer Inst* 2006 ; 98 : 1443-4.
15. Bantscheff M, Hopf C, Savitski MM, *et al.* Chemoproteomics profiling of HDAC inhibitors reveals selective targeting of HDAC complexes. *Nat Biotechnol* 2011 ; 29 : 255-65.

NOUVELLE

Ramollir le cortex

Un prérequis à l'asymétrie de la division ovocytaire

Agathe Chaigne[1,2], Marie-Hélène Verlhac[1,2], Marie-Emilie Terret[1,2]

[1] Centre interdisciplinaire de recherche en biologie, CNRS-UMR7241, Inserm-U1050, Équipe labellisée Ligue contre le cancer, Collège de France, 11, place Marcelin Berthelot, 75005 Paris, France.
[2] Memolife Laboratory of Excellence and Paris Science Lettre, Paris, F-75005, France.
marie-emilie.terret@college-de-france.fr
marie-helene.verlhac@college-de-france.fr

oryon diploïde néces-
commun de la moitié
père et de la mère. La
des gamètes (ovocyte
e) s'accompagne donc
du nombre de chromo-
r d'une cellule diploïde
loïde. Cette réduction
tique se produit lors de
ccompagne d'une divi-
t d'une spécialisation
au développement du
Chez la femelle, tout en
é du génome, l'ovocyte
ximum de cytoplasme
serves stockées lors de
qui est indispensable

jusqu'à la puberté chez les mammifères. Puis, tous les mois, un pic de LH (hormone lutéinisante) provoque la reprise de la méiose et sa dernière étape, la maturation méiotique. Le premier événement remarquable est la rupture de l'enveloppe nucléaire (NEBD : *nuclear envelope breakdown*) qui est suivie par la formation d'un fuseau de microtubules autour des chromosomes répliqués et appariés au niveau des chiasma *(Figure 1)*. Ce fuseau se forme à l'emplacement du noyau, quasiment au centre de la cellule. Chez la souris, cinq à six heures après NEBD, le fuseau migre selon son grand axe vers le cortex le plus proche [1], et, huit à neuf

L'asymétrie des divisions méiotiques est permise par le positionnement périphérique des fuseaux de division dans cette très grosse cellule de 80 µm de diamètre. Quels sont les mécanismes de positionnement du fuseau?

Les mécanismes de positionnement du fuseau

Lors de la division des cellules somatiques, le fuseau est positionné grâce aux microtubules astraux, nucléés par les centrosomes qui organisent également pôles et microtubules du fuseau. Les ovocytes sont dépourvus de centrosomes canoniques et possèdent à la place des MTOC (*microtubule organizing*

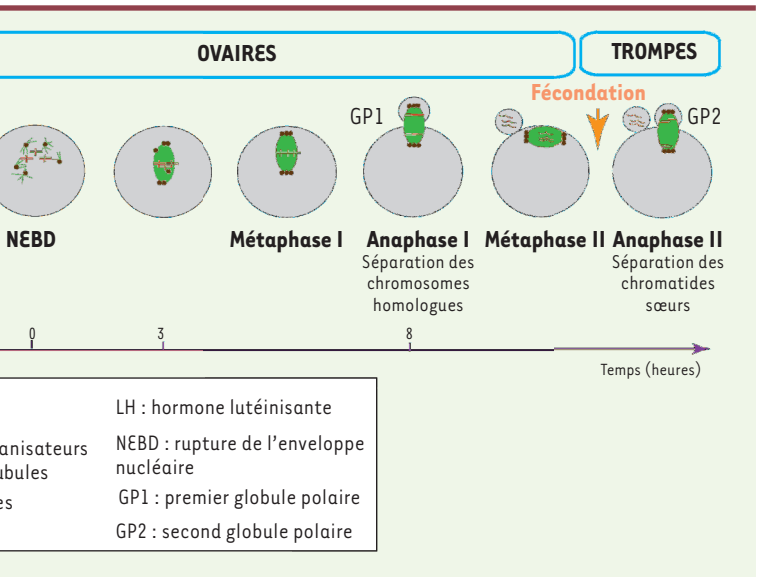


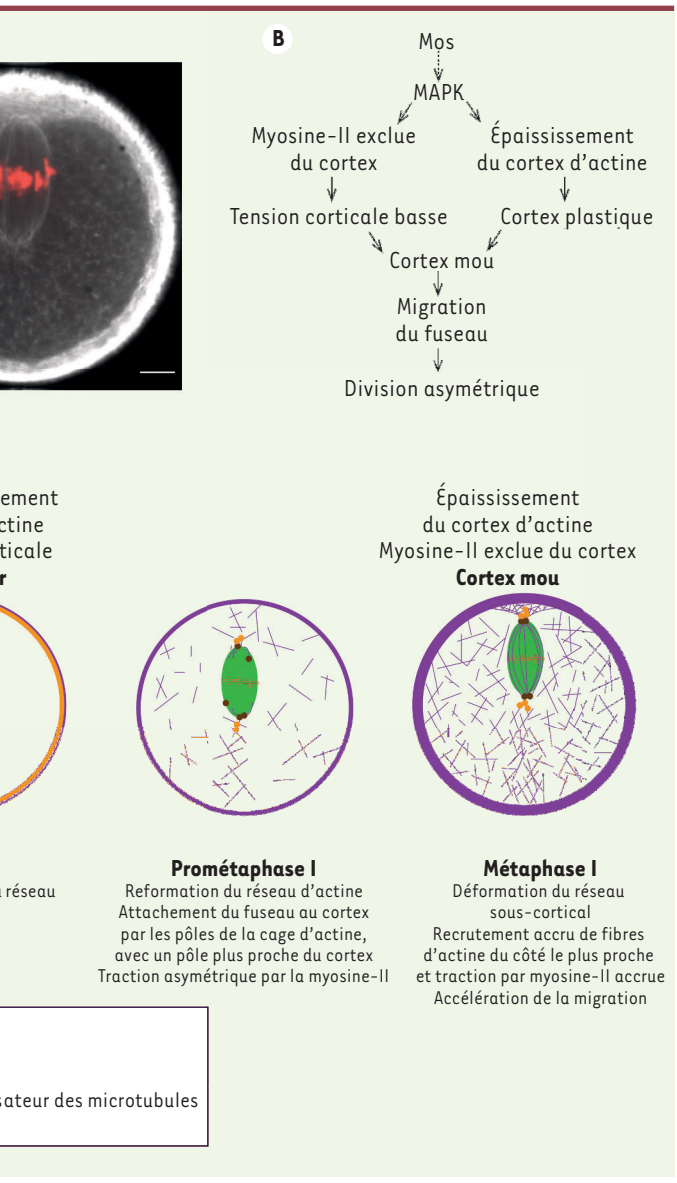
Figure 1. ***Principaux événements de la maturation méiotique de l'ovocyte de souris.*** L'ovocyte est arrêté dans l'ovaire en prophase de première division de méiose (prophase I). La maturation méiotique est déclenchée par le pic de LH (hormone lutéinisante) qui provoque la rupture de l'enveloppe nucléaire (NEBD). Le fuseau de microtubules est formé environ trois heures après NEBD et il migre au cortex à partir de NEBD + 6 h. L'anaphase I, qui consiste en la séparation des chromosomes homologues, est suivie de la cytokinèse, ici l'extrusion du premier globule polaire (GP1). Le fuseau se reforme ensuite parallèlement au cortex, et cté en métaphase II. L'anaphase II, qui séparera les chromatides sœurs, sera déclenchée dans les trompes par la fécondation, n du second globule polaire (GP2).

its d'actine [4-7], de d'un ensemble de vési- situées aux nœuds du et qui recrutent ces Ce réseau d'actine et nt indispensables à la eau puisque dans des édant pas la formine-2 ant une quantité dimi- [8], ou dont la dyna- ne est abolie [10], le pas à la périphérie (ou ocyte. Par ailleurs, le du fuseau dépend éga- e mos/MAPK (*mitogen kinase*) [1].

articipe au

Malgré la présence de ce réseau très épais, il a été montré par la technique d'aspiration à l'aide de micropipettes que dans les ovocytes de souris, la tension du cortex diminue au cours de la maturation méiotique [12]. Au contraire, la tension corticale augmente dans les cellules somatiques qui se divisent, leur permettant de s'arrondir et de positionner leur fuseau *via* l'interaction entre microtubules astraux et cortex rigide. Afin de comprendre ce paradoxe, nous avons mesuré la tension corticale dans différentes conditions : dans des ovocytes contrôles (*wt*), qui présentent à la fois un réseau de microfilaments cytoplasmiques et un épaississement cortical en fin de méiose I,

cellulaires ; en particulier ces protéines sont responsables de l'augmentation de la tension corticale dans la plupart des cellules mitotiques. Dans les ovocytes, la myosine-II est enrichie au cortex des ovocytes en prophase contribuant ainsi à une tension élevée, puis elle est progressivement exclue du cortex, ce qui est reflété par la chute de tension corticale dans les stades tardifs de la méiose I. Cet évènement est également contrôlé par la voie mos/MAPK [11] ; ainsi dans les ovocytes *mos-/-* dépourvus d'épaississement cortical, la myosine-II est toujours enrichie au cortex en méiose I, ce qui corrèle avec le maintien d'une tension corticale élevée. En outre, l'épaississement du cortex d'actine



e cortex : un prérequis à l'asymétrie de la division ovocytaire. A. Réseaux vocyte en fin de méiose I (actine en blanc, chromosomes en rouge ; barre ***B.*** Rôle central de mos dans l'asymétrie de la division de l'ovocyte de souris ive la voie des MAPkinases, qui contribue à ramollir le cortex en délocalisant

ce côté [15]. La force de traction qui s'exerce sur le fuseau agit en retour sur le cortex de l'ovocyte, provoquant une déformation de l'épaississement du cortex d'actine *(Figure 2A)*. D'après un modèle mathématique soutenu par les mesures de tension, si la tension est trop forte (cas des *mos-/-*), le cortex ne peut pas se déformer et amplifier le mouvement du fuseau ; la vitesse du fuseau reste faible, ce qui expliquerait que dans les ovocytes *mos-/-*, le fuseau demeure central pendant le temps de la division. En conditions physiologiques, le cortex se déforme asymétriquement, permettant le recrutement de plus de fibres d'actine et une amplification du mouvement : le fuseau accélère vers le cortex en fin de méiose I [1, 5, 13] *(Figure 2C)*.

Conclusion

Dépourvus des centrosomes qui positionnent les fuseaux des cellules somatiques, les ovocytes possèdent des mécanismes originaux actine-dépendants assurant l'asymétrie de leurs divisions, en modulant en particulier les propriétés physiques du cortex. Il est intéressant de remarquer que l'exclusion de la myosine-II du cortex ainsi que l'épaississement d'actine permettant de ramollir le cortex et faire migrer le fuseau sont tous les deux contrôlés par la même voie de signalisation, la voie mos/MAPK *(Figure 2B)*. En outre, l'augmentation de la plasticité en fin de méiose I pourrait également jouer un rôle dans l'expulsion d'un petit globule polaire, assurant un maintien de la

cé par la Ligue nationale
12012/LNCC/MHV). Agathe
cée par l'École Normale
Paris.

re C, Guillaud P, *et al.* Asymmetric
cytes: with or without Mos. *Curr*
-6.
elopment of cortical polarity in
ment of the meiotic apparatus.
382-94.
rget V, *et al.* Symmetry breaking
quires transient F-actin meshwork
elopment 2011 ; 138 : 2903-8.
rget V, *et al.* Spindle positioning
ies on a dynamic meshwork of
Biol 2008 ; 18 : 1514-9.

5. Schuh M, Ellenberg J. A New model for asymmetric spindle positioning in mouse oocytes. *Curr Biol* 2008 ; 18 : 1986-92.
6. Dumont J, Million K, Sunderland K, *et al.* Formin-2 is required for spindle migration and for the late steps of cytokinesis in mouse oocytes. *Dev Biol* 2007 ; 301 : 254-65.
7. Leader B, Lim H, Carabatsos MJ, *et al.* Formin-2, polyploidy, hypofertility and positioning of the meiotic spindle in mouse oocytes. *Nat Cell Biol* 2002 ; 4 : 921-8.
8. Pfender S, Kuznetsov V, Pleiser S, *et al.* Spire-type actin nucleators cooperate with formin-2 to drive asymmetric oocyte division. *Curr Biol* 2011 ; 21 : 955-60.
9. Schuh M. An actin-dependent mechanism for long-range vesicle transport. *Nat Cell Biol* 2011 ; 13 : 1431-6.
10. Holubcová Z, Howard G, Schuh M. Vesicles modulate an actin network for asymmetric spindle positioning. *Nat Cell Biol* 2013 ; 15 : 937-47.
11. Chaigne A, Campillo C, Gov NS, *et al.* A soft cortex is essential for asymmetric spindle positioning in mouse oocytes. *Nat Cell Biol* 2013 ; 15 : 958-66.
12. Larson SM, Lee HJ, Hung PH, *et al.* Cortical mechanics and meiosis II completion in mammalian oocytes are mediated by myosin-II and ezrin-radixin-moesin (ERM) proteins. *Mol Biol Cell* 2010 ; 21 : 3182-92.
13. Yi K, Rubinstein B, Unruh JR, *et al.* Sequential actin-based pushing forces drive meiosis I chromosome migration and symmetry breaking in oocytes. *J Cell Biol* 2013 ; 200 : 567-76.
14. Simerly C, Nowak G, Lanerolle P de, *et al.* Differential expression and functions of cortical myosin IIA and IIB isotypes during meiotic maturation, fertilization, and mitosis in mouse oocytes and embryos. *Mol Biol Cell* 1998 ; 9 : 2509-25.
15. Maro B, Verlhac MH. Polar body formation: new rules for asymmetric divisions. *Nat Cell Biol* 2002 ; 4 : E281-E283.

NOUVELLE

some
acteur de la tumorigenèse ?

, Frédéric Catez, Hichem C. Mertani,
Diaz

Centre de recherche en cancérologie de Lyon,
UMR Inserm 1052 CNRS 5286, Centre Léon Bérard,
28, rue Laennec, F-69373, Lyon, France ; Université de Lyon,
F-69003, Lyon, France ; Université Lyon 1, ISPB, Lyon,
F-69622, France, F-69000 Lyon, France.
jean-jacques.diaz@lyon.unicancer.fr

s les années 1950, les
des complexes ribo-
es qui traduisent les
(ARNm) en protéines.
tants efforts ont été
terminer la structure
lle des ribosomes.

Ces dernières années ont également vu l'émergence de caractéristiques inattendues des ribosomes, qui ouvrent de nouvelles perspectives dans la compréhension de leur rôle biologique. En effet, les ribosomes montrent une certaine hétérogénéité de composi-

Ribosome et régulation de la traduction

Le ribosome humain est composé de 80 protéines et de quatre ARN ribosomiques (ARNr) organisés en deux sous-unités (40S et 60S) [2]. Le cœur du ribosome, qui comporte les sites cata-

Tension corticale et positionnement du fuseau dans l'ovocyte de souris

Résumé: Les divisions méiotiques sont très asymétriques en taille et génèrent une très grosse cellule, l'ovocyte, et deux petites cellules, les globules polaires. Cette asymétrie est permise par la migration du fuseau lors de la première division jusqu'au cortex le plus proche. Cette migration ne dépend pas des microbutules mais de la Myosin-II et d'un réseau de filaments d'actine nucléé par la coopération des nucléateurs de filaments droits Formin-2 et Spire1/2. Des observations préliminaires effectuées au laboratoire ont décrit un épaississement du cortex d'actine pendant la migration du fuseau, mais pourtant il avait été montré que la tension corticale, un paramètre décrivant la rigidité de l'ovocyte, diminue pendant la migration du fuseau. J'ai montré que cet épaississement est indispensable à la migration du fuseau et est nucléé par le nucléateur de filaments branchés Arp2/3, sous le contrôle de la voie Mos/MAPK. De plus, il provoque la diminution de la tension corticale en délocalisant la Myosin-II, ce qui est indispensable à la migration du fuseau. Finalement, j'ai montré que le chute de tension est un mécanisme d'amplification du déséquilibre des forces présent initialement (grâce au léger décentrage du noyau) qui déclenche la migration du fuseau.

Mots-clefs: filaments d'actine, tension corticale, Méiose I, division asymétrique

Cortical stiffness: a gatekeeper for spindle positioning in mouse oocytes

Abstract: Meiotic divisions are highly asymmetric divisions in size, generating a big cell, the oocyte, and two tiny cells, the polar bodies. This asymmetry is ensured by the migration of the first meiotic spindle to the closest cortex. This migration does not depend on microtubules but on Myosin-II and an F-actin meshwork nucleated by cooperation of straight filament nucleators Formin-2 and Spire1/2. Preliminary studies in the lab described a thickening of the F-actin cortex during spindle migration, but paradoxically cortical tension, a physical parameter describing the stiffness of the cell, drops during spindle migration. I have shown that this thickening is required for spindle migration and nucleated by the branched actin nucleator Arp2/3, under the control of the Mos/MAPK pathway. Furthermore, it promotes the decrease in cortical tension by triggering the delocalization of Myosin-II from the oocyte cortex, which is crucial for spindle migration. Finally, I have shown that the drop in cortical tension is an amplificatory mechanism to the initial unbalance of forces (due to a slight off-centered position of the nucleus) triggering the motion of the spindle.

Keywords: F-actin, cortical tension, Meiosis I, asymmetric division